Modelling of Environmental Effects on Clay Permeability

Ara Mouradian

A Thesis

in

The Department

of

Civil Engineering

Presented in Partial Fulfillment of the Requirements
for the Degree of Master of Applied Science at
Concordia University
Montreal, Quebec, Canada

September 1993

ISBN 0-315-90865-3

Canada

ABSTRACT

Modelling of Environmental Effects on Clay Permeability

Ara Mouradian

In recent years, the use of low hydraulic conductivity material (less than 1E -07 cm/s) to line waste facilities has become mandatory throughout North America This has been accomplished by the use of synthetic or clay-soil liners. Clay-soil liners have extremely low hydraulic conductivities and therefore have the potential to adequately contain these wastes, for significantly low costs The problem with using the clay-soil liner has been that variation in environmental factors effect its hydraulic conductivities

This study was done to produce information about the change of hydraulic conductivity with variations in environmental factors such as electrolyte concentration, type of electrolyte, temperature and hydraulic gradient as well as other factors such as clay type, clay density and sand / clay content. This information could serve as a guideline for an engineer constructing clay based liners. To provide this information, a theoretical model based on Kozeny-Carmen equation and Diffuse Double Layer theory was developed which can predict the change of hydraulic conductivity, K, with variations in these factors

A combination of variables were employed in this study and their effect was analyzed on the hydraulic conductivity of three kinds of clay minerals, montmorillonite, illite and kaolinite. For soils containing illite or kaolinite, K depends mainly on dry density and temperature. For soils containing montmorillonite, K depends on electrolyte concentration, type of electrolyte, hydraulic gradient, temperature and clay density The model also showed the existance of the threshold gradient and its variation with electrlolyte concentration, type of electrolyte, temperature and clay density

ACKNOWLEDGEMENTS

This research was funded by Faculty Research and Development Program (FRDP - I416) of the Concordia University. This support is gratefully acknowledged.

The author wishes to express his gratitude to his thesis supervisor, Dr. Steven Cheung, for the great amount of time and guidance he gave to help complete this thesis.

TABLE OF CONTENTS

TABLE OF CONTENTS (cont'd)

TABLE OF CONTENTS (cont'd)

LIST OF SYMBOLS

A	Area (cm^2)
A^o	Angstrom
B	Boltzman Constant (cm/mmole)
C	Contaminant Concentration (moles/litre)
C_o	Electrolyte Concentration in The Free Solution (moles/litre)
C_c	Electrolyte Concentration at The Midpoint Between Two Parallel Plates (moles/litre)
D	Diffusion Coefficient (cm^2/s)
D_c	Clay Dry Density (used in Figures) (g/cm^3 or Mg/m^3)
D_l	Longitudinal Coefficient Of Dispersion (cm^2/s)
d_c	Half Distance Between Clay Platelets in a Cluster (nm)
e	Electronic Charge ($=4.77 \times 10^{-10}$ esu)
G_c	Specific Gravity of Clay
g	Gravitational Acceleration (m/s^2)
i	Hydraulic Gradient
K	Hydraulic Conductivity (cm/s)
k	Permeability (cm^2)
l	Coordinate Direction Along The Flow Line
M	Molar Concentration
m	Pore Shape Factor
N_i	Concentration of Ions of Species i ($ions/cm^3$)
n_s	Fractional Volume of Solids
n_w	Fractional Volume of Liquid, Porosity
n'_w	Effective Porosity
P	Osmotic Pressure (kg/cm^2)

LIST OF SYMBOLS (cont'd)

P_c	Osmotic Pressure Midway Between Two Particles (kg/cm^3)
P_h	Hydraulic Pressure (kg/cm^3)
q	Rate of Water Flow Per Unit Area (cm/s)
q'	Rate of Water Flow(cm^3/s)
Q	Volume of Water Flow (cm^3)
R	Gas Constant = 0.0848 (kg litre / cm^2 ^oK)
S	Specific Surface Area of Clay per Unit Mass (m^2/kg)
S_e	Effective Cluster Specific Surface Area per Unit Mass (m^2/kg)
S_o	Specific Surface Area of Solids Per Unit Volume (m^2/m^3)
t	Time (s)
T	Absolute Temperature (^oK)
V	Flow Velocity (cm/s)
$\overline{v_l}$	Average Linear Velocity Along The Flow Line (cm/s)
W	Water Content in wt , %
W_i	Work Done in bringing an ion where the potential is ψ_i (J)
X	Distance from Particle Surface (nm)
X_d	Half Distance Between Two Parallel Plates (nm)
X'_d	Effective Half Distance Between Two Parallel Plates (nm)
X_i	Thickness of Immobilized Layer (nm)
Z	Valence of Exchangeable Cations
Z_i	Ionic Valence
γ_c	Clay Dry Density (g/cm^3 or Mg/m^3)
γ_{cc}	Cluster Dry Density (g/cm^3 or Mg/m^3)
γ_d	Bulk Density (g/cm^3 or Mg/m^3)
γ_w	Water Density (g/cm^3)

LIST OF SYMBOLS (cont'd)

ε	Dielectric Constant
μ	Permeant Viscosity (N s/m^2)
σ	Surface Charge Density (esu/cm^2)
τ	Tortuosity
ψ	Electrical Potential (mV)
ψ_c	Electrical Potential at Half Distance Between Parallel Plates (mV)

LIST OF TABLES

LIST OF TABLES (cont'd)

LIST OF FIGURES

LIST OF FIGURES (cont'd)

LIST OF FIGURES (cont'd)

LIST OF FIGURES (cont'd)

LIST OF FIGURES (cont'd)

CHAPTER 1

INTRODUCTION

1.1 Subject

The safe disposal of hazardous waste is one important component in dealing with the global environmental problem. The difficulties of assessing what constitutes 'safe', in terms of final disposal, is further complicated by the fact that industry is producing ever-increasing numbers of chemicals which add to both the variety and complexity of the chemicals found in hazardous waste. Environmental geotechnologists (geotechnical engineers, soil scientists, geologists, hydrogeologists, etc.) can contribute in many different ways to solving the problem of how to dispose of hazardous wastes safely. Dense clay-based materials are increasingly used as hydraulic barriers in many engineering projects. In Canada, for example, a compacted mixture of bentonite (Montmorillonite rich clay mineral) and sand is being evaluated for potential use in a nuclear fuel waste disposal vault (Hancox, 1986). Clay liners are also used to contain industrial waste products (see Figure 1.1). However, the failure of some soil liners to contain these hazardous wastes has resulted in the contamination of the underlying geologic deposits and local water supplies.

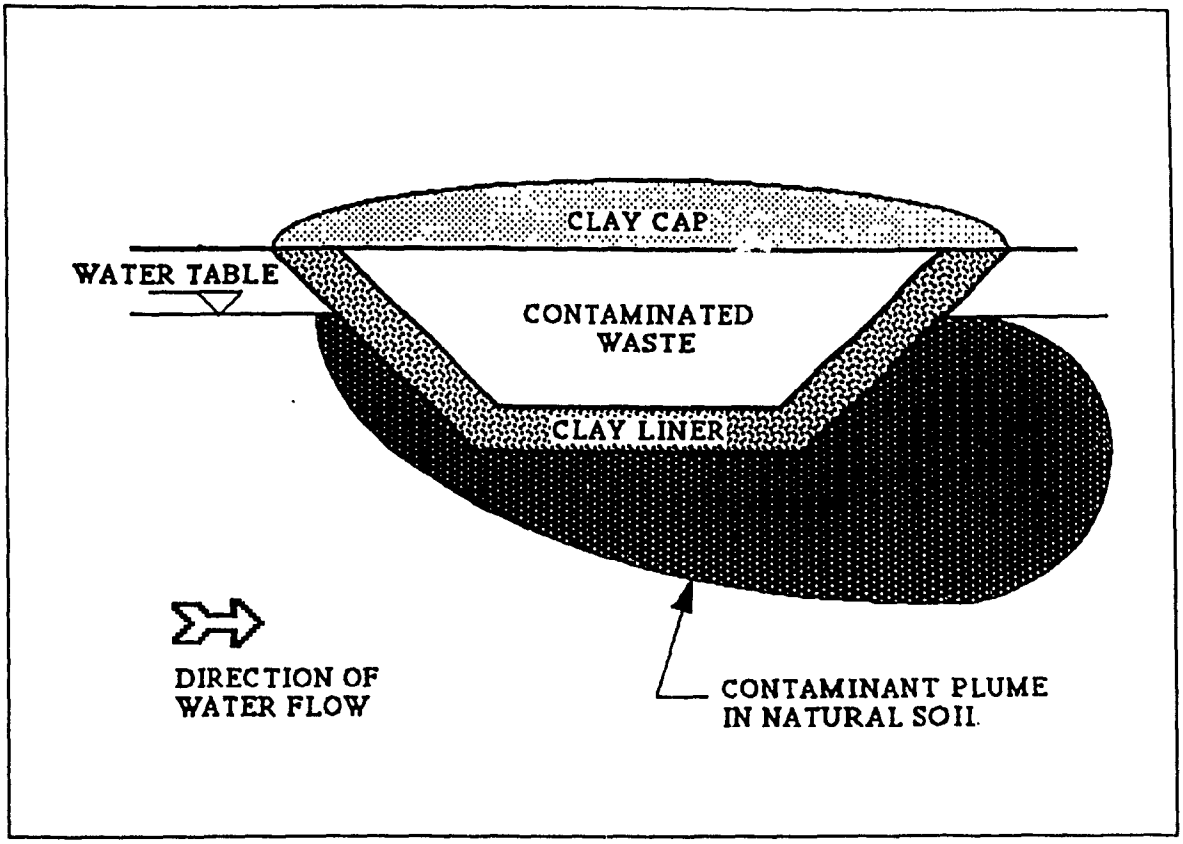

Figure 1.1 Schematic Example of a Clay Liner

Both government and industry have responded to the contamination of the environment by requiring waste containment facilities that reduce the movement of hazardous fluids to the subsoils to an environmentally acceptable level. Government agencies often establish guidelines or laws requiring soil liners with minimum thicknesses and minimum hydraulic conductivities. These minimum hydraulic conductivities can vary from 1×10^{-6} to 1×10^{-7} cm/sec. Permeability of soils with a low hydraulic conductivity is an important step in the design of soil liners which can meet these requirements.

The main obstacle to achieving the design and construction of a 'perfect' barrier lies in our limited knowledge of the complex physical, chemical and biological interactions that take place between the myriad of constituents found in any given landfill and the barrier

material. Protection barrier design has received the attention of many researchers in recent years.

1.2 Need

To assess the safety of the disposal site, a knowledge of the contaminant transport mechanism is needed. The two main mechanisms of contaminant transport through these clay liners are advection and diffusion. Advection depends on hydraulic conductivity (K) and diffusion depends on diffusion coefficient (D). The relative magnitudes of K and D of the clay liner will determine whether contaminants will be transported via advection or chemically controlled diffusion.

Literature shows that hydraulic conductivity is affected by several environmental factors, but this effect is not clear. To design such liners, the effect of clay type, sand content, density, temperature, water salinity, type of electrolyte and hydraulic gradient on the hydraulic conductivity have to be known. Laboratory permeability tests are usually performed in an attempt to evaluate the hydraulic conductivity of these liners. However, these tests are very time consuming and their results are often unclear. A model, describing the effects of these parameters, to be used as a guideline for laboratory tests is needed.

Another problem is the existence of a threshold gradient (a gradient below which there will be no flow) and the variation of this gradient with different environmental factors and clay densities. The establishment of the threshold gradient is very important, since high hydraulic gradient is generally used in the laboratory to determine permeability as compared to the field gradient which may be much lower than the threshold gradient. If the existence of such a gradient in a specific type of clay barrier is proved to exist, then the only mechanism of contaminant transport in that clay is through diffusion.

1.3 Objectives

This study is divided into two parts. One part deals with Kozeny-Carmen equation for flow and its validity in fine grained soils. While the other deals with the existence of a threshold gradient and its variation with clay density.

I The first objective is to examine the effects of clay type, sand content, density, temperature, water salinity, type of permeant, hydraulic gradient, and soil fabric on hydraulic conductivity. Using the Kozeny-Carmen equation and the diffuse double layer theory, a theoretical model is developed to establish relationships between hydraulic conductivity and various parameters. The theoretical results are compared with those from laboratory tests in literature. The implications of the conclusions of this study for the design of hydraulic barriers are discussed and related to engineering parameters that can be used to select appropriate clay-based barrier materials.

II The second objective is to investigate the existence of threshold gradient. A model based on the Kozeny-Carmen equation and the diffuse double layer theory is used to predict the threshold gradient and its variation with changes in environmental factors and clay density. The existence of the threshold gradient is then demonstrated by comparing the predicted results with those from literature.

CHAPTER 2

LITERATURE REVIEW

Several authors have discussed over the years the various aspects of contaminant transport and retention through porous media. The many details related to the advective transport of pollutants (including the determination of hydraulic permeabilities), as well as their diffusive transport (hydrodynamic dispersion and molecular diffusion) have been the subject of numerous recent theses and articles (Cheung and Mouradian, 1992).

The retention of contaminants has received increasing attention from researchers in environmental geotechnology, who have been borrowing from soil sciences not only the theories and concepts about the matter (e.g. double layer theory), but also the techniques to obtain the relevant parameters used to explain retention phenomena during contaminant transport (e.g. cation exchange capacity, distribution coefficients, buffering capacity, etc.)

In order to predict contaminant migration, a series of advection / dispersion / diffusion models have been proposed and/or adapted, most of them based on the law of conservation of mass and Fick's first law (Freeze and Cherry, 1979). It's one-dimensional formulation is presented in Equation (2.1) by

$$D_l \frac{\partial^2 C}{\partial l^2} - \overline{v_l} \frac{\partial C}{\partial l} = \frac{\partial C}{\partial t} \qquad (2.1)$$

Where l is the coordinate direction along the flow line,

D_l the longitudinal coefficient of dispersion and

$\overline{v_l}$ the average linear velocity along the flowline.

Independent of the model and its degree of complexity, there remains the problem of finding reliable input parameters. Experimental techniques guided by theoretical models have to be developed or perfected, either in the field or in the laboratory, in order to obtain such parameters.

In this research work, the interest is placed in the advective characteristics of contaminant migration. The diffusive characteristics of contaminant migration are not analyzed. Velocity is the parameter which describes advective flow, and it can be evaluated by executing permeability tests.

2.1 Fluid Flow

The flow of fluids through a soil may be the result of hydraulic conduction, thermo-osmosis, electro-osmosis, or chemical-osmosis (Mitchell, 1976). Hydraulic conduction is the flow of a fluid induced by a difference in hydraulic head across the soil. Thermo-osmosis, electro-osmosis, and chemical-osmosis are in turn, the flow of fluid induced by a difference in temperature, voltage, or chemical concentration across the soil, respectively. This study deals only with hydraulic conduction.

Hydraulic conduction was first studied by Henry Darcy in 1856. Darcy developed an empirical law which stated that the rate of flow through a medium was proportional to the hydraulic gradient. This law is now known as Darcy's Law and is expressed below:

$$q' = KiA \tag{2.2}$$

$$V = \frac{Q}{At} = Ki \tag{2.3}$$

where

q'	is the rate of flow through the soil
K	a basic property of the soil known as hydraulic conductivity
i	the potential or driving force known as hydraulic gradient and is numerically equal to the difference in hydraulic head across the soil divided by the length of the soil.
A	the area of soil through which flow is taking place
Q	the volume of water flow
t	the time of flow
V	the flow velocity

The hydraulic conductivity, K, is a measure of the resistance of the soil to flow of water.

2.2 Clay Mineralogy

A thorough knowledge of clay mineralogy is essential to fully understand the factors which affect the hydraulic conductivity of clay soils. Clay soils are composed primarily of various types of clay minerals. Each of these clay minerals has its own engineering properties. In many cases, the hydraulic conductivity depends on type of clay mineral.

Clay minerals are small crystalline particles formed by chemical weathering of rock-forming minerals. Silicates are the most important group comprising over 90 percent of the clay minerals on the earth (Lambe and Whitman, 1979). The most common

members of the silicate group are kaolinite, illite and montmorillonite. The properties of these three clay minerals vary widely. Kaolinite is a fairly inert and stable clay which is relatively unaffected by the fluids surrounding it. In contrast, montmorillonite is known for its ability to swell many times its original volume when hydrated with an unlimited supply of water. Illite is a clay mineral whose properties are intermediate between those of kaolinite and montmorillonite (Details on Clay Mineralogy is found in Appendix A).

2.3 Clay Soil Fabric

The geometrical arrangement of the group units, identified as fabric units, constitutes the first-order recognition pattern. The geometrical arrangement of single particles within each fabric unit in turn constitutes the second-order fabric recognition pattern. Response behaviour in clay soils is through fabric unit interaction and through the various bonding mechanisms between units (Details on Clay Soil Fabric are found in Appendix A).

2.4 Double Layer Theory

2.4.1 Introduction

The swelling behavior of clay minerals such as montmorillonite is described by the Diffuse Double Layer Theory. This diffuse double layer (or water hull) around the clay particles is caused by the hydration of water to the clay surface and to the adsorbed cations. It was first formulated by Gouy in 1910 and Chapman in 1913, and is often called the Gouy-Chapman Theory of the Diffuse Double Layer. The Theory indicates that the

behavior of swelling clays is controlled by the subsurface properties (i.e. negative surface charge) rather than the mass properties (i.e. gravity).

Water is a polar molecule where the geometrical arrangement of atoms in the molecules causes one side of the molecule to be positively charged, and the other negatively charged. Thus, in an electrical field such as that existing around a negatively charged clay particle, water molecules are oriented so that their positively charged side is towards the negatively charged clay mineral. This orientation effect on the water molecules occurs only up to a few water-molecule diameters away from the clay surface. Hence, only a thin water layer a few molecules thick is hydrated to the clay mineral surface (Van Olphen, 1977).

Water is also hydrated to the exchangeable cations located on the clay mineral surface. The exchangeable cation becomes much larger once hydrated. The radius of a hydrated sodium ion is 7.8 Angstroms compared to only 0.98 Angstroms for the unhydrated form. The hydrated sodium ions are too large to fit onto the surface of the clay mineral, and are forced to move away to points of equilibrium (Lambe and Whitman, 1979).

The distribution of cations close to the clay surface after hydration is conceptually shown in Figure 2.1. This distribution is caused by electrostatic forces which tend to attract cations to and repel anions from the negatively charged clay surfaces, and a diffusion process which tends to diffuse cations away from each other to points of lower concentration. This distribution of cations and the surface of the clay mineral is often called the diffuse double layer. Some authors call it also diffuse-ion-layer (Yong, Mohamed and Warkentin, 1992). The interaction between a negatively charged soil particle surface and the cations in the soil-water will generate an electric double layer.

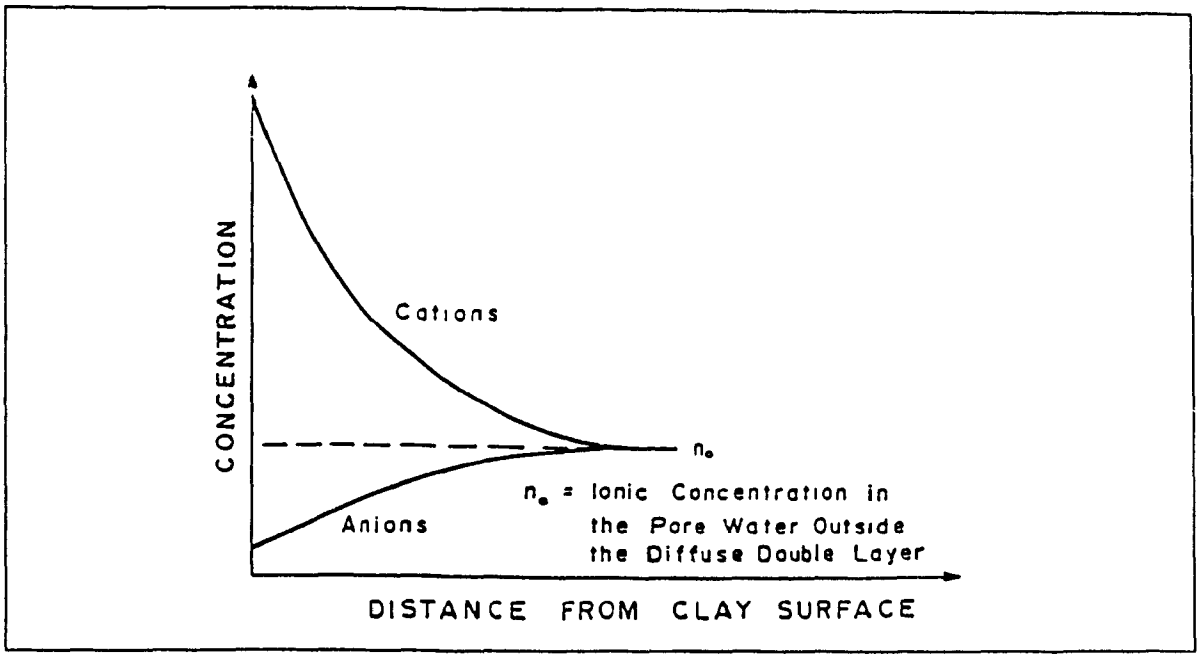

Figure 2.1 Distribution of Cations in the Diffuse Double Layer

2.4.2 Chemical Osmosis

Chemical osmosis is the flow of water caused by salt concentration gradients (Mitchell, 1976). When a semi-permeable membrane such as a clay soil separates two liquids with different salt concentrations, both water and salt move across the membrane in an attempt to equalize concentrations. Water molecules tend to move from the low concentration to the high, while salt molecules tend to move from high concentration to low. However, the movement of water molecules through a clay is much more efficient than the movement of salt molecules. Thus, the net effect of chemical osmosis is the flow of water through the soil from low concentration to high concentration. When this flow is prohibited a pressure is developed known as osmotic pressure. This pressure is referred hereto as swelling pressure.

2.4.3 Gouy-Chapman Theory

The Gouy-Chapman theory considers a negatively charged plate of counter-ion and co-ions and is discribed by the following equations:

The Poisson Equation

$$\frac{d^2\psi}{dX^2} = \frac{4\pi\sigma}{\varepsilon} \tag{2.4}$$

and

The Boltzmann Equation

$$N_i = N_o \, exp\left(\frac{-W_i}{BT}\right) \tag{2.5}$$

with

$$W_i = Z_i \, e \, \psi_i \tag{2.6}$$

where

ε = Dielectric constant,

e = electronic charge,

B = Boltzmann constant,

N_i = the concentration of ions of species i at a point where the potential is ψ_i,

T = the absolute temperature,

W_i=work done in bringing an ion to point where the potential is ψ_i,

X = distance from particle surface,

Z_i = ionic valence,

σ = surface charge density and

ψ = electrical potential.

Equation (2.6) shows the relationship between the electric potential and the distance from the particle surface. From Equation (2.5), the local concentration of ions at a distance x from the particle surface can be written as a function of the electric potential.

According to double layer theory, the swelling of clays is due to the osmotic pressure arising from concentration difference between the mid-plane of adjacent particles and the bulk solution. Assuming ideal behavior of the ions and neglecting the attractive forces between the particles, the osmotic pressure can be quantified by the Van't Hoff equation (Schofield, 1946) which states:

$$P = R\,T\,(N_i - N_O) \tag{2.7}$$

in which P denotes the osmotic pressure and R is gas constant. Substituting Equations (2.5) and (2.6) into Equation (2.7) and considering both anions and cations of a symmetrical electrolyte, it becomes

$$P = 2\,R\,T\,N_o\,(\cosh\frac{Z\,e\,\psi_c}{B\,T} - 1) \tag{2.8}$$

From this equation, the factors influencing the osmotic or swelling pressure are concentrations of electrolyte solution, valence of ions, electric potential, electric charge and absolute temperature, provided that the Gouy-Chapman theory is valid. The swelling pressure can be calculated by (see Appendix B)

$$P = R\,T\,(\frac{\pi^2}{\beta\,Z_i^2\,(X_d + X_o)^2} - 2\,N_o) \tag{2.9}$$

where

$$X_o = \frac{\varepsilon BT}{2\pi Z_i e \sigma}, \qquad \beta = \frac{8\pi e^2}{\varepsilon BT},$$

σ is the surface charge density of the clay and

X_O is a constant depending on the valence of the exchangeable ions and the charge density on the clay particles (it varies from 1 to 4 A^O and is approximately equal to 4 A^O for Na-montmorillonite according to Yong et al.,1959).

Based on parallel arrangement of clay particles the relationship between water content, W, and half distance between particles, X_d in A^O is given by (Yong and Warkentin, 1975)

$$W = \frac{SX_d}{100} \tag{2.10}$$

in which W = water content in wt., % and

S = specific surface area of clay per unit mass, m^2/g.

These calculations adequately predict the measured swelling pressures for the high-swelling Na-montmorillonite at low salt concentrations as shown in Figure 2.2. The measured pressures of Na-montmorillonite exceed the calculated values at higher salt concentrations. They probably result from the errors in using concentrations rather than activities of the exchangeable cations, and from neglecting the tactoid structure.

The thickness of the diffuse double layer for small concentrations of clay minerals in water is described by the Gouy-Chapman Theory and is given by Equation (2.11)

$$THICKNESS = \sqrt{\frac{\varepsilon BT}{8\pi N_o e^2 Z^2}} \tag{2.11}$$

In this expression, thickness is described as the distance from the clay surface to the centre of gravity of the charge distribution.

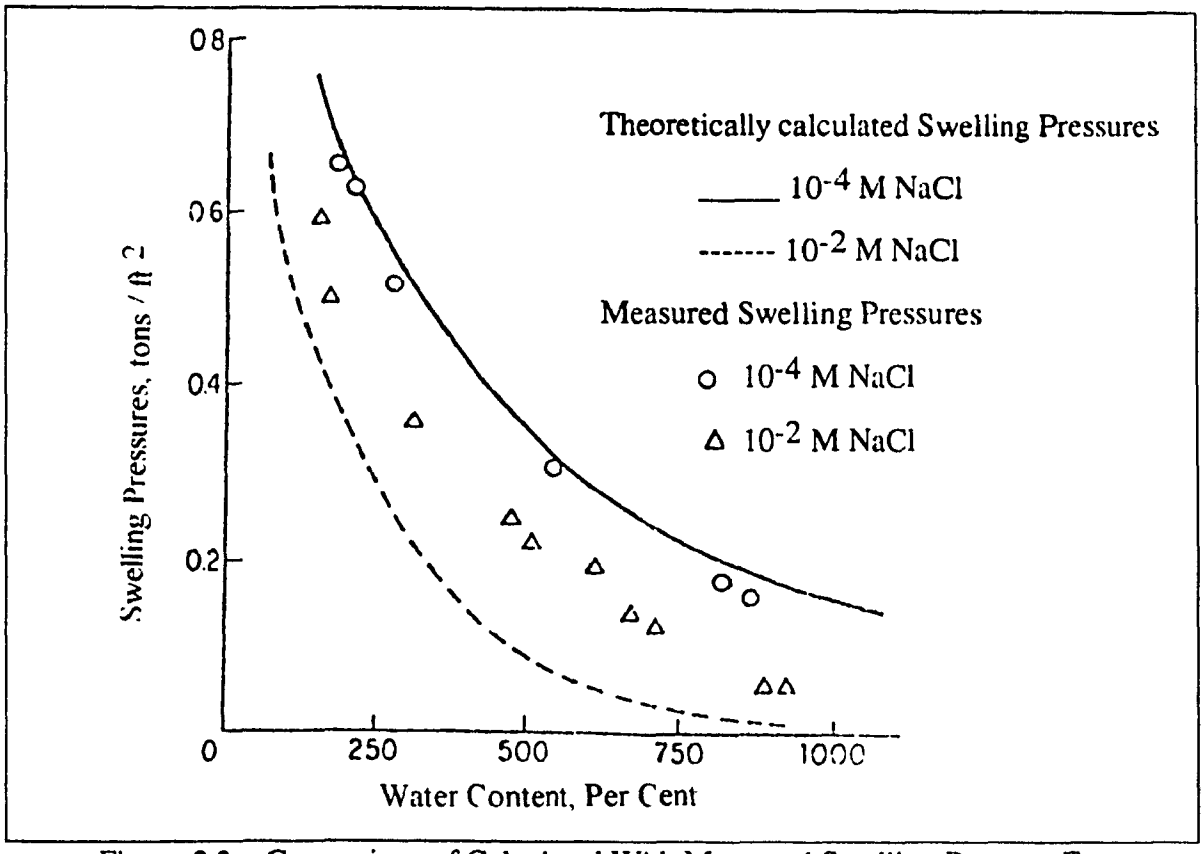

Figure 2.2 Comparison of Calculated With Measured Swelling Pressure For Sodium Montmorillonite at Two Salt Concentrations

The Gouy - Chapman Theory describes how the diffuse double layer is compressed or extended with changes in the physical and chemical environment. Examples of the change in thickness of the diffuse double layer is shown in Table 2.1. It can be seen that the type of exchangeable cation and the ionic concentration are important factors affecting the thickness of the diffuse double layer. A change in the exchangeable cation from the sodium to calcium reduces the thickness of the diffuse double layer by one half, while an increase in the ionic concentration by 2 orders of magnitude decreases the thickness of the

diffuse double layer by one order of magnitude. It should also be noted that in Table 2.1 an increase in temperature theoretically causes the diffuse double layer to decrease in thickness, while a simple examination of Equation (2.11) will indicate that it should increase. This anomoly is caused by the decrease in dielectric constant with an increase in temperature (Appendix A).

Table 2.1 Effects of Changes in Physical / Chemical Environment on the Thickness of the Diffuse Double Layer

Exchangeable Cation	*Temperature (°C)*	*Concentration*	*Thickness A°*
Na	10	0.0001 M NaCl	307.2
Na	20	0.0001 M NaCl	305.3
Na	30	0.0001 M NaCl	303.3
Na	20	0.001 M NaCl	96.5
Na	20	0.01 M NaCl	30.5
Ca	10	0.0001 M $CaCl_2$	153.6
Ca	20	0.0001 M $CaCl_2$	152.6
Ca	30	0.0001 M $CaCl_2$	151.6
Ca	20	0.001 M $CaCl_2$	48.3
Ca	20	0.01 M $CaCl_2$	15.3

The thickness of the diffuse double layer around a clay particle has a significant effect on the permeability of a fine-grained soil. It is generally felt that an increase in the thickness of the diffuse double layer stops or impedes the flow of the water past the clay minerals. It is also generally held that the viscosity of this water near the clay surface is high and decreases with distance from the clay surface until it is the same as the pore fluid.

2.5 Factors Affecting Hydraulic Conductivity

The factors affecting hydraulic conductivity can be subdivided into three areas;

i) the properties of the soil particles,

ii) the properties of the permeant, and

iii) the properties of the soil mass.

The properties of the soil particles which affect hydraulic conductivity include the type of clay mineral, as well as the type of adsorbed cation which is present in the diffuse double layer. The permeant affects the hydraulic conductivity directly through the viscosity and density, and indirectly through the changes in the diffuse double layer surrounding the clay particles. Lastly, the soil mass affects hydraulic conductivity through the structure of the soil particles. This structure is also known as the soil fabric and is used to describe the arrangement of soil particles, particle groups, and the pore spaces in a soil.

2.5.1 Properties of the soil Particles

The hydraulic conductivity of a soil is strongly influenced by the properties of its particles, such as the type of adsorbed cation. Variation in these properties may result in many orders of magnitude change in hydraulic conductivity.

Lambe (1954) reported that the hydraulic conductivity of various clay minerals decreased in the following order:

Kaolinite > Attapulgite > Montmorillonite

Mesri and Olson (1971) tested slightly different types of clay minerals and found the following order for the hydraulic conductivity:

Kaolinite > Illite > Montmorillonite

In general, the data by both Lambe (1954), and Mesri and Olson (1971) indicates that there is from 2 to 3 orders of magnitude difference in the hydraulic conductivities of kaolinite, and attapulgite or illite; and from 2 to 3 orders of magnitude difference in the hydraulic conductivities of attapulgite or illite, and montmorillonite.

Lambe (1954) also reported that the hydraulic conductivity of the various ionic forms of the clay minerals decreased in the following order:

Ca > Mg > K > Na

Rolfe and Aylmore (1977) indicated that at low electrolyte concentrations the hydraulic conductivity of the various ionic forms decreased as follows:

Cs > La > Ba > Ca > Na

The decrease in hydraulic conductivity as the adsorbed cation is changed to sodium is substantial. Lambe (1954) indicated that at a void ratio of 7, the ratio of hydraulic conductivities of sodium montmorillonite to that of calcium montmorillonite was about 1:300. A much less reduction in hydraulic conductivity was reported when attapulgite and kaolinite were considered. In addition, Harris (1931) reported that there was almost a two order of magnitude decrease in hydraulic conductivity in a heavy, calcarous, alkali soil as the adsorbed calcium was replaced by sodium.

Thus, the hydraulic conductivity of a soil can be altered by a change in the clay mineral or adsorbed cation. Of these, changes in the clay mineral is the most critical with possible alterations in the hydraulic conductivity of 4 to 6 orders of magnitude as the clay mineral is changed from kaolinite to montmorillonite. In comparison, a change in adsorbed cation from calcium to sodium alters the hydraulic conductivity from one (1) to two (2) orders of magnitude. The lowest hydraulic conductivity is achieved when the clay mineral is montmorillonite, and the adsorbed cation is sodium.

2.3.2 Properties of the Permeant

The viscosity μ and density γ_w of the permeant are factors which directly affect the hydraulic conductivity of a soil. The expression showing this relationship is given by Equation (2.12).

$$K = \frac{k \gamma_w g}{\mu} \tag{2.12}$$

where γ_w is the water density,

g is the acceleration due to gravity,

μ is the permeant viscosity and

k is the permeability.

Both the viscosity and density of a permeant in Equation (2.12) are a function of temperature and pressure (Dorsey, 1968; and Fredlund, 1973); of these, the most important relationship affecting hydraulic conductivity is the variation of viscosity with

temperature. Data presented in Appendix A show that an increase in temperature from 10°C to 20°C decreases the viscosity of water by 23 percent while only decreasing density by 0.15 percent. They also show that a large increase in pressure of 10 atmospheres increases both density and viscosity by less than 0.12 percent. The combined effect of this temperature and pressure change increases hydraulic conductivity approximately 29 percent. This change is due almost entirely to the variation in viscosity with temperature.

The hydraulic conductivity of a soil is also affected indirectly by the type of permeant which surrounds the clay mineral. A permeant which produces thick diffuse double layers results in a low hydraulic conductivity because of the constricting of flow paths. Conversly, a permeant which produces thin diffuse double layers results in high hydraulic conductivity. Thus, permeants with low ionic concentration, low ionic valency, and/or high dielectric constant results in lower hydraulic conductivities than permeants with high ionic concentration, high ionic valency, and/or low dielectric constant. Kinsky, Frydman and Zaslavsky (1971) studied the effect of liquids with different dielectric constants on the hydraulic conductivity of an initially dry soil. In their experiments, bentonite was compacted dry to a density of 1.5 Mg/m3 and then permeated with fluids varying from formamide (with a dielectric constant of 109) to pure dioxane (with a dielectric constant of 2.2). The resulting hydraulic conductivities are summarized in Table 2.2. As shown, the hydraulic conductivity can be increased by several orders of magnitude with decreasing dielectric constant of the liquid. Kinsky, Frydman and Zaslavsky (1971) also found that the changes in the hydraulic conductivity of a soil caused by treatment with various liquids may not be completely or readily reversed.

Table 2.2 Results of Permeability Tests Performed with Different Liquids on a Bentonite Soil Data after Kinsky, Frydman and Zazlavsky, 1971)

Liquid	*Dielectric Constant*	*Hydraulic Conductivity, cm/s*
Dioxane 100%	2.2	1.00×10^{-4}
Dioxane 10%	41.0	9.10×10^{-6}
Dioxane 5%	70.0	3.10×10^{-6}
Dioxane 3%	74.0	9.10×10^{-7}
Dioxane 1%	78.0	5.10×10^{-7}
Ethanol	24.3	2.10×10^{-7}
Dimethylsulphoxide	48.9	4.10×10^{-7}
Water	80.0	3.10×10^{-8}
Formamide	109.0	3.10×10^{-8}

Mesri and Olson (1971) also studied the effects of various liquids on the hydraulic conductivity of a soil. Their studies looked at the effect of dielectric constant and dipole moment on the hydraulic conductivity of kaolinite, illite and montmorillonite (Table 2.3). They found that for all types of clay minerals the hydraulic conductivity was lowest for liquids with high dielectric constants and dipole moments (i.e. water), and highest for liquids with low dielectric constants and dipole moments (i.e. carbontetrachloride and benzene). They also found that montmorillonite was the most sensitive of the clay minerals to changes in permeant. It had a five and one-half order of magnitude increase in hydraulic conductivity when the permeant was changed from a solution of NaCl to a solution of carbontetrachloride and benzene. The corresponding increase in hydraulic conductivity for illite and kaolinite was three orders of magnitude and a factor of 3, respectively.

Table 2.3 Hydraulic Conductivity of Various Clay Minerals at a Void Ratio of 2. (Data after Mesri and Olsen, 1971)

Fluid	*Kaolinite, cm/s*	*Illite, cm/s*	*Montmorillonite cm/s*
Water (NaCl)	1.4×10^{-6}	2.0×10^{-9}	8.0×10^{-12}
Water ($CaCl_2$)	4.0×10^{-6}	1.0×10^{-8}	6.0×10^{-10}
Ethyl Alcohol	4.0×10^{-6}	4.0×10^{-7}	6.0×10^{-8}
Methyl Alcohol			
Carbon TetraChloride	4.3×10^{-6}	4.3×10^{-6}	4.3×10^{-6}

Thus, the most important properties of the permeant in evaluating hydraulic conductivity are viscosity and density (i.e. direct factors), and the effect of permeant's chemistry on the thickness of the diffuse double layer (i.e. indirect factors). However, the most important of these are the indirect properties since they may change the hydraulic conductivity by up to six orders of magnitude. Variation in hydraulic conductivity due to temperature related viscosity effects is the most important of the direct factors. It may change the hydraulic conductivity by up to 30 percent over a change in temperature of $10^{o}C$.

2.5.3 Properties of the Soil Mass

The property of the soil mass which has the greatest effect on hydraulic conductivity is the structure of the clay particles, or soil fabric. The arrangement of soil particles, particle groups, and pore spaces determines the configuration of the flow paths by which a permeant must pass through the soil. There is a wide possible variation in the fabric of a clay soil as shown with the idealized structures shown in Figure 2.3. An open structure with large pore spaces allows free passage of a permeant and results in a high hydraulic conductivity. Another consideration in the structure and fabric of clay soils is the nature and magnitude of forces originating from the soil particles and fabric units, and between soil and permeant.

The pores between fabric units are defined as macropores, and the pore spaces between particles within the fabric units as micropores. Soil behaviour in relation to permeant flow, requires a knowledge of characteristics of permeant movement in the macro and micropores and also the rearrangement of fabric units and distortion of individual units. The movement of permeant in macropores and micropores will be controlled by different sets of forces and conditions. Overall hydraulic conductivity will

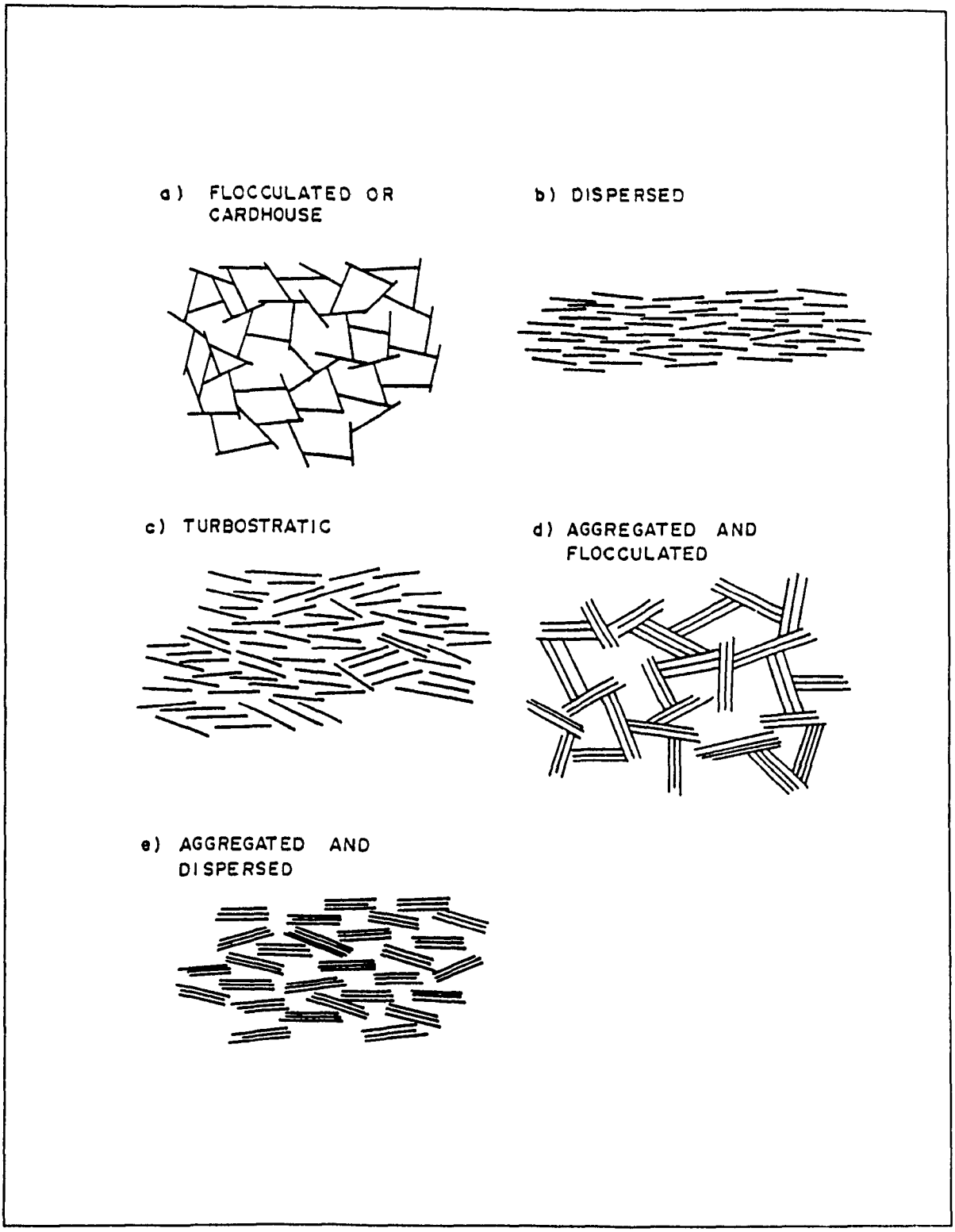

Figure 2.3 Idealized Clay Structure

reflect the average value of hydraulic conductivity through physical testing which in fact is due to two seperate physical phenomena of permeant flow through macro and micropores.

The most important aspect of clay structure on hydraulic conductivity is the distribution of pore sizes. Lambe (1932) showed theoretically that the hydraulic conductivity of a soil was proportional to the square of the diameter of the flow channels. Therefore, two soil samples of similar composition and void ratio do not necessarily have the same hydraulic conductivity. A soil with a few large pores could have a greater hydraulic conductivity than the same soil with numerous smaller pores.

The variation in the distribution of pore spaces in clay soils is a function of many factors. Two major factors are: 1) the moisture content in the soil at the time of compaction, and 2) the method of compaction. Lambe (1954) showed that the hydraulic conductivity of a compacted soil (in Figure 2.4) was a function of the molding moisture content. He also found that the minimum hydraulic conductivity was achieved when the soil was compacted at, or slightly above the optimum moisture content. Mitchell, et al. (1965), and Dunn and Mitchell (1984) showed that at the same level of effort, different methods of compaction could have significant effects on hydraulic conductivity. Mitchell, et al (1965) showed that when the soil was compacted dry of optimum moisture content, there was little effect on hydraulic conductivity. However, when the soil was compacted wet of optimum, the method of compaction was very important. Wet of optimum, the highest hydraulic conductivity was achieved when the static method of compaction was used. Both Mitchell et al (1965) and Dunn and Mitchell (1984) found that there could be as much as one order of magnitude difference in hydraulic conductivity with these methods of compaction. Benson and Daniel (1990) found that the hydraulic conductivity of a highly plastic, compacted clay soil is significantly influenced by the size of clods used in preparing the soil for compaction. For soil compacted dry of optimum, hydraulic conductivity is 1,000,000 times smaller when the soil is prepared from small (4.6 mm)

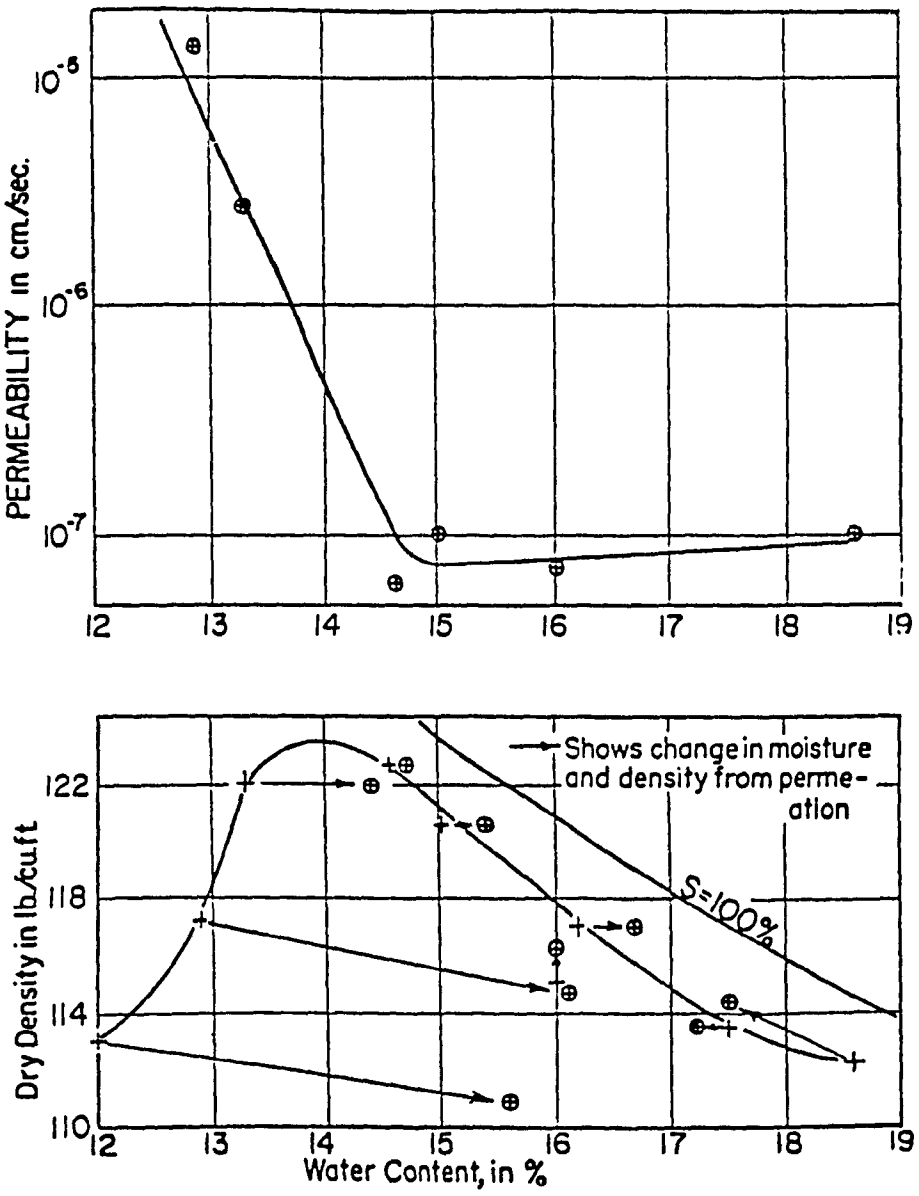

Figure 2.4 Effect of Molding Moisture Content and Proctor Density on the Hydraulic Conductivity (After Lambe, 1954)

rather than large (19 mm) clods. For soil compacted wet of optimum clod size is unimportant.

Results from Yang and Barbour (1991) reveal that the alteration of hydraulic conductivity is strongly related to the initial soil and the level of confining stress. They observed no significant change in the microfabric of the clay; however, the size of inter-aggregate pores appeared to increase as a result of the physico-chemical volume change that occurred during brine permeation.

Two theories have been proposed to account for the variation in hydraulic conductivity with moisture content. Both of these theories explain the variation in hydraulic conductivity in terms of clay structure; one theory uses microstructure and the other uses macrostructure. Lambe (1958a,b), theorized that the relationship shown in Figure 2.4 was the result of the microstructure of the clay particles. It was proposed that soils compacted dry of optimum moisture content had a random orientation of the clay particles (i.e. flocculated structure). This led to large individual pores which resulted in large hydraulic conductivities. Soils compacted wet of optimum were theorized to have more parallel arrangement of the soil particles (i.e. dispersed structure). This led to small individual pores and a lower hydraulic conductivity.

Olsen (1962), proposed that a compacted soil consisted of clusters of soil particles. At high void ratios the majority of flow occurred in the large voids between the soil clusters; very little flow actually occurred through clusters. As the soil was compressed, the large voids were closed and consequently more flow took place within clusters in the smaller voids between the soil particles.

The work conducted to date clearly shows that hydraulic conductivity is a function of the size and distribution of pore spaces in the soil. The size and frequency of larger pore spaces can be reduced by compacting the soil at a moisture content which is wet of

optimum and by using an impact type of compaction. This can significantly lower the hydraulic conductivity of the compacted soil.

2.6 Kozeny-Carmen Relationship

A widely used equation for the prediction of permeability k, in saturated porous media, was proposed by Kozeny (1927) and later modified by Carmen (1937, 1956). The resulting equation is known under the name Kozeny-Carmen equation, although the two scientists never published together (Derivation in Appendix B) and is given by

$$k = n_w^3/m \, . \, \tau^{\,2} \, . \, S_o^2 \, . \, n_s^2$$

where

n_w is the fractional volume of liquid,

m is the pore-shape factor,

τ is the tortuosity,

S_o is the specific surface area of the solids per unit volume,

n_s is the fractional volume of solids ($n_s = 1 - n_w$).

The values of m and τ are approximately 2.5 and 1.41 respectively (Yong and Warkentin,1975)

The principal assumptions in this equation are;

- Darcy's law is valid,
- Viscous flow obeys Poiseuille's law,
- The tortuosity of the flow channels is a constant and
- The flow channels or pores are equal in size.

The Kozeny-Carmen equation has been found to work well in the case of many sands, however it is inadequate in the case of clays. It fails to predict the magnitudes and the porosity dependencies of hydraulic flow rates, as well as to account for their dependence on the chemical compositions of the clay and the permeant.

Olsen (1962) compared the experimental values of flow rates with those predicted by the equation in Figure 2.5. The predicted flow rates per unit gradient were based on the specific surface area values for each clay obtained from nitrogen adsorption and glycol retention measurements. The ratio of measured to predicted flow rate is shown to depend on porosity, clay type, and the chemical compositions of the clay and the permeant.

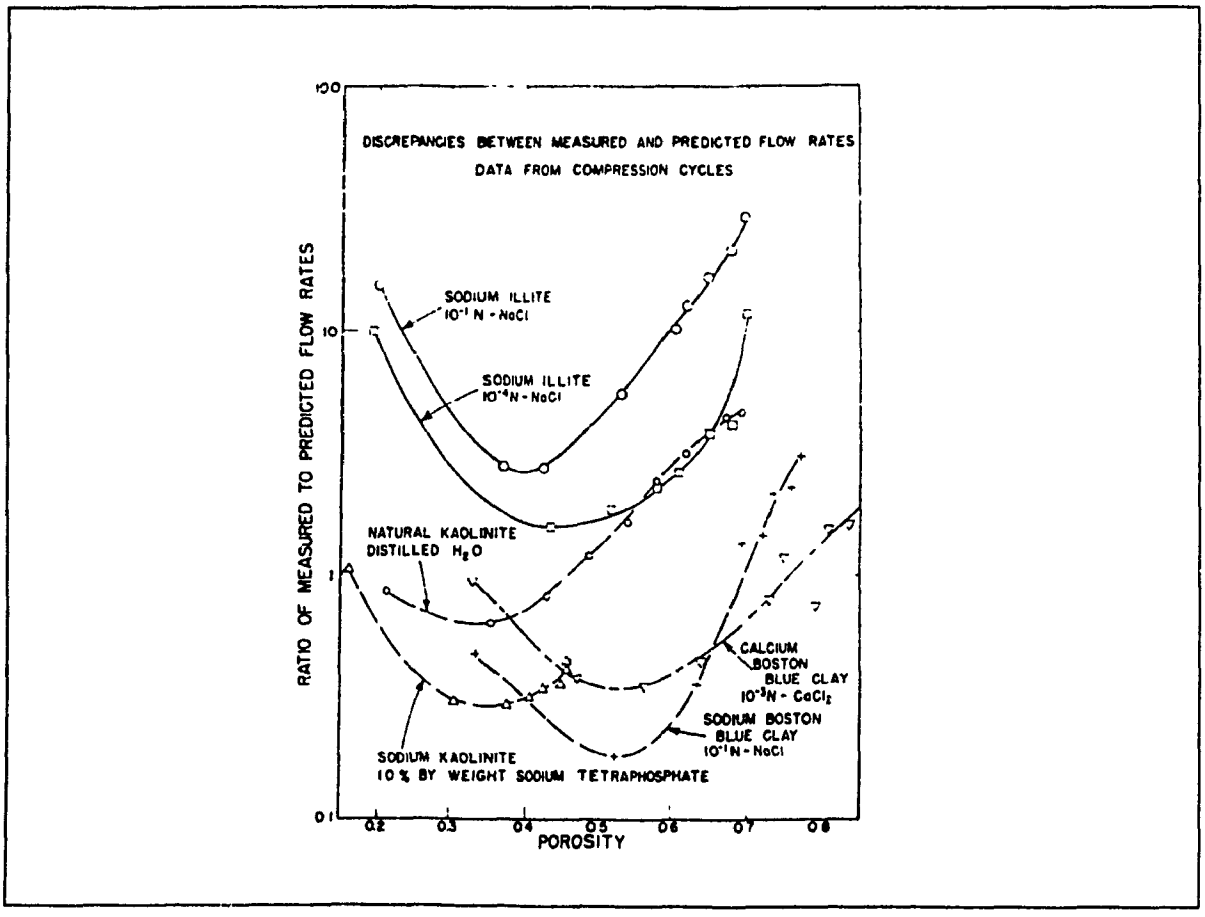

Figure 2.5 Discrepancies between measured and predicted flow rates (Olsen, 1962)

According to Olsen (1962), the major factor responsible for failure of the equation in fine grained soils is ascribed to the nonuniform pore size distribution. Olsen (1962) also concluded that the hydraulic conductivity is mainly controlled by the percentage of fine particles in soil. A small percentage of fines can clog the pores of an otherwise coarse material and result in manyfold lower hydraulic conductivity.

According to Chapuis and Montour (1992) ther could be experimental reasons such as; unprecise specific surface area, unsaturated soil samples and temperatures different than 20 ^{o}C. It might also have theoretical reasons such as; immobile water attached on the clay surface.

2.7 Effect of Hydraulic Gradient

The general law governing the flow of fluids through porous media (Darcy's Law, Figure 2.6a) states that there is a linear relationship between the rate of flow through a soil and hydraulic gradient. While this is generally considered valid, deviations from this law have been documented by many researchers. It has been found that the rate of flow through a soil may not be proportional to the gradient, and that the resulting hydraulic conductivity may increase or decrease as the applied gradient changes. The most common of the reported deviations are shown in Figure 2.6b to d.

Deviations at low gradients as shown in Figure 2.6b have been found by many researchers including von Engelhart and Tunn (1955), Hansbo (1960), Mitchell and Younger (1967), Younger and Lim (1972) and Kharaka and Smalley (1976). Generally, the hydraulic conductivity increased non-linearly with gradient until some specific gradient was reached. After this point, the hydraulic conductivity no longer deviated from Darcy's Law. The gradient at which deviations no longer occured varied considerably.

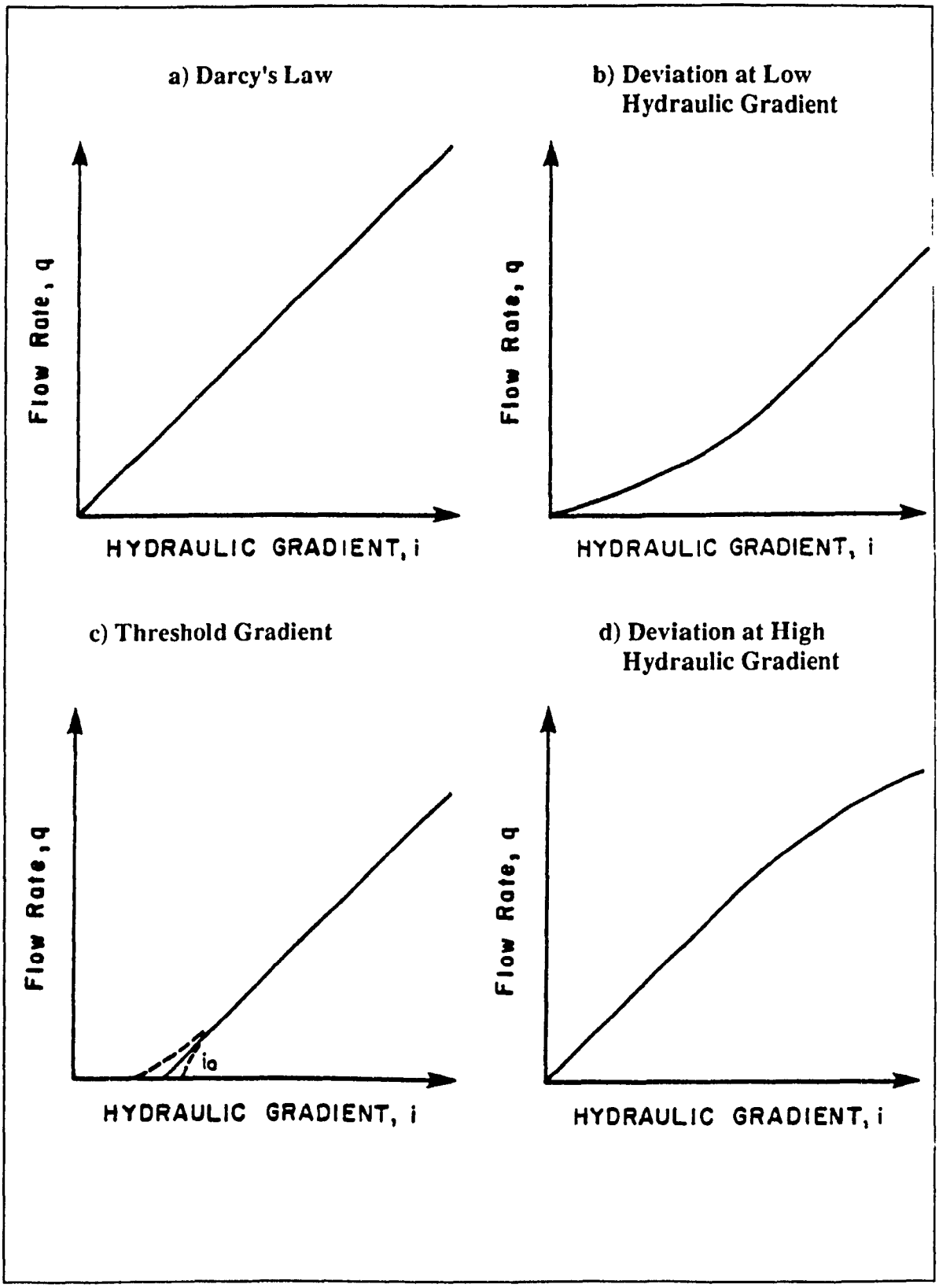

Figure 2.6 Darcy's Law and Some of the Deviations From Darcy's Law

Von Engelhardt and Tunn (1955) reported deviations up to gradients of 170, while Lutz and Kemper (1959) reported them up to gradients of 900, and Mitchell and Younger (1967) indicated them up to gradients of 16. As well, Younger and Lim (1972) found complex deviations below a gradient of 12, though it should be noted that the maximum applied gradient was also 12. These deviations could be due to type of clay mineral, type of permeant and concentration of electrolyte.

A number of researchers including Miller and Low (1963), Law and Lee (1981), have reported that flow through soil did not begin until a critical or threshold hydraulic gradient was reached (Figure 2.6c). Miller and Low (1963) found threshold gradients varied that from 10 to 50, and that the threshold gradient decreased with decreasing clay content and increasing temperature. Law and Lee (1981) reported threshold gradients that varied from 0.09 to 2.93. Foreman and Daniel (1986) found a threshold hydraulic gradient below which the hydraulic conductivity of heptane was zero. The results of their study show also order-of-magnitude differences in hydraulic conductivity depending on testing apparatus and procedures. However, many researchers have not been able to find threshold gradients in their test programs (Olsen, 1965; Mitchell and Younger, 1967). As well, it should be noted that Matyas (1967) indicated that if the soil is completely saturated there is no evidence of a threshold gradient and Darcy's Law is completely obeyed. Deviations at high gradients, as shown in Figure 2.6d, indicates that the hydraulic conductivity decreases as the gradient increases. This has been reported by Lutz and Kamper (1959), Olsen (1962), and Miller and Low (1963). This type of deviation could be as a result of clogging of the pores due to particle migration.

Complex deviations have been reported in addition to those shown in Figure 2.6. Kutilek (1972) has summarized the many forms of deviations found in the literature and along with Mitchell and Younger (1967) and Younger and Lim (1972) have indicated that

the exact deviation may depend upon whether the test is performed with the hydraulic gradient increasing or decreasing.

Many reasons have been proposed to explain the deviations from Darcy's Law. These include quasi-crystalline water, electrokinetic coupling, consolidation, mobility of fines, experimental error and turbulent flow.

The effect of quasi-crystalline water on hydraulic conductivity has been discussed by Von Engelhardt and Tunn (1955), Lutz and Kemper (1959), Hansbo (1960), and Miller and Low (1963). A rigid or more viscous structure is induced upon the water in the diffuse double layer by the clay-water interaction and a finite energy is required to break down this structure. Quasi-crystalline water would produce the deviations shown in Figure 2.6b, and 2.6c. However, Olsen (1962) performed an analysis using this concept and concluded that high viscosity could not account for any discrepancies found in his studies.

Electrokinetic coupling, referred to as electro-osmotic counter flow, is the interaction which occurs between the electrical and viscous flow. Adsorbed cations in the diffuse double layer exert a resistance to flow that decreases as the gradient increases (Kemper, 1960; Swartzendruber, 1966, 1967). Electrokinetic coupling would produce the deviations shown in Figure 2.6b. However, Micheals and Lin (1954), Hansbo (1960), and Miller et al. (1969) have concluded that such effects are insignificant and cannot begin to account for the reported deviations.

Consolidation as a cause of deviations from Darcy's Law has been proposed by Olsen (1962) and Kutilek (1972). A rising gradient causes the porosity of the soil to decrease and results in the deviation shown in Figure 2.6d.

Mobility of the fines in a soil sample has also been used to explain changes in hydraulic conductivity (Bodman, 1937; Younger and Lim, 1972; Hansbo, 1960, 1973; Hardcastle and Mitchell, 1974; Chen and Banin, 1975; Frenkel and Rhoades, 1978; and others). This theory suggests that clay particles may be stripped from the sides of flow paths by the movement of water and this may cause an increase in the size of the flow

paths. This in turn may cause an increase in hydraulic conductivity. As well, the stripped clay particles may block flow paths downstream and cause a decrease in hydraulic conductivity. Mitchell and Younger (1967) considered many possible discrepancies in their tests and concluded that particle migration was the most likely cause. They also indicated that fewer particles were available for movement, and less pore spaces were available for particles to migrate through, as the density of the soil increased. As well, Hansbo (1960, 1973) reported that scanning electron microscope studies showed that many fine particles do not have a load carrying function and that an increase or reversal in the gradient can cause movement of these fines.

Experimental error as a reason for discrepancies from Darcy's Law has been considered by Olsen (1965), Mitchell and Younger (1967) and Kutilek (1972). Olsen (1965) showed that atmospheric contamination in the conventional use of air-water menisci and air bubbles in capillary tubes for measuring flow rates can cause the hydraulic gradient to increase by as much as 10. This error was of sufficient magnitude to account for many of the published deviations from Darcy's Law such as those reported by Hansbo (1960), and Miller and Low (1963). Kutilek (1972) reviewed many of the reported deviations from Darcy's Law and indicated that swelling of a soil, changing degree of saturation, consolidation and growth of bacteria may also be a source of error.

Darcy's Law is no longer valid once flow changes from laminar to turbulent. This occurs when the Reynold's number reaches some critical value between 0.1 and 75 (Lambe and Whitman, 1979). However, turbulent flow is a factor for sands and gravels only and needs not be considered for fine-grained soils.

Thus it is apparent that the hydraulic gradient applied to a soil sample during permeability testing may significantly affect permeability measurements. Changes in hydraulic conductivity with changes in gradient may occur and may be caused by factors normally beyond the direct control of the researcher such as quasi-crystalline water,

electrokinetic coupling, consolidation, and mobility of fines. However, they may also be caused by experimental error which is directly controlled by the researcher.

Table 2.4 The Influence of Density and Hydraulic Gradient on Hydraulic Conductivity of Illite and Na-Montmorillonite Systems (Literature results)

Density (Mg/m3)	Pore fluid	Hydraulic Gradient (i)	Hydraulic Conductivity (cm/s)
Illite (γ_d)			
1.42	DDW[t]	159	1.1×10^{-10}
	DDW	319	7.6×10^{-10}
1.52	Saline	60	1.6×10^{-9}
	DDW	320	8.3×10^{-10}
1.77	DDW	720	1.0×10^{-10}
	DDW	1 444	1.1×10^{-10}
2.07*	DDW	30	3.5×10^{-10}
	DDW	269	5.6×10^{-10}
Montmorillonite (γ_c)			
0.6**	DDW	3 000	6.1×10^{-9}
	Saline[tt]	3 000	7.0×10^{-8}
1.02	DDW	460	2.6×10^{-13}
		1 700	6.3×10^{-13}
1.12	DDW	1 550	4.5×10^{-14}
		3 100	1.6×10^{-12}
		> 3 100	3.1×10^{-13}
1.24	Saline	1 560	1.0×10^{-13}
	DDW	1 560	5.0×10^{-13}
	DDW	3 120	3.5×10^{-13}
	DDW	> 3 120	3.2×10^{-13}
1.42***	DDW	2 000	1.9×10^{-13}
		5 000 to 10 000	2.1×10^{-13}
1.43	DDW	1 700 to 3 400	1.8×10^{-13}
1.46	Saline	1 600 to 8 000	1.8×10^{-13}
1.50***	DDW	2 000	1.9×10^{-13}
1.80***	DDW	2 000	9.0×10^{-14}
		5 000 to 10 000	1.1×10^{-13}

* Radhakrishna & Chan, 1985
** Bucher et al., 1986
*** Pusch, 1980

t Distilled Deionized Water
tt Saline solution 70g/l TDS

Note: TDS is Total Dissolved Solids

Table 2.4 shows the values of hydraulic conductivities for selected mixtures containing montmorillonite or illite, measured under hydraulic gradients ranging from 30 to 10 000. These results show that hydraulic conductivity increases as the hydraulic gradient increased. The phenomenon of increasing hydraulic conductivity with increasing hydraulic gradient has been also shown to exist by Yong and Warkentin (1975) in clays

2.8 Summary

From the literature review we see the importance of surface forces in clay soils. These forces are explained by the diffuse double layer theory and the hydraulic conductivity of clay soils is affected by their interaction. Kozeny-Carmen equation does not take into account these surface forces, it only deals with surface area relating to pore sizes through porosity. It fails also to consider the structure of the clay soil. A model to include the effect of surface forces on the pore sizes determined from the Kozeny-Carmen relationship could be very useful in determining the hydraulic conductivity of clay soils

CHAPTER 3

MODEL DEVELOPMENT

3.1 Introduction

In this chapter, a theoretical model based on Kozeny-Carmen relationship and the Diffuse-ion-layer theory is developed. The model predicts qualitatively the environmental effects such as temperature, porewater chemistry, type of permeant, clay type, clay density and clay content on the permeability of clay soil.

3.2 The Model

The rate of water flow through a water-saturated porous medium is commonly described by Darcy's Law

$$q = K\,i \tag{3.1}$$

where q is the rate of water flow per unit area (cm/s), i is the hydraulic gradient across the material and K is the hydraulic conductivity (cm/s).

Conventionally, K is given by the equation

$$K = k\,\gamma_w\,g\,/\,\eta \tag{3.2}$$

where γ_w is the fluid density, g the acceleration due to gravity, η the fluid viscosity, and k (cm^2) the permeability which depends on the shape and size distribution of the pores.

Using n_w as the fractional volume of liquid, m as the pore shape factor, τ as the tortuosity, S_o as the specific surface area of the solids per unit volume, and n_s as the fractional volume of solids (= 1 - n_w), Kozeny and Carmen suggested that

$$k = n_w^3\,/\,m\,\tau^2\,S_o^2\,n_s^2 \tag{3.3}$$

where m and τ are approximately 2.5 and $2^{1/2}$, respectively (Yong and Warkentin, 1975). Because surface forces are not considered, the Kozeny - Carmen equation is generally satisfactory for sand. However, in clay soils, not all the water can be mobilized for flow: this is related to interparticle forces arising from the surface charge of clay particles. The fractional volume of potentially mobile water (free water), termed here as effective porosity, n_w', has to be substituted for n_w in Equation (3.3).

The interparticle forces arise mainly from the interaction of the diffuse double layers around clay plates, and may be considered to be osmotic in origin. The osmotic pressure, P_c, developed between two parallel plates can be calculated using the following equations (Yong & Warkentin, 1975),

$$P_c = RT(C_c - 2C_o), \tag{3.4}$$

$$C_c = \pi^2/Z^2\beta(X_d+X_o)^2\ 10^{-16}, \tag{3.5}$$

$$\beta = 8\pi e^2/\epsilon BT \quad \text{and} \tag{3.6}$$

$$X_o = \epsilon BT/2\pi Ze\sigma \tag{3.7}$$

where R is the gas constant, T the absolute temperature, C_o the electrolyte concentration in the free solution (water not influenced by the particle forces), C_c the electrolyte concentration at the midpoint between two parallel plates, Z the valence of the exchangeable cations, X_d (^oA) the half distance between two parallel plates, e the electronic charge, ϵ the dielectric constant, B the Boltzmann constant, σ the surface charge density.

From Equations (3.4) and (3.5), P_c is predicted to increase with increasing T or decreasing X_d and C_o. Good agreement between experimental and theoretical values of P_c, particularly for bentonite systems, has been found (Yong & Warkentin, 1975).

The forces holding water to the clay plates (P_c) will influence flow; the force driving flow (hydraulic gradient) must exceed P_c before water can be mobilized. If the hydraulic pressure, P_h, per unit length of the soil is less than or equal to P_c, all the water is immobilized, and no flow will occur. When P_h exceeds P_c, previously bound water flows, the rate of flow increasing with increasing P_h. The thickness of this immobilized layer of water (bound water) depends on the interparticle forces (P_c) and the hydraulic gradient.

The thickness of the immobilized water layer, X_i, adjacent to each clay platelet can be calculated from Equations (3.4) and (3.5) by substituting $X_d = X_i$ and $P_c = P_h$. The effective porosity, n_w', can be calculated for parallel arrangement of clay plates with uniform particle spacing using the following equations, (Yong and Warkentin, 1975)

$$n_w' = \gamma_c \, S \, X'_d / 10^6, \tag{3.8}$$

$$X'_d = X_d - X_i \quad \text{and} \tag{3.9}$$

$$X_d \, (\text{nm}) = (1/\gamma_c - 1/G_c) \, 10^6 / S \, \text{(Derived in Appendix B)} \tag{3.10}$$

where γ_c is the clay dry density (g/cm^3), S the specific surface area per unit mass of clay in m^2/kg and G_c the specific gravity of clay. In this analysis G_c is taken to be 2.65 and S of 800000, 85000 and 20000 m^2/Kg is used for Montmorillonite, Illitic and Kaolinitic clays respectively (Mitchell, 1976).

The model suggests that the permeability k depends on n_w', that in turn, depends on T, C_o, S, i, and γ_c. For soils with relatively limited interparticle forces, P_c, such as illite and kaolinite, K is principally dependent on γ_c. For soils with relatively high P_c, K may be expected to decrease with increasing S, T, and γ_c, or decreasing C_o and i. This is why threshold hydraulic gradients are found to exist in soils with high swelling pressure, P_c.

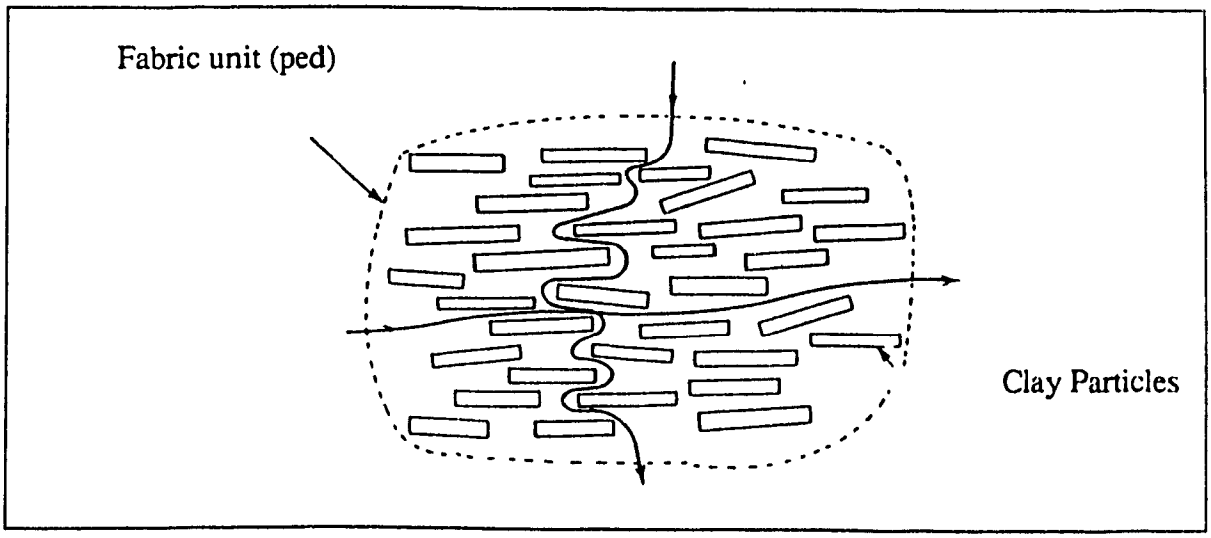

Figure 3.1 Clay Particles and Water Flow

One of the assumptions of the model is that the clay soil is completely (100%) saturated. The second is that the permeant flows through all the pores and around every single clay platelet. The third assumption is that flow channels are equidimensional and uniformly distributed throughout the soil. Another important assumption is the parallel arrangement of the clay particles.

3.3 Sand-clay Mixtures

The model has been developed for pure clay systems, but can be applied to sand-clay mixtures. Like pure clay, the permeability of sand-clay mixtures is controlled by the relative proportions of free and bound water. Compared with clays, sand has a very small specific surface area and surface charge density. Thus, in sand-clay mixtures, S for the mixture is almost directly attributable to the clay fraction. Other properties have also been found to be dictated by clay content (Cheung and Dixon, 1987). Separating the volume of sand in the mixture, the clay density,γ_c can be calculated from the percent of clay content and bulk dry density, γ_d. As an example, for a mixture of sand clay with 9 % Na-Bentonite (montmorillonite rich clay) and γ_d = 1.8 g/cm^3 (or Mg/m3) the procedure of calculation is as follow;

V = 1 cm^3

W solids = 1.8 x 1 = 1.8 g

W sand = 1.8 x 0.91 = 1.64 g

V sand = W sand / S. G. sand = 1.64 / 2.65 = 0.62 cm^3

V clay + water + voids (if not 100 % saturated) = 1 - 0.62 = 0.38 cm^3

W clay = 1.8-1.64 = 0.16 g

γ clay = W clay / V clay + water + voids = 0.16 / 0.38 = 0.42 g/cm^3

Once γ_c is calculated the procedure is the same as for pure clay. Table 3.1 shows an example for relationship between γ_d and γ_c for different clay percentages. One of the assumptions in this case is that sand is inert. The second is that clay particles cover uniformly all the surfaces of sand grains. Thus, all the flow is through the clay soil.

Table 3.1 The Relationship Between Sand Content and γ_c for montmorillonite

Sand Content %	75	60	50	25	0
Dry Density, γ_d (Mg/m3)	1.94	1.78	1.75	1.50	1.25
Clay Density, γ_c (Mg/m3)	1.07	1.19	1.31	1.31	1.25

Figure 3.2 shows that at a certain γ_d the value of γ_c varies depending on % of Bentonite (Montmorillonite rich clay) or clay content.

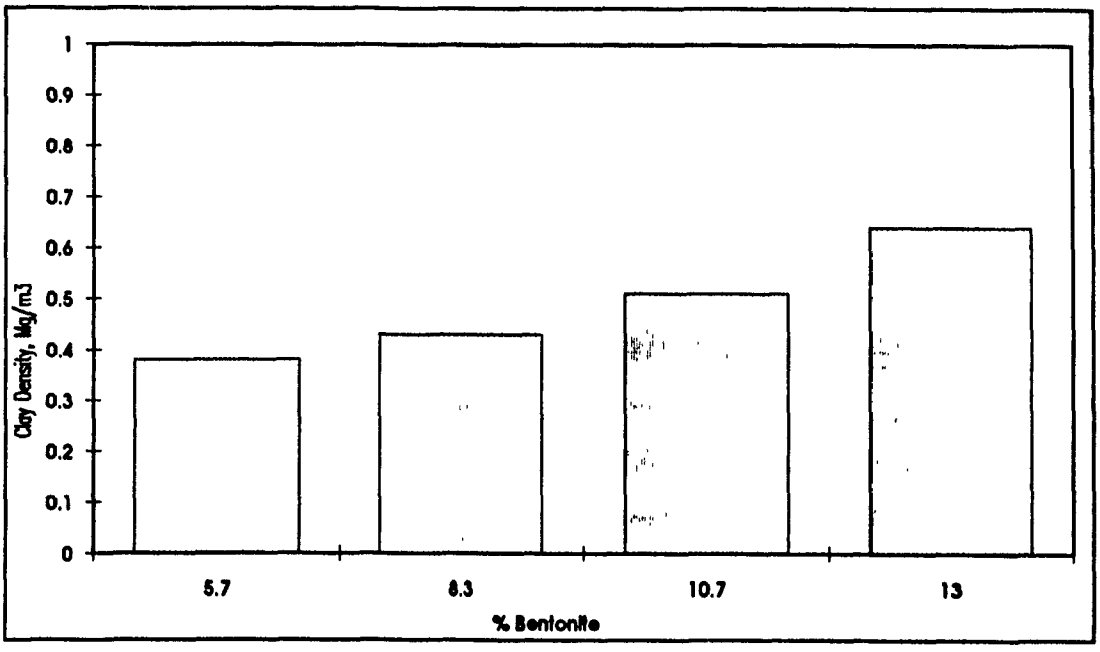

Figure 3.2 Variation of Clay Density with Precentage of Bentonite Content in Clay-Sand Mixtures

3.4 Highly Compacted Montmorillonite

A parallel arrangement of particles is unlikely in nature and some water will exist in large pores, and not be significantly affected by interparticle forces. This water is referred to as free water and can be easily mobilized for flow. The amount of this water is expected to depend mainly on γ_c, but also depends on soil fabric. The Stern water layer, x_o, is a layer of water molecules and associated cations that are very tightly bound to the clay surface, and would not, in practice, be influenced by i (or P_h). This is important for clays with high surface charge density and high specific surface area. For example, for montmorillonite clays, the Stern water layer is estimated to be 0.4nm. In parallel arrangement, plates < 0.8nm apart will not allow the passage of water. In a material with S = 800 m^2/g, G_c = 2.65 and a clay density (γ_c) of approximately 1.25 Mg/m^3 platelets have a calculated particle separation of 0.8nm. In such a system, a K of zero would be expected.

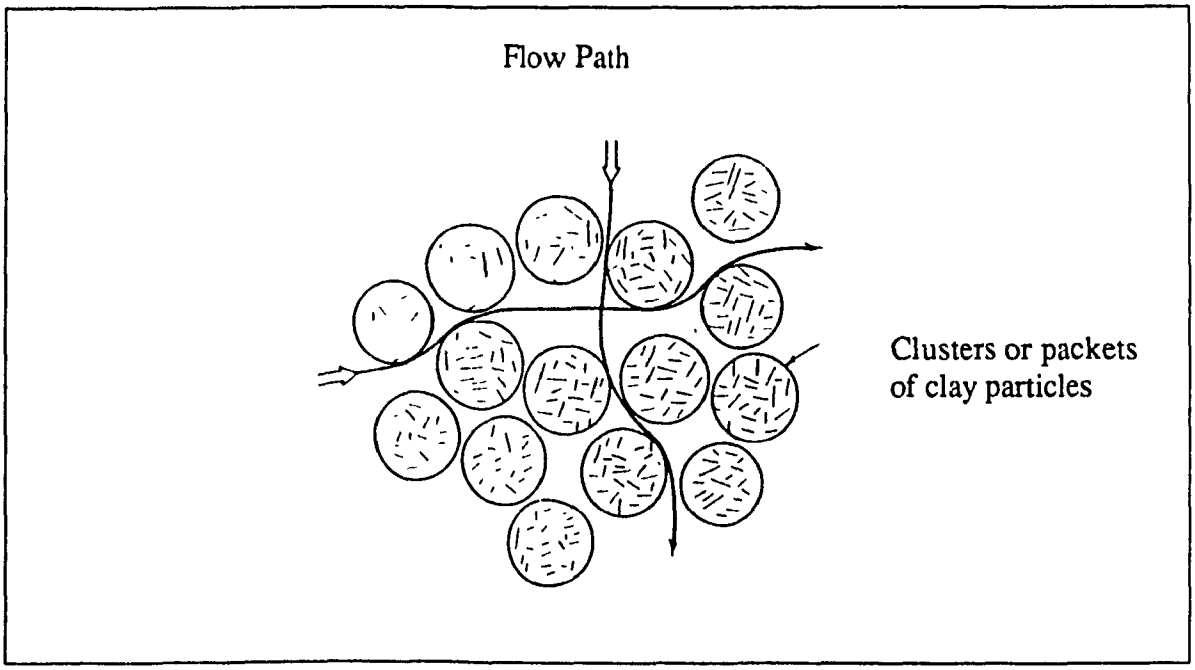

Figure 3.3 Flow through clusters or packets

Experimental K values are reported in the literature for $\gamma_c > 1.25$ Mg/m^3. This can be attributed to the soil fabric where clay platelets form clusters with interparticle distance less than 0.8 nm, thus forming macropores and allowing the passage of water through the soil around the clusters. The size and magnitude of the macropores depend on the number of particles and the interparticle distance in a cluster and depends upon soil system (dispersed, flocculated or, aggregated) and clay dry density γ_c.

In this case X_d is calculated based on Equation (3.10) by the following way,

$$X_d = (1/\gamma_c - 1/\gamma_{cc})\, 10^6 / S_e \qquad (3.11)$$

where

S_e is the effective cluster specific surface area per unit mass of clay in m^2/kg and

γ_{cc} the dry density of the cluster.

The dry density of the cluster γ_{cc} can be calculated from the following equation.

$$d_c = (1/\gamma_{cc} - 1/G_c)\, 10^6 / S \qquad (3.12)$$

where

d_c is the half distance between clay platelets in a cluster; it depends upon the number of hydrated water layers present between these platelets which depend upon clay dry density, γ_c. The calculated values of γ_{cc} are 2.1, 1.7 and 1.45 Mg/m^3 for one (d_c = 0.25/2 nm), two (d_c = 0.5/2 nm) and three (d_c = 0.75/2 nm) layers of hydrated water respectively. Giving priority to minimum number of platelets in a cluster and maximum number of hydrated layers such that; X_d will be greater than 0.4nm, one can calculate at different clay

densities the effective surface area (S_e), effective porosuty (n'_w) and consequently the hydraulic conductivity.

The effective surface area is calculated from the number of platelets in a cluster (Yong and Warkentin, 1975) by the following way. If montmorillonitic clay has ten particles per cluster, the surface area is reduced by ten times, neglecting the surface area of edges which is only a few per cent of the total. Only the two outer surfaces of the 20 particle surfaces are involved for the flow. Surface area measured by nitrogen absorption experiments could be also used as effective surface area. Some of these values are shown in Table 3.2.

Table 3.2 Effective Surface Area at Different Clay Densities and Number of Platelets

γ_c, Mg/m^3	γ_{cc}, Mg/m^3	Number of Platelets	S_e, m^2/kg
1.1	1.7	3	267000
1.3	1.7	4	200000
1.4	1.7	5	160000
1.9	2.1	12	67000

3.5 Model Variables

In this study the model was tested for three kinds of clay minerals. Montmorillonite with a surface area of 800 m^2/g, Illite, with a surface area of 85 m^2/g and kaolinite, with a surface area of 20 m^2/g. These three types of clay minerals were chosen because they are commonly found in the field, montmorillonite and kaolinite represent the two extremeties

of clay minerals in terms of surface area and surface forces activities while illite is midway between the two

Different environmental factors were considered like temperature, salinity, type of permeant and hydraulic gradient as well as other factors like clay density and clay content

The range of temperatures tested were between 20°C and 90°C This range of temperatures is likely to exist in different disposal facilities For example in chemical waste disposal the temperatures vary between 20-30°C and in high level nuclear waste disposal it could vary between 20-100°C (Hancox, 1986). Variation in salinities and type of permeant could be due to groundwater quality or due to the type of waste contained Since groundwater is dominated by Na, Ca and Cl; the types of permeants tested are NaCl and $CaCl_2$; in addition to two kinds of water soluble organic liquids The solution concentrations for NaCl varied between 0.01M and 6M (highly saline brine) to simulate groundwater. The two kinds of organic liquids are Ethanol and Dioxane

Hydraulic gradient could be varied due to the natural conditions present at the site and in the laboratory depends on the type of equipment used in the test The natural gradients are generally very low as compared to those used in the laboratory, a range of hydraulic gradient 200-2000 is considered basically to simulate laboratory conditions in studying the effect of hydraulic gradient on the hydraulic conductivity Density of clay could change due to overburden pressure Moreover, different densities and clay type could exist in the field and need to be examined to define the performance of the clay barrier. Since hydraulic conductivity is dictated by clay content, only the clay densities of 0.3 to 2.1 Mg/m^3 will be tested in the model.

CHAPTER 4

MODEL RESULTS

4.1 Introduction

In this chapter the variation of hydraulic conductivity, K in clay soil was tested, through the theoretical model developed, with changes in environmental factors. These model results are presented and discussed. The model was tested for three types of clay soil minerals; montmorillonite, illite and kaolinite at different temperatures, hydraulic gradients, clay densities, permeant salt concentrations and types of permeant.

4.2 Montmorillonite

Because clay soils containing high percentages of montmorillonite minerals are very sensitive to changes in environmental factors as discussed earlier, and that Bentonite which is widely used as clay liner is composed mainly of montmorillonite, this type of clay mineral will be examined more thoroughly than others. In the following sections the scheme and results of model tests will be presented and discussed.

4.2.1 Effect of Clay Density, γ_c

Figure 4.1 shows results of Log K vs clay density, γ_c for NaCl concentrations of 0.5 molar and saline solution, with hydraulic gradients varying from 200 to 2000. Hydraulic conductivity decreases with increasing clay density. A simple explanation is that; the denser is the clay soil the lower is its porosity and the narrower are the flow channels resulting in lower hydraulic conductivity. The results are shown up to γ_c = 1 Mg / m^3; there is a very significant decrease (not shown in the figure) of hydraulic conductivity for γ_c between 1 and 1.25 Mg / m^3. Similar results are shown in Figures C-1 to C-3 for NaCl of 3 molar and $CaCl_2$ of 0.5 and 3 molars in Appendix C.

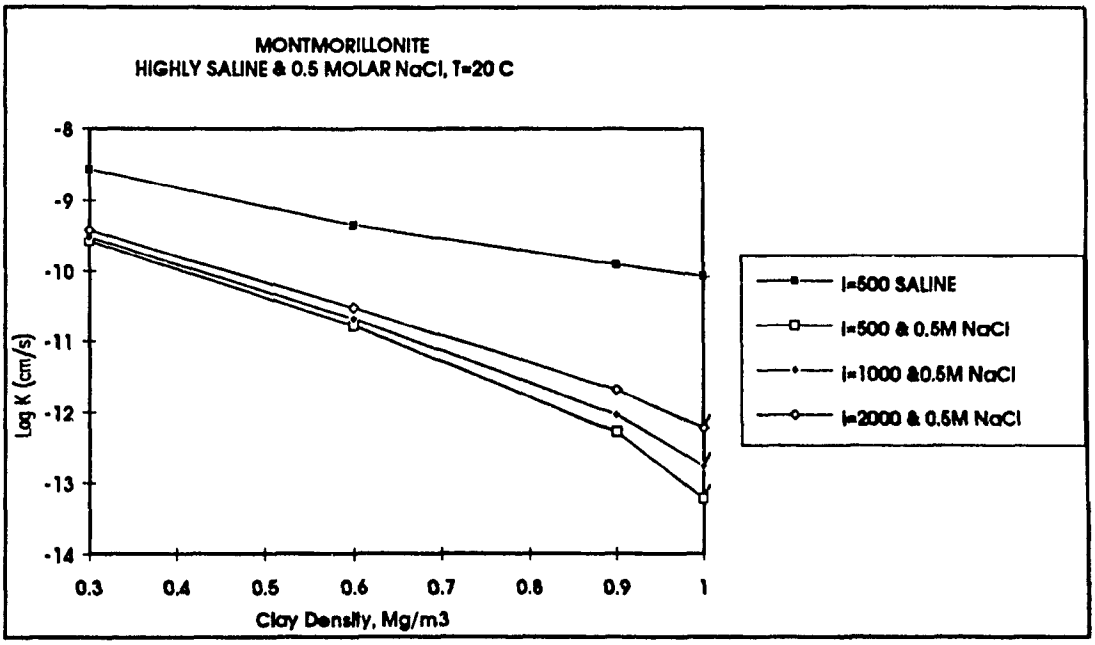

Figure 4.1 Montmorillonite, Log K vs γ_c at 0.5 M NaCl and different Hydraulic Gradients (Model results)

4.2.2 Effect of Salt Type

The effect of NaCl and $CaCl_2$ concentration for Montmorillonite at different clay densities of 0.3 and 1 Mg / m^3 and hydraulic gradients of 200, 1000 and 2000 is shown in

Figures C-4 to C-6 in Appendix C. Typical result is shown in Figure 4.2. At the same hydraulic gradient, the same clay density and the same salt concentration, permeants with $CaCl_2$ in Figure 4.2 are shown to have a higher hydraulic conductivity than permeants with NaCl. This is due to the fact that for Ca^{++} ions the thickness of the diffuse double layer is less than that with Na^+ ions, leaving a larger space unaffected by surface forces for permeant flow resulting in higher hydraulic conductivities. This effect is more dominant at lower concentration and higher density because the diffuse double layers are highly interacted as compared to those which are mostly compressed at lower density under the applied gradient.

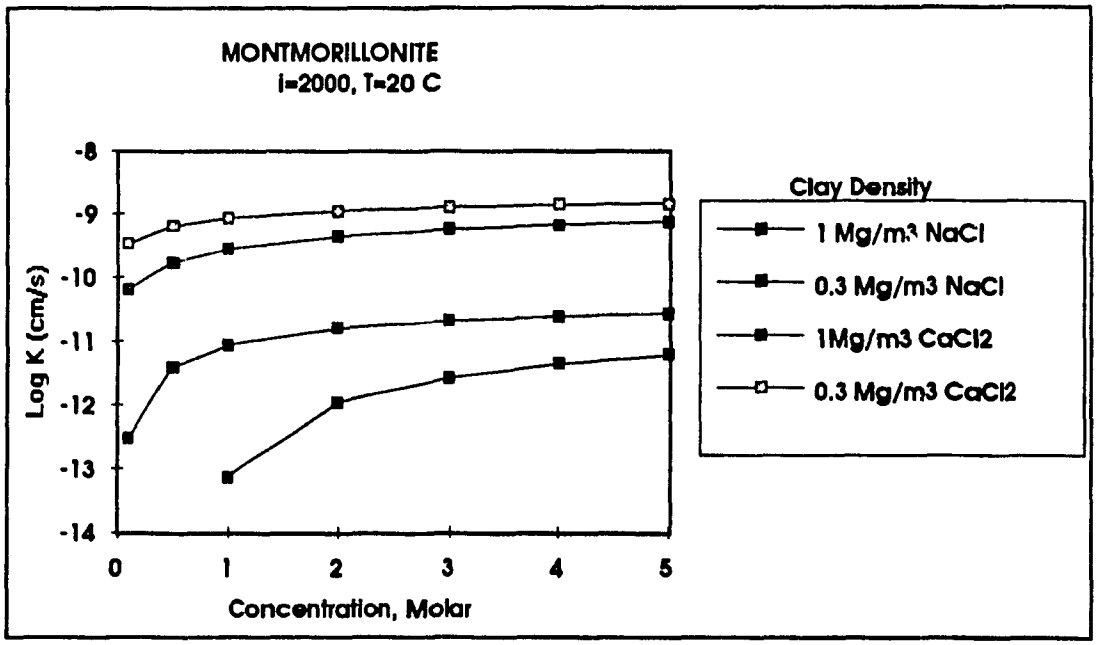

Figure 4.2 Montmorillonite, Log K vs NaCl and $CaCl_2$ Concentration at $\gamma_c = 0.3$ and 1 Mg / m^3 and i = 2000 (Model results)

4.2.3 Effect of Temperature

The series of Figures C-7 to C-13 in Appendix C show Log K vs NaCl and $CaCl_2$ concentration for two temperatures T = 20 ^oC and T = 90 ^oC at clay densities of 0.3, 0.6

and 1 Mg / m^3 and hydraulic gradients of 200, 500, 1000 and 2000. A typical result is shown in Figure 4.3. The effect of the variation of the temperature on the hydraulic conductivity is of two parts. One part is due to the change in the viscosity of the permeant which is, in the case of water, in the range of around three times (Appendix A, Table A-2). The higher is the temperature the higher is the hydraulic conductivity due to viscosity change. This viscosity effect is almost constant for the range of concentrations considered. The second part is due to the temperature effect on the diffuse double layer. The higher the temperature the larger is the diffuse double layer so the lower is the hydraulic conductivity. This effect varies with concentration; at low concentrations the diffuse double layer is large and the effect of the temperature is more, while at high concentrations the diffuse double layer is depressed and the effect of temperature on the diffuse double layer and hence on the hydraulic conductivity is less. The net result is that at low concentrations we have a balancing effect while at high concentration the change is due to viscosity.

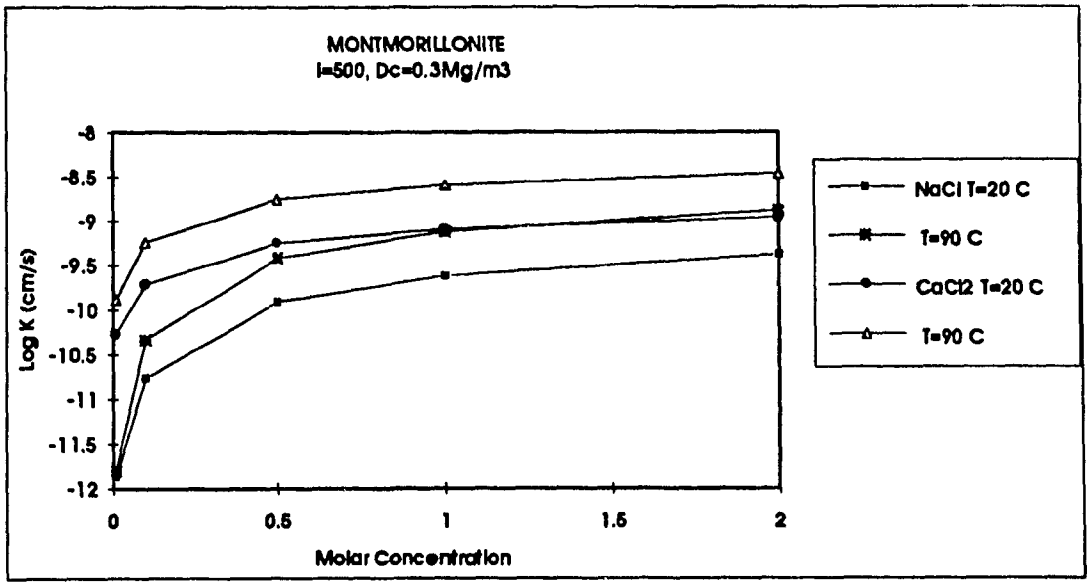

Figure 4.3 Montmorillonite, Log K vs NaCl and $CaCl_2$ concentration at T=20 and 90°C, γ_c = 0.3 Mg / m^3 and i=500 (Model results)

In Figure 4.3 the variation due to different type of permeant solution is also clear, at low concentration the difference between K90 and K20 (Hydraulic conductivities at T = 90 and 20 respectively) for NaCl is less than that for $CaCl_2$. In this case, three types of effects need to be considered . The first is the effect of temperature on viscosity, this is a positive effect on the hydraulic conductivity. The second is the effect of temperature on the diffuse double layer, this is a negative effect. The third is the effect of type of permeant solution; in this case, it is a positive effect from NaCl to $CaCl_2$. The net effect is the summation of these three.

For easier comparison ratios of K90 / K20 vs NaCl and $CaCl_2$ concentrations for hydraulic gradients of 1000 and 2000, and clay densities of 0.3 and 1 Mg / m^3 are plotted in Figures C-52 to C-57 in Appendix C. At low clay densities, K90 / K20 varies between 2.6 and 3 which is due to viscosity variation.Typical example is given in Figure 4.4. At high clay densities, K90 / K20 varies between 1 and 3, due to the combined effect of diffuse double layer and viscosity.

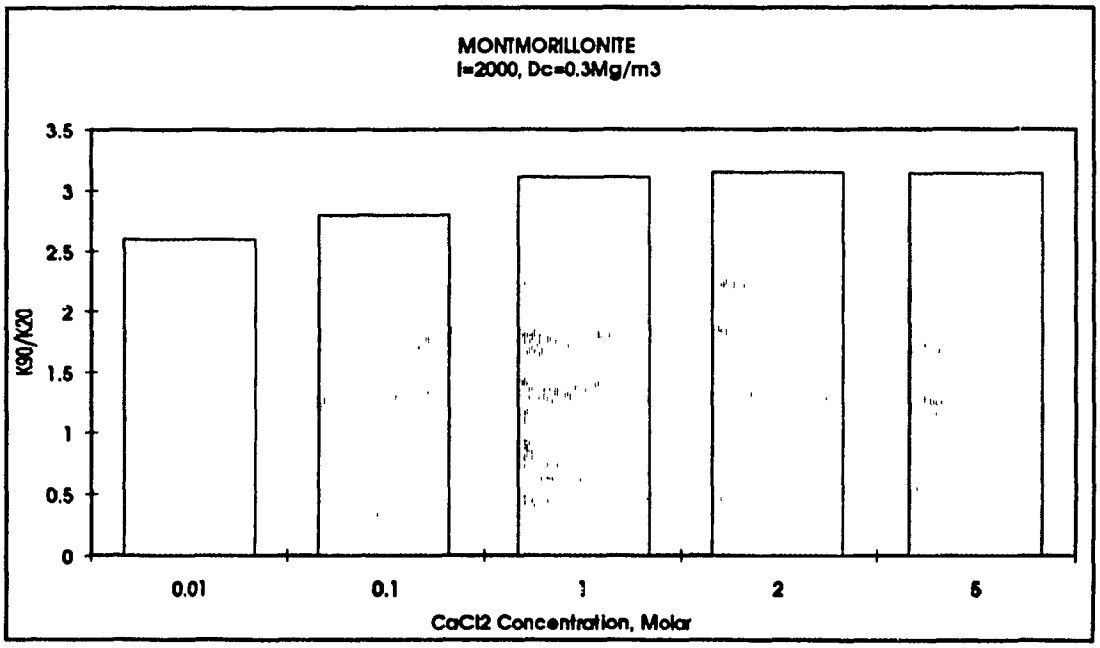

Figure 4.4 Montmorillonite, K90/K20 vs $CaCl_2$ concentration at i = 2000 and γ_c = 0.3 Mg / m^3 (Model results)

4.2.4 Effect of Hydraulic Gradient, i

Results in Figure 4.5 show that at high concentrations the hydraulic conductivity is constant and is not affected by the hydraulic gradient, while, at low concentrations the hydraulic conductivity increases with increasing hydraulic gradient. The reason for this is that at low concentrations the diffuse double layer is large and the applied gradient can only mobilize some of the bound water. As the hydraulic gradients get higher, the force holding the bound water is exceeded, more bound water is mobilized leaving larger space for free water flow. Similar results in Figures C-16 to C-22 (Appendix C) at different NaCl and $CaCl_2$ concentrations and clay densities are shown.

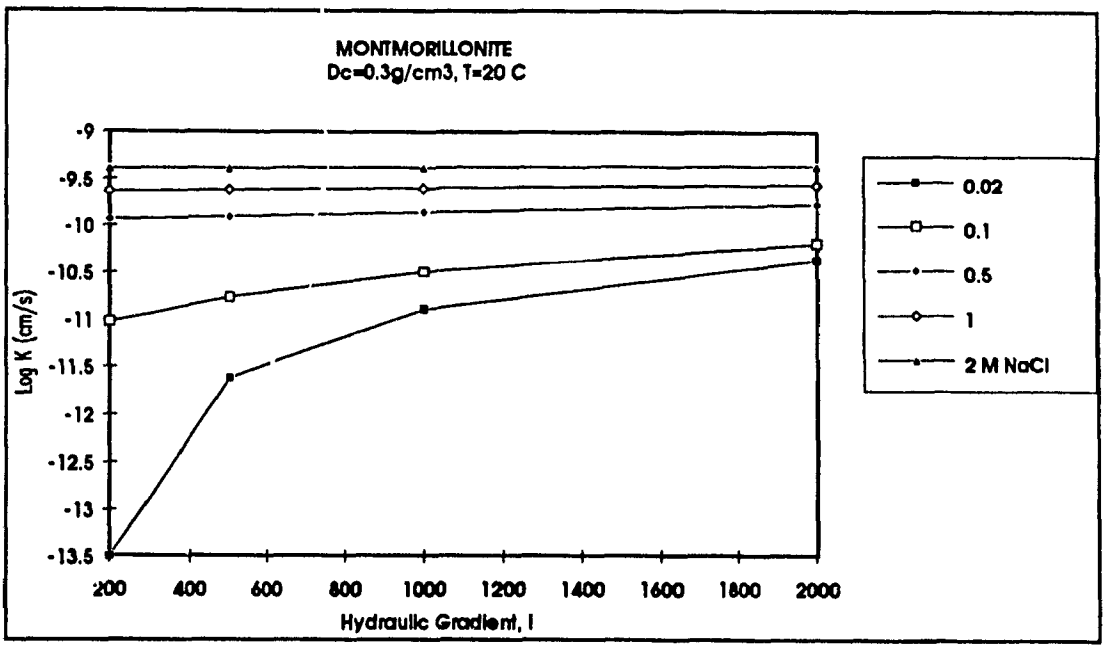

Figure 4.5 Montmorillonite, Log K vs Hydraulic Gradient i at different NaCl concentration and $\gamma_c = 0.3$ Mg / m^3 (Model results)

4.2.5 Effect of Concentration

The effect of concentration is discussed in connection with hydraulic gradient, i, clay density, γ_c and Temperature as follows.

i) Concentration and Hydraulic gradient

Figures 4.6 and 4.7 show that at low molar concentrations the hydraulic conductivity varies with hydraulic gradient. The lower is the hydraulic gradient the lower is the hydraulic conductivity, because the lower is the pressure to shear the interacted diffuse ion layers. While, at higher concentrations the thickness of the diffuse double layer is less and the interaction between them is limited so the hydraulic conductivity is not affected by the hydraulic gradient. The effect of the type of permeant solution is also clear. For NaCl solution the hydraulic conductivity is affected more by the hydraulic gradient than for $CaCl_2$ solution.

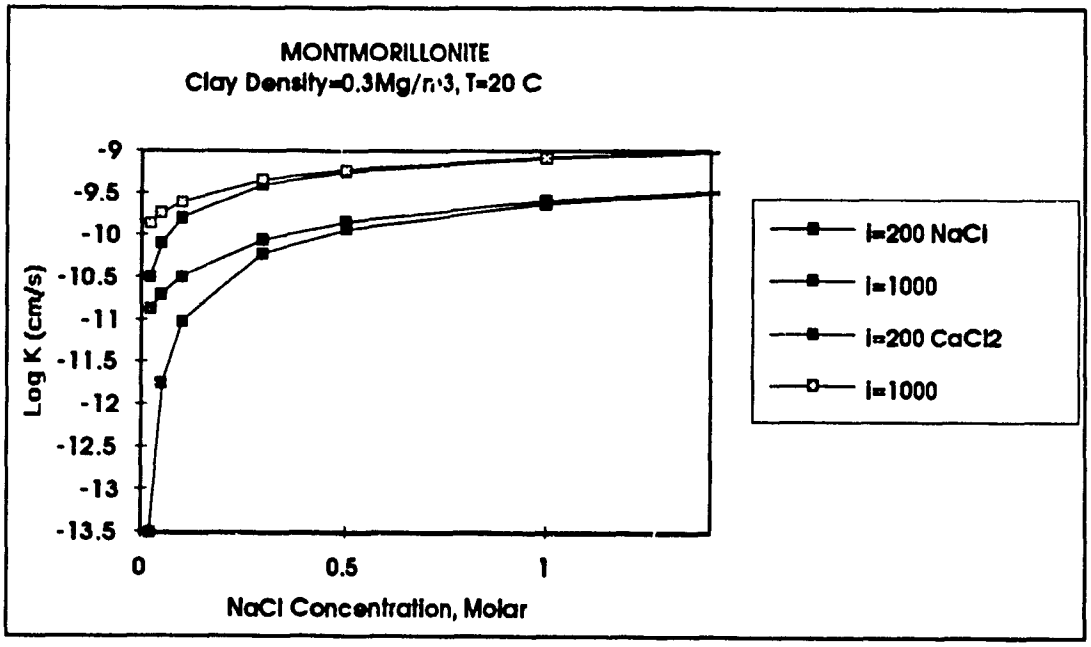

Figure 4.6 Montmorillonite, Log K vs NaCl and $CaCl_2$ concentration at i = 200 and 1000 and $\gamma_c = 0.3$ Mg / m^3 (Model results)

Similar results are found in Figures C-14, C-15 and C-23 to C-27 in Appendix C which show Log K vs NaCl and $CaCl_2$ concentration at temperature T = 20 ^oC and clay densities of 1 and 0.3 Mg / m^3 and hydraulic gradients varying between 200 and 2000.

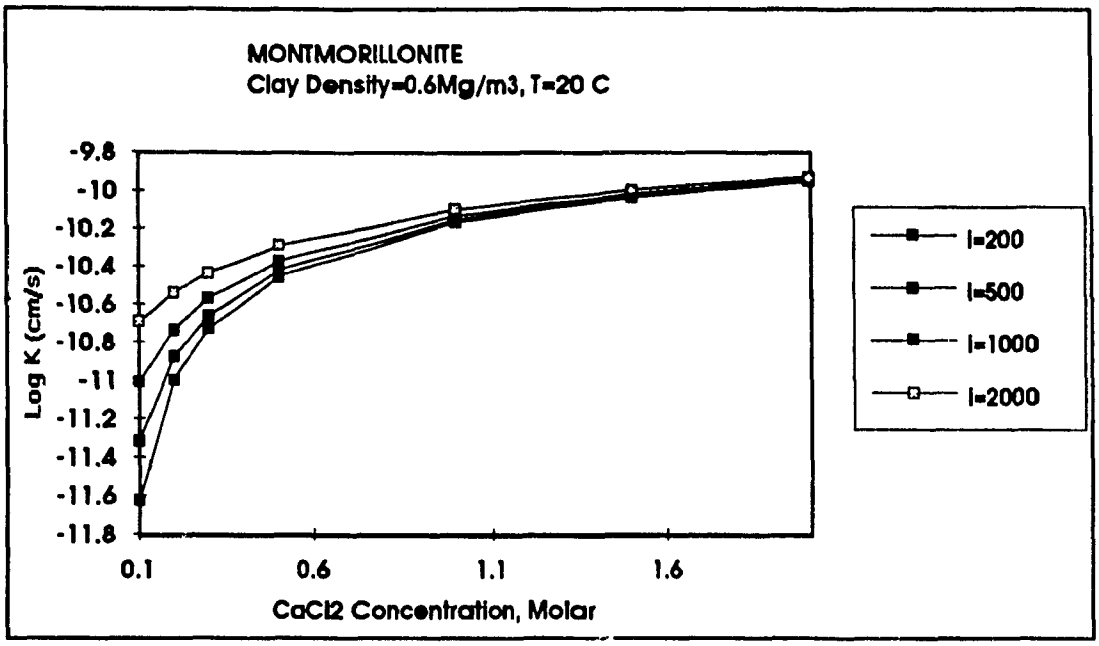

Figure 4.7 Montmorillonite, Log K vs $CaCl_2$ concentration at different Hydraulic Gradient i and γ_c = 0.6 Mg / m^3 (Model results)

ii) Concentration and Clay Density, γ_c

Figure 4.8 shows the variation of the hydraulic conductivity with clay density. It can be seen that the higher the clay density the lower the hydraulic conductivity. At high clay densities, the hydraulic conductivity is affected more by concentration because the diffuse double layers are interacted and any change in the concentration will affect the diffuse double layers and hence their interaction resulting in changes in the hydraulic conductivity. More results are shown in Figures C-28 to C-34 in Appendix C for show Log K vs NaCl and $CaCl_2$ concentrations at different clay densities and hydraulic gradients.

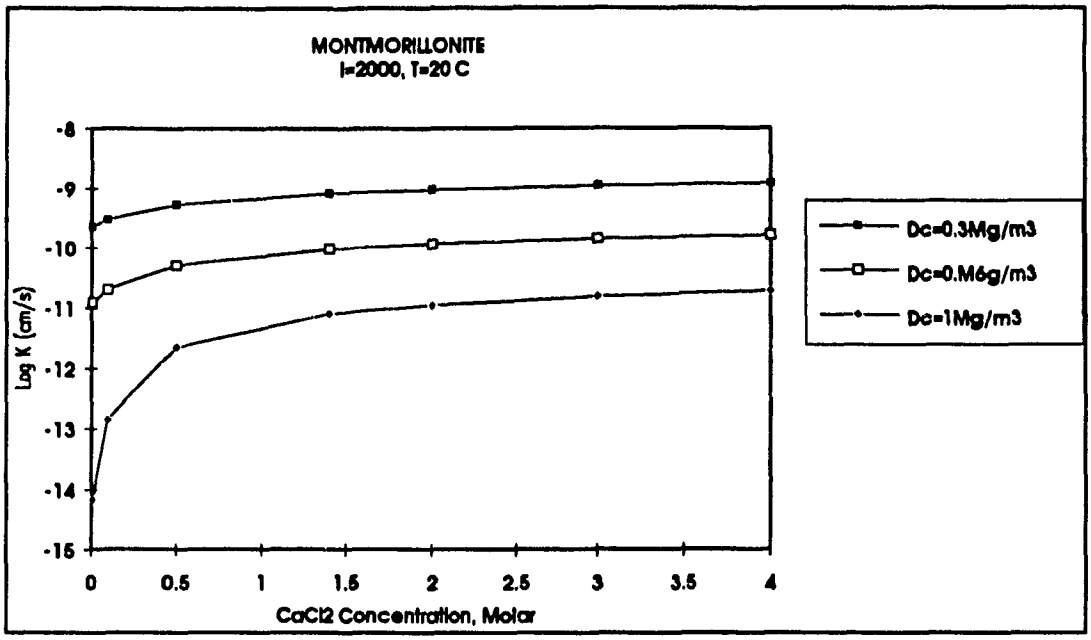

Figure 4.8 Montmorillonite, Log K vs $CaCl_2$ concentration at different γ_c and i=2000 (Model results)

iii) Concentration and Temperature

Figure 4.9 show the variation of hydraulic conductivity with temperature and concentration. Hydraulic conductivity is shown to increase with increasing concentration up to about 1M and then remain constant. The constant values of K suggest that surface forces are absent and hence not affected by concentration. The difference of K values with temperature is mainly due to change in water viscosity. At concentration < 0.4M, the changes of K are due to the combined effect of diffuse double layer and water viscosity with temperature. Similar results in Figures C-35 to C-51 in Appendix C are presented for Log K vs NaCl and $CaCl_2$ concentrations at different temperatures 20, 40, 70 and 90° C, clay densities of 0.3, 0.6 and 1 Mg / m^3 and hydraulic gradients of 200, 500, 1000, 2000.

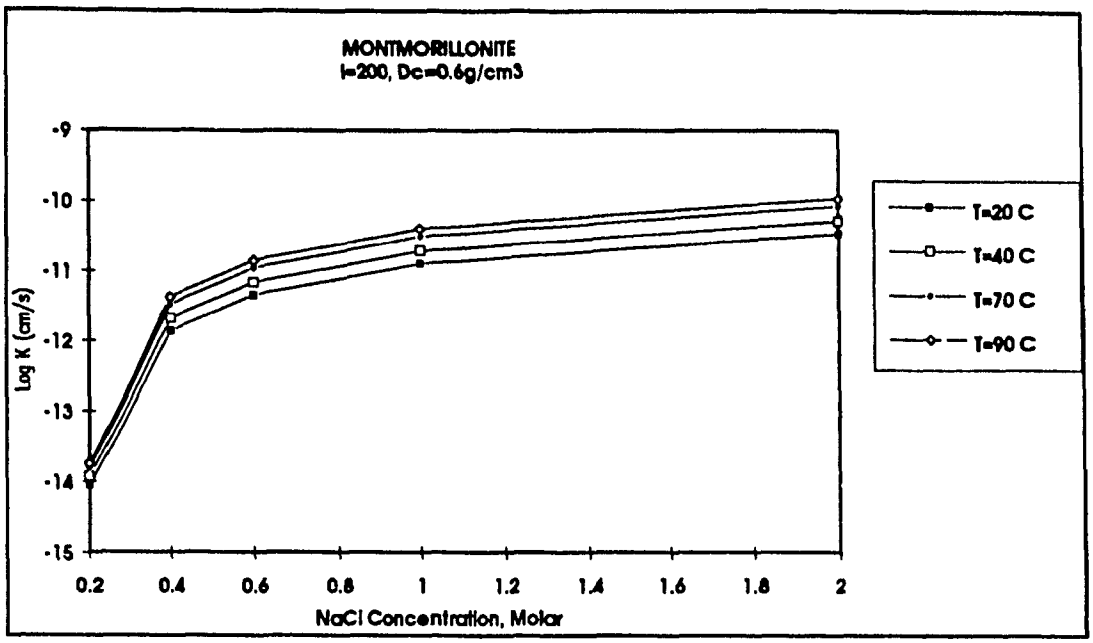

Figure 4.9 Montmorillonite, Log K vs NaCl concentration at T=20, 40, 70 and 90°C, γ_c = 0.6 Mg / m^3 and i = 200 (Model results)

4.2.6 Threshold Gradient Analysis

A set of graphs were drawn for flow rate per unit area, q and hydraulic gradient, i for different NaCl and $CaCl_2$ concentrations and clay densities. Through these graphs the existence of threshold gradient (a gradient at which there is insignificant flow) and its variation with salt type, salt concentration, clay density and temperature were examined. These graphs were drawn using q = Ki at each point where the q and the i were plotted. These results are shown in Figures C-58 to C-73 in Appendix C. The effect of each variable is analysed in the following sections

i) Effect of Clay Density, γ_c

Due to surface forces there is a nonlinear relationship at low and high clay densities. These results are very similar to experimental results. The existence of the threshold gradient is evident. Figures 4.10 and 4.11 show that the higher the clay density the higher is the threshold gradient; this could be explained by the fact that at higher

densities clay particles are closer to each other and diffuse double layers interact largely. Higher pressures are needed to shear these interacted diffuse double layers.

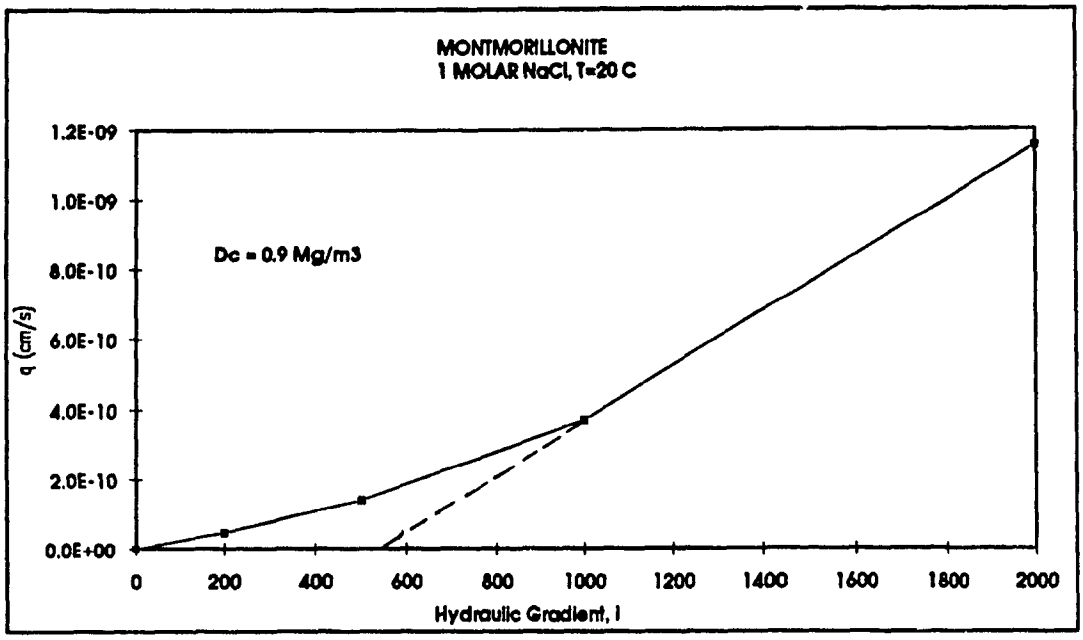

Figure 4.10 Montmorillonite, q (cm/s) vs i at 1 Molar NaCl concentration and $\gamma_c = 0.9$ Mg / m^3, (Model results)

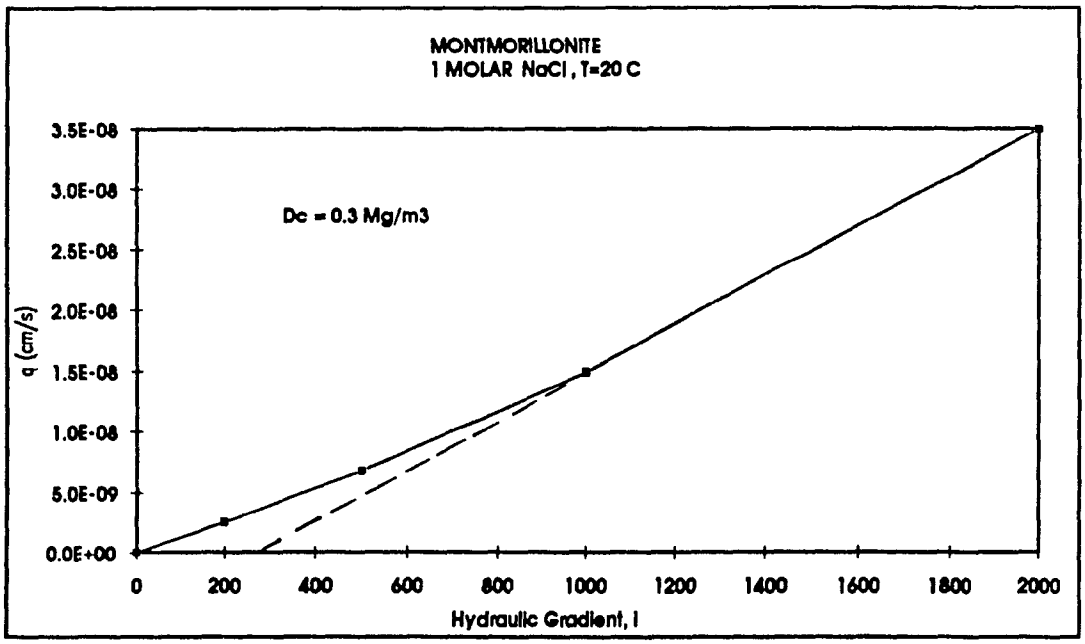

Figure 4.11 Montmorillonite, q (cm/s) vs i at 1 Molar NaCl concentration and $\gamma_c = 0.3$ Mg / m^3, (Model results)

ii) Effect of Salt Type and Concentration

Figures 4.10 and 4.12 show that; at the same concentration and the same clay density; permeants with NaCl solution have larger threshold gradients than those with $CaCl_2$ solution. This is explained by the fact that for NaCl solution the diffuse double layer is larger and the interaction of these layers are more than that of the $CaCl_2$ solution, thus more pressure is required and higher values of threshold gradient are obtained. Figure 4.13 shows the variation of threshold gradient with variation in concentration, the higher is the concentration the lower is the threshold gradient. This is again explained by the fact that at high concentrations the diffuse double layer is fully depressed allowing easier flow of the permeant through the clay soil.

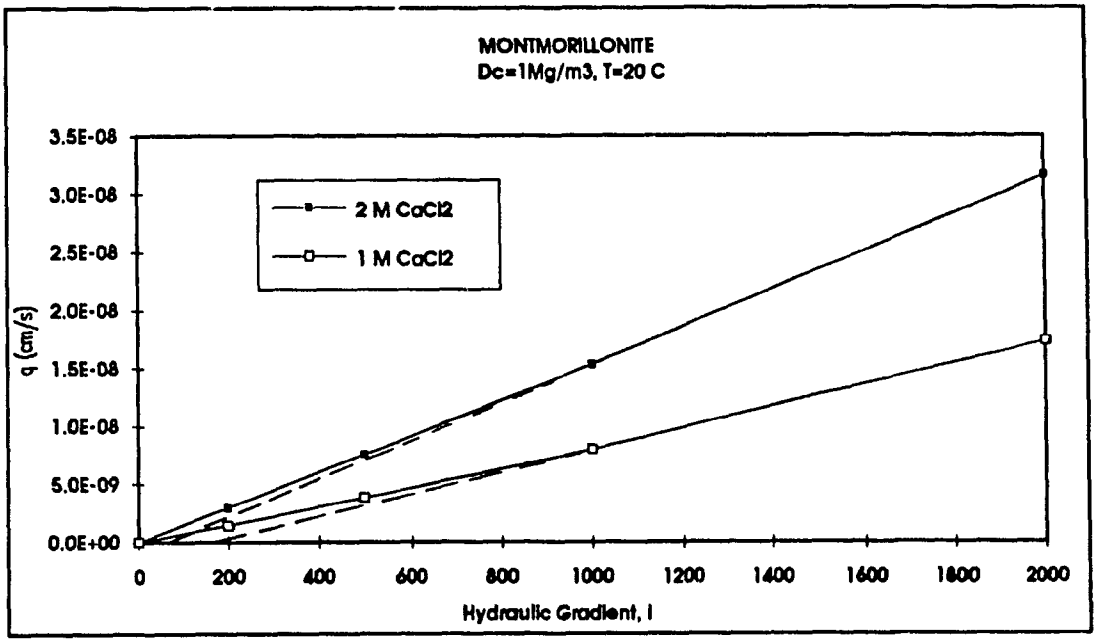

Figure 4.12 Montmorillonite, q (cm/s) vs i at 1 M and 2M $CaCl_2$ and γ_c = 1 Mg / m^3 (Model results)

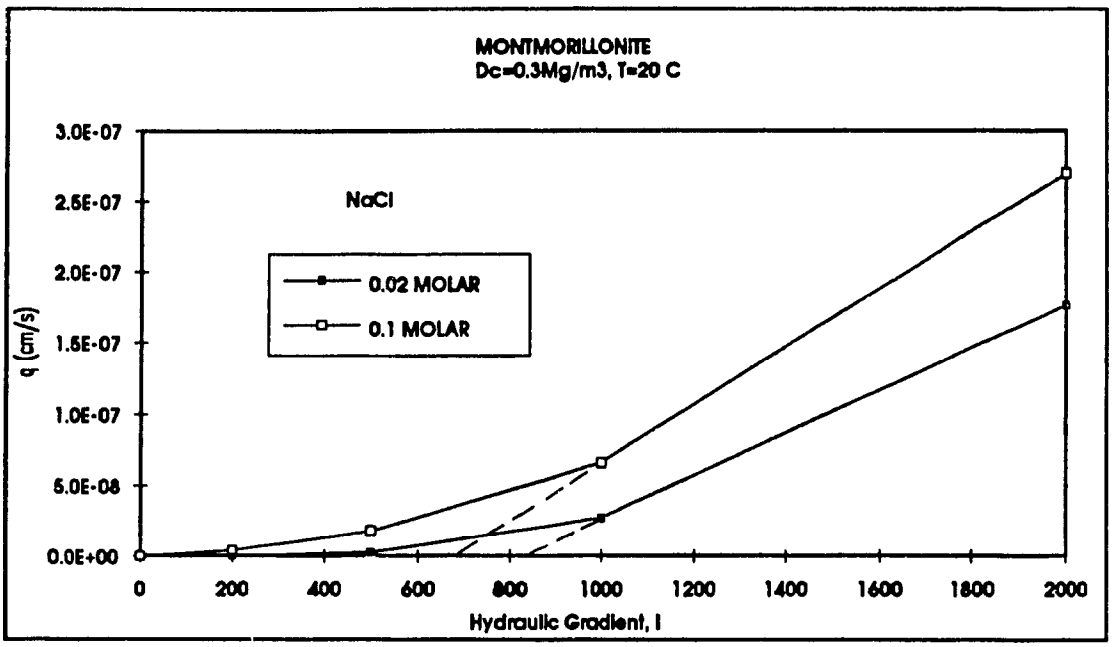

Figure 4.13 Montmorillonite, q (cm/s) vs i at 0.1 M and 0.02M NaCl and $\gamma_c = 0.3$ Mg/m^3 (Model results)

iii) Effect of Temperature

The model was also tested for the effect of temperature changes on the threshold gradient. Figure 4.14 is a typical result which shows that, as the temperature increased from 20 to 90°C the threshold gradient decreased. The effect of the temperature change on the hydraulic conductivity is due to viscosity and the diffuse double layer factors; these two factors have opposite effects. At high concentrations, the diffuse double layer is small and the effect of temperature variation is mainly due to viscosity factor. At low concentrations the threshold gradient may not be affected with temperature due to the balancing effect of the two factors (see Figures C-70 to C-73 in Appendix C).

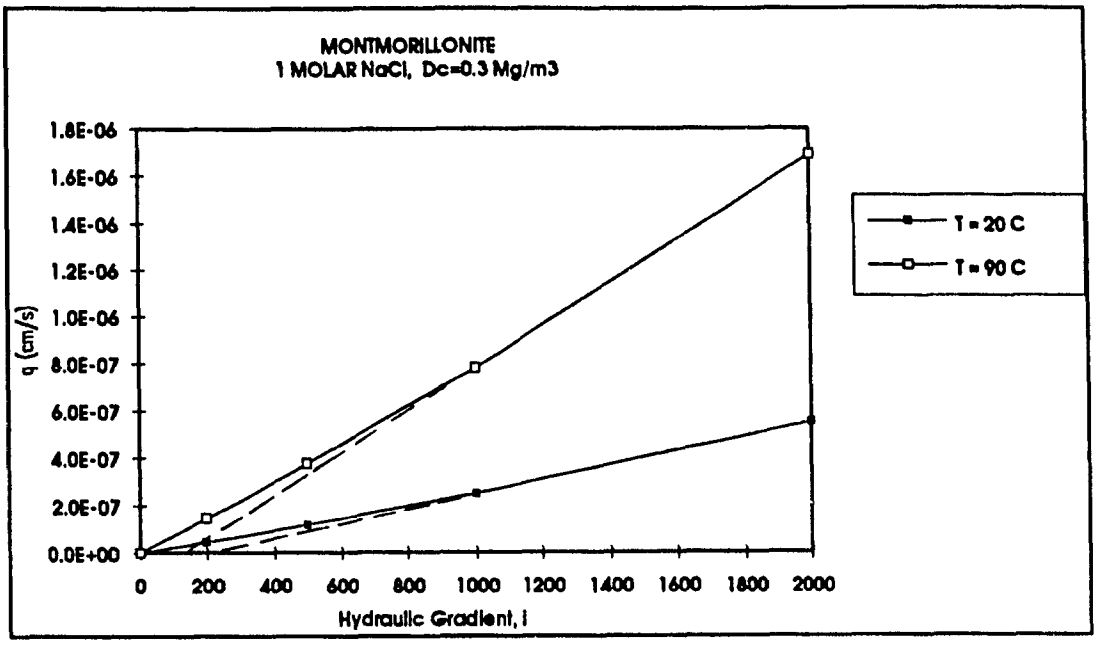

Figure 4.14 Montmorillonite, q (cm/s) vs i at T=20 and 90°C, 1M NaCl and γ_c = 0.3 Mg/m^3 (Model results)

4.2.7 Highly Compacted Montmorillonite

Figure 4.15 shows the results of Log K vs. clay density, based on the theory developed in section 3.4 for highly compacted montmorillonitic clays. Hydraulic conductivity decreases as clay density increases and we have two boundary; lines one for highly saline solution and the other for distilled water. The higher the clay density the more is the number of particles in a cluster thus increasing the size of a cluster and decreasing the effective surface area, but since with larger clusters we have more immobilized water between the clay particles we still have a decrease in the hydraulic conductivity but at a lesser rate.

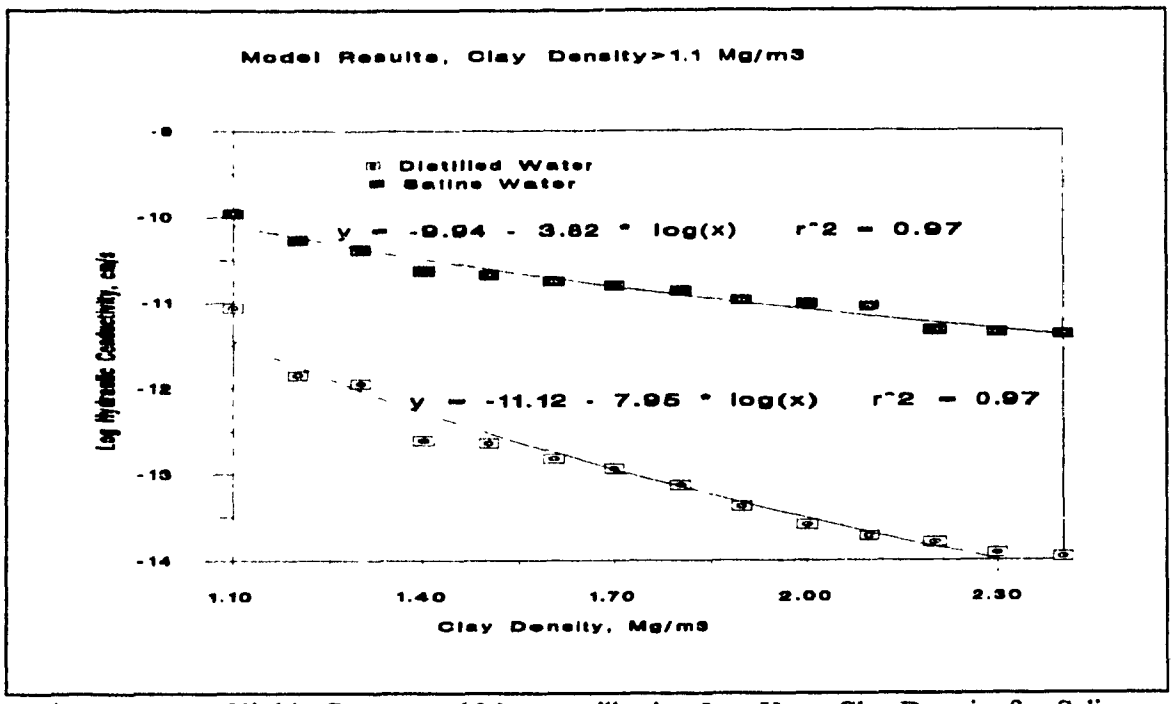

Figure 4 15 Highly Compacted Montmorillonite, Log K vs. Clay Density for Saline Solution and Distilled Water (Model results)

4.3 Illite

In this section the hydraulic conductivity of illite clay mineral is tested through the theoretical model for the variation in the environmental factors.

4.3.1 Effect of Salt Concentration

Typical result in Figure 4.16 show that, at low concentrations (< 1M) there is little variation of hydraulic conductivity; while at higher concentrations the hydraulic conductivity is constant. From these results we conclude that in illitic clay minerals surface forces are less active. Of course, as it is evident the hydraulic conductivity varies with clay density, the higher the clay density the lower is the hydraulic conductivity. More of model results in Figures C-74 to C-76 in Appendix C, for Log K vs NaCl and $CaCl_2$

concentrations are plotted at different clay densities ranging between 0.3 and 2 Mg/m^3 and hydraulic gradients between 200 and 1000.

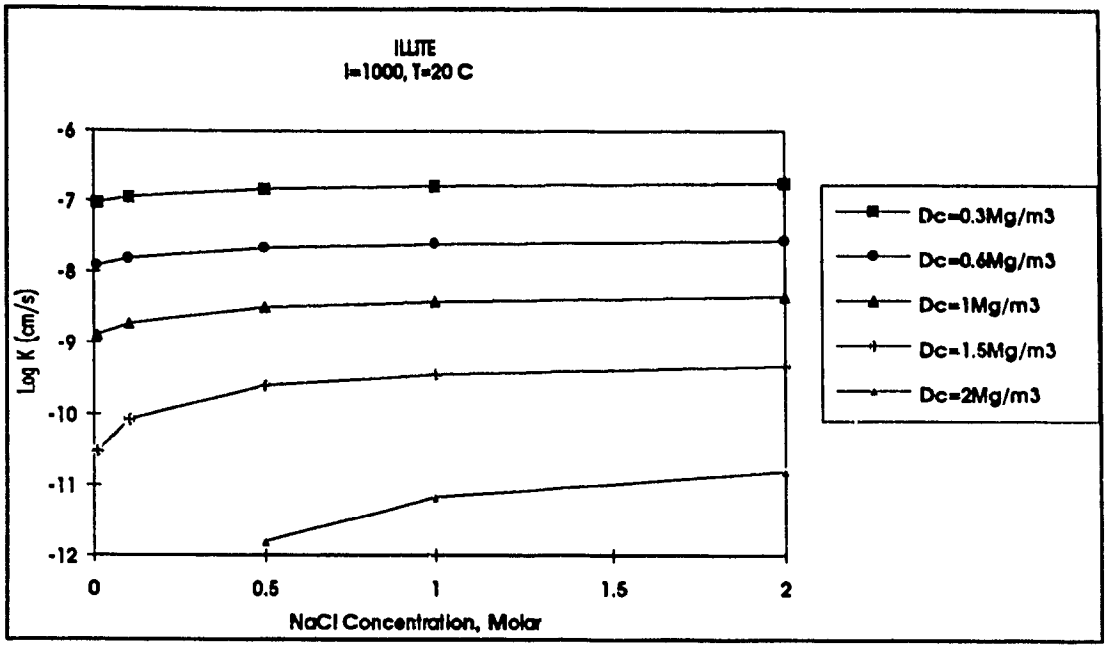

Figure 4.16 Illite, Log K vs NaCl concentration at γ_c = 0.3, 0.6, 1, 1.5, 2 Mg/m^3 and i = 1000 (Model results)

4.3.2 Effect of Temperature

At low densities (0.3 Mg / m^3) the only variation of hydraulic conductivity with variation in temperature is due to the change in the viscosity which is in the order of 3 for K90 / K20. Typical results in Figures 4.17 and 4.18 show that at higher densities (>1.3 Mg / m^3) and low concentrations (< 0.2M in the case of NaCl) K90 / K20 is in the range of 2.4 to 2.8 because of the combined effect of the diffuse double layer interaction and the change in the viscosity; while at the same high density but at high concentration, K90 / K20 is in the order of 3, in this case the diffuse double layer is depressed due to high concentration and the change in hydraulic conductivity is due to viscosity effect. In Figures C-77 to C-82 in Appendix C Log K vs NaCl and $CaCl_2$ concentrations are plotted

at different temperatures T = 20, 40, 70 and 90 °C and clay densities of 0.3 and 1.3 Mg / m^3 and hydraulic gradients of 200 and 1000.

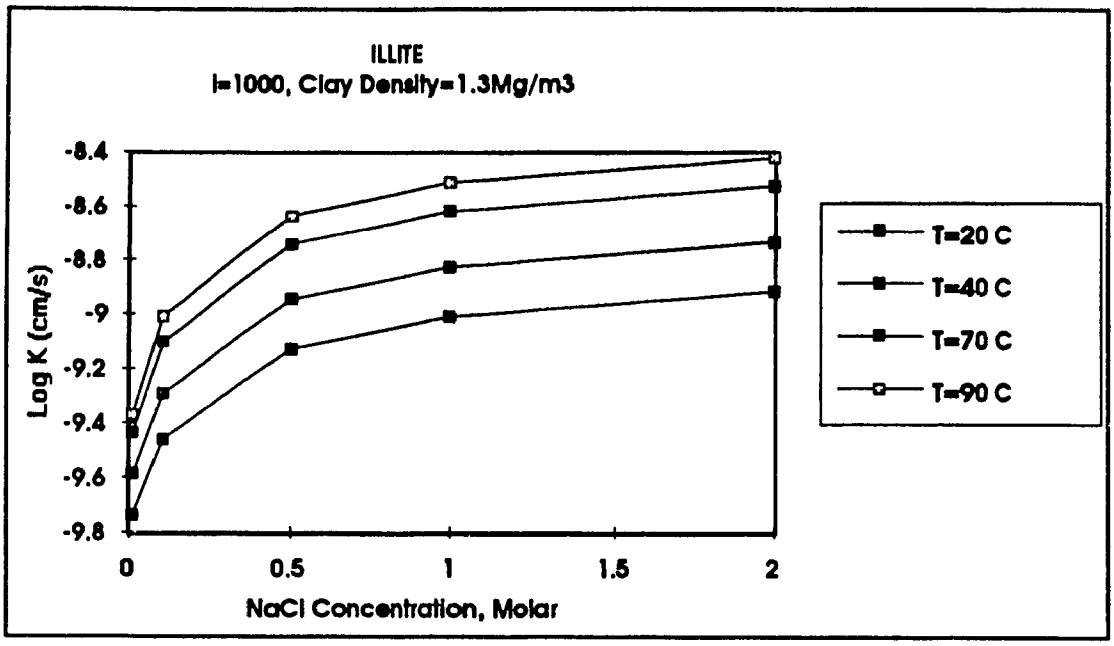

Figure 4.17 Illite, Log K vs NaCl concentration at T = 20, 40, 70 and 90°C, i = 1000, γ_c = 1.3 Mg / m^3 (Model results)

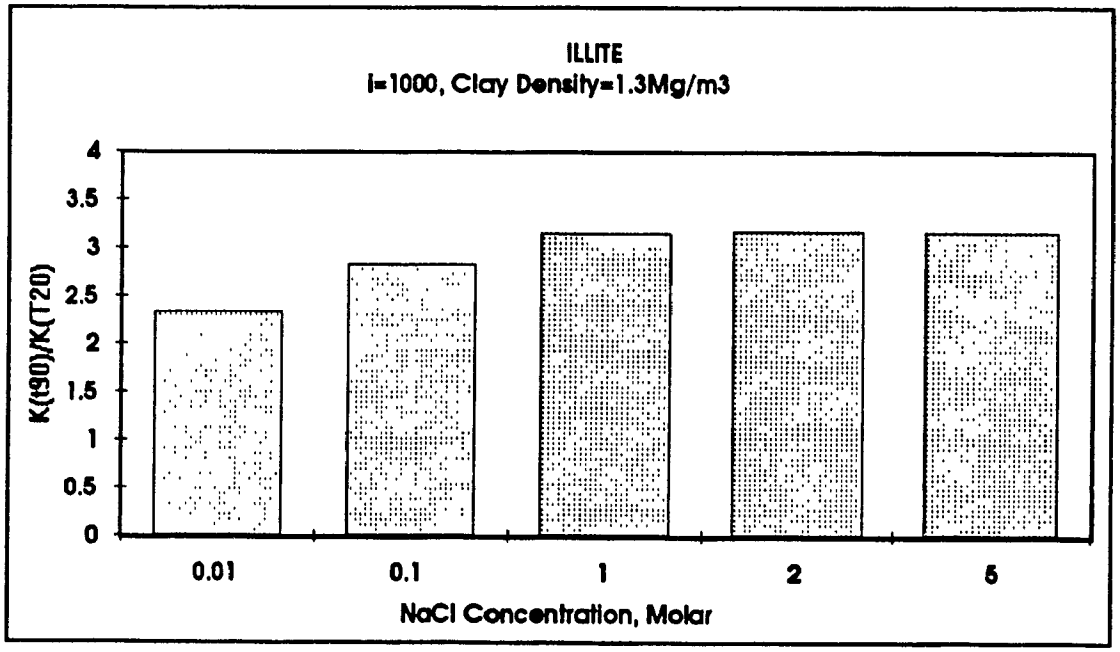

Figure 4.18 Illite, K90/K20 vs NaCl concentration at i = 1000 and γ_c = 1.3 Mg / m^3, (Model results)

4.3.3 Effect of Clay Density, γ_c

Results in Figure 4.19 show that hydraulic conductivity varies with clay density the higher the clay density the lower the hydraulic conductivity. Figure 4.19 also shows that at high molar concentrations (1 Molar) all the graphs representing different hydraulic gradients coincide meaning that K is not affected by the hydraulic gradient. At low Molar concentrations (0.01 Molar, Figure C-83) hydraulic gradient has a little effect on K. More of these results are shown in Figures C-83 to C-85 in Appendix C for Log K vs clay density for NaCl and $CaCl_2$ concentrations of 0.01 and 1 Molar and hydraulic gradients ranging between 200 and 2000.

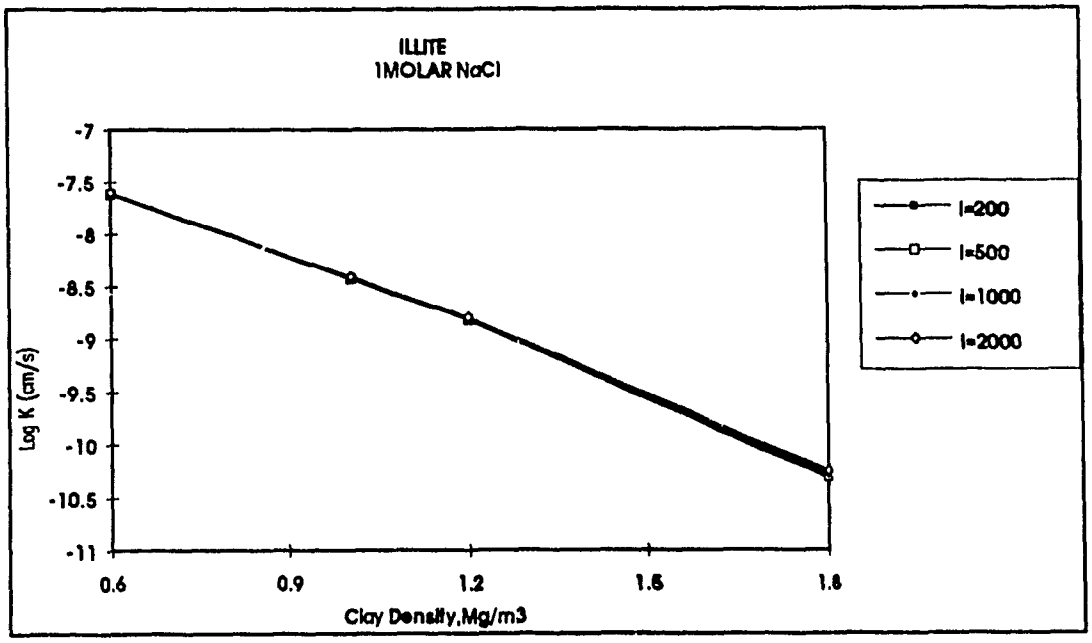

Figure 4.19 Illite, Log K vs γ_c at different Hydraulic Gradient and 1M NaCl concentration (Model results)

4.3.4 Effect of Hydraulic Gradient, i

Typical results in Figure 4.20 show that at low densities (1 Mg/m^3) and high concentrations (> 1 Molar) there is no variation in hydraulic conductivity for different hydraulic gradients. While, at high densities and low concentrations there is very little

variation. This is due to the fact that at high densities clay particles are very close and at low concentrations the diffuse double layers are thick resulting in higher interaction. More results found in Figures C-86 to C-88, C-117 and C-118 in Appendix C show Log K vs NaCl and $CaCl_2$ concentration at clay density 1, 1.3 and 1.8 Mg / m^3 and hydraulic gradients of 200, 500, 1000 and 2000.

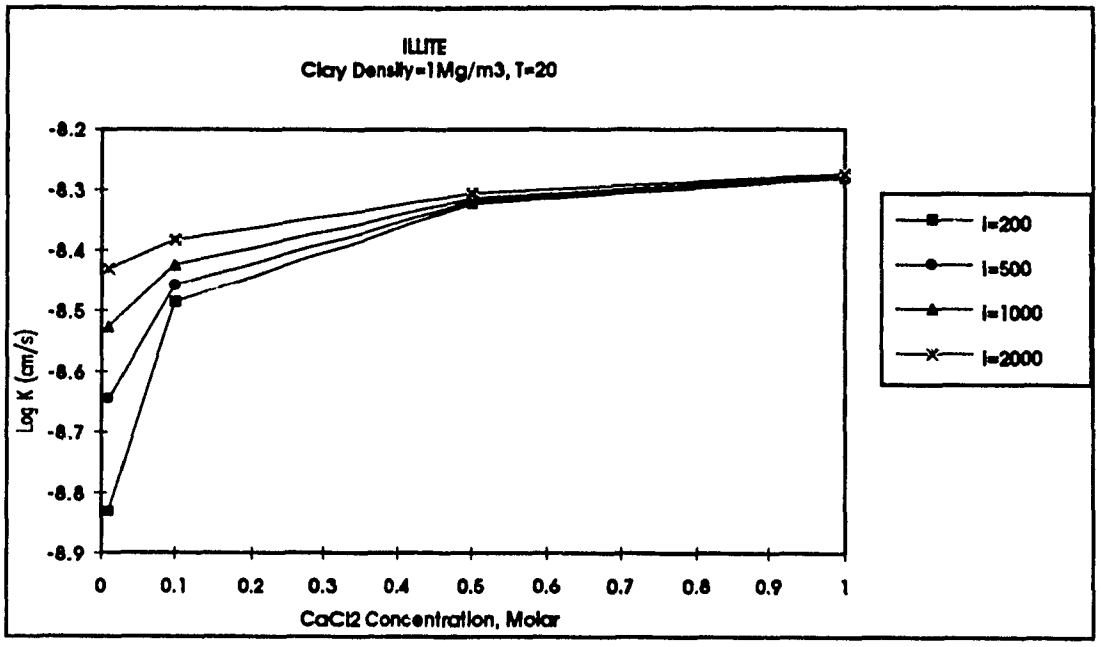

Figure 4.20 Illite, Log K vs $CaCl_2$ concentration at different Hydraulic Gradient and $\gamma_c = 1$ Mg / m^3 (Model results)

4.3.5 Effect of Salt Type

Figure 4.21 shows the effect of salt type on the hydraulic conductivity of Illite clay mineral. Hydraulic conductivity has little variation with salt type at low hydraulic gradients; while at higher hydraulic gradients the variation is lesser. More results are shown in Figures C-89 and C-90 in Appendix C for Log K vs hydraulic gradient for NaCl

and $CaCl_2$ concentrations of 0.1 and 1 Molar at different clay densities of 1 and 1.5 Mg/m^3.

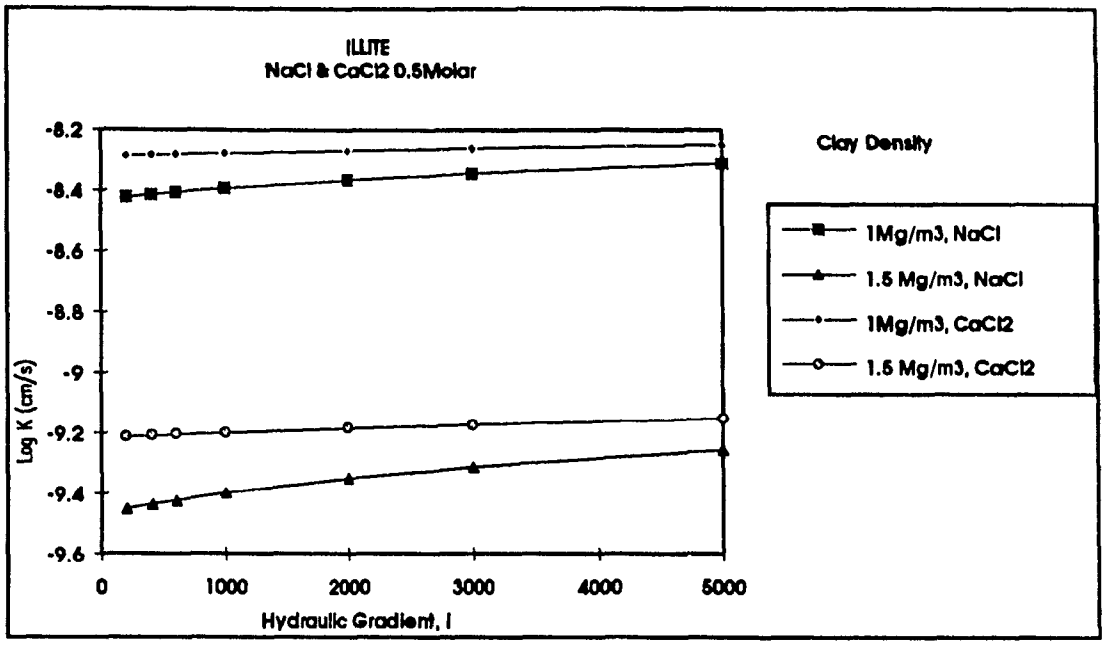

Figure 4.21 Illite, Log K vs Hydraulic Gradient i for 0.5M NaCl and $CaCl_2$ and γ_c = 1 and 1.5 Mg / m^3 (Model results)

4.3.6 Threshold Gradient

In this section the existence of threshold gradient is investigated for illitic clay minerals. Figures C-91 to C-95 in Appendix C are plotted for the flow rate per unit area q and the hydraulic gradient i. Threshold gradients exist for illite at high densities and low concentrations, except that the values of threshold gradients are smaller than that of montmorillonite. Typical graph is shown in Figure 4.22; at high Molar concentrations the curve for q vs i gets linear and threshold gradient does not exist.

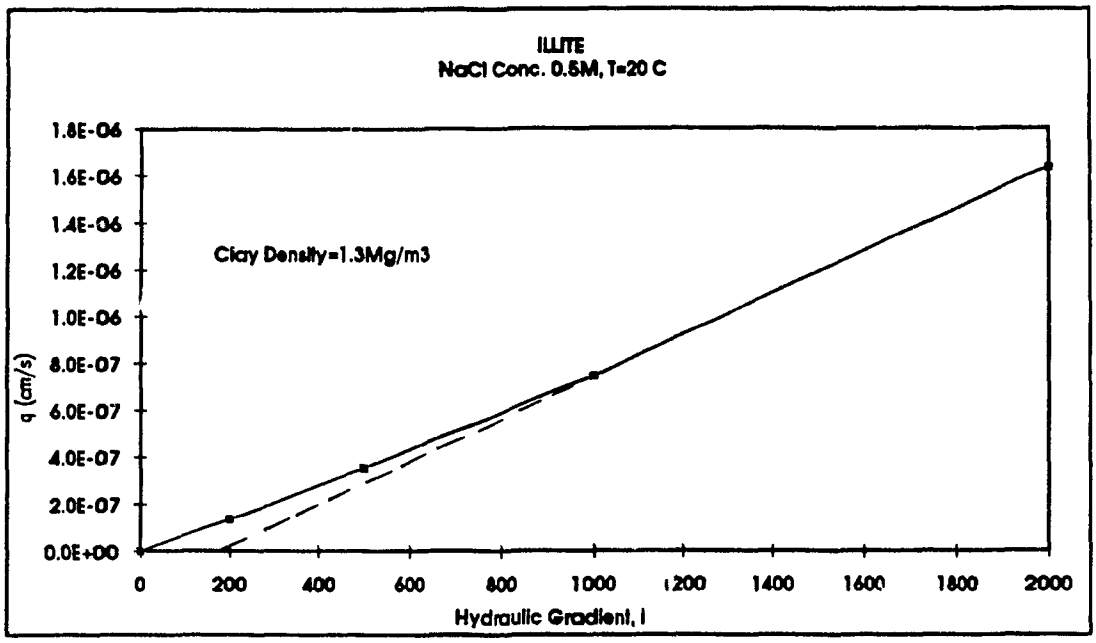

Figure 4.22 Illite, q (cm/s) vs i at 0.5 M NaCl concentration and γ_c = 1.3 Mg / m^3 (Model results)

4.4 Kaolinite

In this section the hydraulic conductivity of Kaolinite clay mineral is tested through the theoretical model for the variation in the environmental factors.

4.4.1 Effect of Salt Concentration

Typical result in Figure 4.23 shows that there is almost no variation in hydraulic conductivity with concentration for kaolinitic clay minerals, this is due to low activities of surface forces. The only variation of hydraulic conductivity is due to density variation which is related to porosity, the higher the density the lower is the hydraulic conductivity. Figures C-96 to C-98 in Appendix C show Log K vs NaCl and $CaCl_2$ concentrations at temperature 20 ^oC, different clay densities and hydraulic gradients of 200 and 1000.

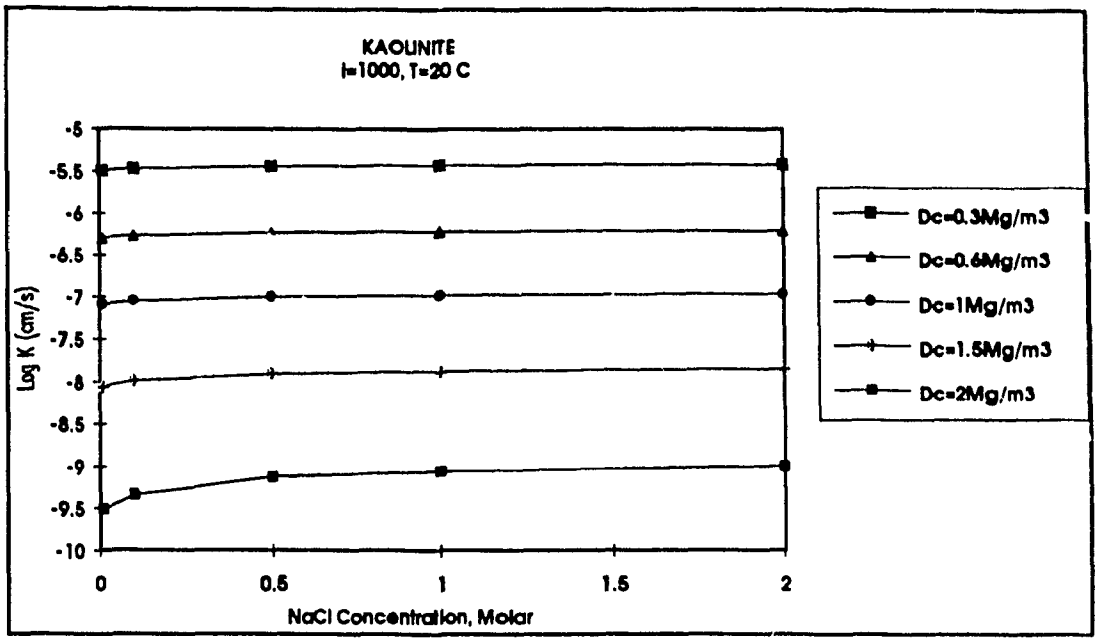

Figure 4.23 Kaolinite, Log K vs NaCl concentration at different γ_c and i = 1000 (Model results)

4.4.2 Effect of Temperature

Results in Figures 4.24 and 4.25 show that the only variation of hydraulic conductivity with temperature is due to the viscosity which is in the range of 3. This is clear in the K90 / K20 graph. Similar results are found in Figures C-99 to C-103 in Appendix C, where Log K vs NaCl and $CaCl_2$ concentrations are plotted at different temperatures T = 20, 40, 70 and 90 ^oC and clay densities of 0.3 and 1.3 Mg / m^3 and hydraulic gradients of 200 and 1000.

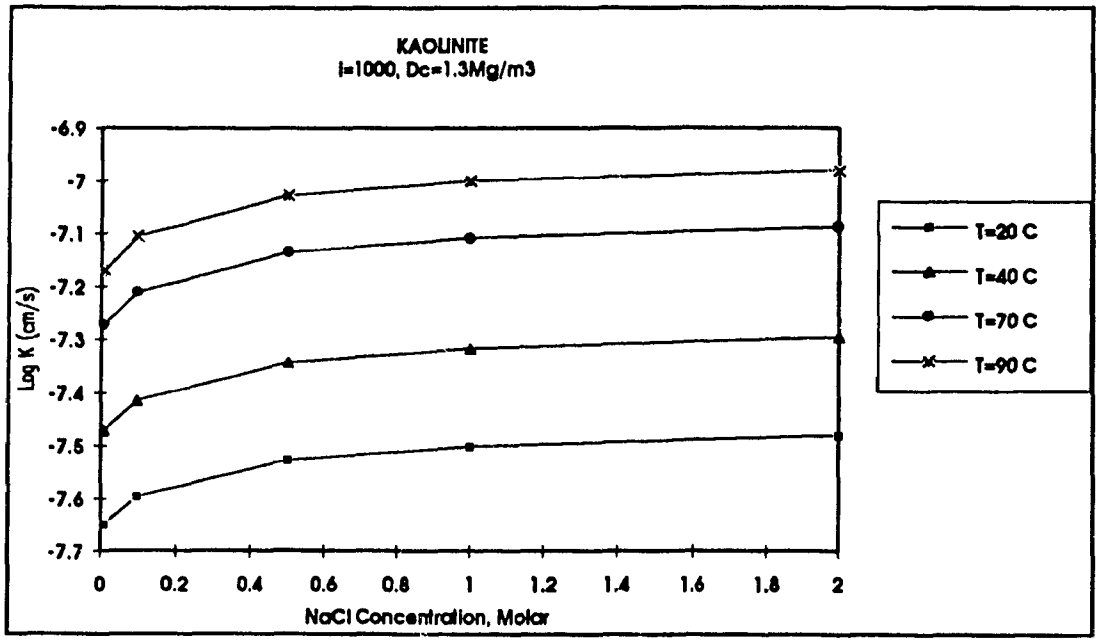

Figure 4.24 Kaolinite, Log K vs NaCl concentration at T=20, 40, 70 and 90°C γ_c = 1.3 Mg / m^3 (Model results)

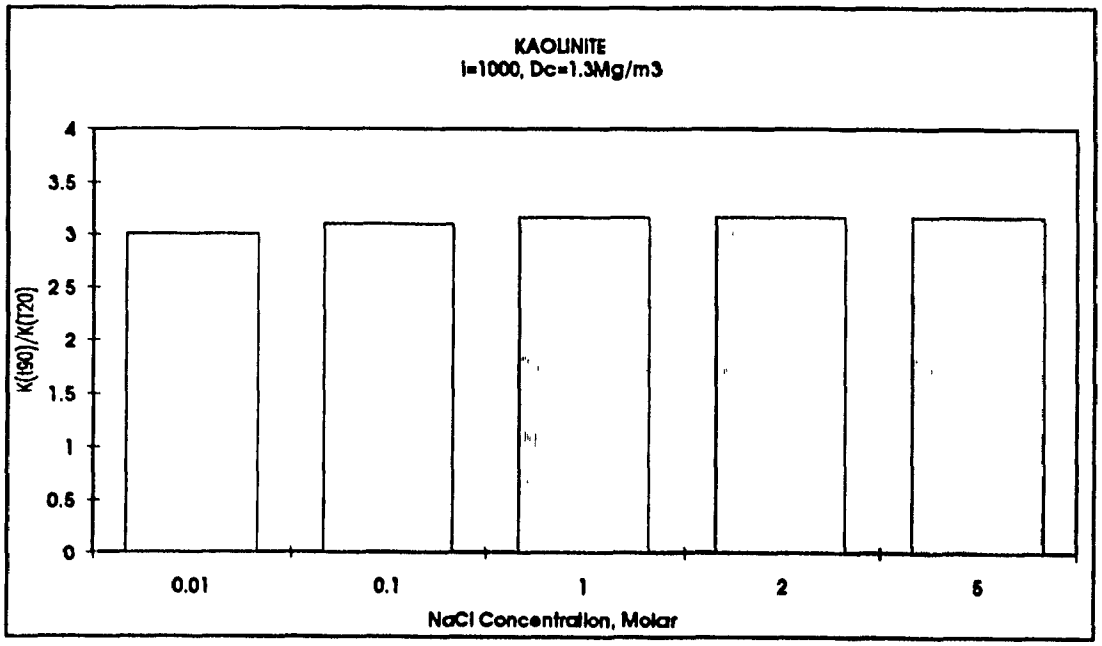

Figure 4.25 Kaolinite, K90/K20 vs NaCl concentration at i=1000 and γ_c = 1.3 Mg / m^3 (Model results)

4.4.3 Effect of Clay Density, γ_c

Figure 4.26 show that hydraulic conductivity is only affected by the clay density, K decreases with increasing clay density. Figures C-104 to C-106 in Appendix C show Log K vs clay density for NaCl and $CaCl_2$ concentrations of 0.01 and 1 Molar and hydraulic gradients ranging between 200 and 2000.

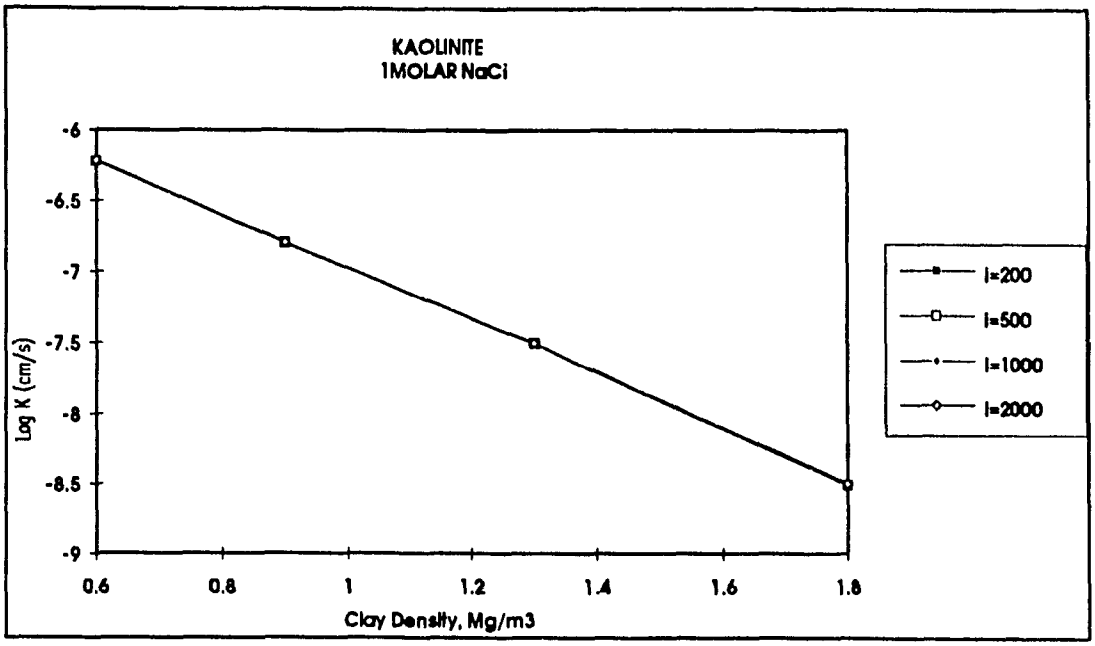

Figure 4.26 Kaolinite, Log K vs γ_c at different Hydraulic Gradient and 1M NaCl concentration (Model results)

4.4.4 Effect of Hydraulic Gradient, i

Typical graph in Figure 4.27 shows that the variation of hydraulic conductivity with hydraulic gradient is very small for kaolinitic clay minerals. This is explained by the fact that surface forces are less dominant in kaolinite. More results in Figures C-107 to C-109 in Appendix C show Log K vs NaCl and $CaCl_2$ concentration at clay densities 1.3 and 1.8 Mg / m^3 and hydraulic gradients ranging between 200 and 2000.

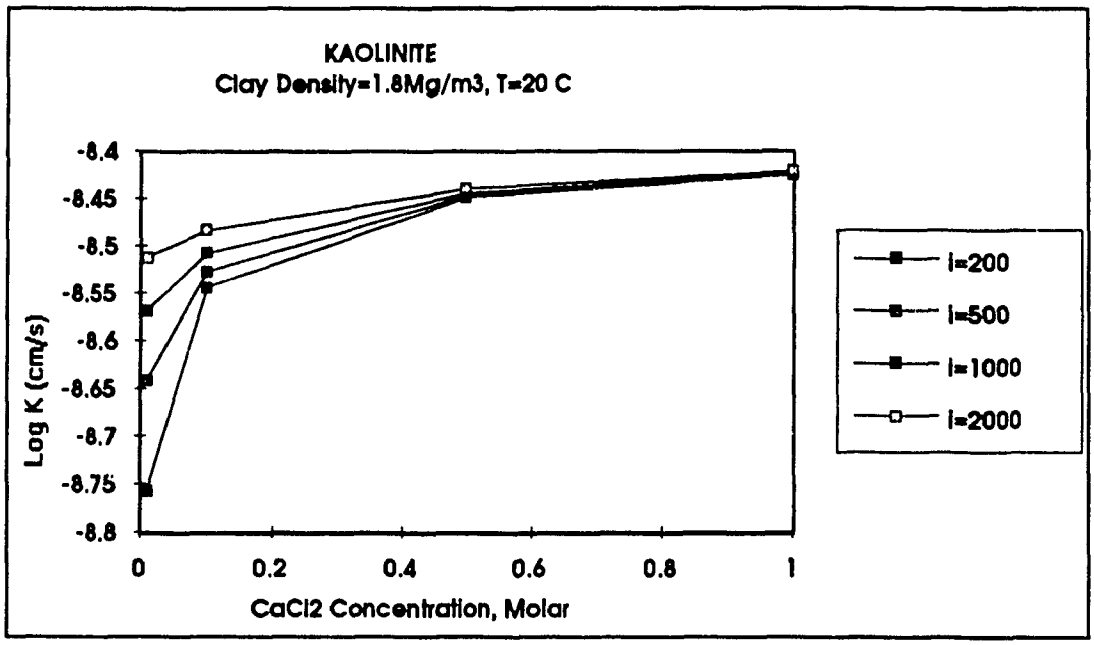

Figure 4.27 Kaolinite, Log K vs $CaCl_2$ concentration at different Hydraulic Gradient and γ_c = 1.8 Mg / m^3 (Model results)

4.4.5 Effect of Salt Type

Figure 4.28 presents Log K vs hydraulic gradient for NaCl and $CaCl_2$ of 0.5 Molar and clay densities of 1 and 1.5 Mg / m^3. Type of permeant solution has no effect on the hydraulic conductivity of kaolinite. It also shows that the hydraulic conductivity is almost constant for all values of hydraulic gradients. Figures C-110 and C-111 in Appendix C show Log K vs hydraulic gradient for NaCl and $CaCl_2$ concentrations of 0.1 and 1 Molar at different clay densities of 1, 1.5 and 1.8 Mg / m^3.

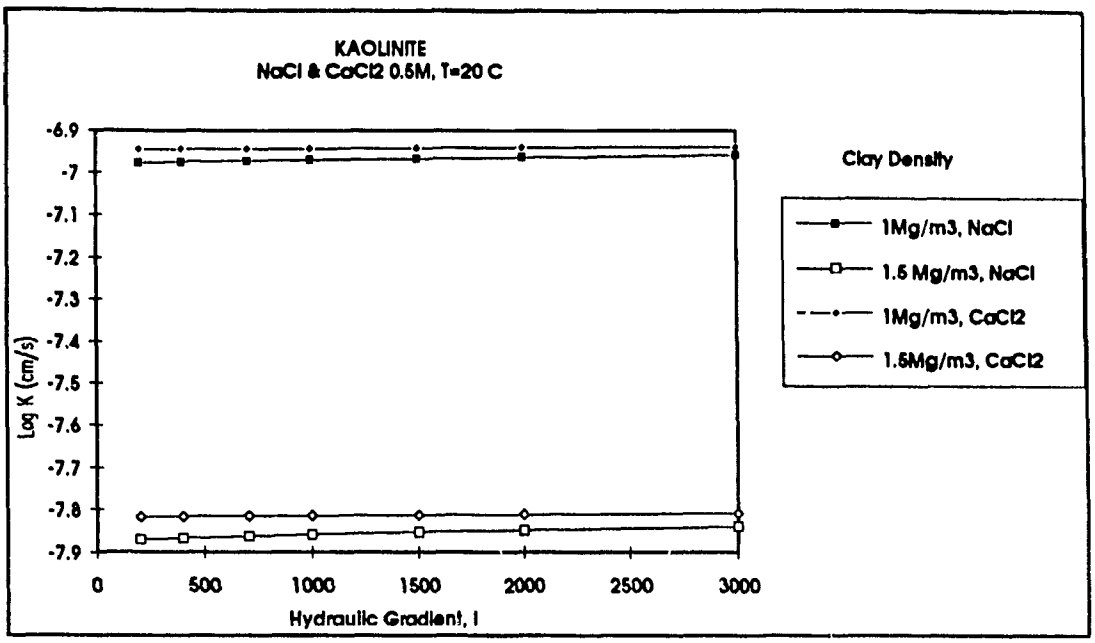

Figure 4.28 Kaolinite, Log K vs Hydraulic Gradient i for 0.5M NaCl and $CaCl_2$ and γ_c = 1 and 1.5 Mg / m^3 (Model results)

4.4.6 Threshold Gradient

Figure 4.29 shows the q vs i curve for kaolinite. The threshold gradient does not exist and the curve is almost linear passing through the origin. This is due to the fact that surface force activities are less in kaolinite and the clay soil starts acting like sand. In Figures C-112 to C-115 in Appendix C a set of graphs were also plotted for the flow rate per unit area q and the hydraulic gradient i.

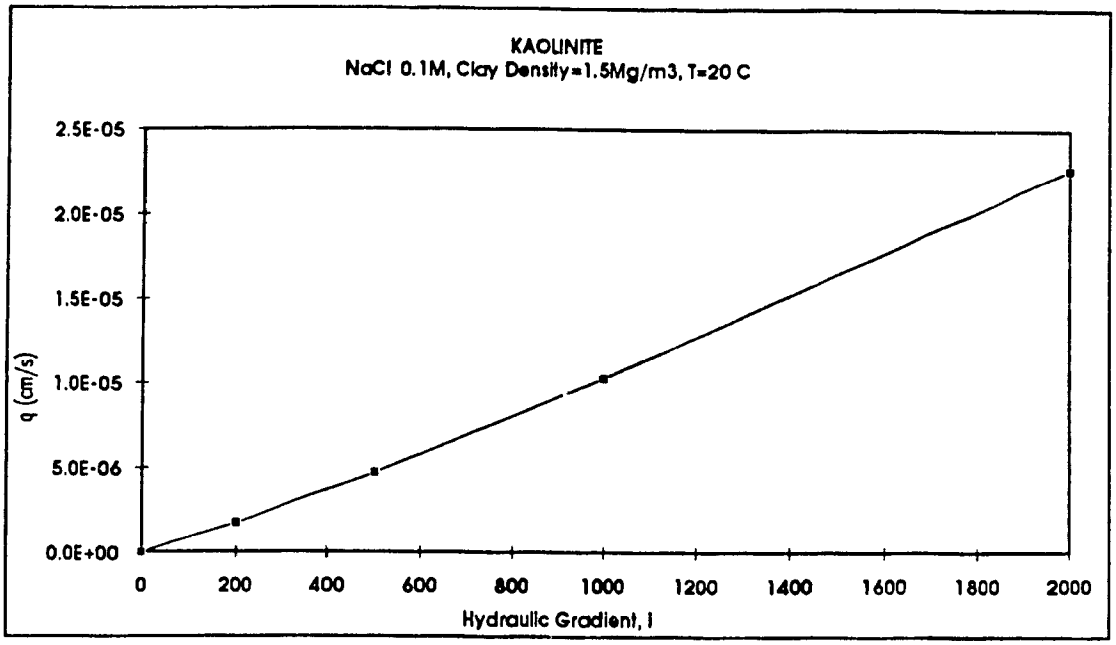

Figure 4.29 Kaolinite, q (cm/s) vs i at 0.1 M NaCl concentration and $\gamma_c = 1.5$ Mg / m^3

4.5 Summary

The modelling results show that hydraulic conductivity depends on the interaction between surface forces and the driving hydraulic gradient The surface forces are dictated by clay type (surface area), clay density, pore water salinity, temperature and soil fabric. The threshold gradient (a gradient at which the flow is insignificant) has been proved to exist specially in montmorillonitic clay minerals

CHAPTER 5

MODEL vs. LITERATURE RESULTS

5.1 Introduction

In this chapter model results are compared with results from available literature. Typical results relevant to this study are introduced from different researchers who did extensive work on the hydraulic conductivity of clay soil. In the first part, model vs. literature results for organic liquids, model results are compared with data from Fernandez 1988. In the second part, model vs. general literature results for inorganic permeants, the effects of changes in each of the environmental factors are compared through literature and model results.

5.2 Model vs. Literature Results For Organic Liquids

In this section the model is tested for two kinds of permeants; water with percentage of Ethanol and water with percentage of Dioxane. Values of kinematic viscosity of the solution and the dielectric constant for different percentages of Ethanol and Dioxane with water are used from Fernandez 1988 (Figures 5.1 and 5.2). Viscosity increases as the hydrocarbon liquid content increase to about 50% and then decreases. The dielectric constant decreases as the hydrocarbon liquid content increases.

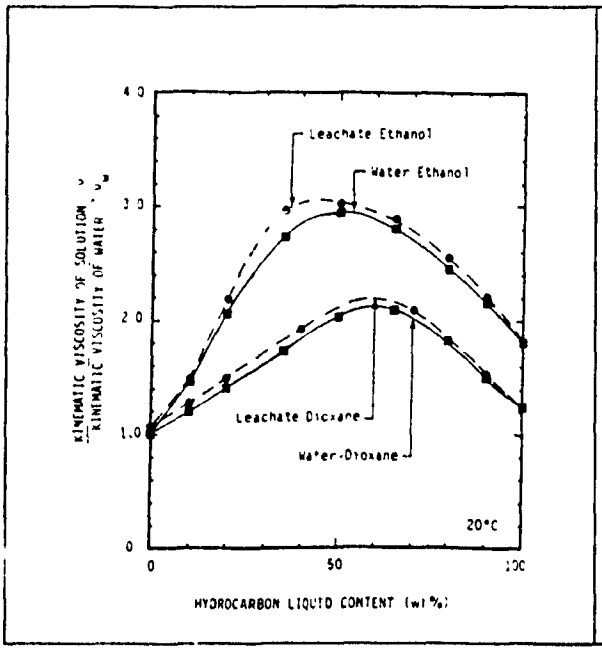

Figure 5.1 Relative viscosity of solutions containing hydrocarbon liquids

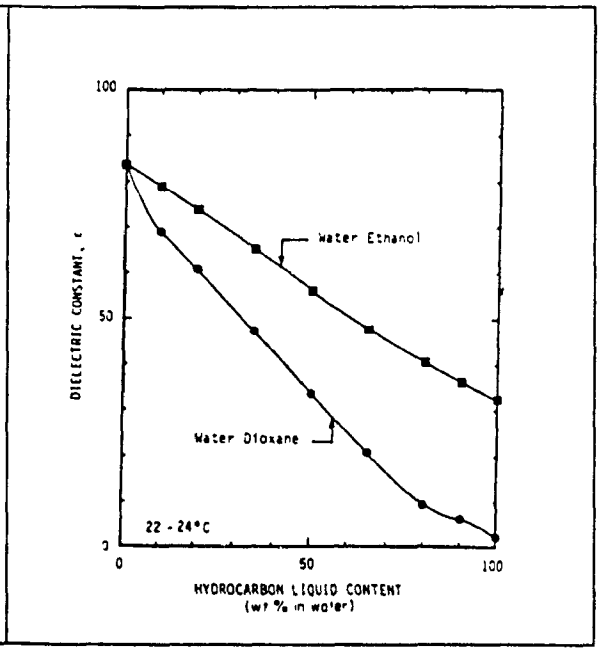

Figure 5.2 Dielectric constant of solutions containing hydrocarbon liquids

The model graphs for hydraulic conductivity and permeability for Ethanol percentages in water are shown in Figures 5.3 and 5.4. These results match qualitatively with the experimental results of Fernandez shown in Figures 5.5 and 5.6.

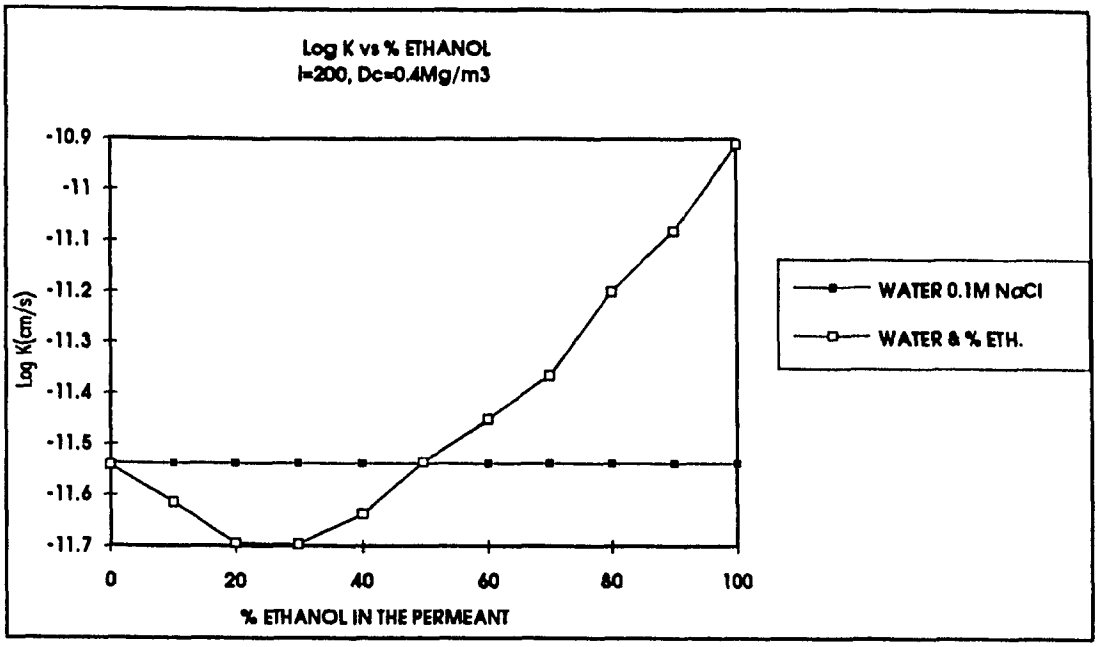

Figure 5.3 Log K vs % of Ethanol in the permeant at Hydraulic Gradient of 200 and $\gamma_c = 0.4$ Mg/m^3 (Model Results)

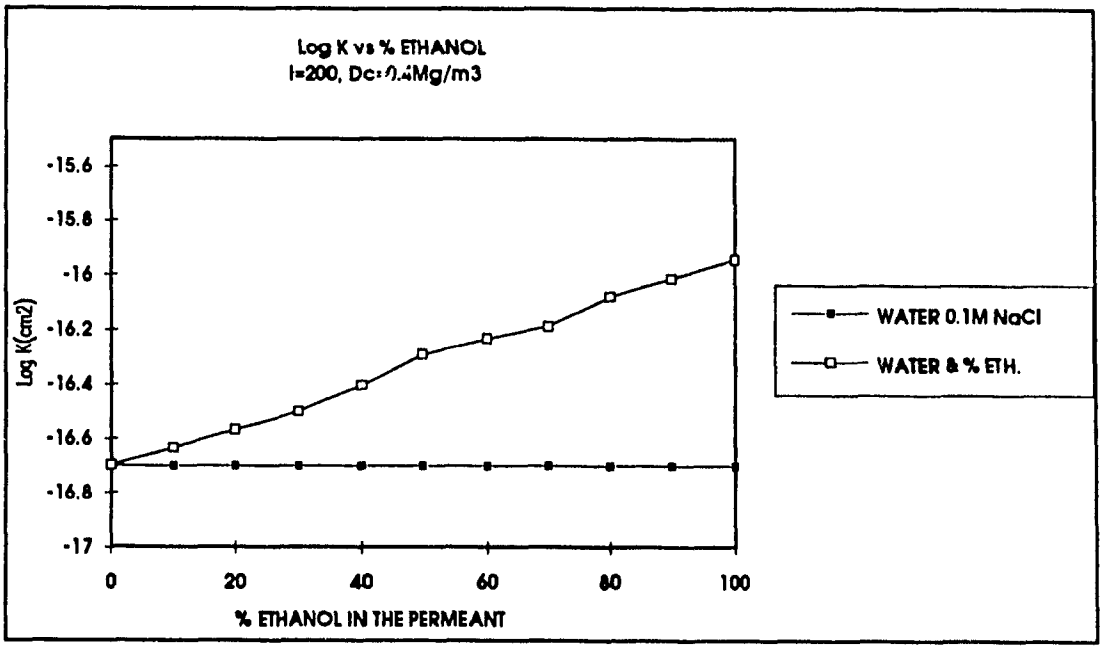

Figure 5.4 Log Permeability vs % Ethanol in the Permeant (Model Results)

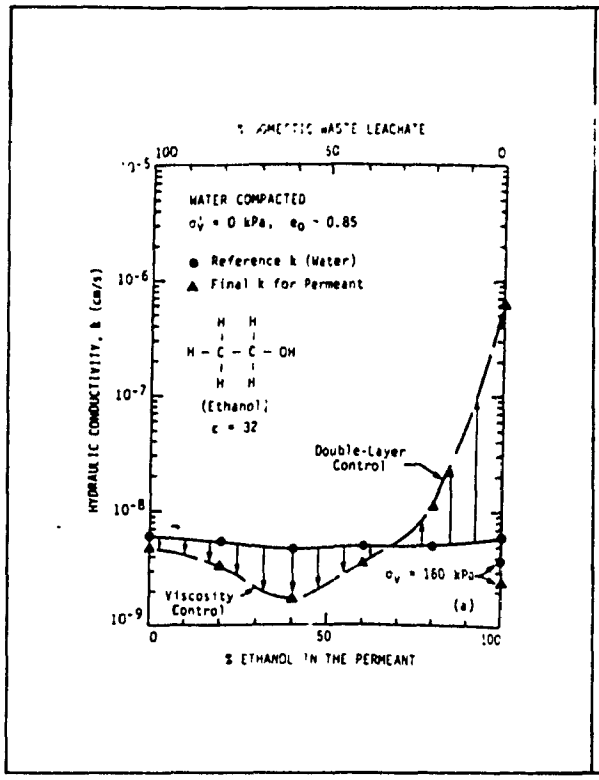

Figure 5.5 Hydraulic conductivity vs % Ethanol in the permeant (Liter. Results)

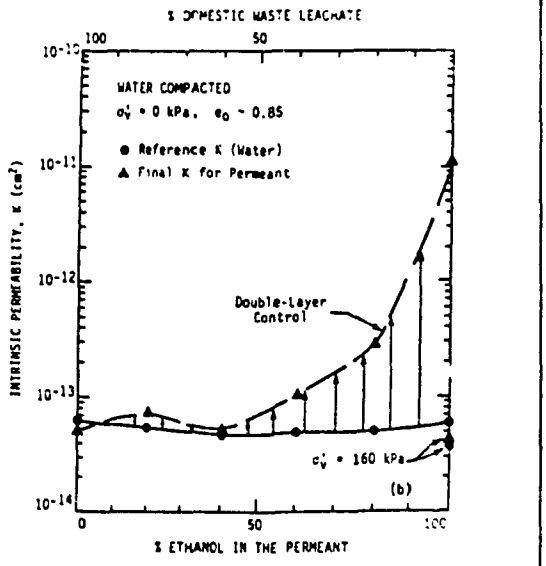

Figure 5.6 Permeability vs % Ethanol in the permeant (Liter. Results)

Hydraulic conductivity variation is due to two effects; one due to viscosity change the second is due to dielectric constant change. An increase in the viscosity decreases the hydraulic conductivity while a decrease in dielectric constant reduces the diffuse double layer and consequently increases the permeability. At low Ethanol percentages viscosity increases and the dielectric constant decreases but as a net effect the increase in the viscosity controls the variation and the hydraulic conductivity decreases. At higher percentages the viscosity starts decreasing and the dielectric constant decreases, in such a case the variation of the dielectric constant controls the system and the hydraulic conductivity increases. As for the variation of the permeability the viscosity has no effect and the double layer controls the permeability, consequently permeability increases as the Ethanol content increases.

The dielectric constant, ε, of a permeant has been widely recognized as a critical parameter affecting the hydraulic conductivity of clays. Liquids having a low dielectric constant may collapse the double layers of water around clay particles, leaving a larger space for permeant flow (at constant void ratio), resulting in large values of permeability.

The same kind of results are obtained for the percentages of Dioxane in the water. The permeants containing up to 70% dioxane produced decreases in hydraulic conductivity, whereas increases were produced by 85 and 100% dioxane. Figures 5.7 and 5.8 show the model and experimental results respectively.

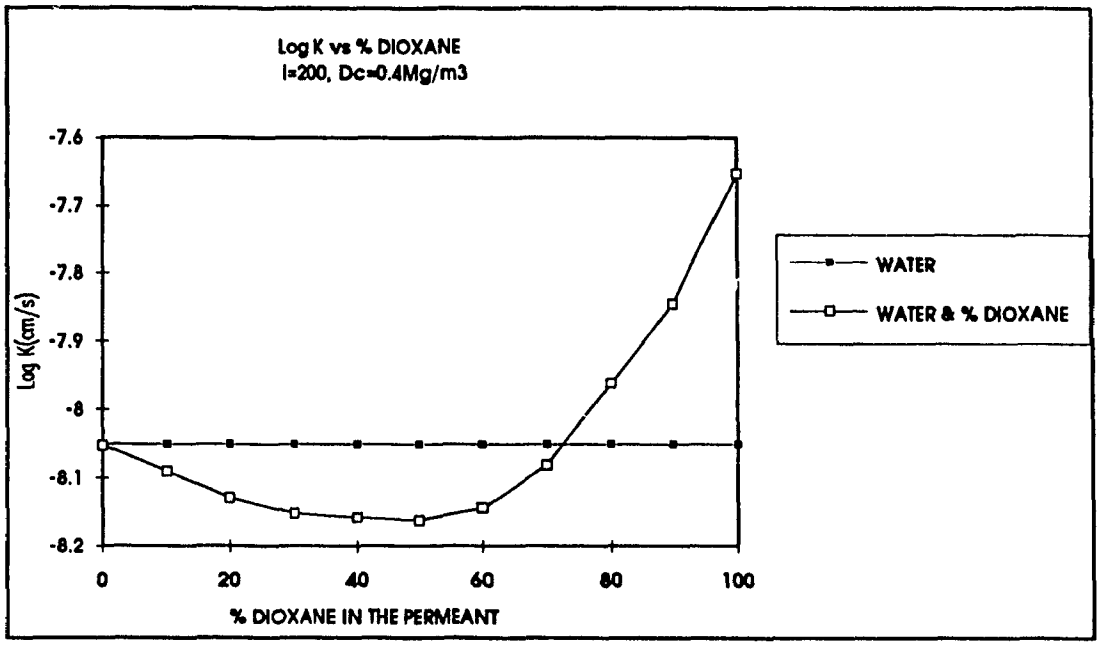

Figure 5.7 Log K vs % of Dioxane in the permeant at Hydraulic Gradient of 200 and $\gamma_c = 0.4$ Mg/m^3 (Model Results)

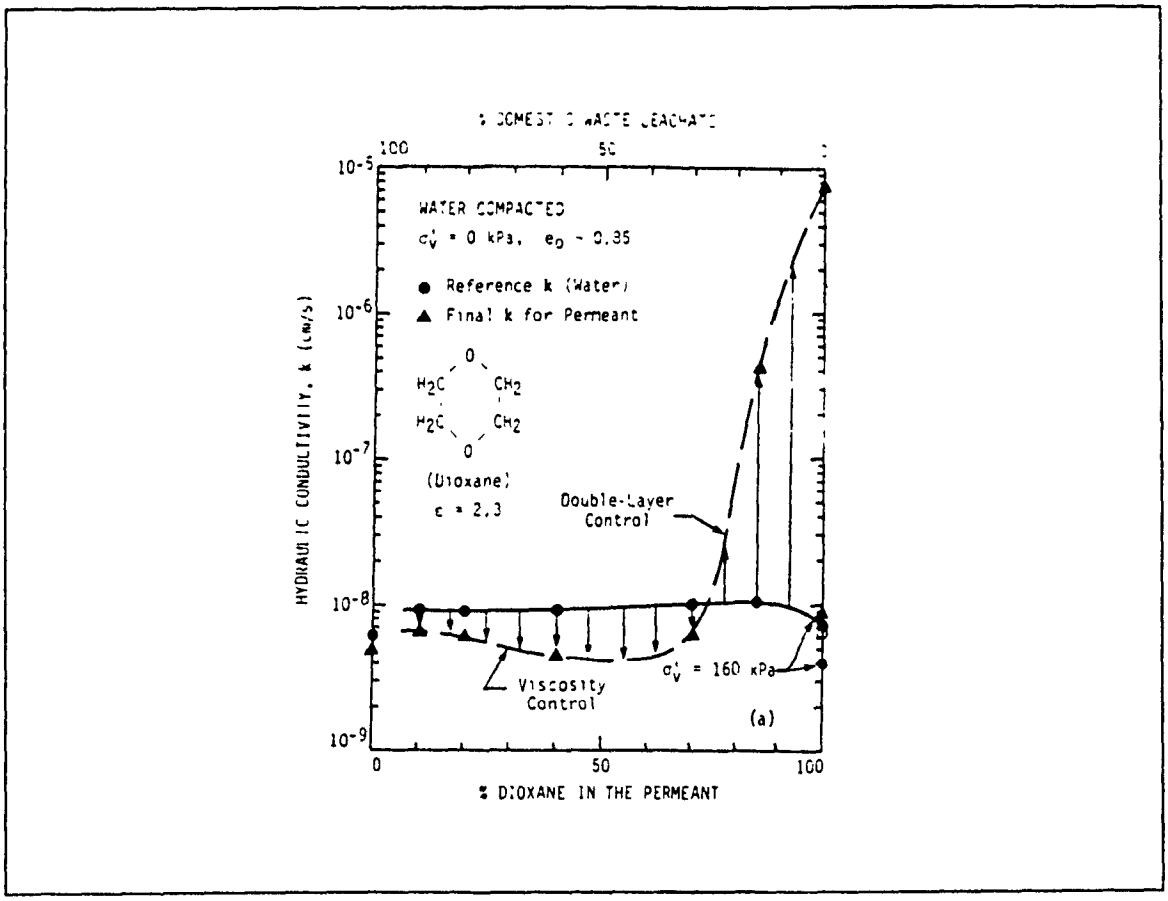

Figure 5.8 Hydraulic conductivity vs % Ethanol in the permeant (Liter. Results)

From this analysis we conclude that the model can predict qualitatively the variation of the hydraulic conductivity and permeability with changes in Ethanol and Dioxane percentages in water. It is also clear the separate effects of viscosity and the diffuse double layer and the dominance of one on the other with respect to the hydraulic conductivity.

5.3 Model vs. General Literature Results (Inorganic Permeants)

5.3.1 Clay Type

At the same dry density, mixtures containing montmorillonite possess much lower hydraulic conductivity than similar mixtures containing kaolinite or illite Table 5.10. This tends to confirm the significance of the surface activity of the clay and the lack of mobility of bound water. The model predicts these results as shown in Figure 5.9.

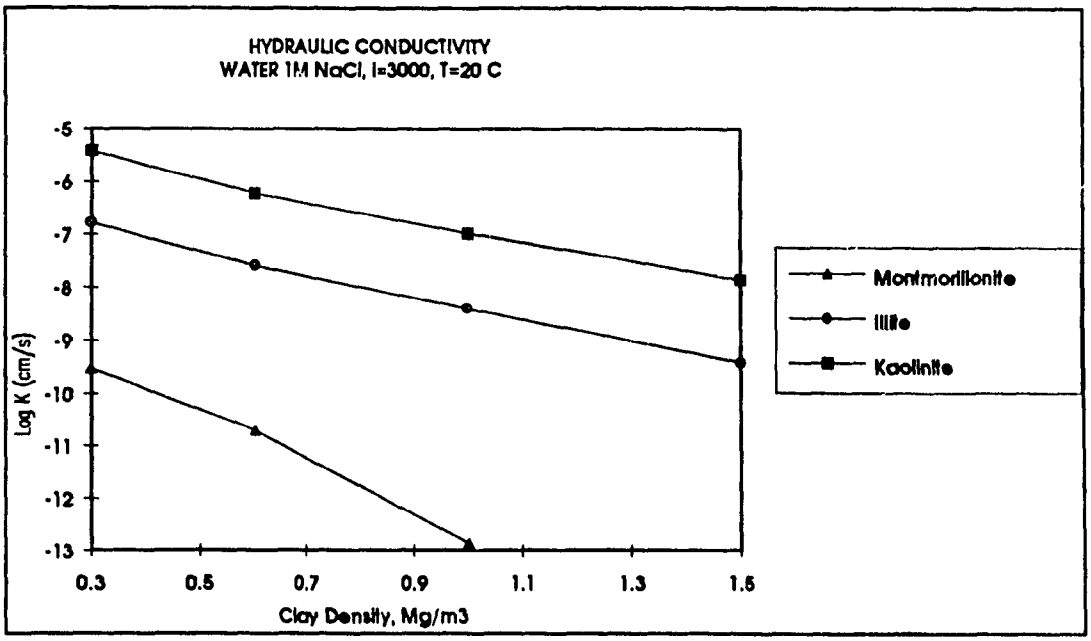

Figure 5.9 Log K vs γ_c for Montmorillonite, Illite and Kaolinite at 1M NaCl and i=3000 (Model Results)

5.3.2 Hydraulic Gradient - i

In the previous chapter it was shown through the model that hydraulic conductivity increases as hydraulic gradient increase. Experimental results (after Zrymiak, 1985) shown

in Table 5.1 agree with this result. At hydraulic gradient of 202 Brine solution was permeated through the soil and the hydraulic conductivity was increased.

Table 5.1 Hydraulic Conductivity vs Hydraulic Gradient, $\gamma_c = 0.38$ Mg/m^3 (Experimental results after Zrymiak 1985)

Hydraulic Gradient, i	Hydraulic Conductivity, cm/s
25	5.2×10^{-8}
51	6.2×10^{-8}
101	1.7×10^{-7}
202	1.2×10^{-6}
202 Brine Solution	2.4×10^{-6}

Table 2.4 (Chapter 2) shows the values of hydraulic conductivities for selected mixtures containing montmorillonite or illite, measured under hydraulic gradients ranging from 30 to 10 000.

The presented data are typical of results in literature, which showed the following:

(i) For most mixtures containing illite as the predominant clay mineral hydraulic conductivity increased as the hydraulic gradient was increased. Model results shown in Figure 5.10 confirm literature data.

(ii) In mixtures containing montmorillonite as the predominant clay mineral, with clay densities less than approximately 1.25 Mg/m3, hydraulic conductivity generally increased as the hydraulic gradient was increased. Figure 5.10 show the model results.

(iii) For montmorillonite soils with densities greater than approximately 1.25 Mg/m3, i had little effect on K. This was explained by the macropores phenomenon.

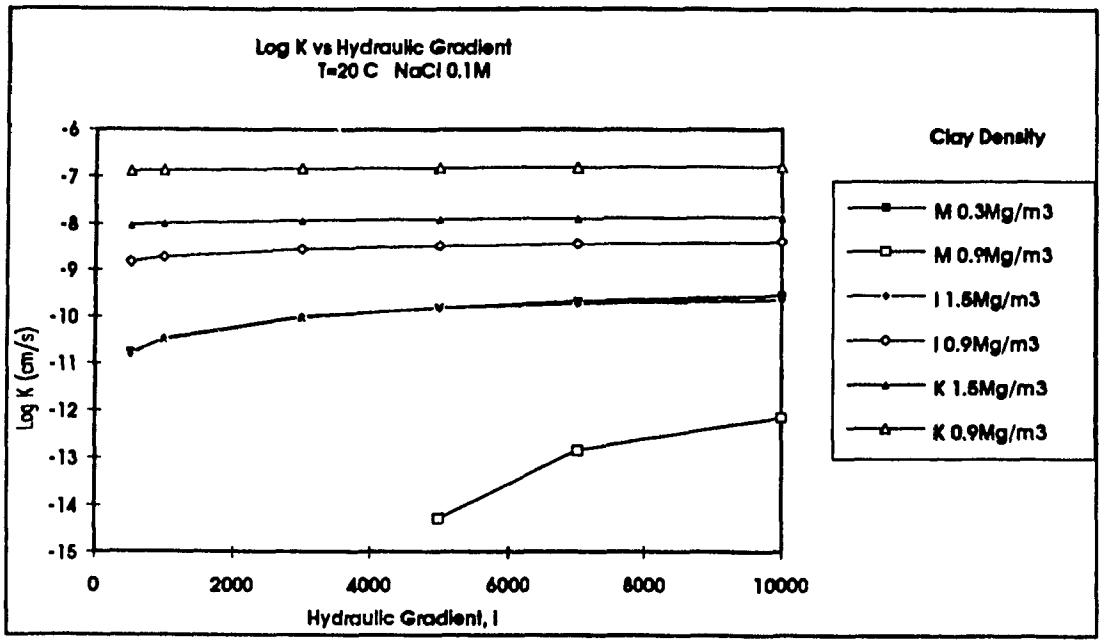

Figure 5.10 Log K vs Hydraulic Gradient for Montmorillonite (M), Illite (I) and Kaolinite (K) at 0.3, 0.9 and 1.5 Mg/m^3 and 0.1M NaCl (Model Results)

Experimental results in literature suggest that, a gradient of less than 400 for illitic and 3000 for montmorillonite systems is insufficient to mobilize all the water in the pore space available for flow. At these gradients, in illitic systems of moderately high densities and in montmorillonitic systems of lower densities, the bonds between the water and the clay are stronger than the shear stress causing the flow. The model predicts this phenomenon by considering the effects of the diffuse double layer.

Table 5.2 shows the effect of pressure on the hydraulic conductivity from experiments by Lutz and Kemper (1958). Changing the pressure differential across the clay sample had varying effects on the different clays. All Na clays were more permeable to water and to electrolyte solutions than would have been predicted from the increase in pressure; that is, the hydraulic conductivity increased proportionally more than the pressure. Apparently the water films were progressively destroyed as the pressure was

increased. In Ca clays, with a restricted diffuse layer and water structure, increasing the pressure had practically no effect on hydraulic conductivity.

5.3.3 Water Salinity

Table 5.2 includes data showing the influence of the ionic concentration in the water on the hydraulic conductivity of Na and Ca-Bentonite. These data show that hydraulic conductivity increases as the electrolyte concentration increase.

Data available for illite indicates that K increased as the total dissolved solids in the water were increased from 0 to 70 g/l. As predicted by the diffuse double-layer theory, the interparticle forces appear to be active in relatively dense illite systems and will influence K. However, the effects of water salinity on K are very small compared with the effects of density. The variation of K with salinity predicted by the model for illite is shown in Figure 5.11.

Table 5.2 Effects of pressure, adsorbed cations, and electrolyte concentration on the permeability of clays (Exp. Results after Lutz and Kemper, 1958)

Soil Type	P. cms. Hg	k ($x10^{-5}$) Water	k ($x10^{-5}$) 0.005N	k ($x10^{-5}$) 0.5N
Na-Bentonite	10	3.18	7.81	35.3
	40	5.18	13.10	42.70
	70	7.50	18.05	48.50
Ca-Bentonite	10	87.0	166.0	329.0
	40	82.0	146.3	280.0
	70	81.5	135.4	264.0

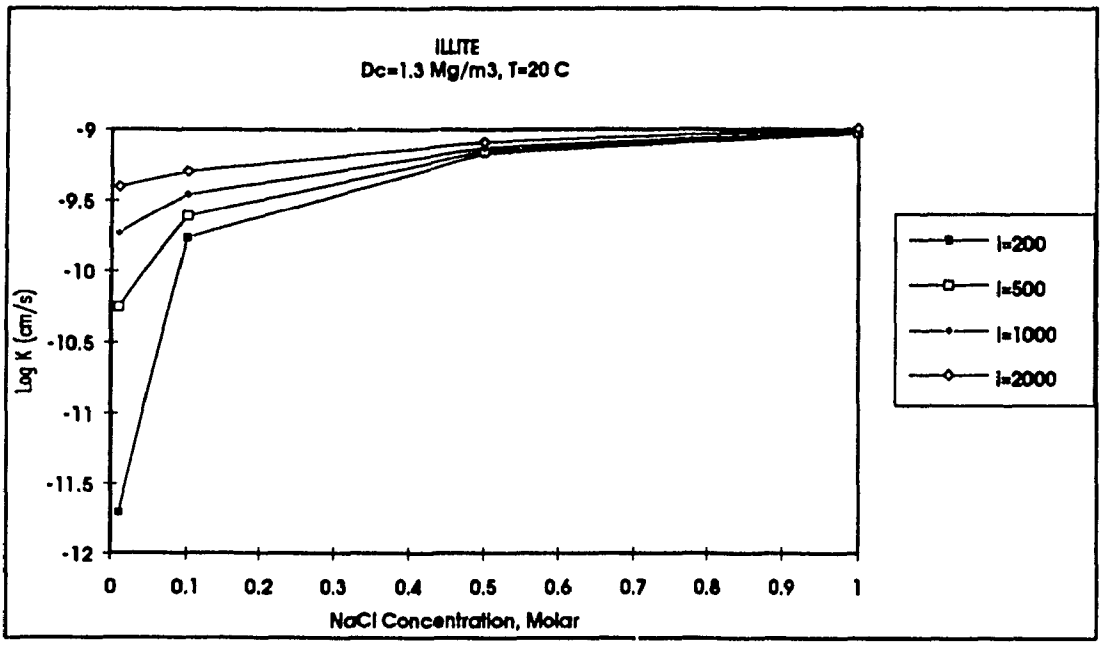

Figure 5.11 Illite, Log K vs NaCl Molar Concentration at Different Hydraulic Gradients and γ_c = 1.3 Mg/m3 (Model Results)

As for kaolinite hydraulic conductivity is almost not affected by the salinity of the water. Figure 5.12 shows the model results of the variation of hydraulic conductivity with hydraulic gradient for montmorillonite, illite and kaolinite at NaCl concentrations of 0.1 and 1 Molar.

5.3.4 Type of permeant

Experimental results (after Zrymiak, 1985) of Log K vs hydraulic gradient for distilled water and brine solution are presented in Figure 5.13. For the soil permeated with brine solution the hydraulic conductivity is higher than with distilled water. This result was predicted by the model and discussed in the previous chapter. Table 5.3 shows values of hydraulic conductivity for distilled water and brine solution at different clay densities γ_c.

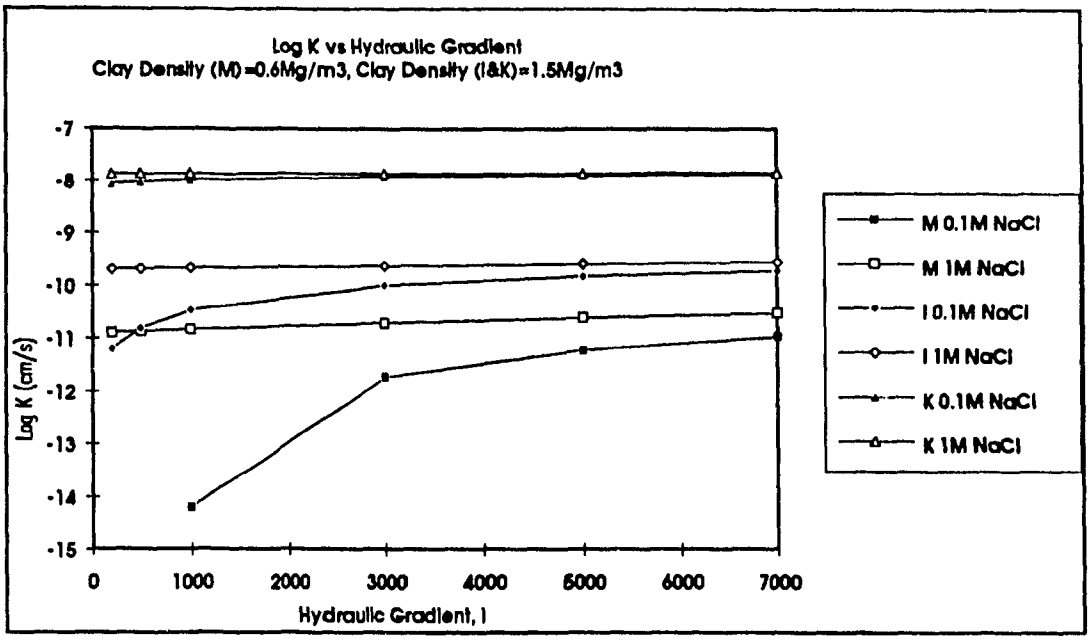

Figure 5.12 Log K vs Hydraulic Gradient for Montmorillonite (M)γ_c = 0.6 Mg/m^3, Illite (I) and Kaolinite (K) γ_c = 1.5 Mg/m^3 at 0.1 and 1 M NaCl (Model Results)

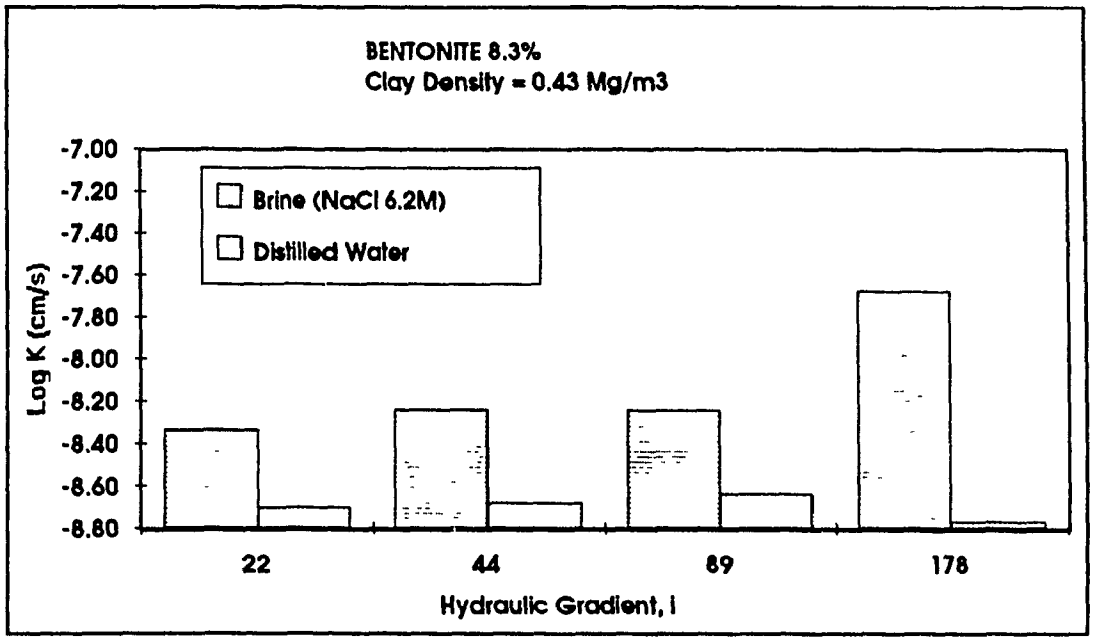

Figure 5.13 Log K vs Hydraulic Gradient at Bentonite content of 8.3% for Brine solution and Distilled Water (Experimental Results, Zrymiak 1985)

Table 5.3 Hydraulic Conductivity of Bentonite for D.W. and Brine Solution (Experimental results after Zrymiak)

Clay Density, γ_c Mg/m^3	K (cm/s), Distilled Water	K (cm/s), Brine
0.38	1.2×10^{-6}	2.4×10^{-6}
0.43	1.7×10^{-9}	5.5×10^{-9}
0.43	1.3×10^{-9}	6.1×10^{-9}
0.51	7.5×10^{-10}	1.8×10^{-9}
0.64	6.0×10^{-10}	7.3×10^{-10}

The model was also tested for NaCl and $CaCl_2$ concentrations in water. For montmorillonite clay K varies with type of salt, for NaCl the hydraulic conductivity is less than that of $CaCl_2$. For illite the variation is less and for kaolinite there is almost no variation. All of these results could be explained to be due to surface activities of clay minerals. The model results are shown in Figure 5.14.

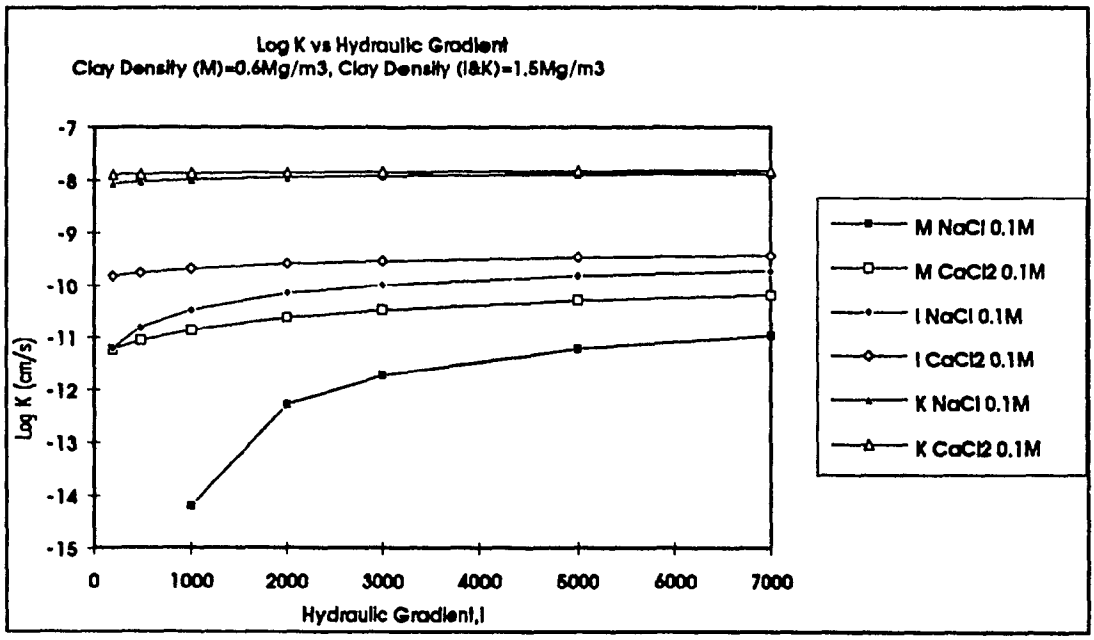

Figure 5.14 Log K vs Hydraulic Gradient for Montmorillonite (M)γ_c = 0.6 Mg/m^3 , Illite (I) and Kaolinite (K) γ_c = 1.5 Mg/m^3 at 0.1M NaCl and $CaCl_2$ (Model Results)

Experimental results in Table 5.2 for Na and Ca - Bentonite, show the variation of hydraulic conductivity with changing the Na to Ca. Two other experimental results are also quoted here, one from P. Rolfe and A. Aylmore (1977) "At the lower electrolyte concentrations permeability increases in the order Na < Ca at a given concentration." The other is from Dunn and Mitchell (1984) " Data from this investigation show the sort of reduction in hydraulic conductivity which may occur due to the use of distilled water in lieu of natural pore water or tap water".

5.3.5 Temperature

Increasing the temperature of a clay-water system potentially increases the hydraulic conductivity by decreasing the viscosity of water or decreases permeability by increasing the osmotic pressure. Because of changes in the viscosity of water alone, increasing the temperature from 25 to 50° or 100°C will increase the hydraulic conductivity by factor of 2 and 3, respectively. Table 5.4 shows literature results for the influence of T on hydraulic conductivity for kaolinite- and montmorillonite-based mixtures.

For kaolinite, the data show that hydraulic conductivity increases with increasing T. The changes are similar to those predicted by the change in water viscosity, and that permeability does not change. This confirms that the interparticle forces are limited in kaolinite and sand/kaolinite mixtures. It is worthwhile here to mention that hydraulic conductivity is affected by viscosity and interparticle forces, while permeability is only affected by interparticle forces. For the mixtures containing montmorillonite, an increase in

Table 5.4 Hydraulic Conductivity of Saturated Clay-Sand Mixtures with Temperature (Literature Results, Dixon and Cheumg, 1985)

	Temperature		
	25°C	50°C	100°C
Montmorillonite, γ_c(Mg/m3)			
1.21 (50% Sand)	4.2×10^{-12}	3.7×10^{-12}	8.0×10^{-12}
1.32 (50% Sand)	2.0×10^{-14}	1.6×10^{-13}	3.0×10^{-13}
Kaolin (Fransham et al., 1981)			
γ_d (Mg/m3)			
1.46 (100% Kaolin)	3.7×10^{-10}	6.0×10^{-10}	1.3×10^{-9}
1.82 (50% Sand)	1.7×10^{-10}	2.4×10^{-10}	6.5×10^{-10}

T does not increase hydraulic conductivity as much as is predicted by the viscosity change relationship. The interparticle forces may play a significant role in determining the effect of temperature on hydraulic conductivity and permeability. Figures 5.15 and 5.16 show ratios of permeability and hydraulic conductivity at 90 and 20 °C for montmorillonite and kaolinite.

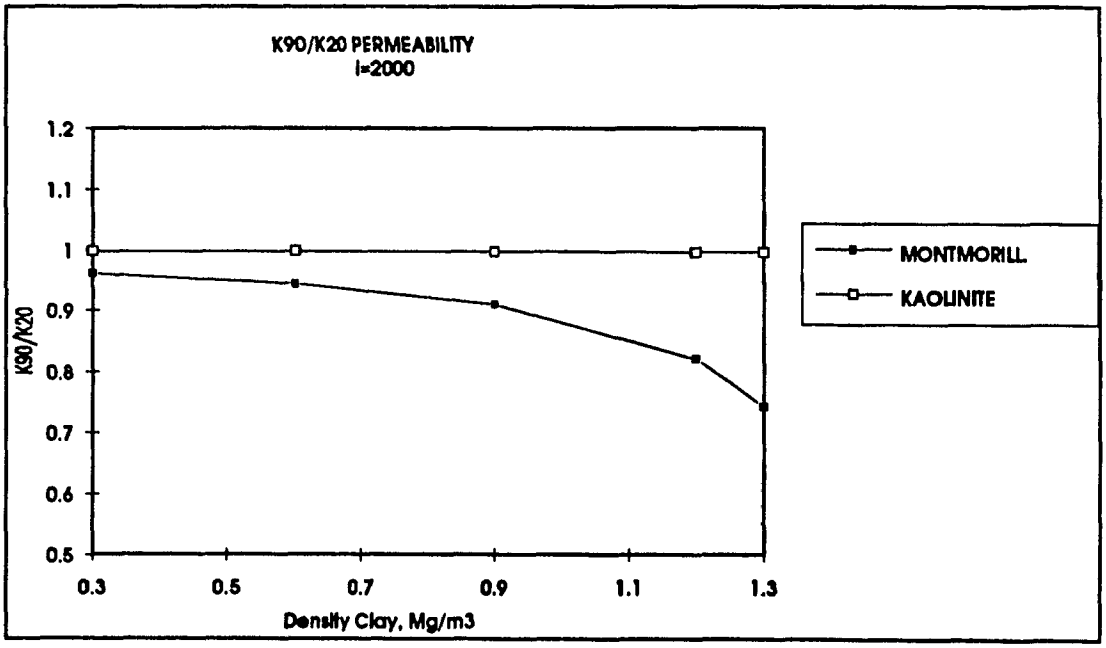

Figure 5.15 Ratio of Permeability (k90/k20) vs Clay Density for Montmorillonite and Kaolinite at i = 2000 (Model Results)

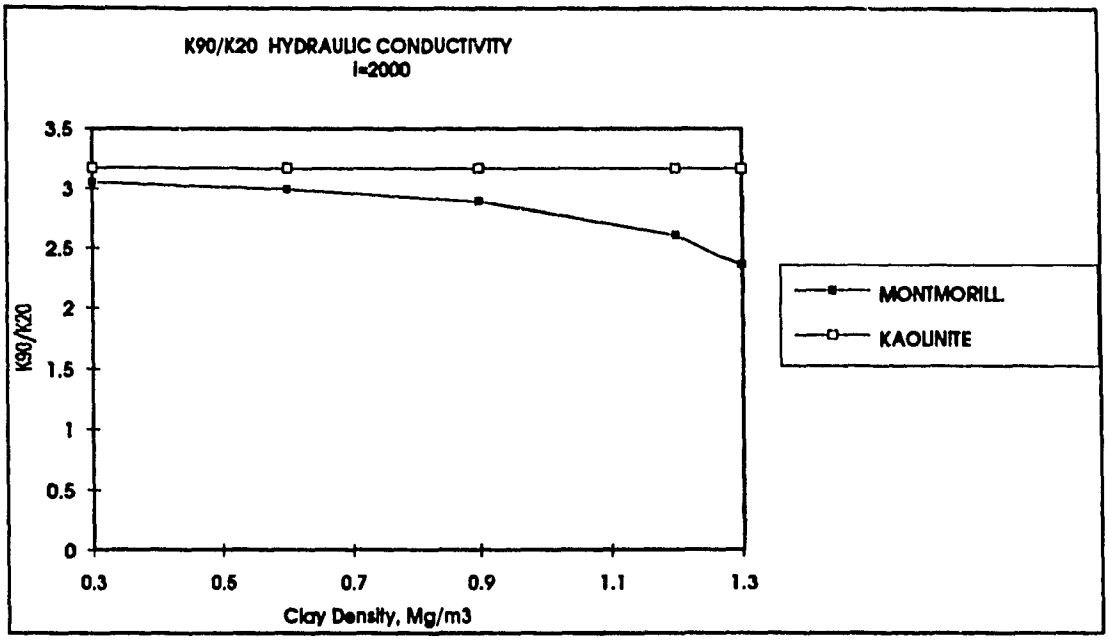

Figure 5.16 Ratio of Hydraulic Conductivity (K90/K20) vs Clay Density for Montmorillonite and Kolinite at i = 2000 (Model Results)

Table 5.5 show experimental data after E. Peterson and S. Kelkar, (1983); from these results we conclude:

i) The ratio of permeability k_{90} / k_{20} is always less than one which means that the higher the temperature the lower is the permeability; this complies with the model results in Figure 5.15.

ii) The ratio of hydraulic conductivity K_{90} / K_{20} is always less than the ratio of the viscosities of the fluid at these temperatures; in the case of water this ratio is ~3.2. These results also comply with the model results in Figure 5.16.

Table 5.5 Hydraulic Conductivity of Bentonite at T = 20 and 90 ^{o} C, i = 3000 (Experimental Results after E. Peterson and S. Kelkar, 1983)

Bentonite (Wt. %)	Saturating Fluid	T ^{o} C	γ_d (Mg/m^3)	k (10^{-9} darcies)	K (10^{-13}m/s)	$\frac{k_{90}}{k_{20}}$	$\frac{K_{90}}{K_{20}}$
100	Deionized water	20 90	2.1	22 12	2.3 3.6	0.545	1.6
100	Brine	20 90	2.15	34 11	1.6 1.7	0.32	1.1
70	Brine	20 90	2.15	205 133	10.3 18.0	0.65	1.75
30	Brine	20 90	2.6	351 160	21.5 23.5	0.46	1.1

As of the variation of threshold gradient with temperature, Miller and Low 1963 did exstensive work on threshold gradient and its variation with temperature. They showed that the threshold gradient decreased with increasing temperature. This same result was obtained through the model as shown in Figure 5.17.

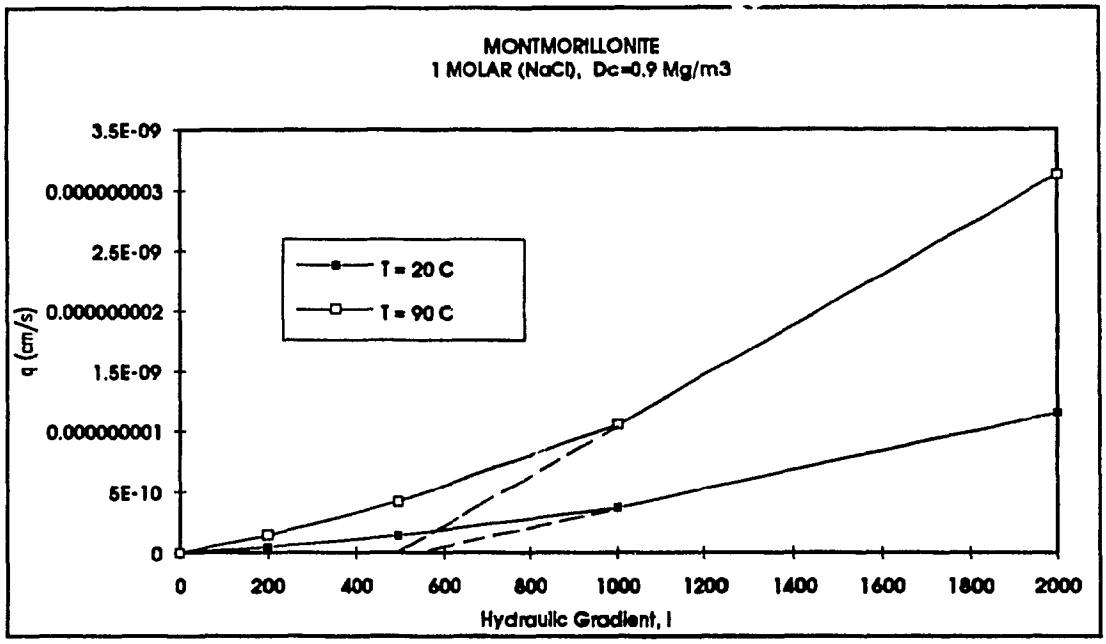

Figure 5.17 Montmorillonite, q (cm/s) vs Hydraulic Gradient for 1M NaCl and γ_c = 0.9 Mg/m^3 at T=20 and 90^{o}C (Model results)

5.3.6 Density, sand content and compaction

This section compares the results of the model with data relevant to density, sand content and compaction. Experimental results, after Zrymiak (1985), for Bentonite contents of 5.7%, 8.3%, 10.7%, 13% by weight, corresponding to different clay densities, at hydraulic gradient of 200 were compared with the model results.

Log K vs clay density γ_c are plotted for model data and experimental data (Figures 5.18 and 5.19). For both cases K decreases as clay density γ_c increases.

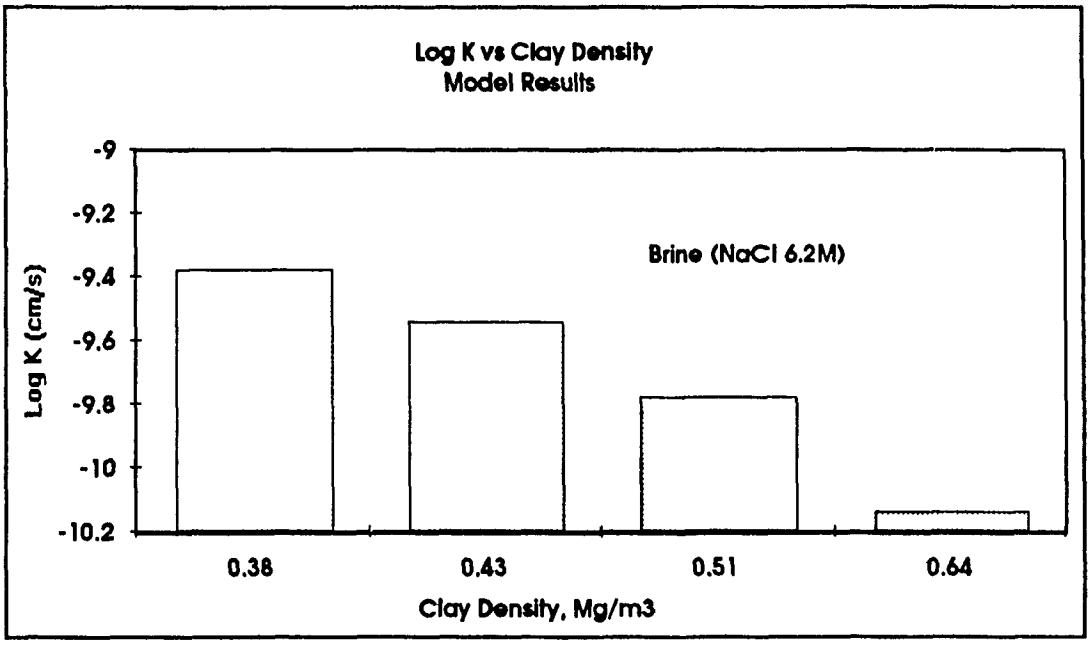

Figure 5.18 Bentonite, Log K vs γ_c for brine (NaCl 6.2M) permeant, (Model Results) Hydraulic Gradient, i = 200

At clay density 0.64 Mg/m^3 the experimental and model values of the hydraulic conductivity are more close than at clay density of 0.38 Mg/m^3. Table 5.6 shows the results in a tabular form. The reason is that higher clay densities are obtained by increasing

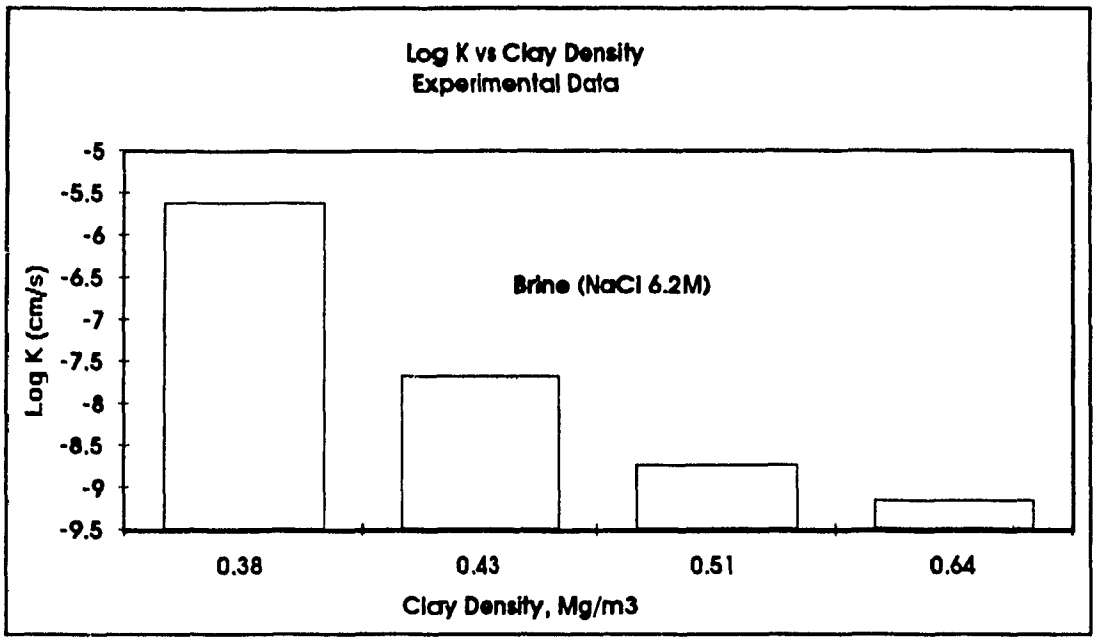

Figure 5.19 Bentonite, Log K vs γ_c for brine (NaCl 6.2M) permeant (Experimental results, after Zrymiak 1985), i = 200

the % Bentonite content by weight. Higher Bentonite contents result in uniform distribution of clay particles around the sand grains thus approaching the assumption that clay particles are uniformly distributed around the sand grains. This gives an insight to the importance of soil fabric in the prediction of soil permeability. We can also conclude that, certain clay content is essential to prevent high water passage.

Table 5.6 Experimental and Model Results of Hydraulic Conductivity with Brine Solution

% Bentonite	γ_d , Mg/m^3	γ_c, Mg/m^3	K model, cm/s	K exp., cm/s
5.7 %	1.90	0.38	4.2×10^{-10}	2.4×10^{-6}
8.3%	1.86	0.43	2.9×10^{-10}	2.1×10^{-8}
10.7%	1.83	0.51	1.6×10^{-10}	1.8×10^{-9}
13%	1.88	0.64	7.0×10^{-11}	6.9×10^{-10}

Figure 5 20 presents experimental (R. Pusch, 1987) and model results for highly compacted montmorillonite. Model results are represented by two curves for highly saline and distilled water. For the highly saline the hydraulic gradient has no effect, while for the distilled water a hydraulic gradient of 5000 is used. Log K is inversely related to γ_c, and n_w' approaches very low values and tends to zero at high γ_c. In fact at these very low n_w' much lower hydraulic conductivities were expected but due to soil fabric, where clay platelets start to form clusters with a lower specific area, the hydraulic conductivity is not decreased as much as it is expected. At these densities the water pathway is in the macropores.

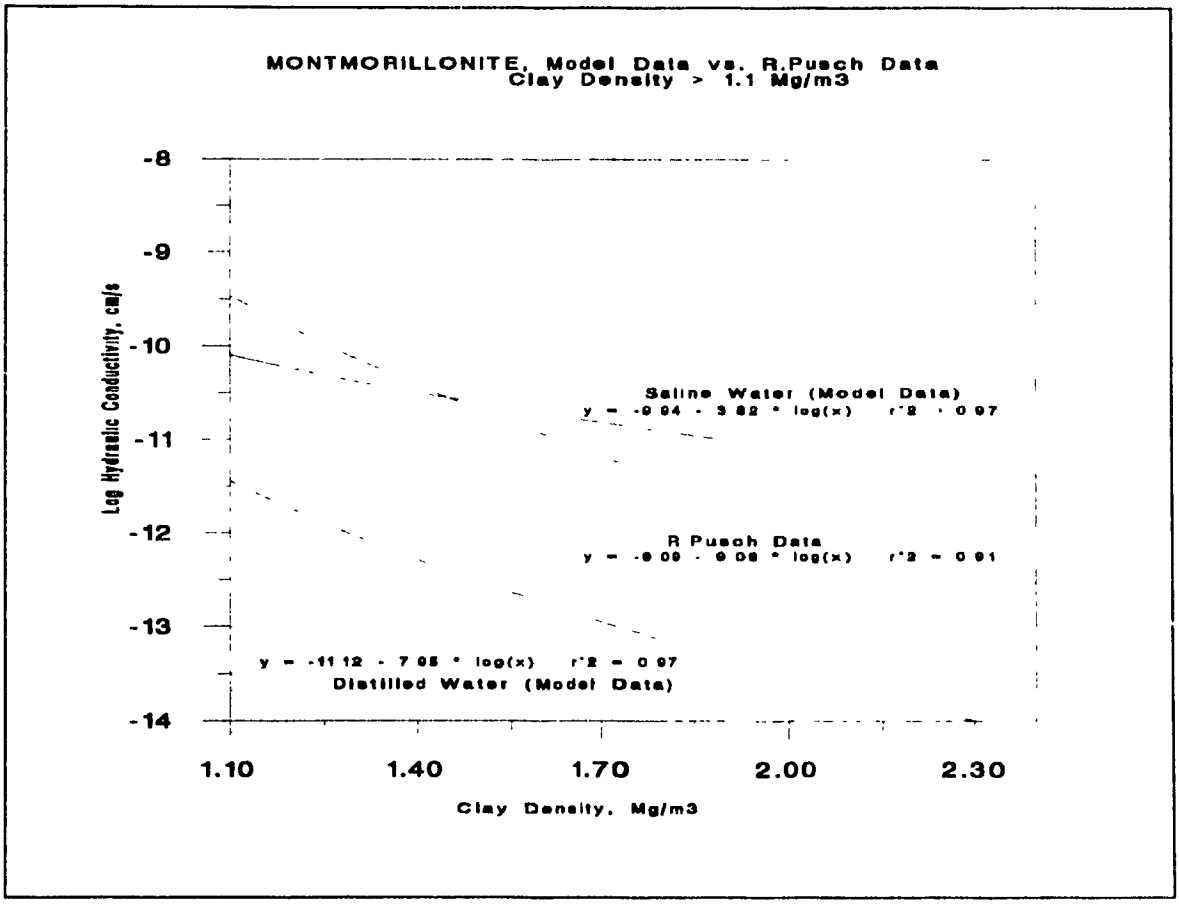

Figure 5.20 Log K vs. γ_c for Highly Compacted Montmorillonite, Experimental Results (R.Pusch,1987) & Model Results

Table 5.7 Maximum Dry Density as a Function of Clay Type, and Sand Content for Sand-Clay Mixtures using the ASTM Modified Compaction Technique (Dixon and Cheung, 1985) Maximum Density Attained (Mg/m3)

% Sand	75	60	50	25	0
Montmorillonite	1.94	1.78	1.75	1.50	1.25
Illite	2.17	2.16	2.15	2.02	1.92
Kaolinite	2.05	1.95	1.82	1.64	1.46

Table 5.8 The Relationship Between Sand Content and γ_c for Montmorillontite

Sand Content %	75	60	50	25	0
Dry Density, γ_d (Mg/m3)	1.94	1.78	1.75	1.50	1.25
Clay Density, γ_c (Mg/m3)	1.07	1.19	1.31	1.31	1.25

Data in Table 5.7 show that increasing the sand content will increase the maximum attainable γ_d. For illitic and kaolinitic systems, there is no significant difference between γ_d and γ_c, hence K decreases with increasing γ_d. Therefore, the addition of a sand component (up to 75% by dry mass) may be advantageous, increasing γ_d and hence reducing the K. For montmorillonitic systems it has been shown that K depends on γ_c rather than γ_d. Table 5.8 presents the results of Table 5.7, recalculated to show the relationship between sand content and γ_c for smectite-sand mixtures. The data show that adding up to 60% of sand (by dry mass) does not significantly alter γ_c of the compacted mixture. This suggests that the effect of sand on the K of a sand-clay system will be insignificant provided that the sand content does not exceed 60%. The γ_c obtained (1.2 Mg/m3) indicates that K is close to the minimum K obtainable for compacted bentonite barriers and further densification will not decrease K.

Data in Table 5.9 are experimental results after Dudson and Chapman, 1981. These experimental results indicate that, the higher the clay content the lower is the

hydraulic conductivity. This same result was obtained by the model knowing that higher clay content at the same dry density resulted in higher clay density and hence lower hydraulic conductivities. We can also see that for Ca-Bentonite between 50% and 100% the hydraulic conductivity has a slight decrease meaning that the addition of bentonite after 50% has no significant effect on the hydraulic conductivity.

Table 5.9 Hydraulic conductivity of Clays and Sand/Clay Mixtures (Experimental Results after Dudson and Chapman, 1981)

Description	Sand : Clay Ratio	K cm/min
Quartz Sand		1.0×10^{-3}
Quartz Sand : mica	9:1	4.6×10^{-4}
	7:3	4.2×10^{-4}
	1:1	5.8×10^{-4}
	0:1	4.9×10^{-4}
Quartz Sand : kaolin	9:1	9.5×10^{-5}
	7:3	8.9×10^{-6}
	1:1	2.5×10^{-6}
	0:1	3.0×10^{-6}
Quartz Sand : Ca bentonite	9:1	4.3×10^{-5}
	7:3	2.1×10^{-6}
	1:1	5.5×10^{-7}
	0:1	2.0×10^{-7}
Quartz Sand : Na bentonite	9:1	1.6×10^{-7}
	7:3	3.0×10^{-8}
	1:1	impermeable
	0:1	impermeable

CHAPTER 6

CONCLUSIONS AND RECOMMENDATIONS

This chapter summarizes the conclusions and recommendations of this thesis. The conclusions are based upon model results compared with available literature results for montmorillonite, illite and kaolinite clays.

6.1 Conclusions

The hydraulic conductivity of compacted clays and sand-clay mixtures depends on clay type, density, electrolyte concentration in the water, type of permeant, hydraulic gradient, temperature and sand content. Changes in the hydraulic conductivity of clay systems related to these variables can be explained by the Kozeny-Carmen relationship and the diffuse double-layer theory. Through the theoretical model developed it was concluded that because of the higher specific surface area and the dominance of bound water in this clay, montmorillonite had a lower K than illite or kaolinite at the same dry density. Montmorillonite and kaolinite represented the two extremeties as of their surface area per gram, while illite represented in between. Results also indicated that montmorillonite was

the clay mineral that was affected the most from changes in environmental factors. The following conclusions are summarized.

- For montmorillonite, an increase in electrolyte concentration resulted in an increase in hydraulic conductivity ranging from one up to three orders of magnitude depending on the hydraulic gradient, clay density and type of electrolyte. For illite, at low concentrations (<1M) and high densities (>1Mg/m^3) there is one order of magnitude increase in hydraulic conductivity with increase in electrolyte concentration. Finally, the hydraulic conductivity of kaolinite is not affected by electrolyte concentration.

- Change of electrolyte from Na+ to Ca++ increased the hydraulic conductivity of montmorillonite by 0.5 to two orders of magnitude depending on concentration, clay density and hydraulic gradient. For illite, at low concentrations (0.1M), low hydraulic gradient (i = 1000) and high clay densities (> 1 Mg/m^3) change of electrolyte from Na+ to Ca++ increased the hydraulic conductivity in the order of five times; while at higher concentrations and higher hydraulic gradients the increase was insignificant. Change of electrolyte had no effect on the hydraulic conductivity of kaolinite.

- Because of the opposite effects of diffuse double layer and viscosity on the hydraulic conductivity of montmorillonite an increase in temperature at low concentrations had no effect, while at high concentrations the increase was due to viscosity. For illite, at low densities the hydraulic conductivity varied with temperature only due to viscosity effect; while, at higher densities and low concentrations it was affected both by the diffuse double layer and the viscosity. As for kaolinite, the variation of hydraulic conductivity with temperature was only due to the variation in the viscosity.

- The hydraulic conductivity can be affected by hydraulic gradient. For montmorillonite clay the hydraulic conductivity increases with increasing hydraulic gradient. For illite clay at low concentrations hydraulic gradient has little effect on hydraulic conductivity; whereas it has no effect at higher concentrations. For kaolinite the hydraulic gradient had no effect on the hydraulic conductivity.

- The hydraulic conductivity decreases with increasing bentonite content in a clay / sand mixture at the same bulk density.

- The hydraulic conductivity in highly compacted clay decreases with increasing clay density. For highly compacted montmorillonite the existence and variation of hydraulic conductivity is due to the presence of macropores.

Through the theoretical model the existence of the threshold gradient and its variation with the environmental factors was demonstrated. For montmorillonite the results are summarized as follows.

- The higher is the electrolyte concentration the lower is the threshold gradient.
- The higher is the temperature the lower is the threshold gradient.
- The higher is the clay density the larger is the threshold gradient.
- The threshold gradient with Na+ electrolyte permeants is greater than with Ca++ electrolyte.

For illite the same effects are found except that the values of the threshold gradients are smaller than for montmorillonite.

For kaolinite, the flow rate versus hydraulic gradient is almost linear and no threshold gradient was detected.

As a final conclusion the model developed can predict qualitatively the effects of environmental factors on the permeability of clay soils. This model could serve as a guideline in setting the ranges of perameters to be tested for permeability tests in the laboratory, depending upon the environmental conditions that might exist in the actual field. Another important conclusion is the existence of the threshold gradient which was proved, through the theoretical model, to exist in montmorillonite clay.

6.2 Applications of Results

In hydraulic barrier design using compacted clay-based materials, it is necessarily required to consider potential changes in the environment under which the barrier will function. Using the model for K developed in this study, it is now possible to assess these parameters and incorporate them into the material selection process.

6.3 Recommendations

Basic research into the following areas should be conducted:

1. A computer program for hydraulic conductivity using the theoretical model developed could be very helpful in designing clay barriers.

2. More experimental work is required to refine the theoretical model through pore size distribution swelling pressure and permeability tests.

REFERENCES

1. Benson, C.H. and Daniel, D.E. (1990). Influence of Clods on Hydraulic Conductivity of Compacted Clay. Journal of Geotechnical Engineering, ASCE, Vol. 116, No. 8, August 1990. pp. 1231-1248.

2. Bodman, G.B. (1937). The Variability of the Permeability "Constant" at Low Hydraulic Gradients During Saturated Water Flow in Soils. Soil Science Society Proceedings, Vol. 2, pp. 45-53.

3. Bucher, F., Jedelhauser, P. and Mayor, P. A. (1986). Quell-Durchlassigkeits- und Schrumpfversuche an Quartzsand-Bentonit-Gemischen, Institut Fur Grundbau und Bodenmechanik, ETH, Zurich, NAGRA Technical Report 86-13.

4. Carmen, P.C. (1956). Flow of gases through porous media, Butterworths, London.

5. Chapuis, R. P. and Montour I. (1992). Evaluation de l'Equation de Kozeny-Carman pour Predire la Conductivite Hydraulique. 45 Canadian Geotechnical Conference, Toronto, October 1992.

6. Chen, Y., and Banin, A. (1975). Scanning Electron Microscope (SEM) Observations of Soil Structure Changes Induced by Sodium-Calcium Exchange in Relation to Hydraulic Conductivity. Soil Science, 120, No. 6, pp. 428-436.

7. Cheung, S.C.H., Gray, M.N. and Dixon, D.A. (1987). Hydraulic and Ionic Diffusion Properties of Bentonite-Sand Buffer Materials, Proc. Symp. on Coupled Processes Associated with Nuclear Waste Repositories, Berkley, California, Academic Press Inc.

8. Cheung, S.C.H., Mouradian, A. and Lee, C.F. (1992). Molecular Diffusion in Dense Bentonite, Proc. 11th Symposium on Engineering Applications of Mechanics, University of Regina, Regina, Saskatchewan.

9. Darcy, H. (1856). Les Fontaines Publiques de la Ville de Dijon (Water Supply of Dijon), Dalmont, Paris.

10. Dixon, D.A., Gray, M.N. and Thomas, A.W. (1985). A Study of the Compaction Properties of Potential Clay-Sand Buffer Mixtures for Use in Nuclear Fuel Waste Disposal. Engineering Geology 21(1985), pp. 247-255. Elsevier Sci. Publ.

11. Dorsey, N.E. (1968). Properties of Ordinary Water-Substance, Hafner Publishing Company, New York.

12. Dudson, P.J. and Chapman N.A. (1981). Geochemical Factors Controlling the Nuclide Release Source Term in Granite: Engineered Barriers for High Level Waste. Environmental Protection Unit, Institute of Geological Sciences, Harwell.

13. Dunn, R.J., and Mitchell, J.K. (1984). Fluid Conductivity Testing of Fine-Grained Soils, Journal of Geotechnical Engineering. ASCE, Vol. 110, No. 11, 1648-1665.

14. Fernandez, F. and Quigley R.M. (1988). Viscosity and Dielectric Constant Controls on the Hydraulic Conductivity of Clayey Soils Permeated with Water-Soluble Organics. Can. Geotech. J. Vol. 25. p 582-589.

15. Foreman, D.E. and Daniel, D.E. (1986). Permeation of Compacted Clay With Organic Chemicals. Journal of Geotechnical Engineering, ASCE, 112 (7), pp. 669-681.

16. Fransham, P.B., Reesor, S., LaHay, C., Roubanis, D. and Hann, F. 1981. Mechanical and Hydraulic Properties of Two Potential Buffer Materials, Vol. 1, Waterloo Research Institute, Final Report to Atomic Energy of Canada Limited., Project 002-08031, Waterloo Ontario.

17. Fredlund, D.G. (1973). Volume Change Behavior of Unsaturated Soils, Ph.D. Thesis, The University of Alberta.

18. Freeze, R.A., and Cherry, J.A. (1979). Groundwater. Prentice-Hall , Englewoods Cliffs, New Jersey.

19. Frenkel, H., Goentzen, J.O., and Rhoades, J.D. (1978). Effects of Clay Type and Content, Exchangeable Sodium Percentage, and Electrolyte Concentration on Clay Dispersion and Soil Hydraulic Conductivity. Soil Sci. Soc. Am. J., Vol. 42, pp. 32-39.

20. Grauer, R., (1986). Bentonite as a Backfill Material in the High-Level Waste Repository: Chemical Aspects. Swiss Federal Institute for Reactor Research, Wurenlingen.

21. Gray, M.N., Cheung, S.C.H. and Dixon, D.A. 1984. Swelling Pressures of Compacted Bentonite/Sand Mixtures. Proc. 44th Mat. Res. Soc. Conference, Boston, Vol. 44, 1984.

22. Hancox, W.T. 1986. Progress in the Canadian Nuclear Fuel Waste Management Program, in Proc. Can. Nuc. Soc. 2nd Intl.Conf. on Radioactive Waste Management, pp. 1-9, Winnipeg, Manitoba.

23. Hansbo, S. (1960). Consolidation of Clay, With Special Reference to Influence of Vertical Sand Drains. Swedish Geotechnical Institute, Proceedings, No. 18, Stockholm.

24. Hansbo, S. (1973). Influence of Mobile Particles in Soft Clay Permeability. Proceedings of the International Symposium of Soil Structure, Gothenburg, pp. 132-135.

25. Hardcastle, J.H., and Mitchell, J.K. (1974). Electrolyte Concentration-Permeability Relationships in Sodium Illite - Silt Mixtures. Clays and Clay Minerals, 22, 143-154.

26. Harris, A.E. (1931). Effect of Replaceable Sodium on Soil Permeability. Soil Science, 31, 435-446.

27. Kemper, W.D. (1960). Water and Ion Movement in Thin Films as Influenced by the Electrostatic Charge and Diffuse Layer of Cations Associated with Clay Mineral Surfaces. Soil Sci. Soc. Amer. Proc., 24, 10-16.

28. Kharaka, Y.K., and Smalley, W.C. (1976). Flow of Water and Solutes Through Compacted Clays. The American Association of Petroleum Geologists Bulletin, 60, No. 6, 973-980.

29. Kinsky, J., Frydman, S., and Zaslavsky, D. (1971). The Effect of Different Dielectric Liquids on The Engineering Properties of Clay. Proc. 4th AsianRegional Conf. on Soil Mech. and Found. Eng., Vol. 1, Bangkok, pp. 367-372.

30. Kutilek, M. (1972). Non- Darcian Flow of Water in Soils - Laminar Region. Fundamentals of Transport Phenomena in Porous Media, International Association for Hydrtaulic Research, Elsevier Publishing Company, pp. 327 - 340.

31. Lambe, H. (1932). Hydrodynamics, 6th Ed., Cambridge University Press, London.

32. Lambe, T.W. (1954). The Permeability of Fine Grained Soils. Symposium on Permeability of Soils, ASTM STP 163, 57th Annual Meeting of ASTM, June 1954, pp. 56-67.

33. Lambe T.W. (1958a). The Structure of Compacted Clay. J. Soil Mech. Found. Div., Proc. of ASCE, 84, No. SM2, Paper 1654, 1-34.

34. Lambe, T.W. (1958b). The Engineering Behavior of Compacted Clay. J. Soil Mech. Found. Div., Proc. of ASCE, 84, No. SM2, Paper 1655, 1-35.

35. Lambe, T.W., and Whitman, R.V. (1979). Soil Mechanics, SI Version, John Wiley & Sons , Inc.

36. Law, K.T., and Lee, C.F. (1981). Initial Gradient in a Dense Glacial Till. 10th Int. Conf. Soil Mech. and Found. Engng. Rotterdam, Vol. 1, pp. 441-446.

37. Lutz, J.F., and Kemper, W.D. (1959). Intrinsic Permeability of Clay as Affected by Clay-Water Interaction. Soil Science, 88, 83-90.

38. Mesri, G. and Olsen, R.E. (1971). Consolidation Characteristics of Montmorillonite. Geotechnique, 21, No. 4, pp. 341-352.

39. Micheals, A.S., and Linn, C.S. (1954). Permeability of kaolinite. Ind. Eng. Chem.,l 46, 1239-1246.

40. Miller, R.J., and Low, P.F. (1963). Threshold Gradient for Water Flow in Clay Systems. Soil Sci. Soc. Am. Proc., 27, No. 6, 605-609.

41. Miller, R.J., Overman, A.R., and Peverly, J.H. (1969). The Absence of Threshold Gradients in Clay-Water Systems. Soil Sci. Soc. Am. Proc., 33, No. 2, pp. 183-187.

42. Mitchell, J.K., Hooper, D.R., and Campanella, R.G. (1965). Permeability of Compacted Clay. J. Soil Mech. Found. Div., Proc. of ASCE, 91, SM4, 41-65.

43. Mitchell, J.K., and Younger, J.S. (1967). Abnormalities in Hydraulic Flow Through Fine-Grained Soils. Permeability and Capillarity of Soils, ASTM STP 417, Am. Soc. Testing Mats., pp. 106-139.

44. Mitchell, J.K. (1976). Fundamentals of Soil Behavior, John Wiley and Sons Inc.

45. Olsen, H.W. (1962). Hydraulic Flow Through Saturated Clays. Clay and Clay Minerals, 11, 131-161.

46. Olsen, H.W. (1965). Deviations from Darcy's Law in Saturated Clays. Soil Sci. Soc. Am. Proc., 29, 135-140.

47. Peterson, E. and Kelkars, S. 1983. Laboratory Tests to determine Hydraulic and Thermal Properties of Bentonite-Based Backfill Materials, Contractor Report, SAND 82-7221, Unlimited Release UC-70.

48. Pusch, R. (1980a). Water Uptake, Migration, and Swelling Characteristics of Saturated and Unsaturated, Highly Compacted Bentonite, SKBF/KBS Technical Report, TR-80-11, Stockholm.

49. Pusch, R. (1980b). Swelling Pressure of Highly Compacted Bentonite, SKBF/KBS Technical Report, TR-80-13, Stockholm.

50. Pusch, R. (1980c). Permeability of Highly Compacted Bentonite, SKBF/KBS Technical Report, TR-80-16, Stockholm.

51. Pusch, R., Hokmark, H. and Borgesson, L. (1987). Outline of Models of Water and Gas Flow Through Smectite Clay Buffers. Swedish Nuclear Fuel and Waste Management Co., Stockholm.

52. Radhakrishna, H.S. and Chan, H.T. (1985). Strength and Hydraulic Conductivity of Clay-based Buffers for a Deep Underground Nuclear Fuel Waste Disposal Vault, Atomic Energy of Canada Limited Technical Record, TR-327.

53. Rolfe, P.F., and Alymore, L.A.G. (1977). Water and Salt Flow Through Compacted Clays: I. Permeability of Compacted Illite and Montmorillonite. Soil Sci. Soc. Am. J., 41, 489-495.

54. Schofield, R.K., (1946). Ionic Force in Thick Films of Liquid Between Charged Surfaces. Trans. Far. Soc. 42B.

55. Swartzendruber, D. (1967). Non-Darcian Movement of Soil Water. Int. Soil Water Symp., pp. 208-222.

56. Van Olphen, H. (1977). An Introduction to Clay Colloid Chemistry, 2nd Ed., John Wiley & Sons, Inc.

57. Von Engelhardt, W., and Tunn, W.L.M. (1955). The Flow of Fluids Through Sandstones. Heidelberger Beitr. Mineral. u. Petrographic 2, pp. 12-55.

58. Yang, N. and Barbour, S.L. (1991). The Impact of Soil Structure and Confining Stress on the Hydraulic Conductivity of Clays in Brine Environments. Proceedings of the 2nd Geo-environmental Copnference, Canadian Geotechnical Engineering, Montreal 1991.

59. Yong, R.N and Warkentin, B.P. (1959). Physico-Chemical Analysis of High Swelling Clays Subject to Loading 1st Pan Amer Conf. on Soil Mech. and Found Eng., Mexico City, Mexico, pp. 108-111.

60. Yong, R.N., and Warkentin, B.P. (1975). Soil Properties and Behaviour, Elsevier Scientific Publishing Co., New York.

61. Yong, R.N., Boonsinsuk P., Xu Da-Ming, August 1985. Study of Development of Backfill Formulations for a Nuclear Waste Disposal Vault, Final Report. Geotechnical Research Centre, McGill University, Montreal Quebec.

62. Yong, R.N., Mohamed, A M.O., and Warkentin, B.P., (1992). Principles of Contaminant Transport in Soils, Developments in Geotechnical Engineering 73, Elsevier Scientific Publication, The Netherlands

63. Younger, J.S , and Lim, C I. (1972). An Investigation Into The Flow Behavior Through Compacted Saturated Fine-Grained Soils With Regard to Fines Content and Over a Range of Applied Hydraulic Gradients. Fundamentals of Transport Phenomena in Porous Media, International Association for Hydraulic Research, Elsevier Publishing Company, pp 312-326.

64. Zrymiak, P.A. (1985). Effects of Brine on the Measured Hydraulic Conductivity and Volume Change of a Compacted Sand-Bentonite Mixture. Master Thesis, Civil Engineering Department, University of Saskatchewan, Saskatoon

APPENDIX A

CLAY MINERALOGY

THICKNESS OF THE DIFFUSE DOUBLE LAYER

VARIATION IN VISCOSITY AND DENSITY WITH TEMPERATURE AND PRESSURE

TABLE OF CONTENTS

A-1 Clay Mineralogy

A thorough knowledge of clay mineralogy is essential to fully understand the factors which affect the hydraulic conductivity of clay soils. Clay soils are composed primarily of various types of clay minerals. Each of these clay minerals has its own engineering properties. In many cases, the hydraulic conductivity depends on type of clay mineral.

Clay minerals are small crystalline particles formed by chemical weathering of rock-forming minerals. Silicates are the most important group comprising over 90 percent of the clay minerals on the earth (Lambe and Whitman, 1979). The most common members of the silicate group are kaolinite, illite and montmorillonite. The properties of these three clay minerals vary widely. Kaolinite is a fairly inert and stable clay which is relatively unaffected by the fluids surrounding it. In contrast, montmorillonite is known for its ability to swell many times its original volume when hydrated with an unlimited supply of water. Illite is a clay mineral whose properties are intermediate between those of kaolinite and montmorillonite.

A-1.1 Structural Units

The structural make-up of clay minerals is chiefly responsible for their engineering behavior. The silicate minerals are comprised of two basic structural units. These basic structural units are the silica tetrahedron, and the aluminum or magnesium octahedron. The silica tetrahedron is formed by four silica atoms surrounding an oxygen atom in a tetrahedron shape. Sheets of silica are formed as various silica tetrahedrons join to share cornering oxygen atoms (Figure A-1).

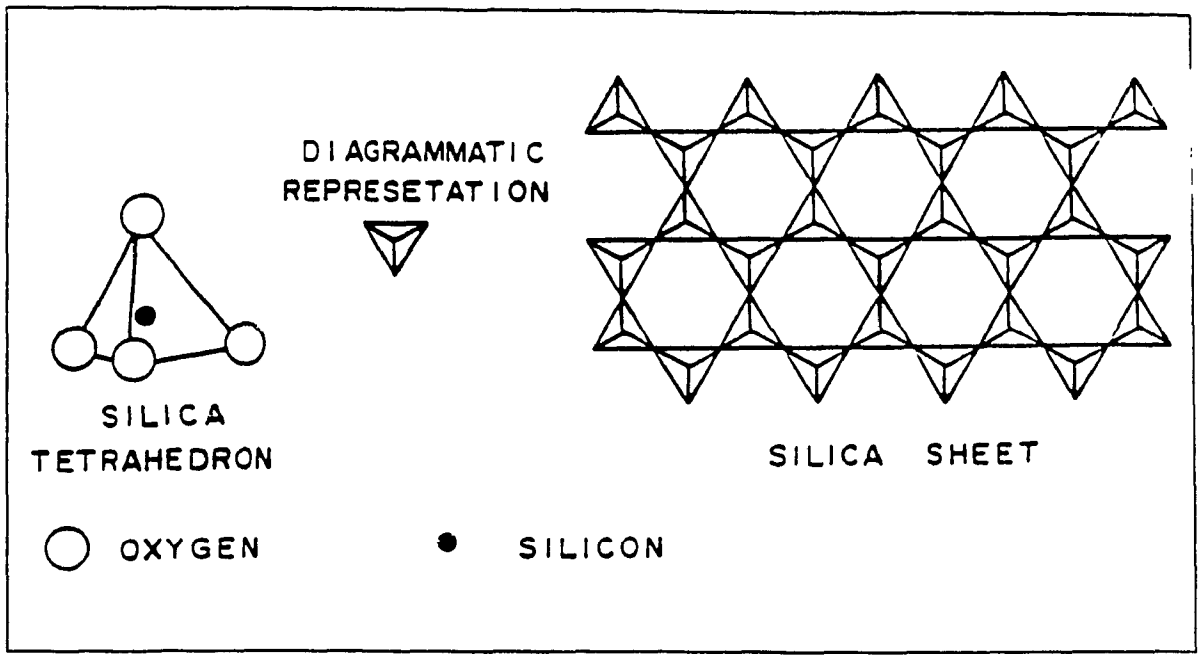

Figure A-1 Silica Tetrahedron and Silica Sheet

The aluminum or magnesium octahedral is formed by six oxygen or hydroxyl atoms surrounding an aluminum or magnesium atom in an octahedral shape (Figure A-2). Various octahedral units share cornering oxygen or hydroxyl atoms to form octahedral sheets. Two types of octahedral sheets are possible. The Gibbsite is formed when most of the cations are aluminum, and the Brucite sheet is formed when most of the cations are magnesium.

A-1.2 Clay Minerals

Clay minerals are formed as the silica and octahedral sheets join to form two or three layer units. The symbols frequently used to diagrammatically depict the various structures found in clay minerals are shown in Figure A-3 with the structures of the three most common clay minerals shown in Figure A-4.

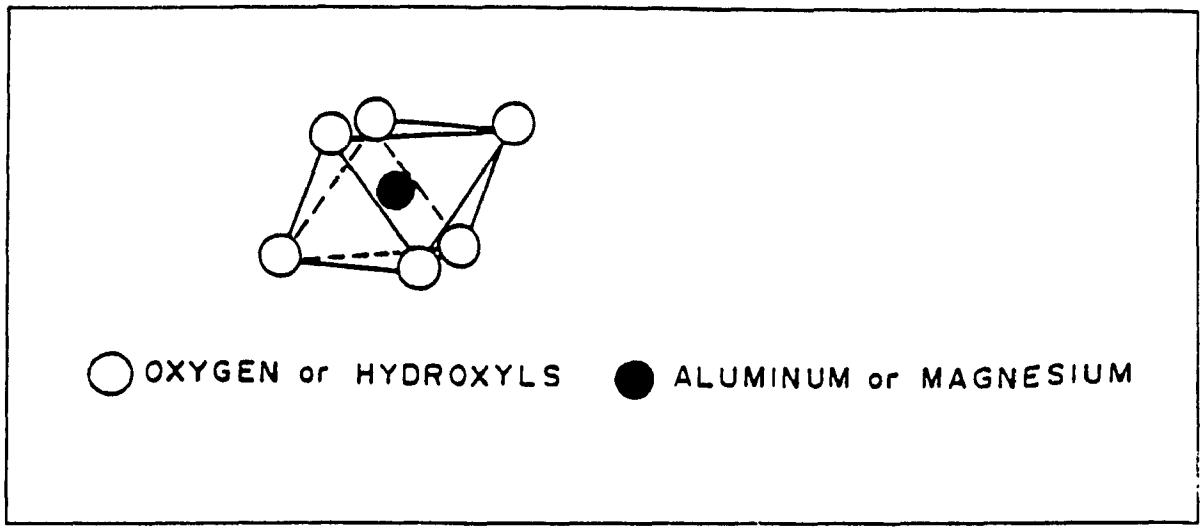

Figure A-2 Octahedral Unit (Re drawn after Mitchell, 1976)

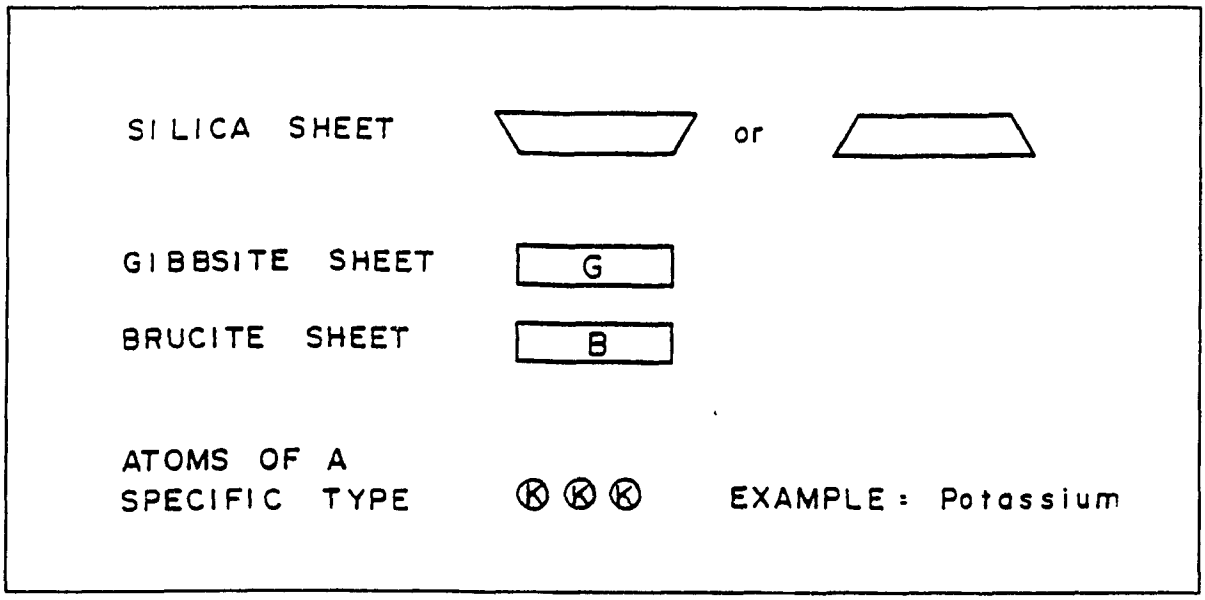

Figure A-3 Symbolic Representation of Silica and Octahedral Sheet

Montmorillonite is a 3 layer clay mineral. It has a net negative charge of - 0.66 per unit cell due to isomorphous substitution of high valency atoms by lower valency atoms in the crystal lattice. Electrical neutrality is reached by the adsorption of cations and other positively charged particles onto the surface of the montmorillonite particle. In a dry state the montmorillonite particles usually exist as stacks held together by Van der Waal forces.

These forces are fairly weak and can be easily broken by the introduction of water. Water molecules are strongly absorbed to the clay surface by electrical forces (termed hydration) and will cause stacks to break into individual particles. The hydrated water molecules which increases the effective size of the montmorillonite particle is the cause of the swelling behavior of montmorillonite soils.

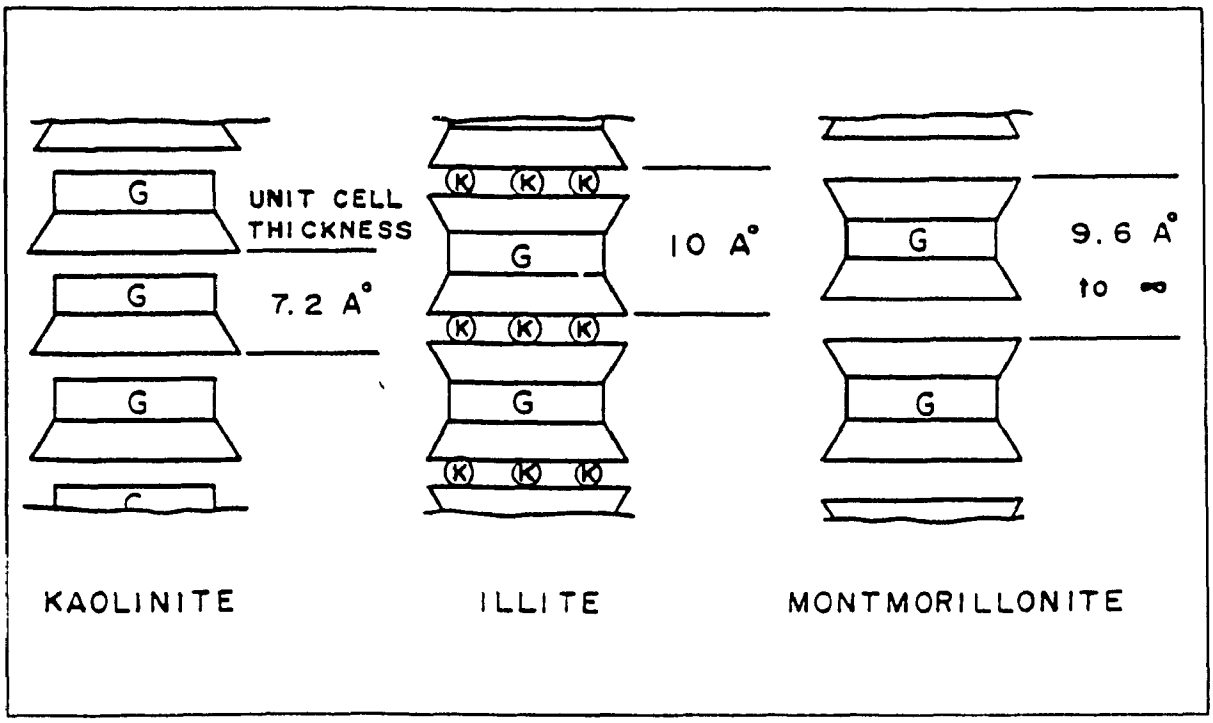

Figure A-4 Symbolic Structure of Kaolinite, Illite, and Montmorillonite

Illite is similar to montmorillonite in structure except that potassium ions strongly bond the individual particles together. Illite has a net negative charge of -1.3 to -1.5 per unit cell, but this is partially offset by the charge of the absorbed potassium ions. Illite exhibits some swelling behavior though the relative amount of swelling is much less than montmorillonite due to the larger size of the clay mineral.

Kaolinite is a two layer clay mineral in which the individual particles are held together by strong hydrogen bonds. The strong hydrogen bonds permits the growth of

large crystals which cannot be easily broken. Kaolinite possesses a small negative charge; however, this clay mineral is not noted for having any appreciable swelling ability.

A-2 Clay Soil Fabric

The geometrical arrangement of the group units, identified as fabric units, constitutes the first-order recognition pattern. The geometrical arrangement of single particles within each fabric unit in turn constitutes the second-order fabric recognition pattern. Response behaviour in clay soils is through fabric unit interaction and through the various bonding mechanisms between units.

A-2.1 Fabric Classification

There are three levels of first-order fabric recognition.

i) Macroscopic: The fabric units are distinguishable with the naked eye. In clay soils, fabric units that can be identified visually with the naked eye, will generally consist of an aggregation of clay particles. These units are defined as "peds".

ii) Microscopic: In the case of clays, single particles will not be distinguishable at this level of viewing. The fabric units identified in the microscopic range consist of several particles or groups of particles and are defined as "clusters". The composition of a cluster is somewhat similar to that of a ped except in regard to size. Clusters can be combined to form peds.

iii) Ultra-Microscopic: Single or individual clay particles can be distinguished at this level. The small fabric units observed and distinguished at this level of viewing are domains or single clay particles. Domain units consist of two or more particles acting as a unit. In general, particles within domains are in parallel array. Several domains could combine to form a cluster.

The most important consideration in the structure and fabric of clay soils is the nature and magnitude of forces originating from the soil particles and fabric units, and between soil and water.

A-2.2 Pore Space and Fabric:

The pores between fabric units are defined as macropores, and the pore spaces within the fabric units as micropores. Soil behaviour in relation to water flow, pore-water extrusion, requires a knowledge of characteristics of water movement in the macro and micropores and also of the rearrangement of fabric units and distortion of individual units. The movement of water in macropores and micropores will be controlled by different sets of forces and conditions.

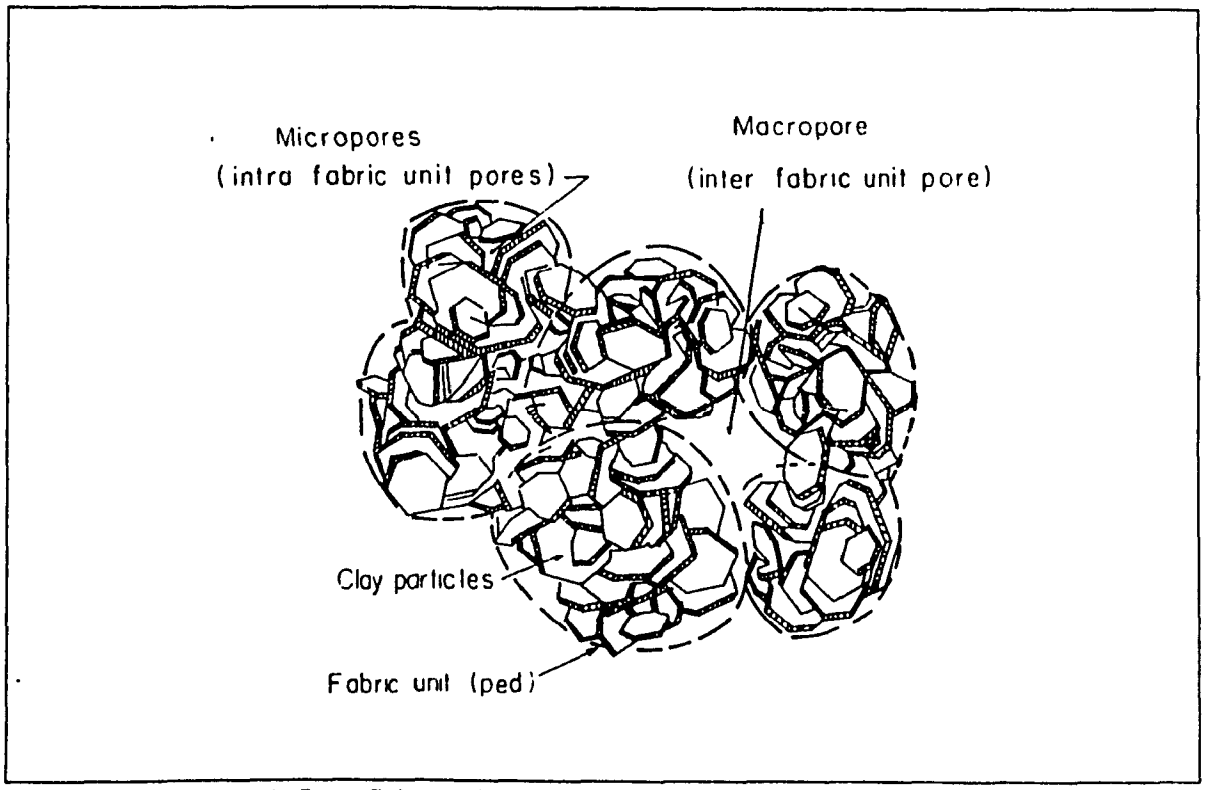

Figure A-5 Schematic diagram showing macro- and micropores
(After Yong and Warkentin, 1975)

Thickness of the Diffuse Double Layer

Thickness of the diffuse double layer (Van Olphen, 1977) :

$$\text{Thickness} = \frac{1}{k} = \sqrt{\frac{\varepsilon BT}{8\pi N_o e^2 Z^2}}$$

where: ε = Dielectric Constant from Table A-1

B = Boltzman Constant, 1.38×10^{-16} erg / ^{o}K

T = Temperature (^{o}K)

N_o = Chemical Concentration (ions / cm^3)

e = Unit electronic charge, 16.0×10^{-20} coulomb, or 4.8×10^{-10} esu

Z = Valence of the adsorbed cation

EXAMPLE:

Type of Adsorbed Cation = Na^+

Temperature = 10 ^{o}C

Concentration = 0.01 M NaCl

N_o = (6.02×10^{23} ions / mole) (0.01 M / liter) (10^{-3} liter / cm^3)

= 6.02×10^{18} ions / cm^3

$$\text{Thickness} = \sqrt{\frac{(84.22)(1.38\times10^{-16})(283)}{8\pi(6.02\times10^{18})(4.8\times10^{-10})^2(1)^2}}$$

= 3.07×10^{-7} cm

= 30.7 A^{o}

Table A-1 Variation of Dielectric Constant of Water with Temperature

°C	°K	Dielectric Constant
0	273	88.25
10	283	84.22
20	293	80.35
25	298	78.49
30	303	76.67
40	313	73.14
50	323	69.78
60	333	66.60
70	343	63.57
80	353	60.61
90	363	58.02
100	373	55.58

Data from Dorsey (1968)

Table A-2 Variation of Viscosity of Water with Temperature and Pressure

Temp. (^oC)	Viscosity (millipoise)	Temp. (^oC)	Viscosity (millipoise)	Temp. (^oC)	Viscosity (millipoise)
0	17.94	17	10.88	34	7.35
1	17.32	18	10.60	35	7.20
2	16.74	19	10.34	36	7.06
3	16.19	20	10.09	37	6.92
4	15.68	21	9.84	38	6.79
5	15.19	22	9.60	39	6.66
6	14.73	23	9.38	40	6.53
7	14.29	24	9.16	45	5.97
8	13.87	25	8.94	50	5.49
9	13.48	26	8.74	55	5.07
10	13.10	27	8.55	60	4.70
11	12.74	28	8.36	65	4.37
12	12.39	29	8.18	70	4.07
13	12.06	30	8.00	75	3.81
14	11.75	31	7.83	80	3.57
15	11.45	32	7.67	85	3.36
16	11.16	33	7.51	90	3.17

Variation in Viscosity with Pressure: Data from Dorsey (1968)

$$v = v_o (1 + KP)$$

where: v = viscosity at temperature, T, and Pressure P

v_o= viscosity at temperature, T, from above

$K = 117 \times 10^{-6}$ per Kg / cm^3

P = Pressure, Kg / cm^2 (1 Kg / cm^2 = 0.9678 atm)

Table A-3 Variation in Density of Air-Free Water with Temperature

Temperature (^{o}C)	Density (gm/cm^3)
0	0.999 8406
5	0.999 9649
10	0.999 7011
15	0.999 1016
20	0.998 2066
25	0.997 0482
30	0.995 6514
35	0.994 0367
40	0.992 2205
45	0.990 2
50	0.988 0
60	0.983 2
70	0.977 8
80	0.971 8
90	0.965 3

Data from Dorsey (1968)

APPENDIX B

DEVELOPMENT OF MODEL EQUATIONS

TABLE OF CONTENTS

Calculation Of Half Distance Between Parallel Plates, X_d

From Yong and Warkentin, 1975

$$W = \frac{S X_d}{100} \qquad \text{(B-1)}$$

in which

W = water content in wt, %

S = surface area of clay, m^2 / g

X_d = half distance between parallel plates, A^o

$$W = \frac{W\,water}{W\,soil} x\,100$$

Assume

W soil = 1 gr.

V water = V soil - V soil particles

$$V\,soil = \frac{1}{\gamma_c}$$

$$V\,soil\,particles = \frac{1}{G_c}$$

Where

γ_C & G_C = soil density and specific gravity g/cm^3

W water = V water x 1

$$W\,water = \left(\frac{1}{\gamma_c} - \frac{1}{G_c}\right)$$

$$W = \left(\frac{1}{\gamma_c} - \frac{1}{G_c}\right) x\,100$$

$$X_d\,(A^o) = 10^4 \left(\frac{1}{\gamma_c} - \frac{1}{G_c}\right) x \frac{1}{S}$$

$$X_d\,(nm) = 10^6 \left(\frac{1}{\gamma_c} - \frac{1}{G_c}\right) x \frac{1}{S\,(m^2/kg)} \qquad \text{(B-2)}$$

Kozeny-Carmen equation

The usual starting point for derivation of Kozeny-Carmen equation is Poiseiulle's law for flow through a round capillary, which gives the average flow velocity according to

$$v_{ave} = \frac{\gamma_p R^2}{8\mu} i_h \tag{B-3}$$

where μ is viscosity, R is tube radius, and γ_p is unit weight of the permeant. Because the flow channels in a soil are of various shapes and sizes, a characteristic dimension is needed to describe average size. The hydraulic radius

$$R_h = \frac{flow\ \ channel\ \ cross\ \ section\ \ area}{wetted\ \ perimeter} \tag{B-4}$$

is useful

For a circular tube flowing full

$$R_h = \frac{\pi R^2}{2\pi R} = \frac{R}{2} \tag{B-5}$$

so Poiseiulle's equation becomes

$$q_{circle} = \frac{1}{2}\frac{\gamma_p}{\mu} R_h^{\,2} i_h a \tag{B-6}$$

where a is the cross-sectional area of the tube. For other shapes of cross section, an equation of the same form will hold, differing only in the value of a shape coefficient C_s, so that

$$q = C_s \frac{\gamma_p R_h^{\,2}}{\mu} i_h a \tag{B-7}$$

For a bundle of parallel tubes of constant but irregular cross section contributing to a total cross sectional area, A (solids plus voids), the area of flow passages A_t filled with water is

$$A_t = SnA \tag{B-8}$$

where S is the degree of saturation and n is the porosity, as shown in Fig. 15.4. For this condition, the hydraulic radius is given by

$$R_h = \frac{A_f}{P} + \frac{A_f L}{PL} = \frac{volume\ \ available\ \ for\ \ flow}{wetted\ \ area} = \frac{V_{water}}{S_o} \quad \text{(B-8)}$$

where P is the wetted perimeter, L is the length of flow channel in the direction of flow, and S_O is the specific surface per unit volume of particles. For void ratio e and volume of solids V_S, the volume of water is

$$V_W = eV_S S \quad \text{(B-9)}$$

Thus

$$q = C_s(\frac{\gamma_p}{\mu}) R_h^2 S n i_h A = C_s(\frac{\gamma_p}{\mu}) R_h^2 S(\frac{e}{1+e}) i_h A \quad \text{(B-10)}$$

and substitution for R_h gives

$$q = C_s V_s^2(\frac{1}{S_o^2})(\frac{\gamma_p}{\mu}) S^3(\frac{e^3}{1+e}) i_h A \quad \text{(B-11)}$$

By analogy with Darcy's law;

$$k_h = C_s V_s(\frac{\gamma_p}{\mu}) \frac{1}{S_o^2}(\frac{e^3}{1+e}) S^3 \quad \text{(B-12)}$$

For the case of full saturation, $V_S = 1$, and $C_S = 1 / k_O \tau^2$ where k_O is a pore shape factor and T is a tortuosity factor, equation (B-12) becomes

$$K = k_h(\frac{\mu}{\gamma_p}) = \frac{1}{k_o \tau^2 S_o^2}(\frac{e^3}{1+e}) \quad \text{(B-13)}$$

Derivation of Gouy-Chapman Theory

The Gouy-Chapman theory considers a negatively charged plate of counter-ion and co-ions. The basic assumptions of the theory are expressed in the following three equations:

The Poisson Equation:

$$\frac{d^2\psi}{dx^2} = \frac{4\pi\sigma}{\varepsilon} \tag{B-14}$$

The Boltzmann Equation:

$$N_i = N_o \, exp\left(\frac{-W_i}{BT}\right) \tag{B-15}$$

with

$$W_i = Z_i \, e \, \psi_i \tag{B-16}$$

where

ε = Dielectric constant

e = electronic charge

B = Boltzmann constant

N_i = the concentration of ions of species i at a point where the potential is ψ_i

T = the absolute temperature

W_i= work done in bringing an ion to point where the potential is ψ_i

x = distance from particle surface

Z_i = ionic valence

σ = surface charge density

ψ = electrical potential

Equation (B-16) shows the relationship between the electric potential and the distance from the particle surface. From Equation (B-15), the local concentration of ions at a distance x from the particle surface can be written as a function of the electric potential.

According to double layer theory, the swelling of clays is due to the osmotic pressure arising from concentration difference between the mid-plane of adjacent particles and the bulk solution. Assuming ideal behavior of the ions and neglecting the attractive forces between the particles, the osmotic pressure can be quantitatively defined by the Van't Hoff equation (Schofield, 1946) which states:

$$P = RT(N_i - N_o) \tag{B-17}$$

in which P denotes the osmotic pressure and R is gas constant. Substituting Equations (B-15) and (B-16) into Equation (B-17) and considering both anions and cations of a symmetrical electrolyte

$$P = 2RTN_o\left(\cosh\frac{Ze\psi_c}{BT} - 1\right) \tag{B-18}$$

From this equation, the factors influencing the osmotic or swelling pressure are concentrations of electrolyte solution, valence of ions, electric potential, electric charge and absolute temperature, provided that the Gouy-Chapman theory is valid.

The value of electric potential, ψ_C can be obtained from the integrated Poisson-Boltzmann equation (Taylor, 1962 and Yang, 1966). The resulting equation derived by Verwey et al, (1948), by assuming infinite surface electric potential is :

$$k X_c = 2\exp\left(\frac{-Y_c}{2}\right)\int_0^{\pi}\frac{d\phi}{\sqrt{1-\exp(-2Y_c)\sin^2\phi}} \tag{B-19}$$

where

$$sin^2\phi = \frac{exp(-Y)}{exp(-Y_c)}$$

$$k = \sqrt{\frac{8\pi Z_i^2 e^2 N_o}{\varepsilon B T}}$$

X_C= the half distance between two parallel plates (Figure B-1).

Y_C= electric potential in the line midway between parallel interacting particles (Figure B-1).

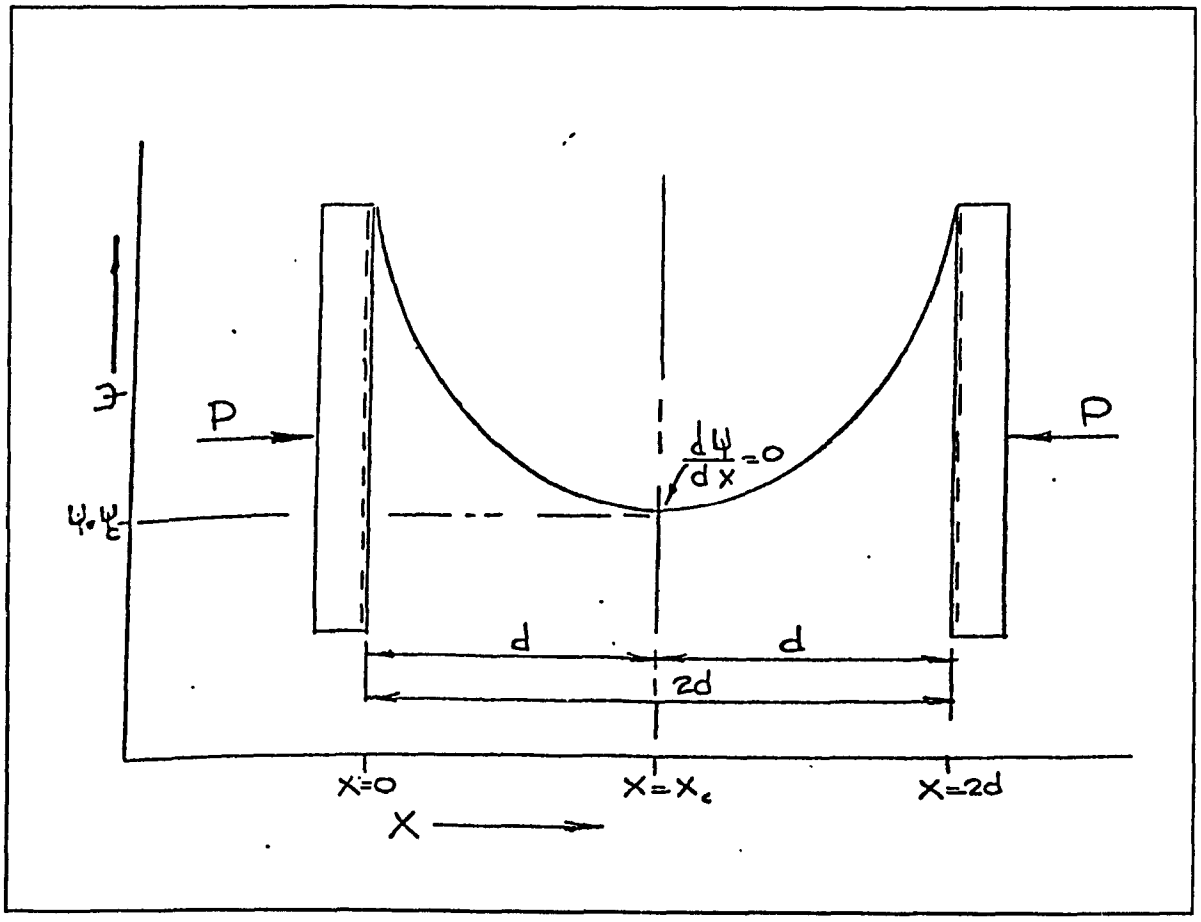

Figure B-1 Variation in Electric Potential ψ Between Parallel Plates
(Taylor, 1962)

For a small amount of overlap, or interaction at relatively large interparticle distances, the resulting electric potential is the algebraic sum of the potentials from single plates. At close spacing of particles, the anions can be neglected. Therefore, the application of Equation (B-19) in practice can be simplified by the substitution of the Langmuir approximation and by a summation of the potentials due to single layers. Equation (B-19) becomes :

$$Y_c = 2\,ln(\frac{\pi}{k\,X_c}) \tag{B-20}$$

and

$$\psi_c = \frac{2\,K\,T}{Z_i\,e}\,ln(\frac{k\,X_c}{\pi}) \tag{B-21}$$

This solution is valid only when $Y_C > 1$.

The accuracy of the approximation methods is shown in Table B-1 from which it is evident that as the Langmuir approximation becomes untrustworthy, the summation of seperate potentials may be successfully applied.

Table B-1: Comparison of Midpoint Potential from Langmuir Approximation and Summation of Seperate Potentials (Taylor, 1962)

kX_C	Y_C *from Eq.(3.6)*	Y_C *from Langmuir*	Y_C *from Potentials*
4.0	0.15	-	0.15
3.0	0.40	0.10	0.40
2.0	0.98	1.03	1.10
1.5	1.50	1.48	1.70
1.0	2.30	2.38	3.10
0.75	2.85	2.86	4.10
0.50	3.60	3.68	5.60

By substituting Equation (B-21) into Equation (B-18) and then by putting

$$\beta = \frac{8\,\pi\,e^2}{\varepsilon\,B\,T}$$

yields (Yang, 1966)

$$P = R\,T\,(\frac{\pi^{\,2}}{\beta\,Z_i^2\,X_c^2} - 2\,N_o) \qquad \text{(B-22)}$$

There is a small error resulting from the assumption that the plane of infinite charge is at the face of the plate. A correction should, therefore, be made to the half distance between two parallel plates. The swelling pressure can then be easily calculated by

$$P = R\,T\,(\frac{\pi^2}{\beta\,Z_i^2\,(X_d + X_o)^2} - 2\,N_o) \qquad \text{(B-23)}$$

where

$$X_o = \frac{\varepsilon\,B\,T}{2\,\pi\,Z_i\,e\,\sigma}$$

σ is the surface charge density of the clay.

X_O is constant depending on the valence of the exchangeable ions and the charge density on the clay particles, and varies from 1 to 4 A^O for clay. For Na-montmorillonite, X_O is approximately 4 A^O (Yong et al,1959).

APPENDIX C

SUPPLEMENTARY MODEL RESULTS

TABLE OF CONTENTS

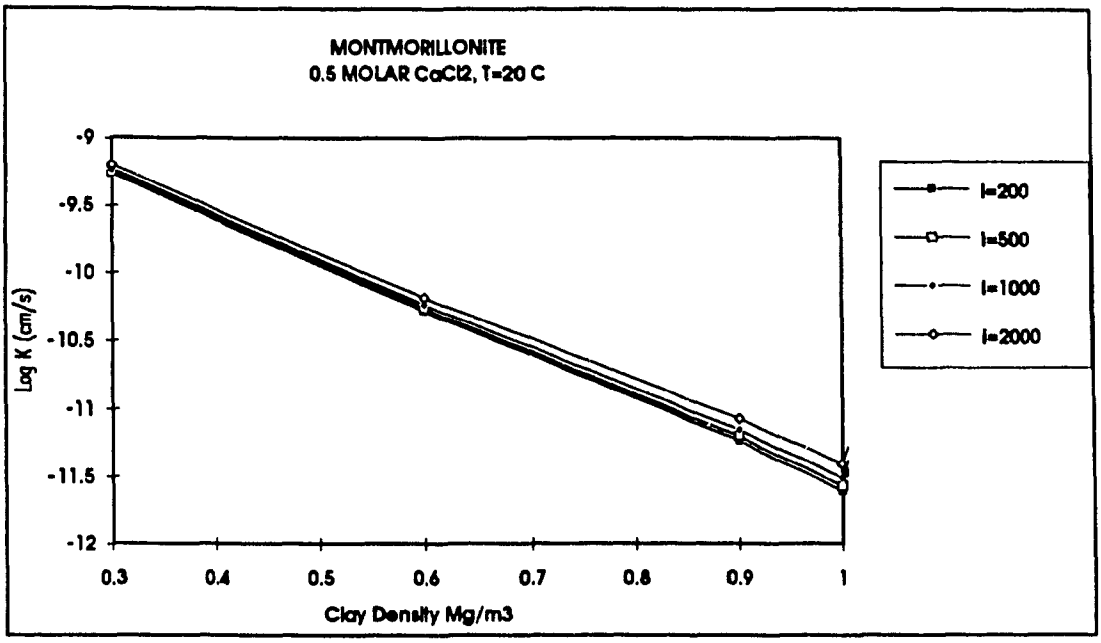

Figure C-1 Montmorillonite, Log K vs γ_c at 0.5 M $CaCl_2$ and different Hydraulic Gradients (Model results)

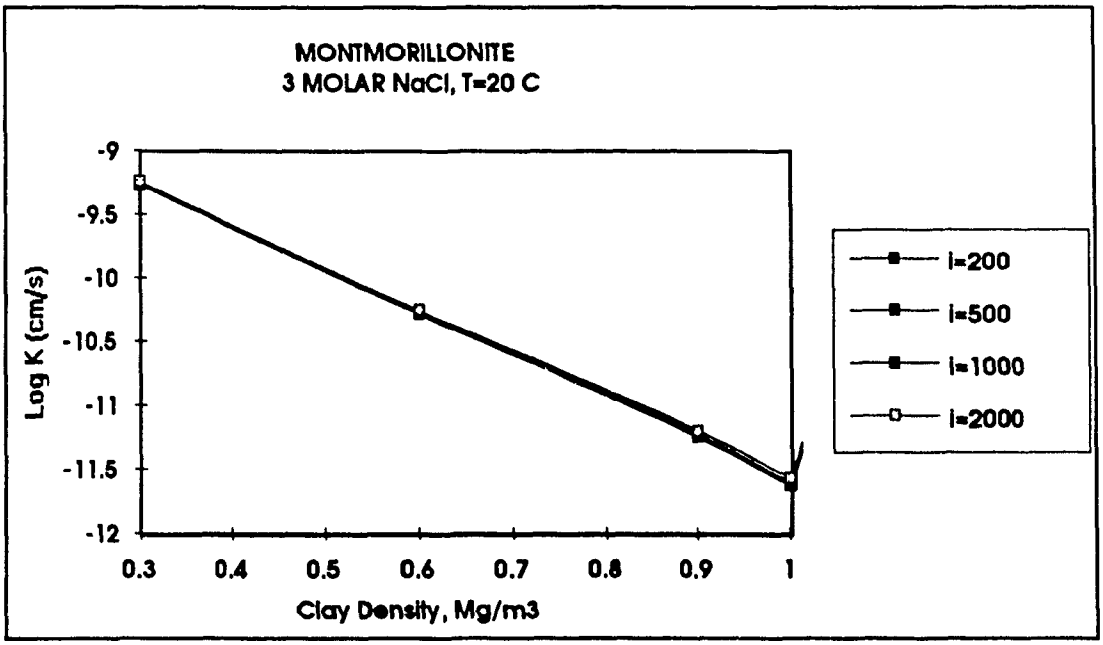

Figure C-2 Montmorillonite, Log K vs γ_c at 3M NaCl and different Hydraulic Gradients (Model results)

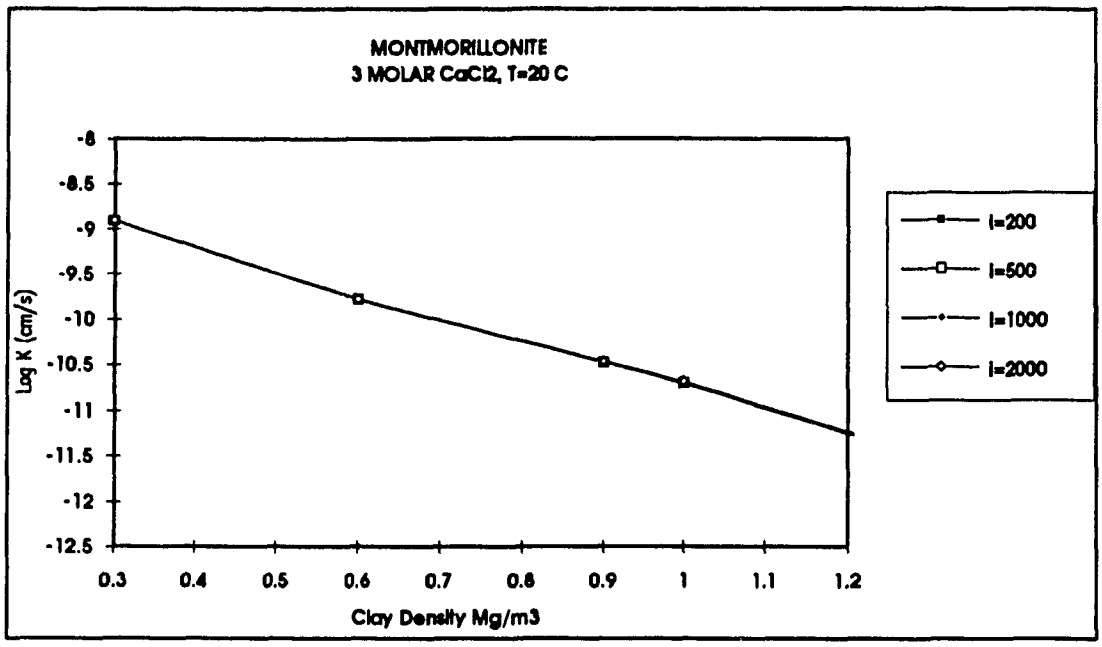

Figure C-3 Montmorillonite, Log K vs γ_c at 3 M $CaCl_2$ and different Hydraulic Gradients (Model results)

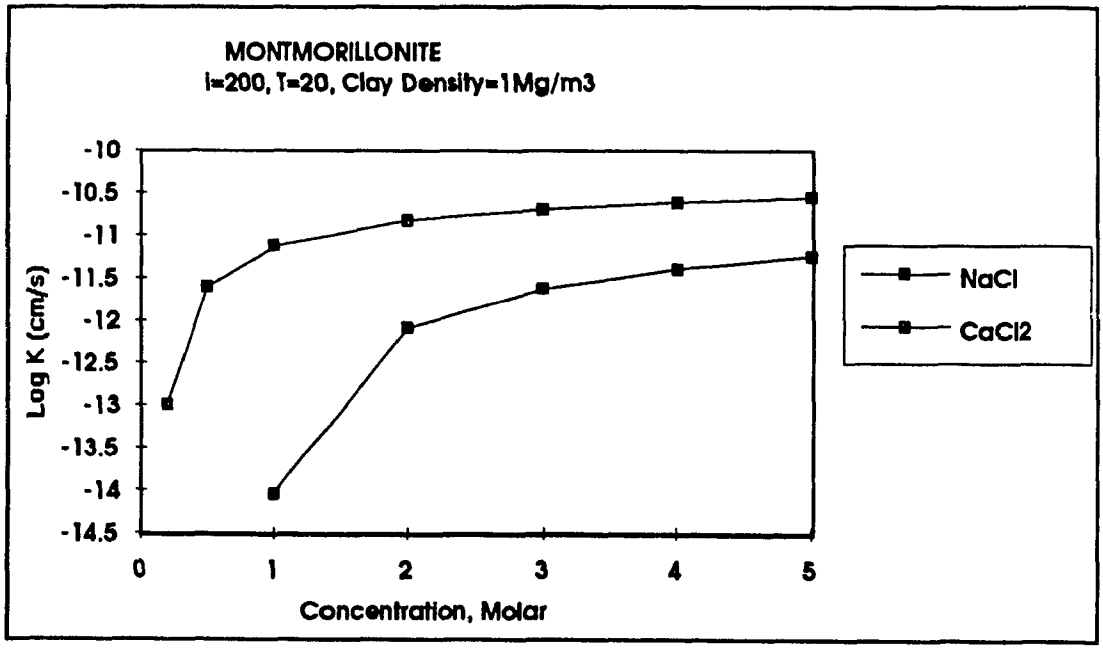

Figure C-4 Montmorillonite, Log K vs NaCl and $CaCl_2$ Concentration at $\gamma_c = 1$ Mg / m^3 and i = 200 (Model results)

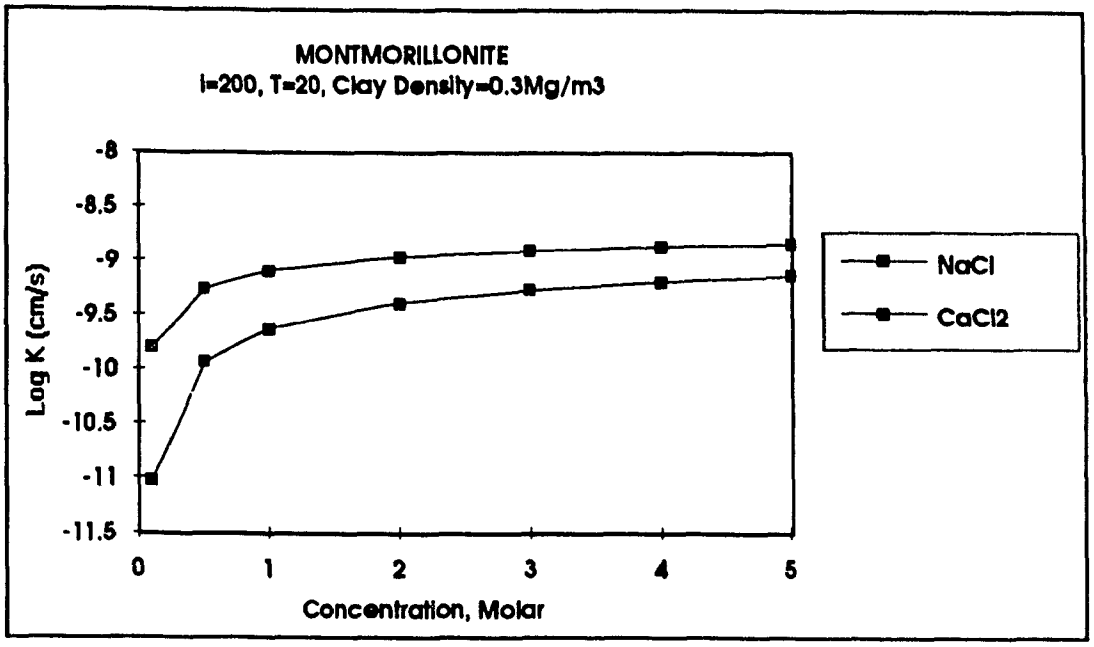

Figure C-5 Montmorillonite, Log K vs NaCl and $CaCl_2$ Concentration at $\gamma_c = 0.3$ Mg / m^3 and i = 200 (Model results)

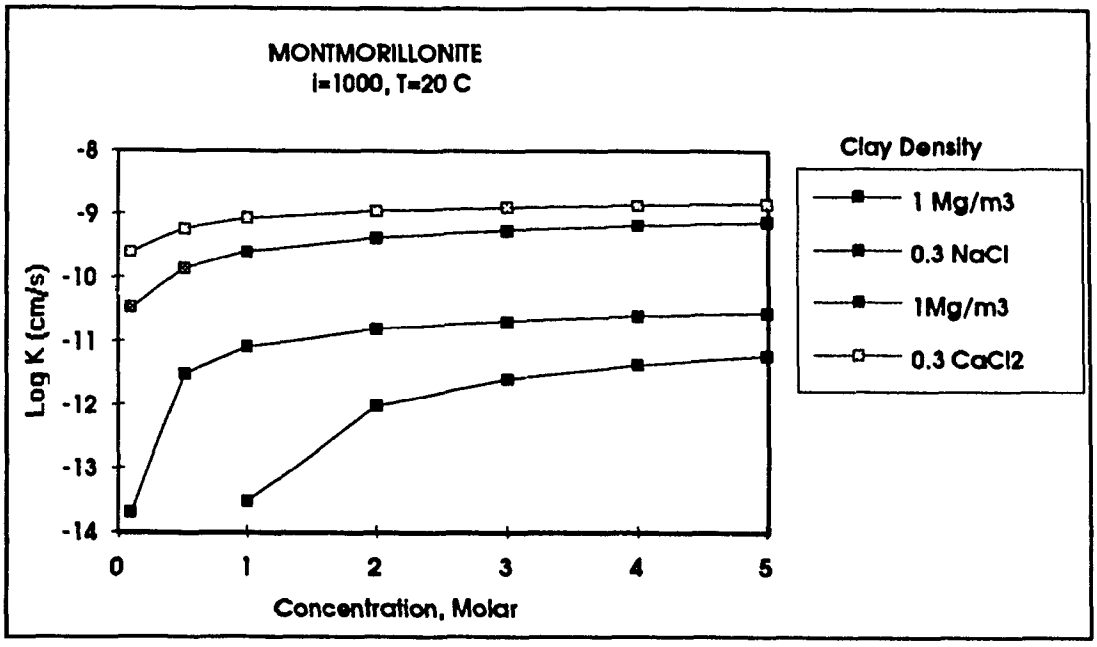

Figure C-6 Montmorillonite, Log K vs NaCl and $CaCl_2$ Concentration at $\gamma_c = 0.3$ and 1 Mg / m^3 and i = 1000 (Model results)

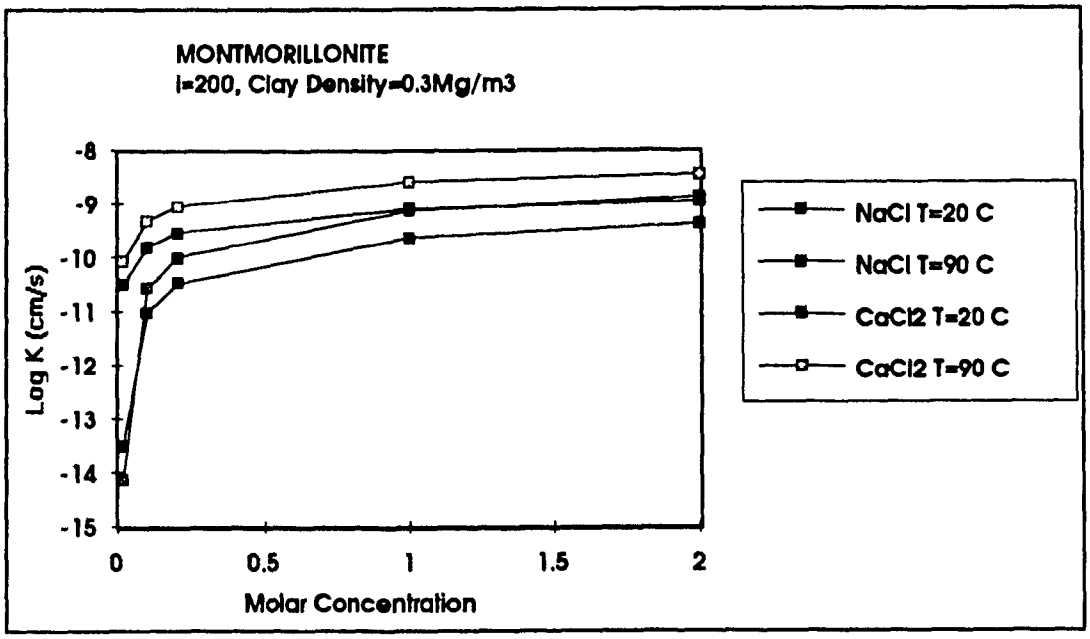

Figure C-7 Montmorillonite, Log K vs NaCl and $CaCl_2$ concentration at T=20 and 90°C, γ_c = 0.3 Mg / m^3 and i=200 (Model results)

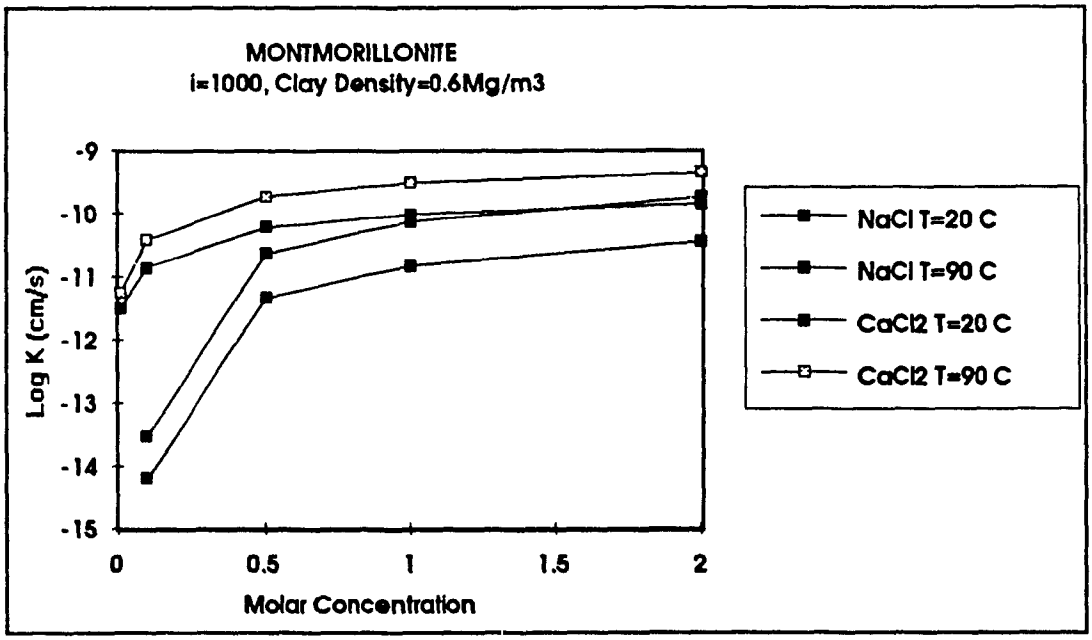

Figure C-8 Montmorillonite, Log K vs NaCl and $CaCl_2$ concentration at T=20 and 90°C, γ_c = 0.6 Mg / m^3 and i=1000 (Model results)

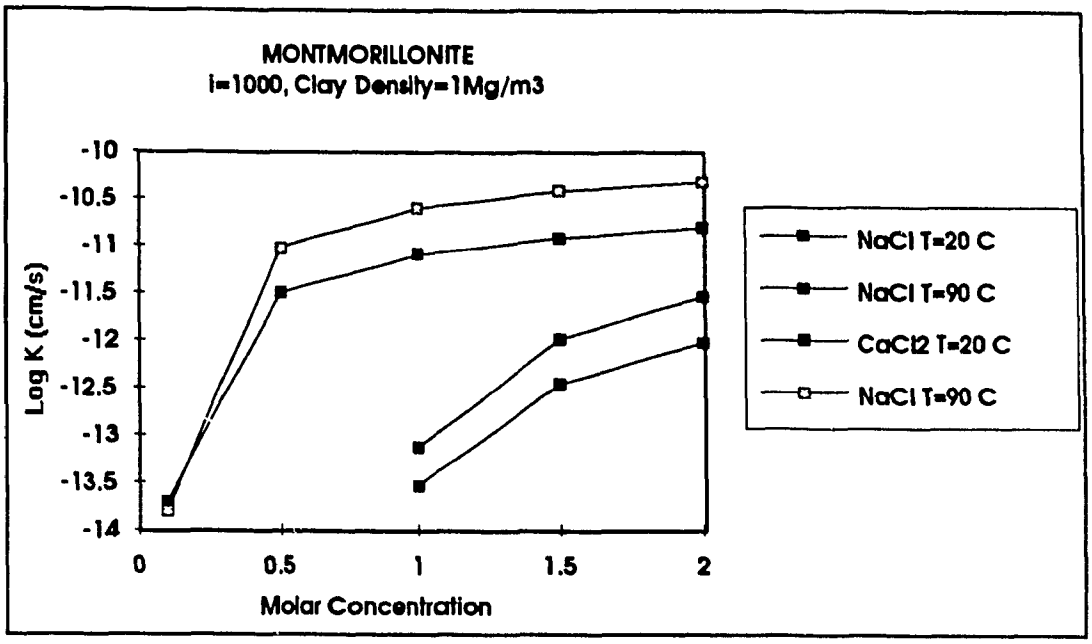

Figure C-9 Montmorillonite, Log K vs NaCl and $CaCl_2$ concentration at T=20 and 90°C, γ_c = 1 Mg / m^3 and i=1000 (Model results)

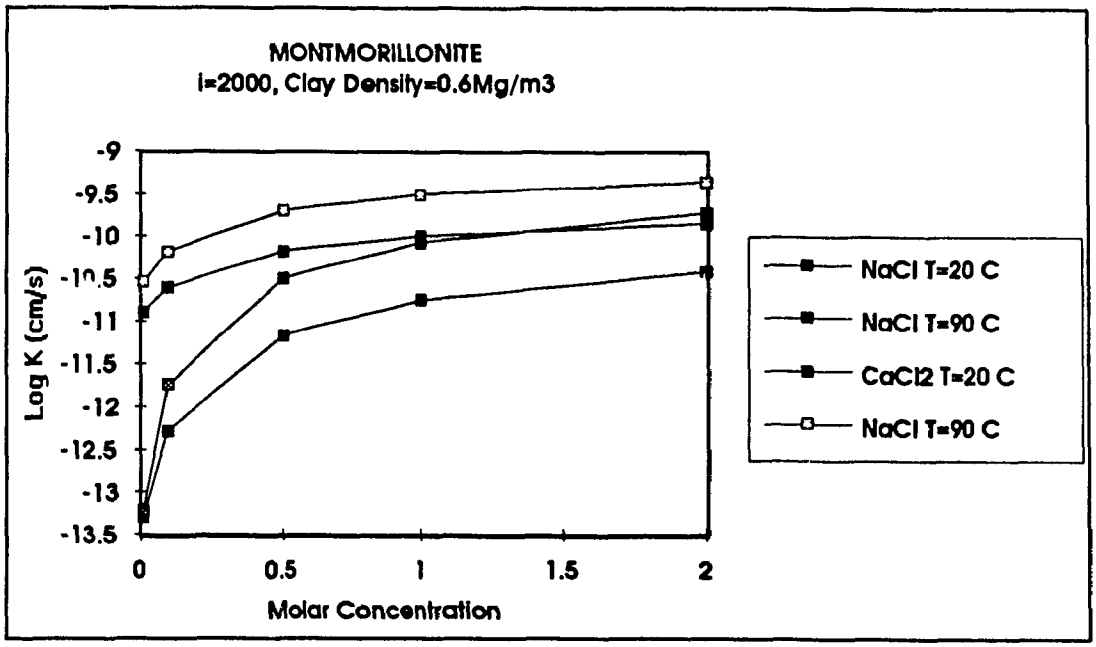

Figure C-10 Montmorillonite, Log K vs NaCl and $CaCl_2$ concentration at T=20 and 90°C, γ_c = 0.6 Mg / m^3 and i=2000 (Model results)

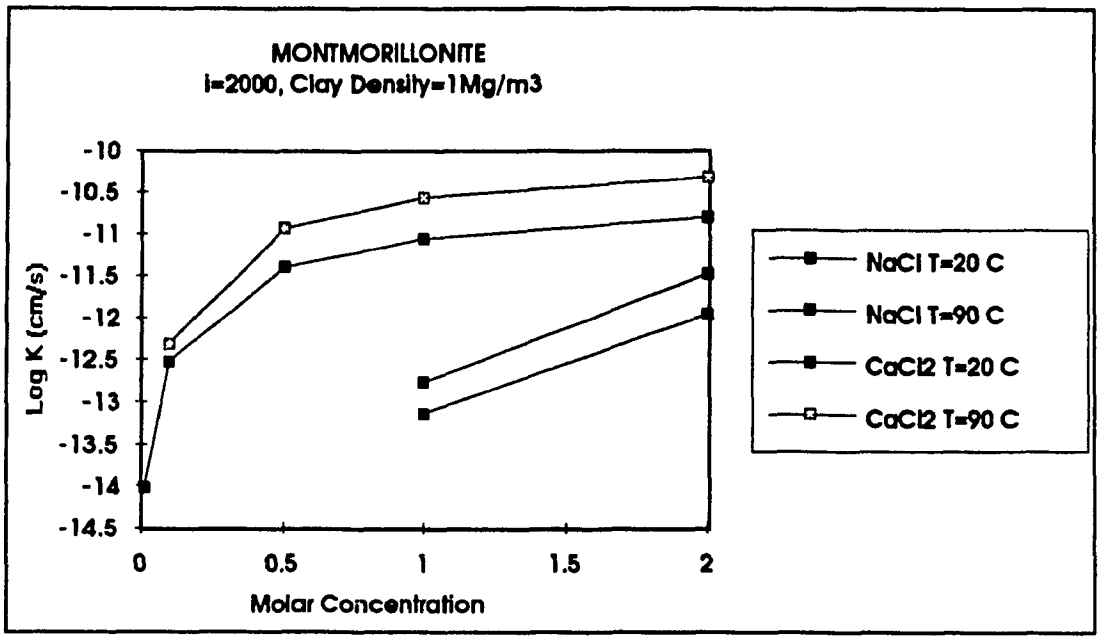

Figure C-11 Montmorillonite, Log K vs NaCl and $CaCl_2$ concentration at T=20 and 90°C, γ_c = 1 Mg / m^3 and i=2000 (Model results)

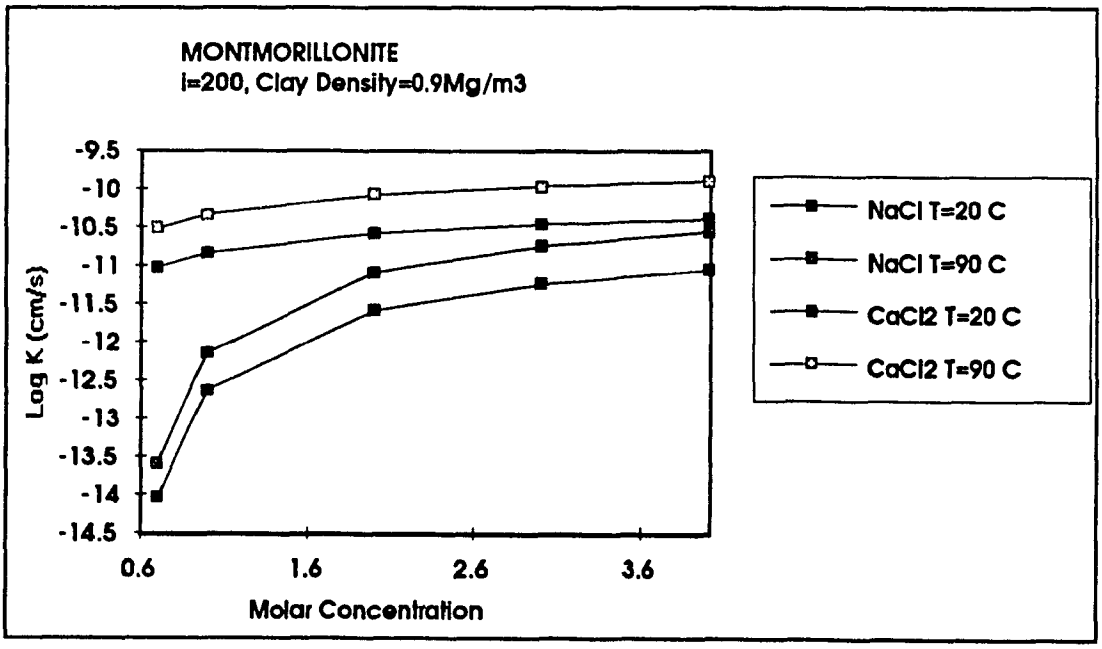

Figure C-12 Montmorillonite, Log K vs NaCl and $CaCl_2$ concentration at T=20 and 90°C, γ_c = 1 Mg / m^3 and i=200 (Model results)

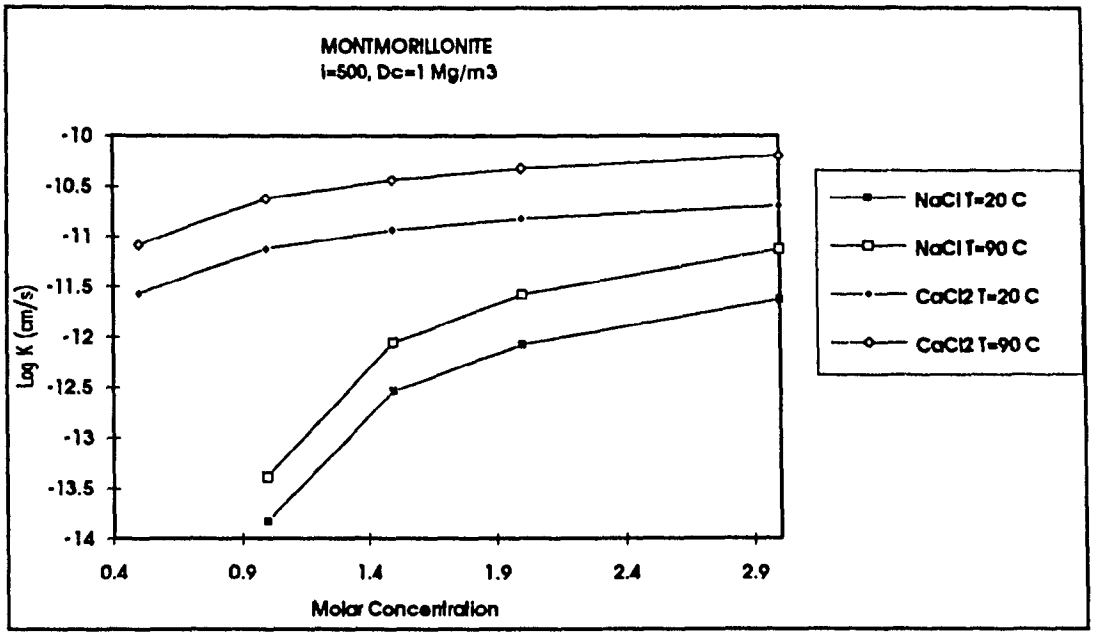

Figure C-13 Montmorillonite, Log K vs NaCl and $CaCl_2$ concentration at T=20 and 90°C, γ_c = 1 Mg / m^3 and i=200 (Model results)

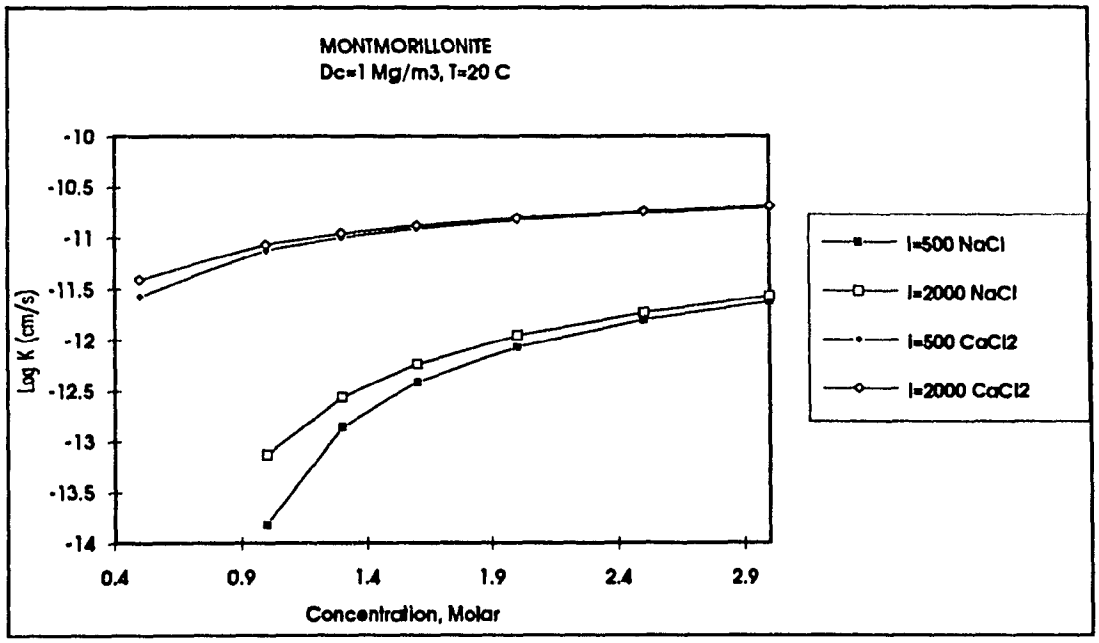

Figure C-14 Montmorillonite, Log K vs NaCl and $CaCl_2$ concentration at i = 500 and 2000 and γ_c = 1 Mg / m^3 (Model results)

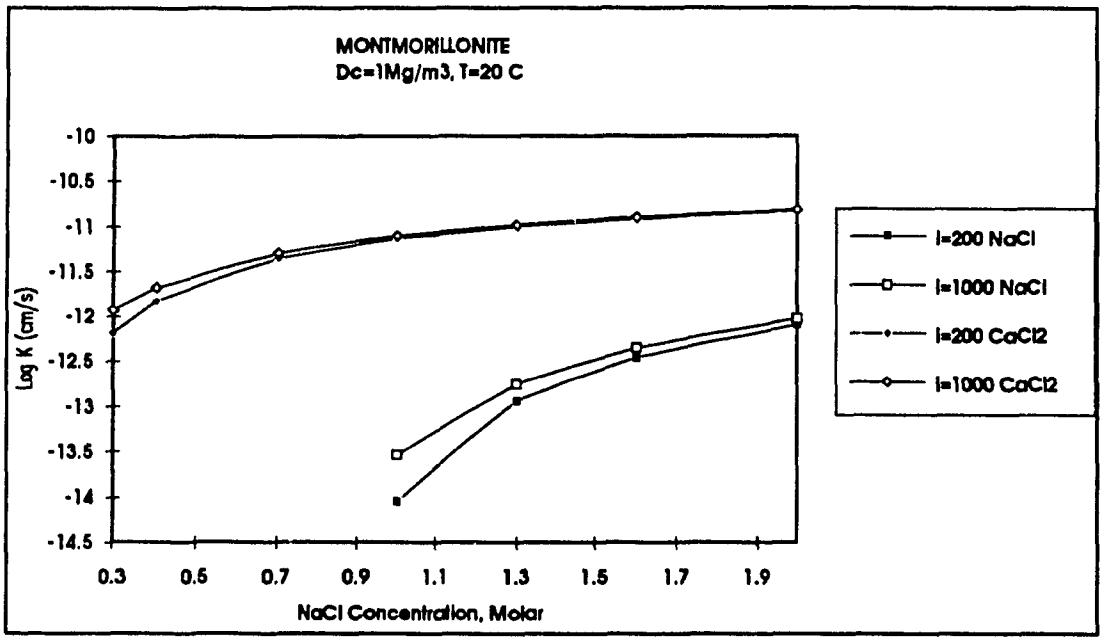

Figure C-15 Montmorillonite, Log K vs NaCl and $CaCl_2$ concentration at i = 200 and 1000 and γ_c = 1 Mg / m^3 (Model results)

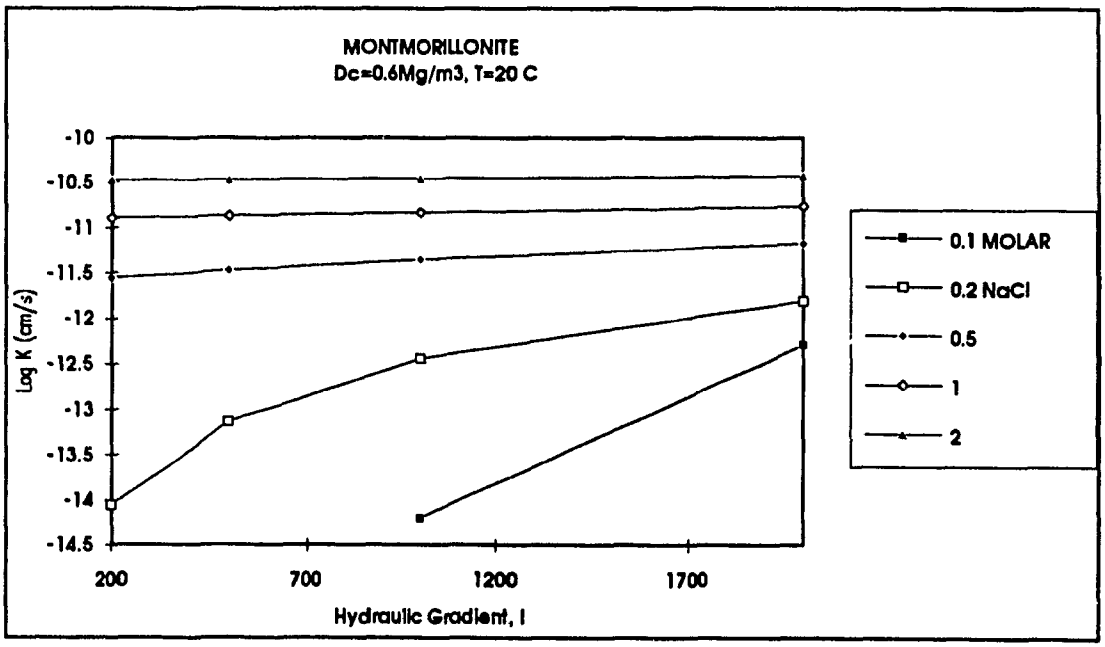

Figure C-16 Montmorillonite, Log K vs Hydraulic Gradient i at different NaCl concentration and γ_c = 0.6 Mg / m^3 (Model results)

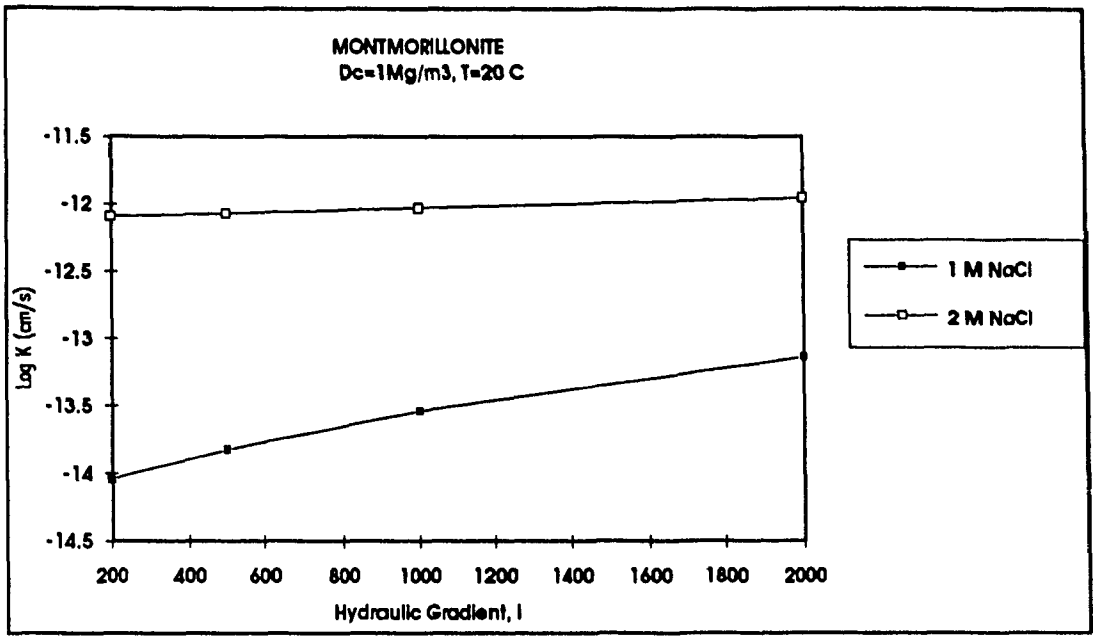

Figure C-17 Montmorillonite, Log K vs Hydraulic Gradient i at different NaCl concentration and γ_c = 1 Mg / m^3 (Model results)

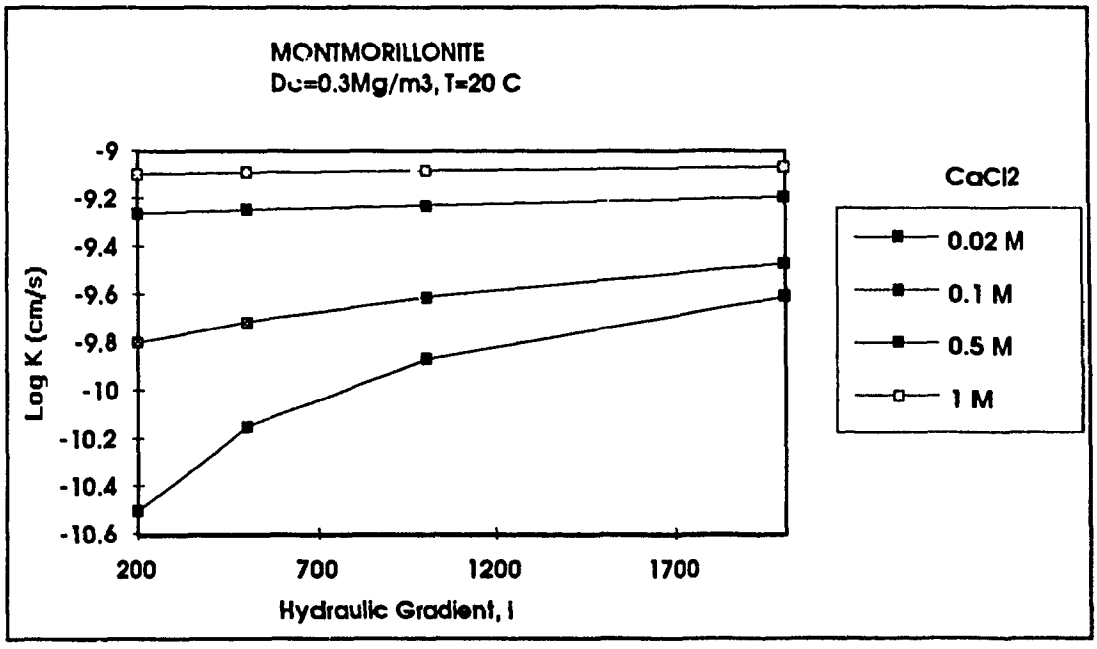

Figure C-18 Montmorillonite, Log K vs Hydraulic Gradient i at different $CaCl_2$ concentration and γ_c = 0.3 Mg / m^3 (Model results)

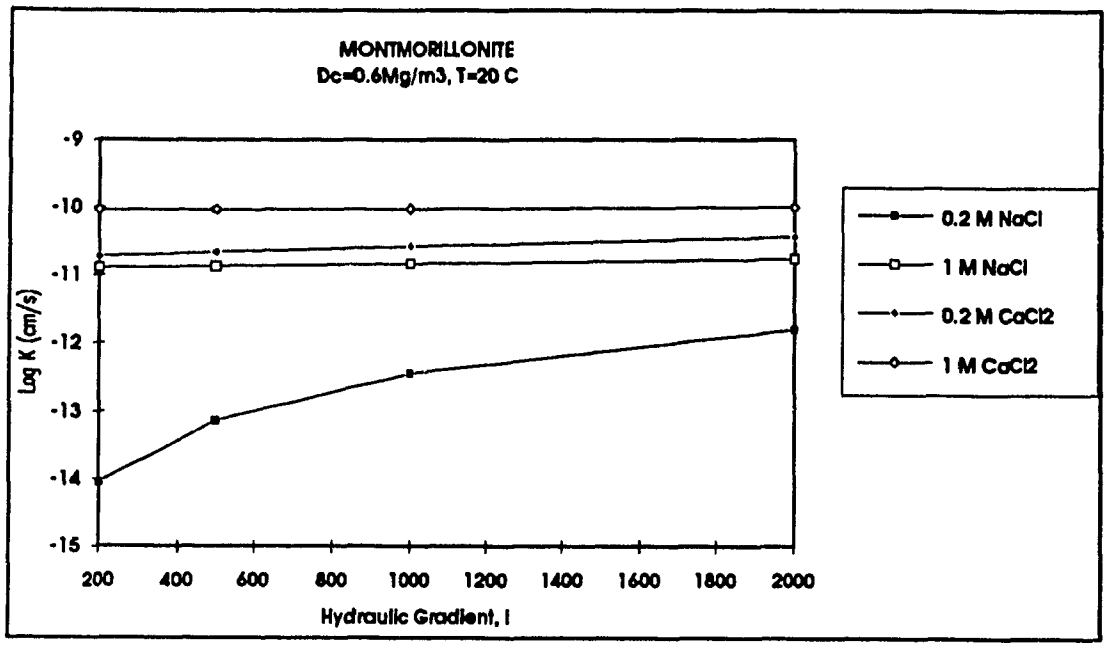

Figure C-19 Montmorillonite, Log K vs Hydraulic Gradient i at different NaCl and $CaCl_2$ concentrations and $\gamma_c = 0.6$ Mg / m^3 (Model results)

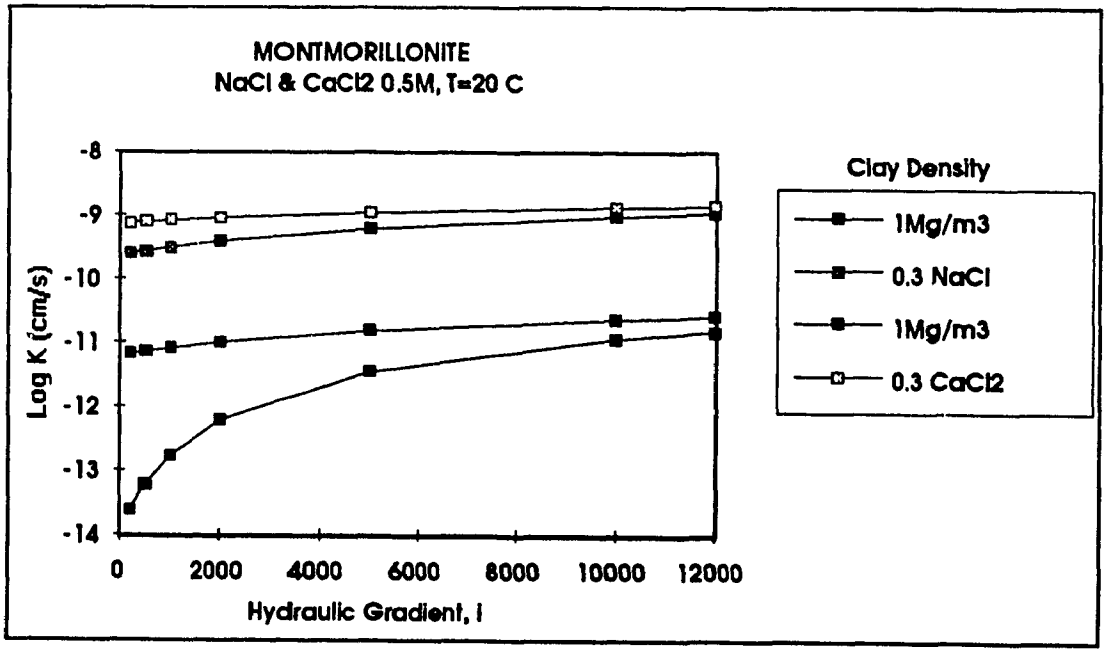

Figure C-20 Montmorillonite, Log K vs Hydraulic Gradient i at 0.5M NaCl and $CaCl_2$ concentration and $\gamma_c = 0.3$ and 1 Mg / m^3 (Model results)

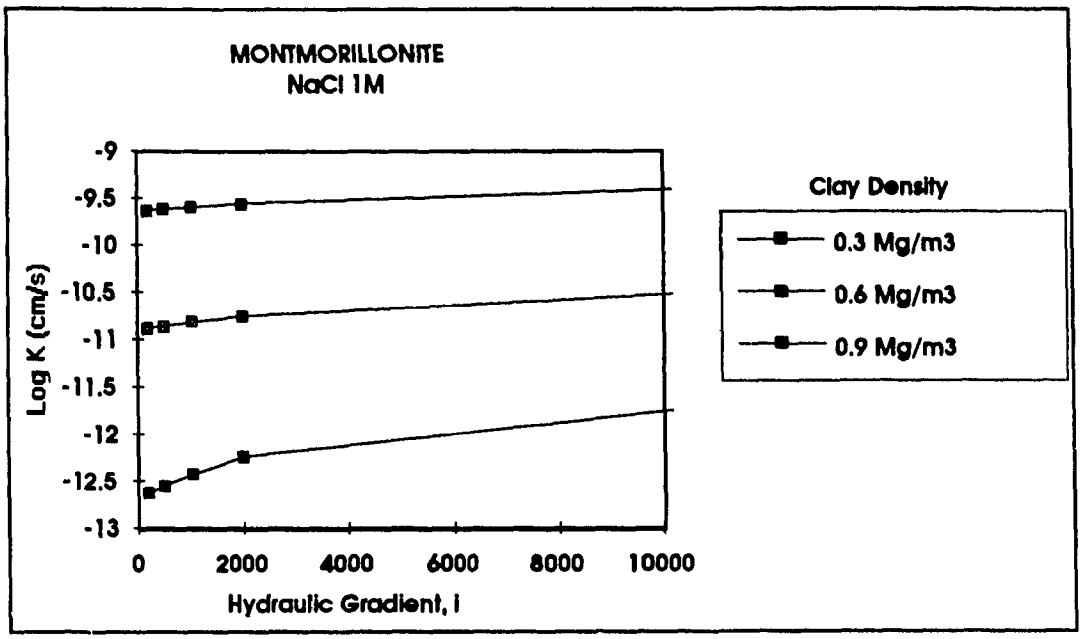

Figure C-21 Montmorillonite, Log K vs Hydraulic Gradient i at 1M NaCl concentration and $\gamma_c = 0.3$,0.6 and 0.9 Mg / m^3 (Model results)

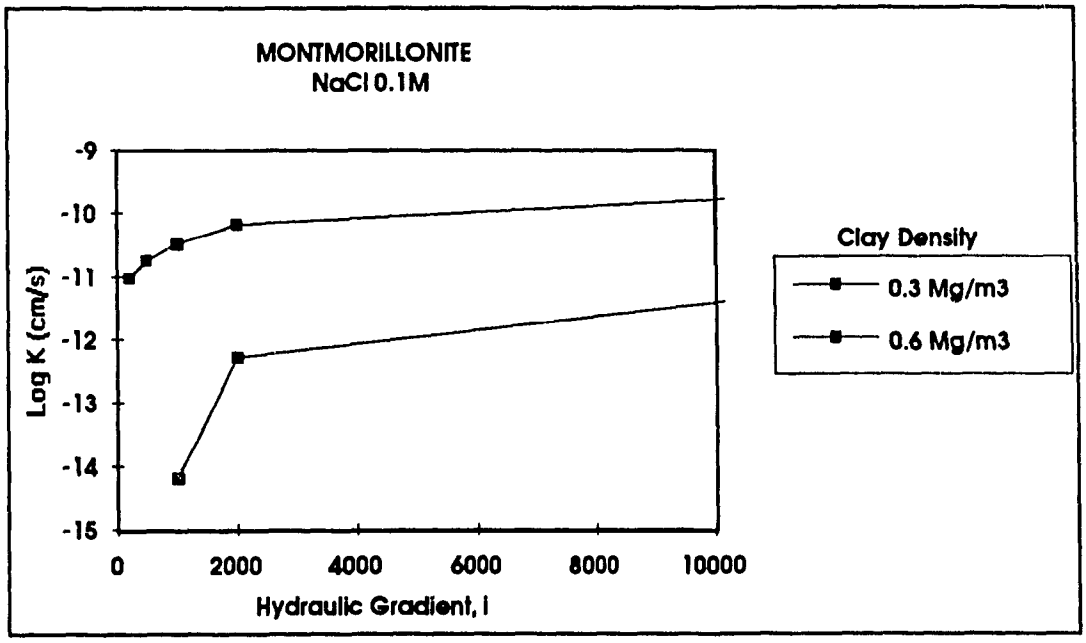

Figure C-22 Montmorillonite, Log K vs Hydraulic Gradient i at 0.1M NaCl concentration and $\gamma_c = 0.3$ and 0.6 Mg / m^3 (Model results)

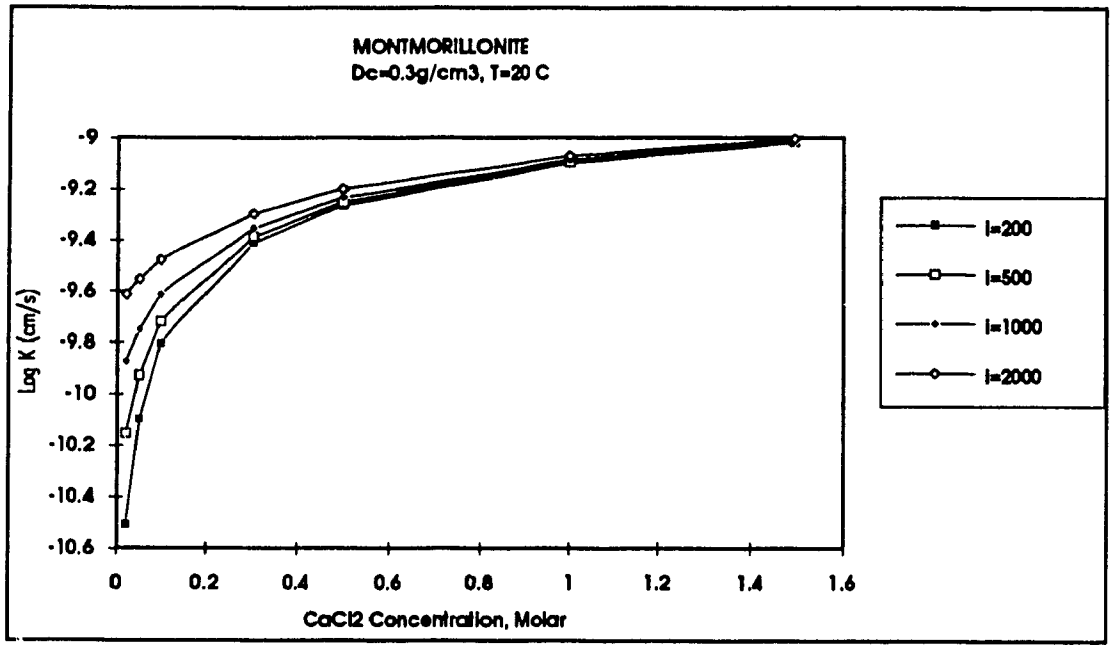

Figure C-23 Montmorillonite, Log K vs $CaCl_2$ concentration at different Hydraulic Gradient i and $\gamma_c = 0.3$ Mg / m^3 (Model results)

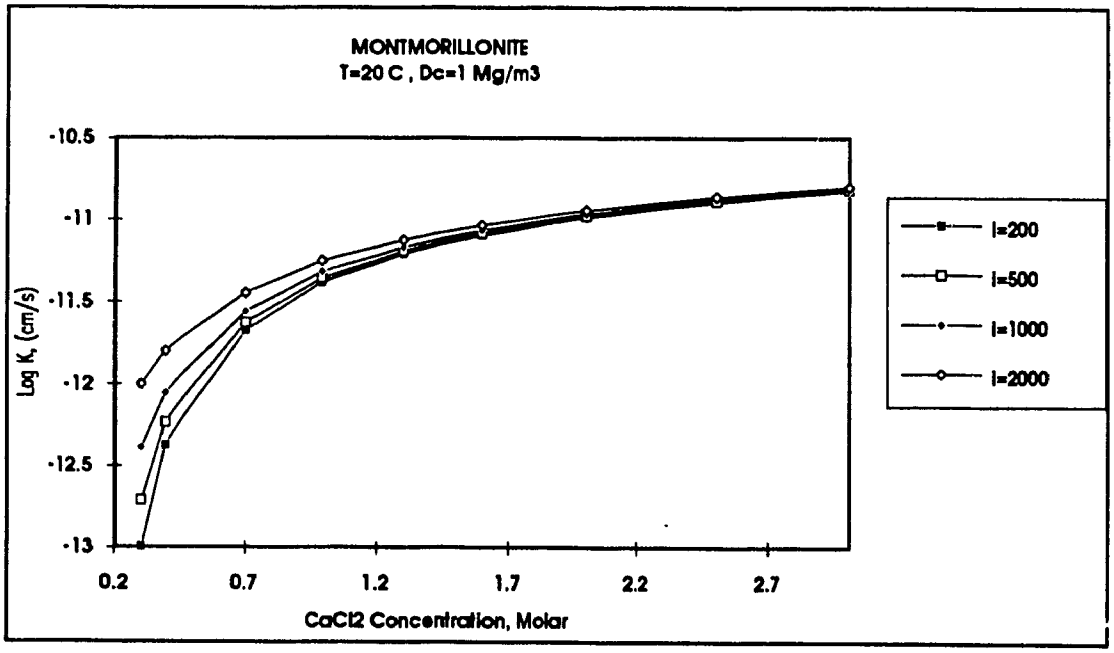

Figure C-24 Montmorillonite, Log K vs $CaCl_2$ concentration at different Hydraulic Gradient i and $\gamma_c = 1$ Mg / m^3 (Model results)

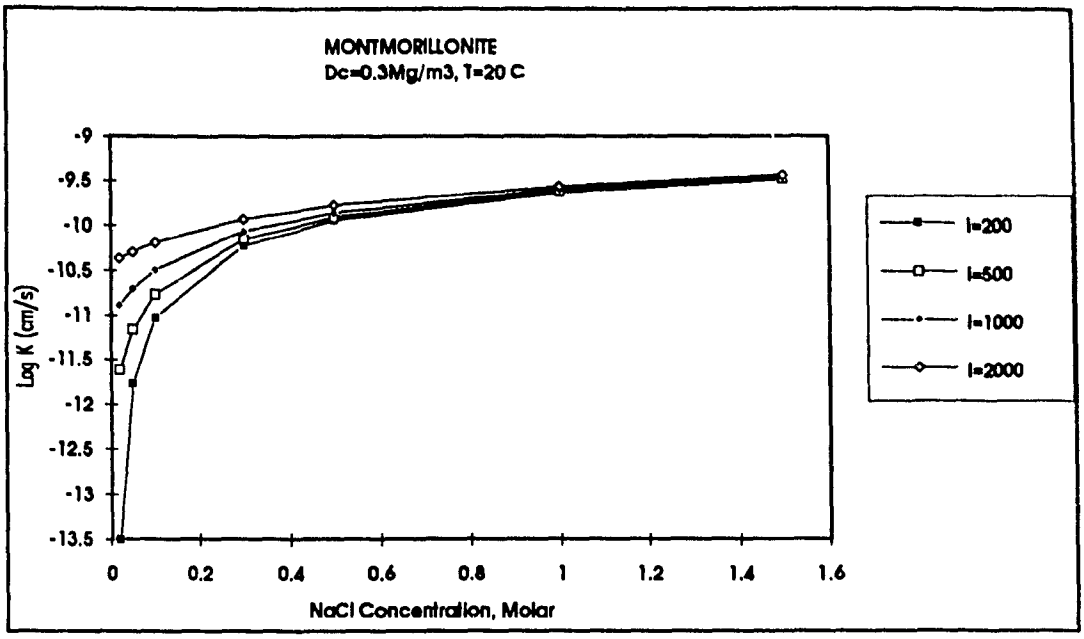

Figure C-25 Montmorillonite, Log K vs NaCl concentration at different Hydraulic Gradient i and $\gamma_c = 0.3$ Mg / m^3 (Model results)

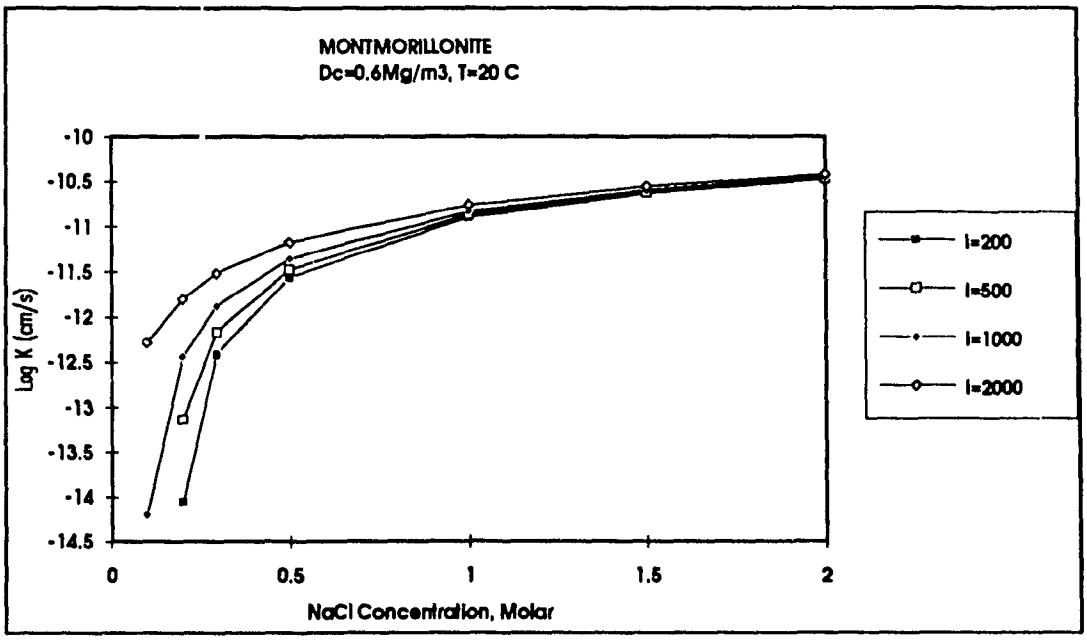

Figure C-26 Montmorillonite, Log K vs NaCl concentration at different Hydraulic Gradient i and $\gamma_c = 0.6$ Mg / m^3 (Model results)

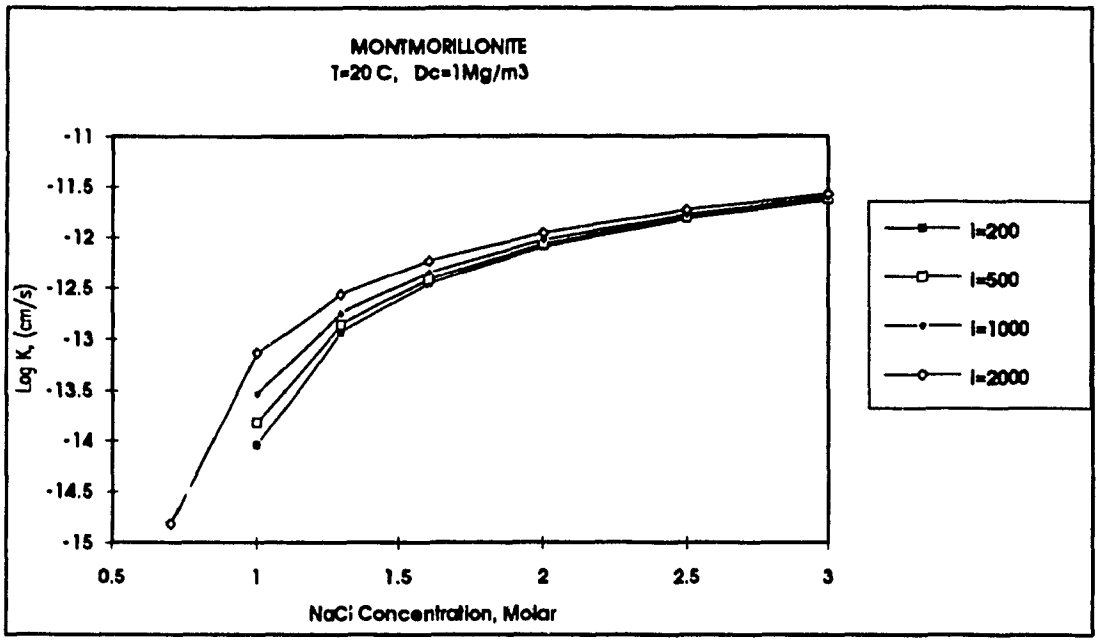

Figure C-27 Montmorillonite, Log K vs NaCl concentration at different Hydraulic Gradient i and γ_c = 1 Mg / m^3 (Model results)

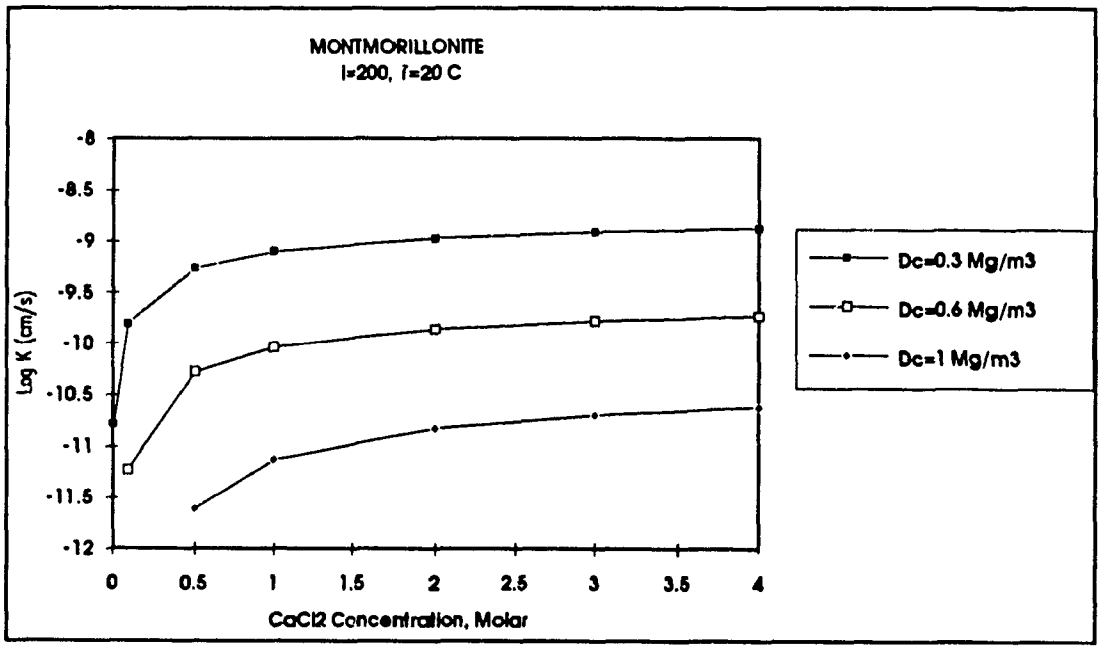

Figure C-28 Montmorillonite, Log K vs $CaCl_2$ concentration at γ_c = 0.3, 0.6 and 1 Mg/m^3 and i=200 (Model results)

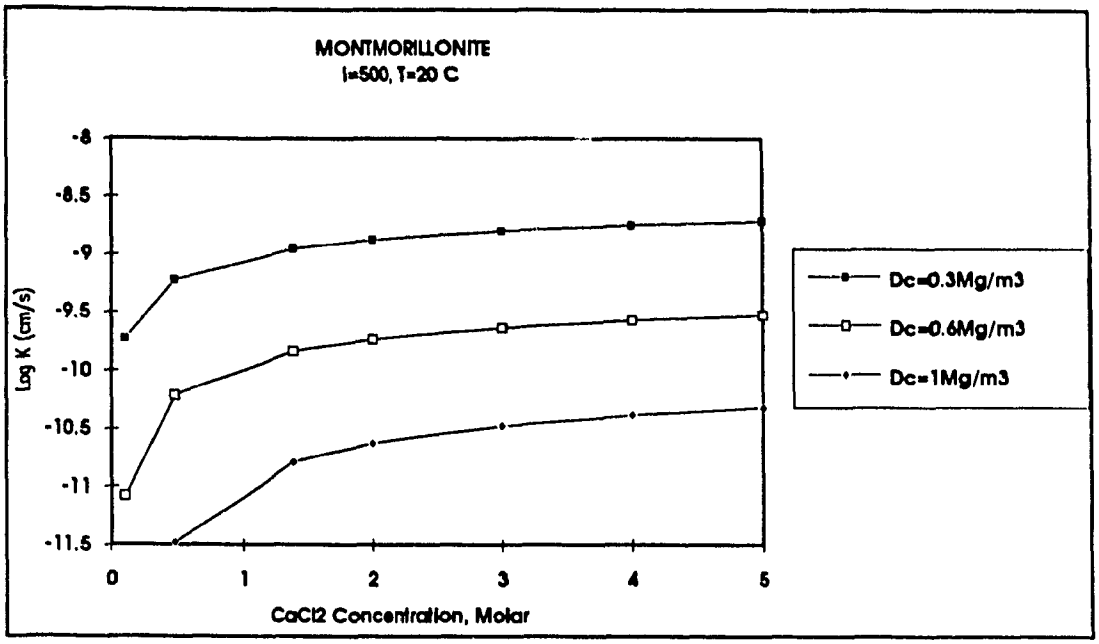

Figure C-29 Montmorillonite, Log K vs $CaCl_2$ concentration at γ_c = 0.3, 0.6 and 1 Mg/m^3 and i=500 (Model results)

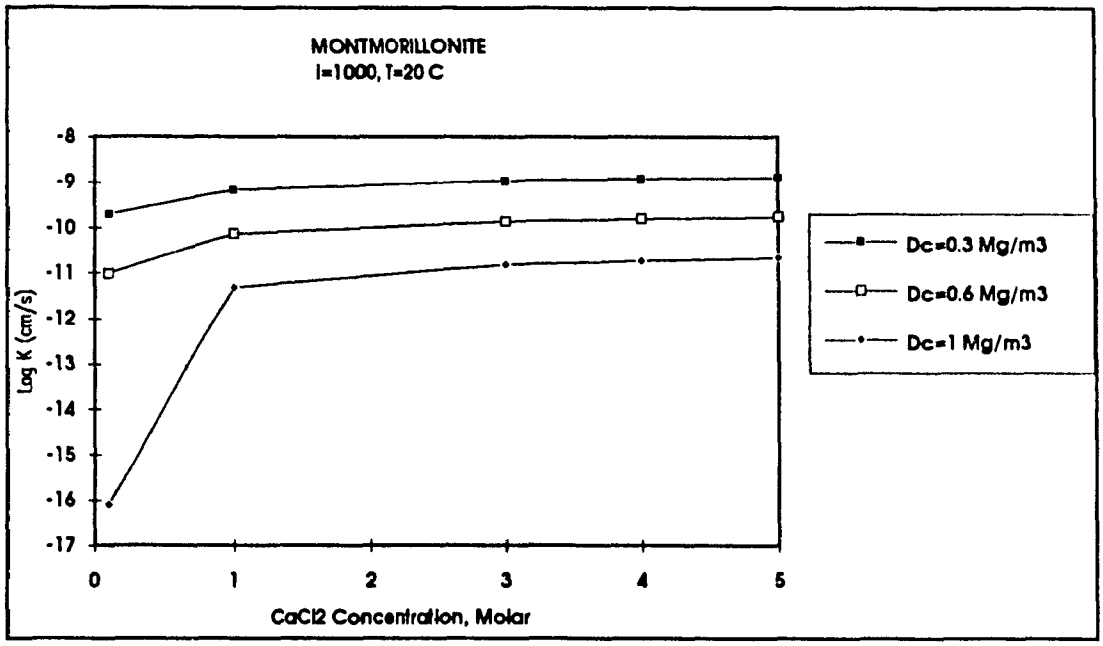

Figure C-30 Montmorillonite, Log K vs $CaCl_2$ concentration at γ_c = 0.3, 0.6 and 1 Mg/m^3 and i =1000 (Model results)

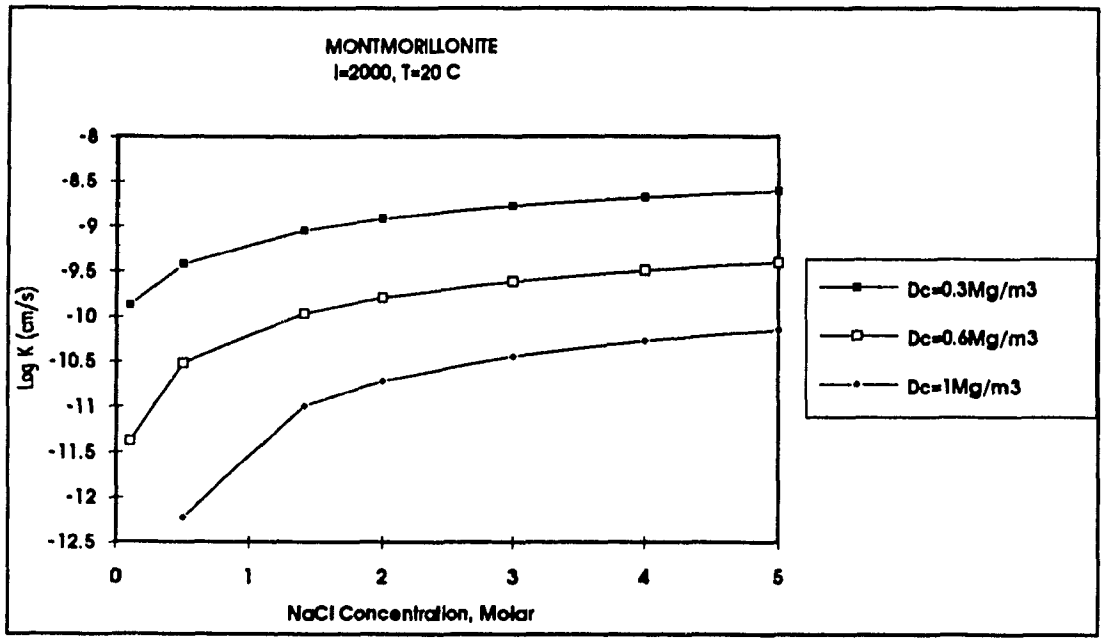

Figure C-31 Montmorillonite, Log K vs NaCl concentration at γ_c = 0.3, 0.6 and 1 Mg/m^3 and i=2000 (Model results)

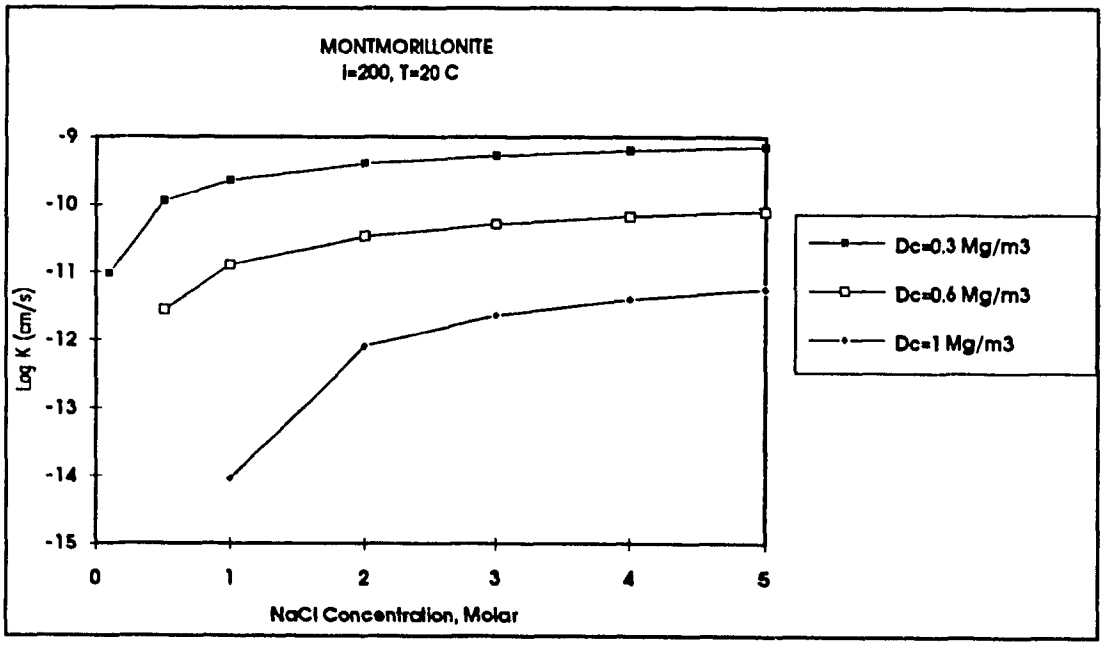

Figure C-32 Montmorillonite, Log K vs NaCl concentration at γ_c = 0.3, 0.6 and 1 Mg/m^3 and i = 200 (Model results)

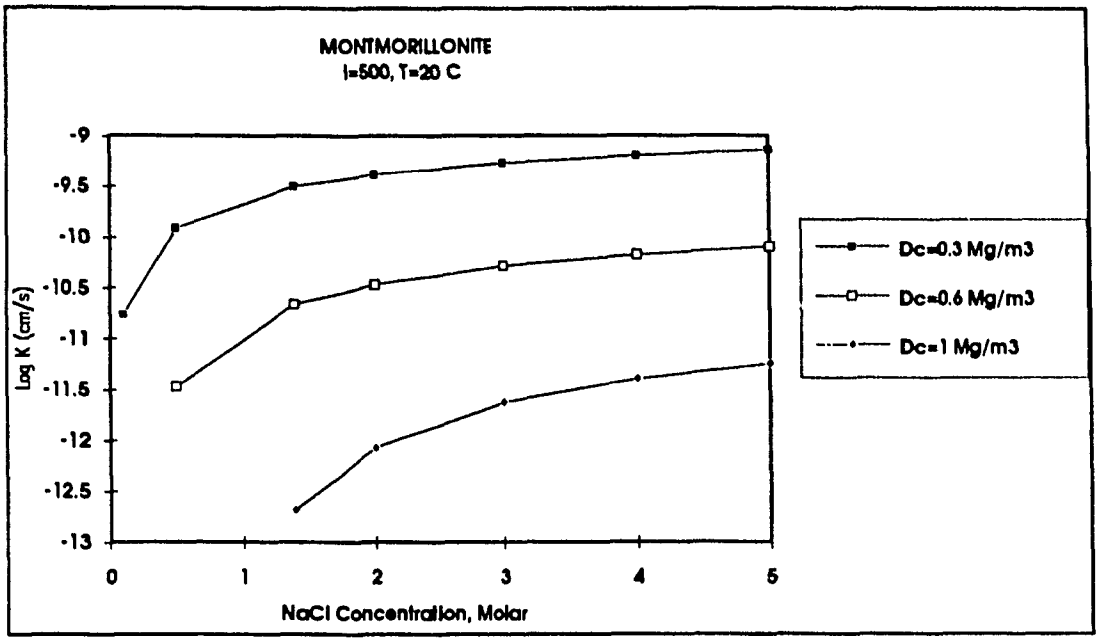

Figure C-33 Montmorillonite, Log K vs NaCl concentration at γ_c = 0.3, 0.6 and 1 Mg/m^3 and i = 500 (Model results)

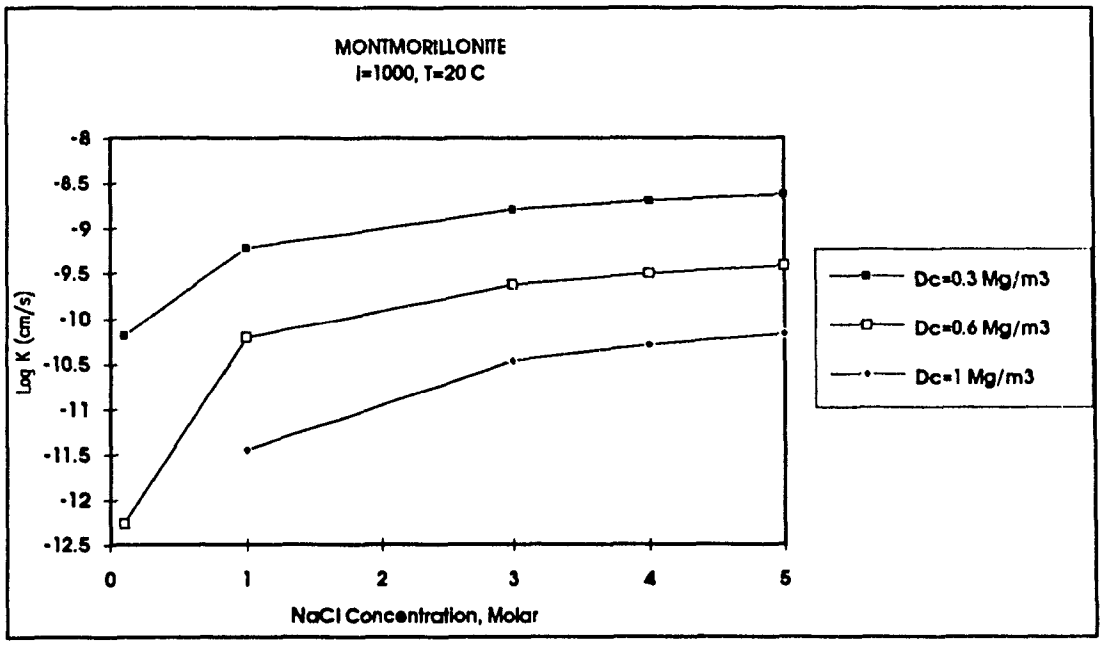

Figure C-34 Montmorillonite, Log K vs NaCl concentration at γ_c = 0.3, 0.6 and 1 Mg/m^3 and i = 1000 (Model results)

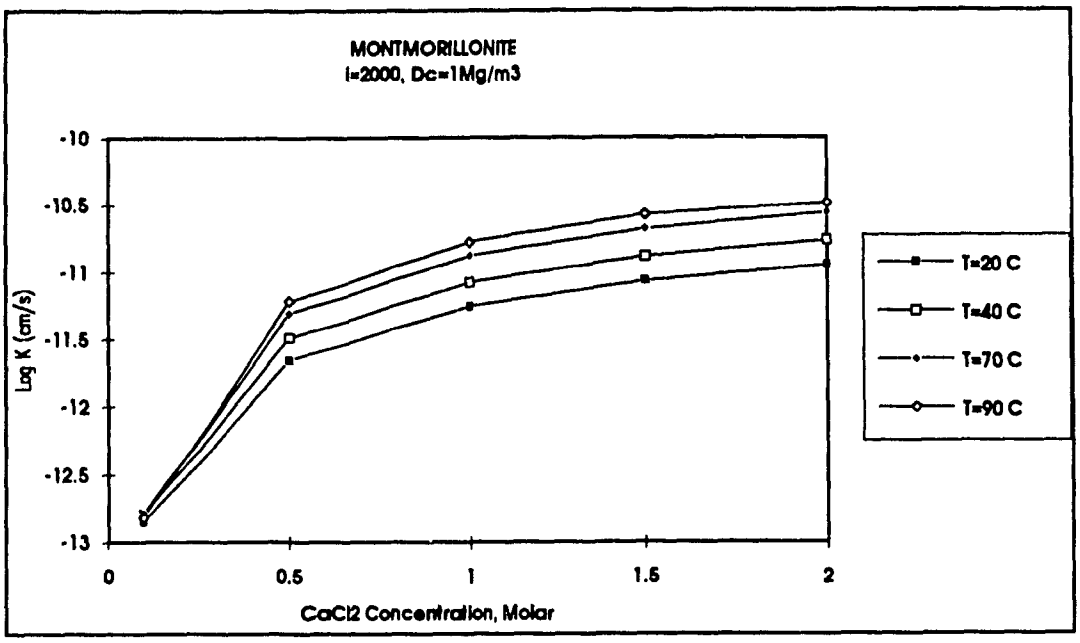

Figure C-35 Montmorillonite, Log K vs $CaCl_2$ concentration at T=20, 40, 70 and 90°C, γ_c = 1 Mg / m^3 and i = 2000 (Model results)

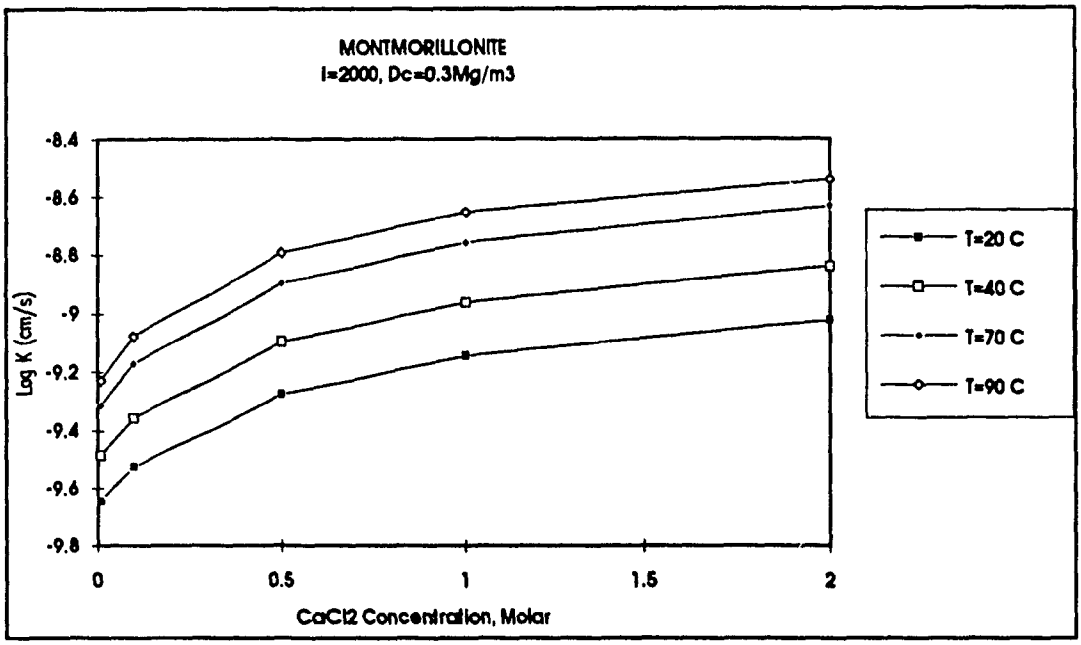

Figure C-36 Montmorillonite, Log K vs $CaCl_2$ concentration at T=20, 40, 70 and 90°C, γ_c = 0.3 Mg / m^3 and i = 2000 (Model results)

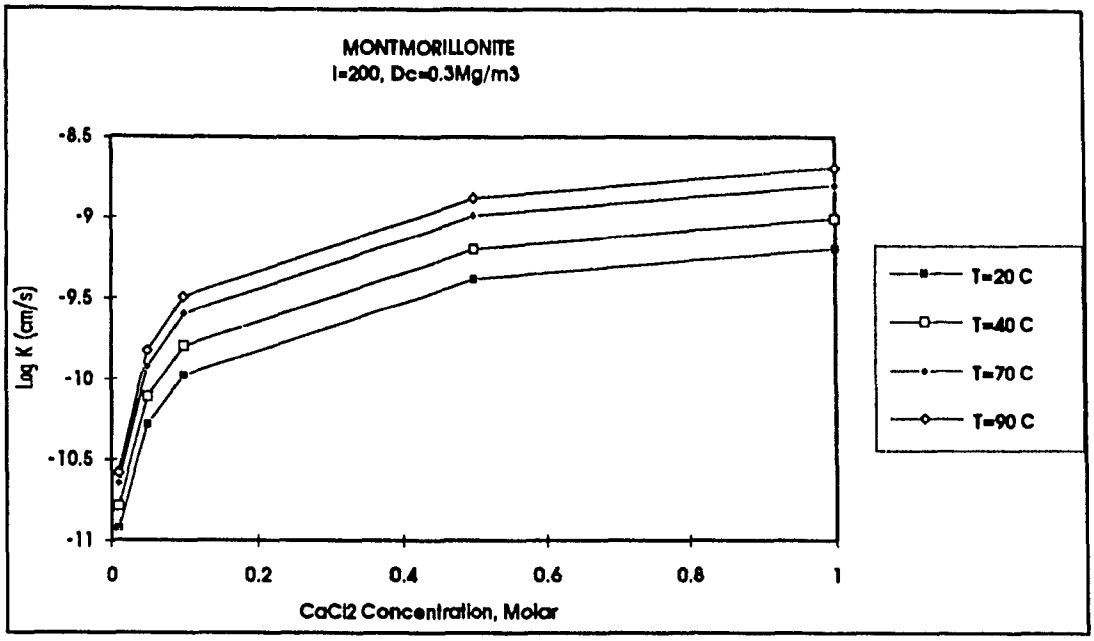

Figure C-37 Montmorillonite, Log K vs $CaCl_2$ concentration at T=20, 40, 70 and 90°C, $\gamma_c = 0.3$ Mg / m^3 and i = 200 (Model results)

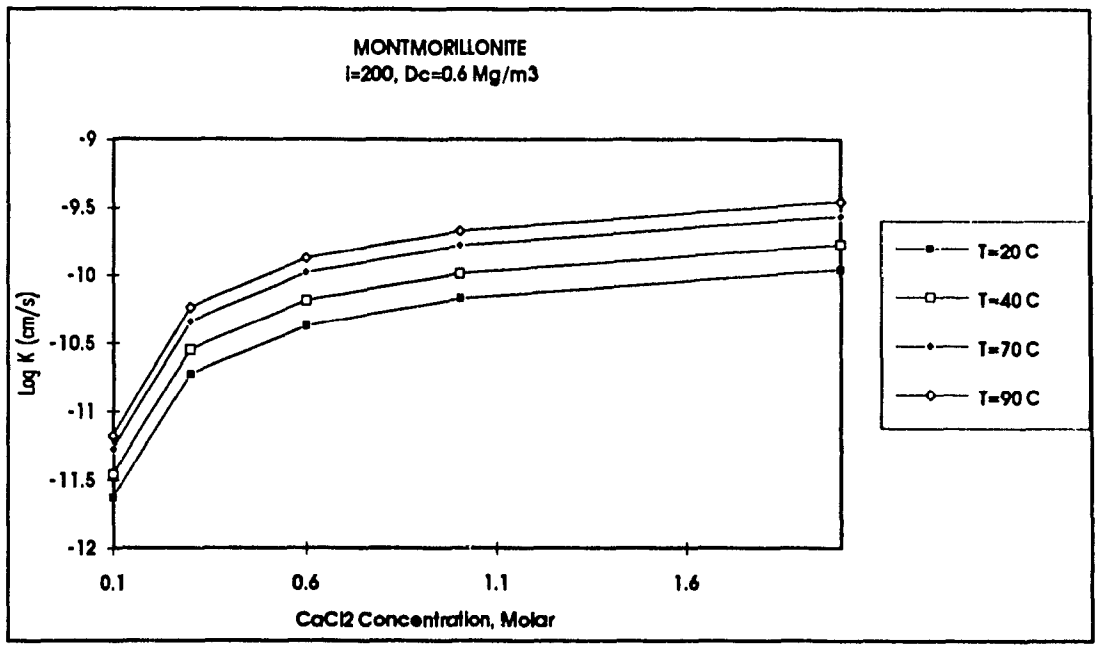

Figure C-38 Montmorillonite, Log K vs $CaCl_2$ concentration at T=20, 40, 70 and 90°C, $\gamma_c = 0.6$ Mg / m^3 and i = 200 (Model results)

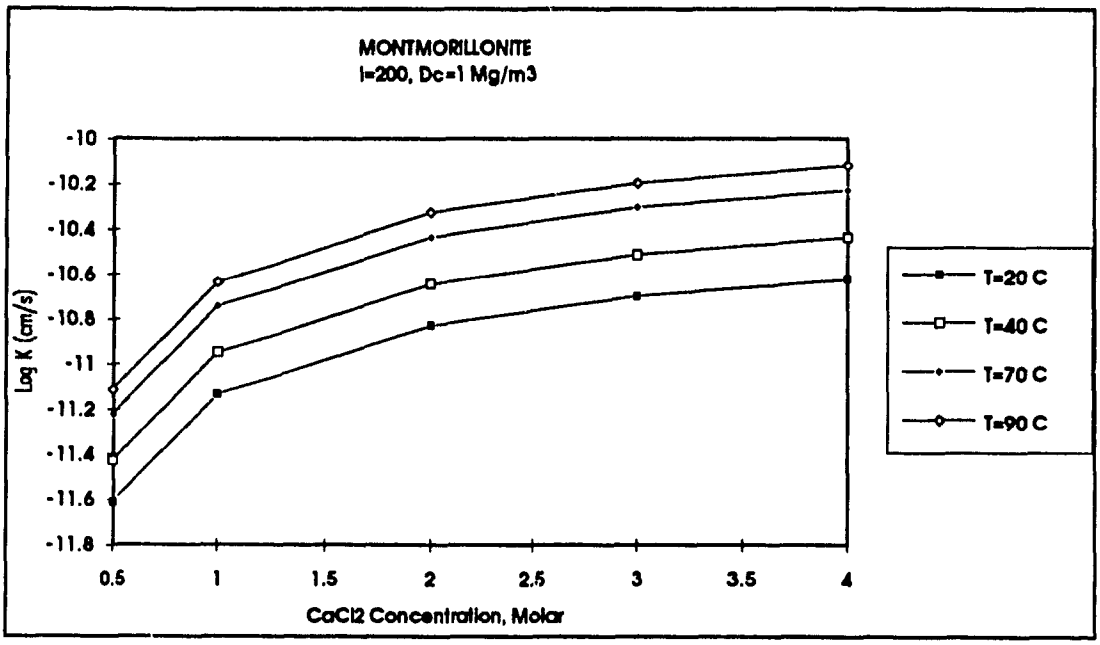

Figure C-39 Montmorillonite, Log K vs $CaCl_2$ concentration at T=20, 40, 70 and 90°C, γ_c = 1 Mg / m^3 and i = 200 (Model results)

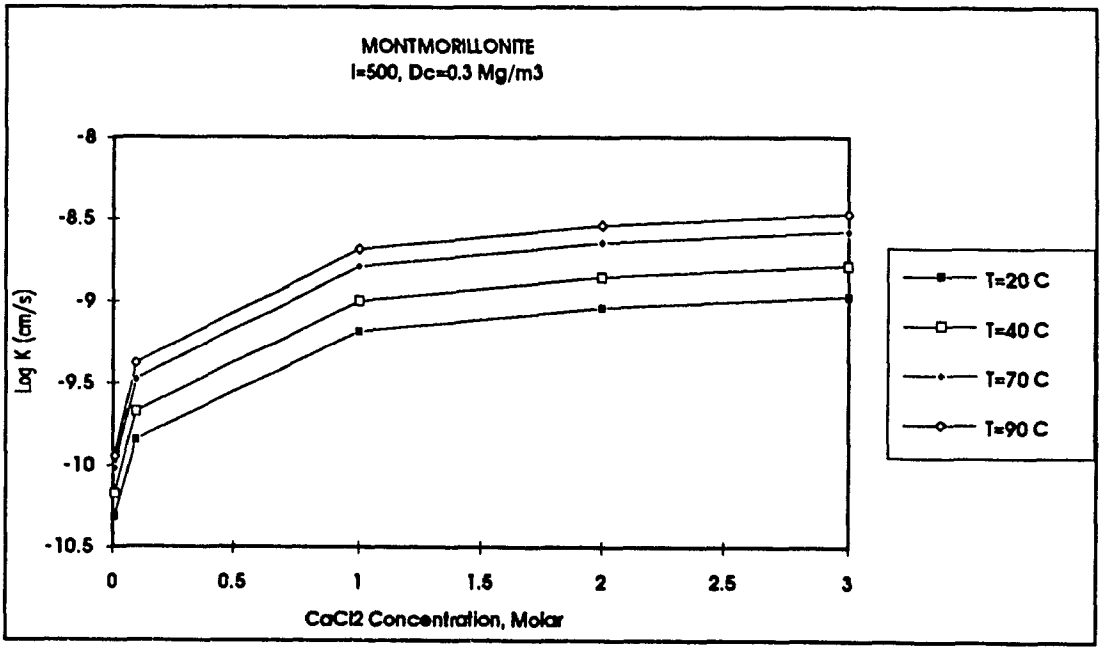

Figure C-40 Montmorillonite, Log K vs $CaCl_2$ concentration at T=20, 40, 70 and 90°C, γ_c = 0.3 Mg / m^3 and i = 500 (Model results)

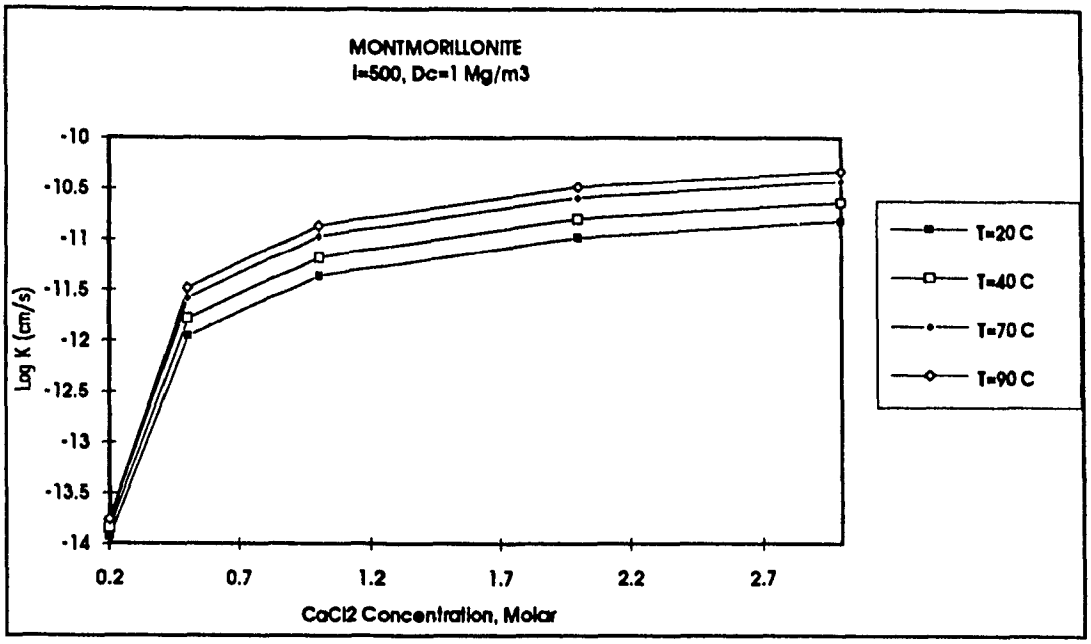

Figure C-41 Montmorillonite, Log K vs $CaCl_2$ concentration at T=20, 40, 70 and 90°C, γ_c = 1 Mg / m^3 and i = 500 (Model results)

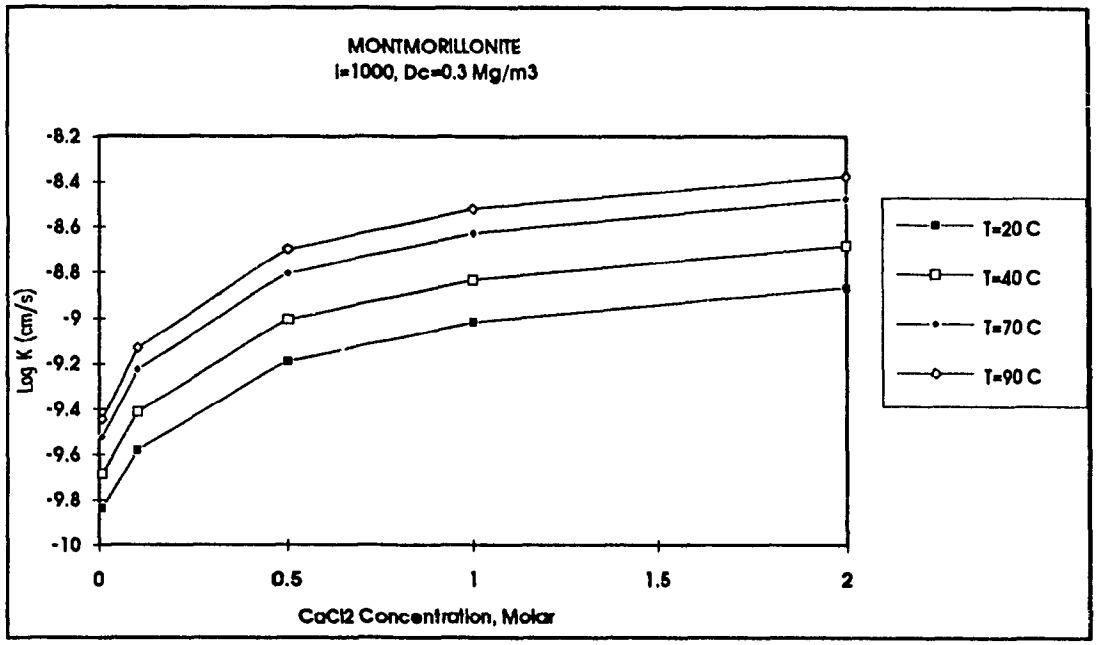

Figure C-42 Montmorillonite, Log K vs $CaCl_2$ concentration at T=20, 40, 70 and 90°C, γ_c = 0.3 Mg / m^3 and i = 1000 (Model results)

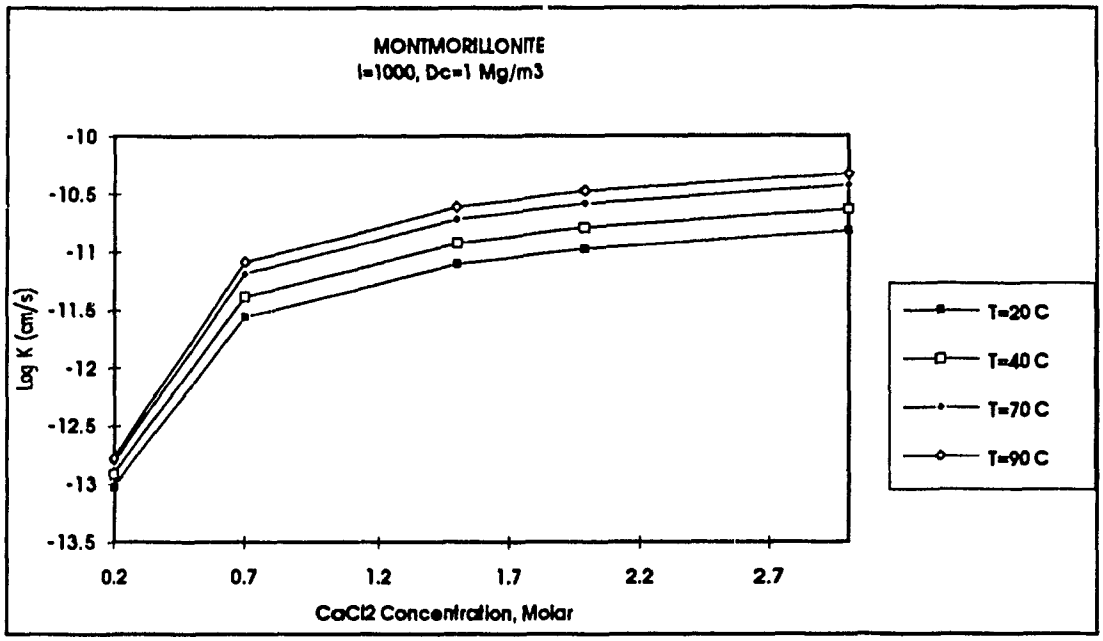

Figure C-43 Montmorillonite, Log K vs $CaCl_2$ concentration at T=20, 40, 70 and 90°C, γ_c = 1 Mg / m^3 and i = 1000 (Model results)

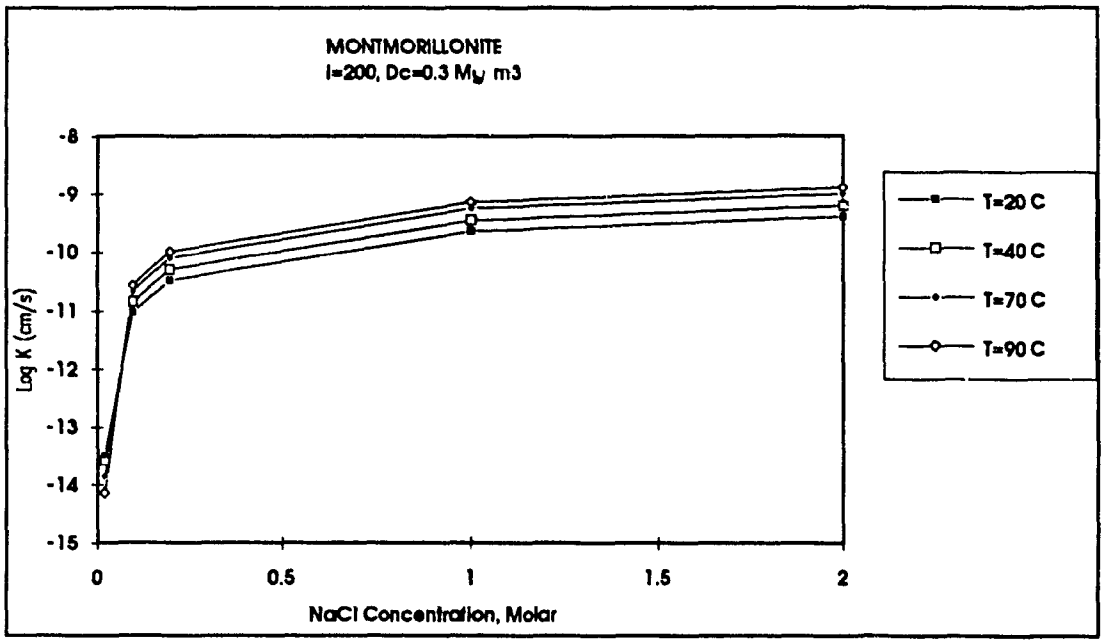

Figure C-44 Montmorillonite, Log K vs $CaCl_2$ concentration at T=20, 40, 70 and 90°C, γ_c = 0.3 Mg / m^3 and i = 200 (Model results)

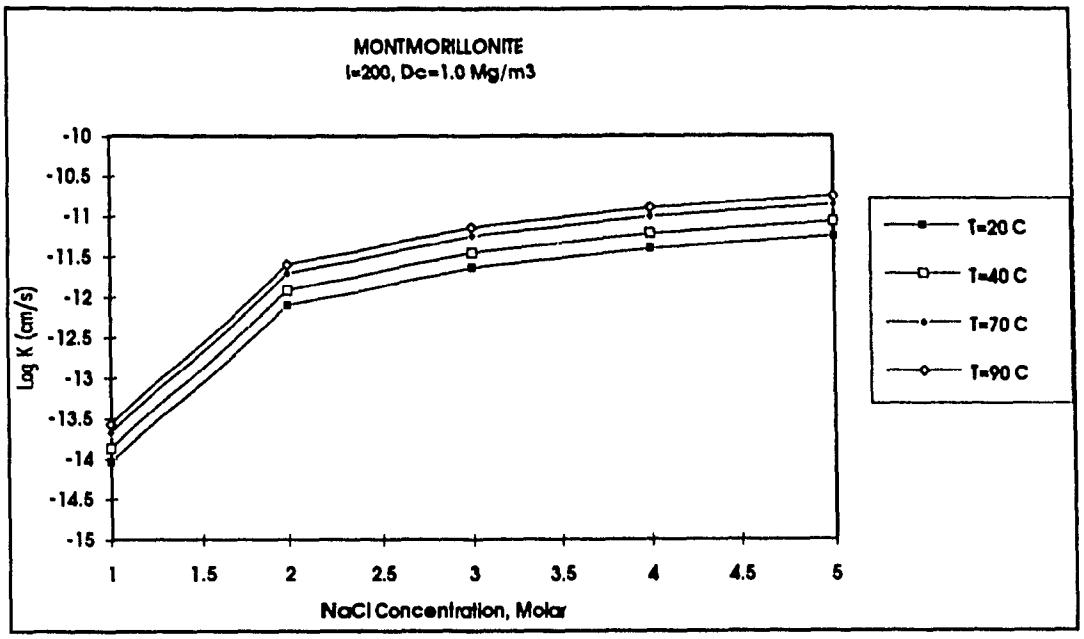

Figure C-45 Montmorillonite, Log K vs NaCl concentration at T=20, 40, 70 and 90°C, γ_c = 1 Mg / m^3 and i = 200 (Model results)

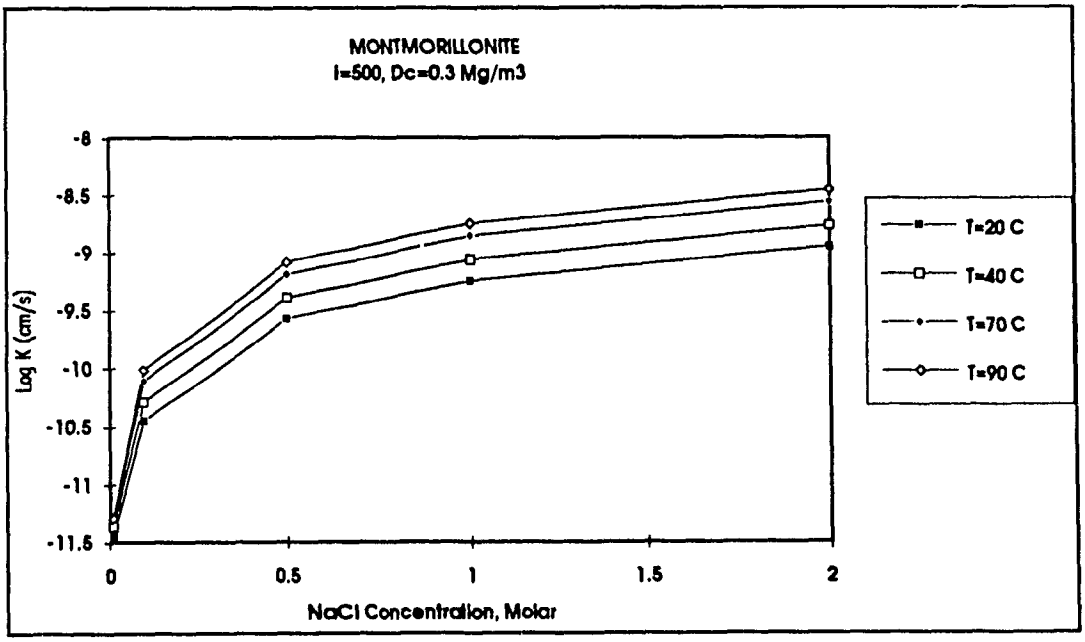

Figure C-46 Montmorillonite, Log K vs NaCl concentration at T=20, 40, 70 and 90°C, γ_c = 0.3 Mg / m^3 and i = 500 (Model results)

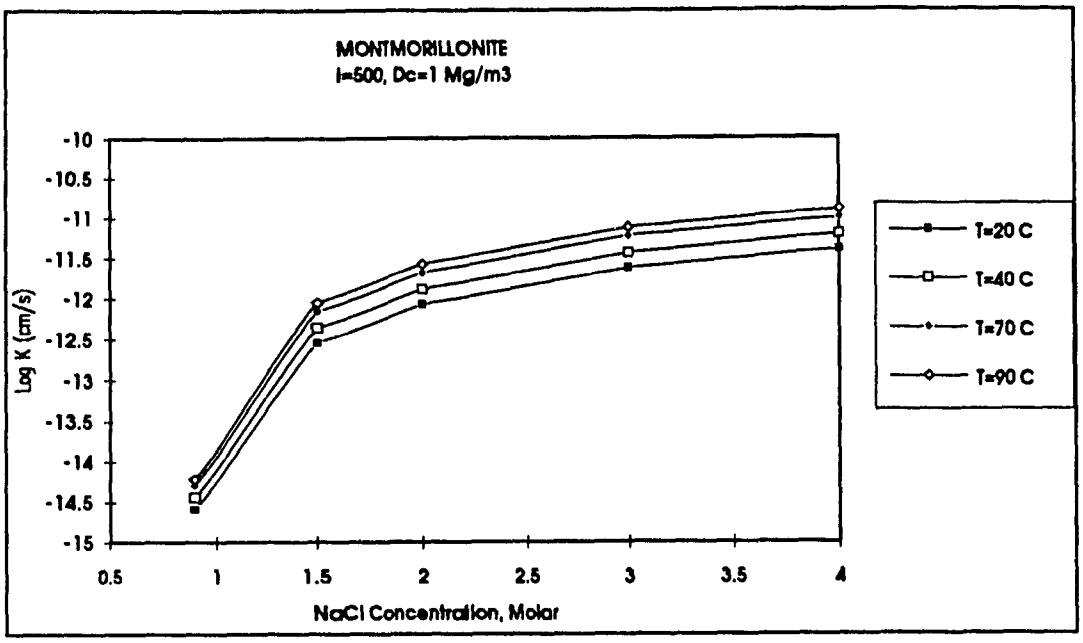

Figure C-47 Montmorillonite, Log K vs NaCl concentration at T=20, 40, 70 and 90°C, γ_c = 1 Mg / m^3 and i = 500 (Model results)

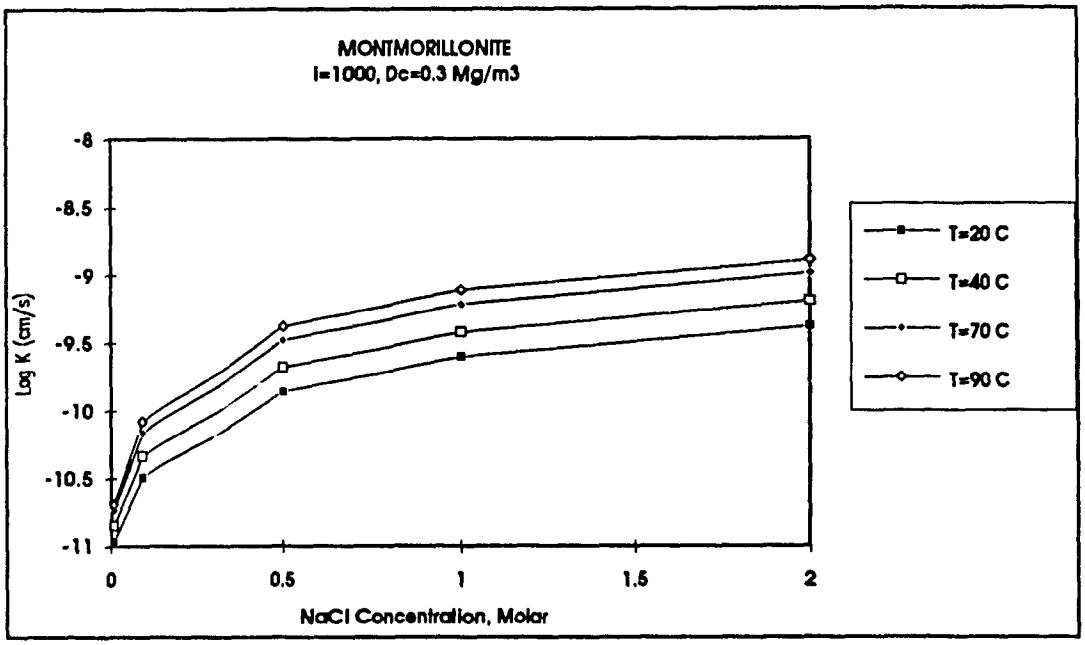

Figure C-48 Montmorillonite, Log K vs $CaCl_2$ concentration at T=20, 40, 70 and 90°C, γ_c = 0.3 Mg / m^3 and i = 1000 (Model results)

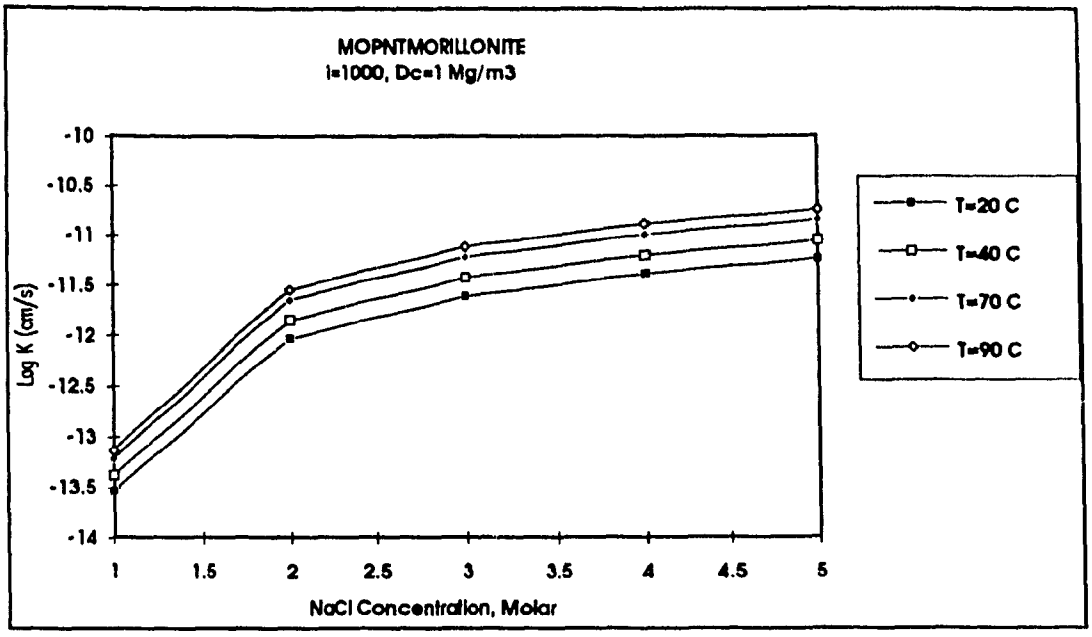

Figure C-49 Montmorillonite, Log K vs NaCl concentration at T=20, 40, 70 and 90°C, γ_c = 1 Mg / m^3 and i = 1000 (Model results)

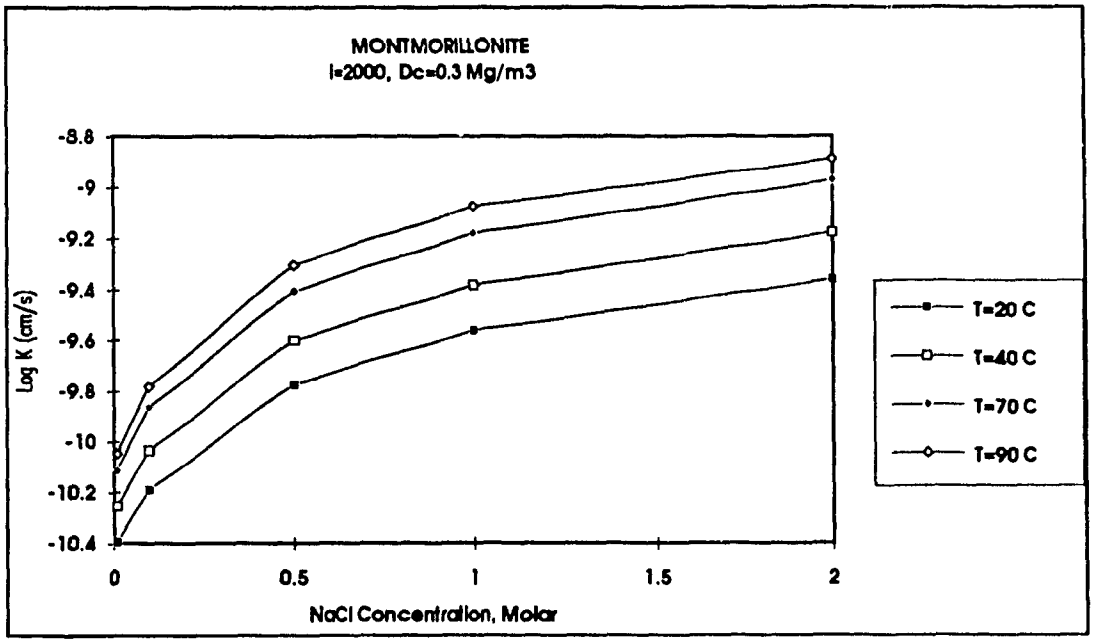

Figure C-50 Montmorillonite, Log K vs NaCl concentration at T=20, 40, 70 and 90°C, γ_c = 0.3 Mg / m^3 and i = 2000 (Model results)

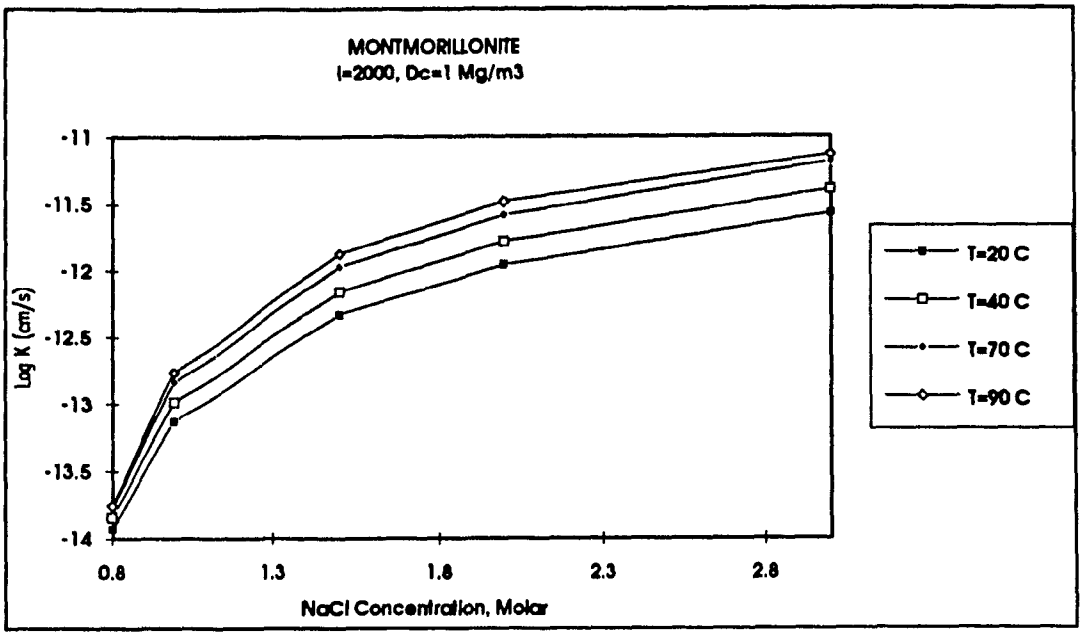

Figure C-51 Montmorillonite, Log K vs NaCl concentration at T=20, 40, 70 and 90°C, γ_c = 1 Mg / m^3 and i = 2000 (Model results)

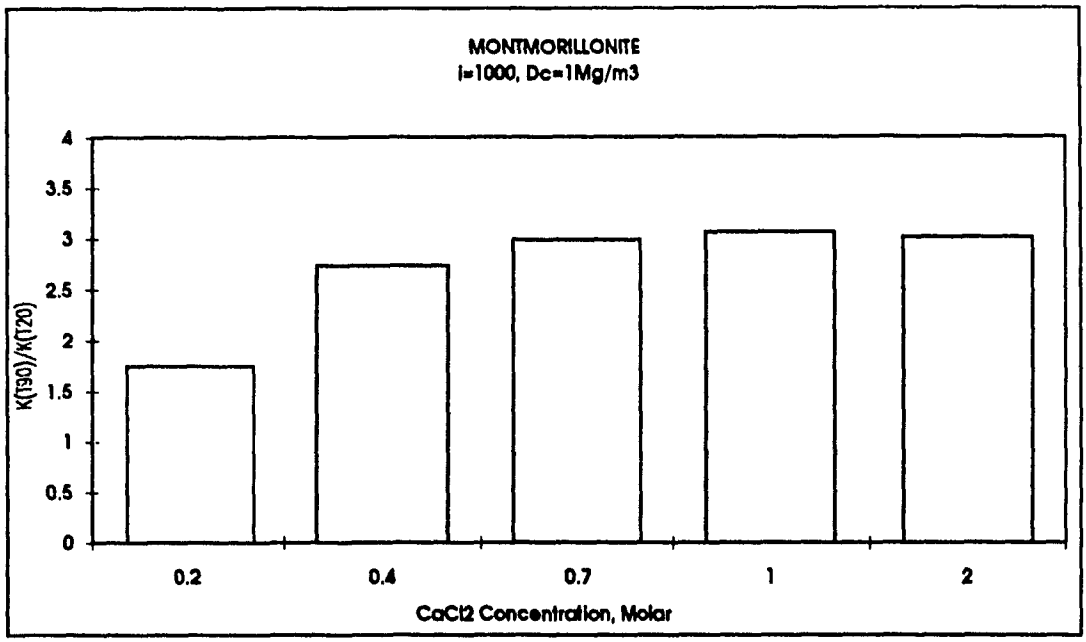

Figure C-52 Montmorillonite, K90/K20 vs $CaCl_2$ concentration at i = 1000 and γ_c = 1 Mg / m^3 (Model results)

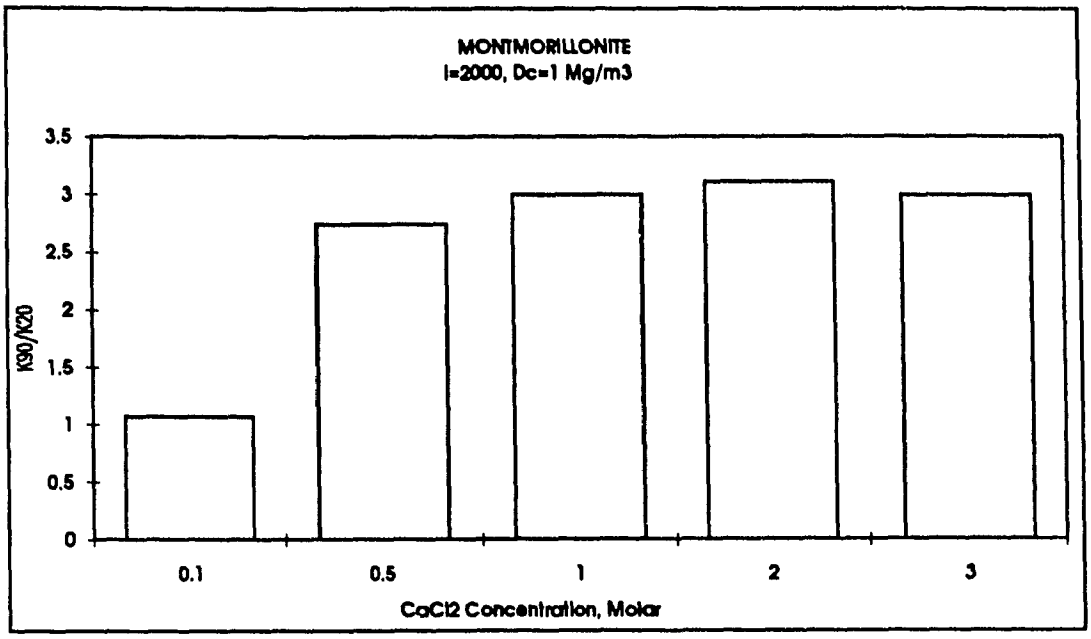

Figure C-53 Montmorillonite, K90/K20 vs $CaCl_2$ concentration at i = 2000 and γ_c = 1 Mg / m^3 (Model results)

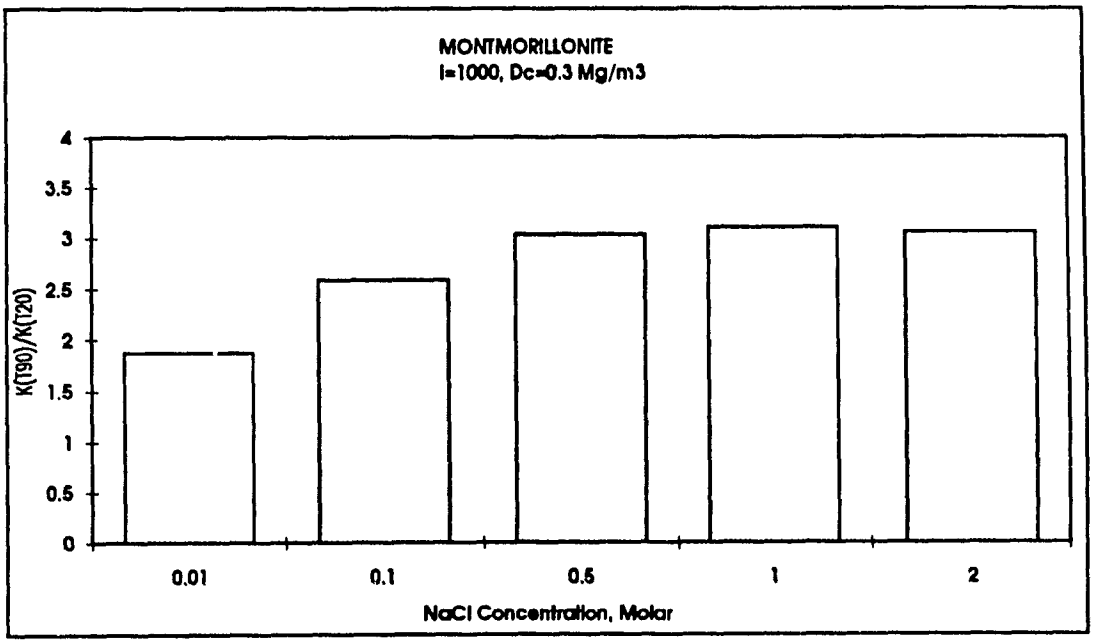

Figure C-54 Montmorillonite, K90/K20 vs NaCl concentration at i = 1000 and γ_c = 0.3 Mg / m^3 (Model results)

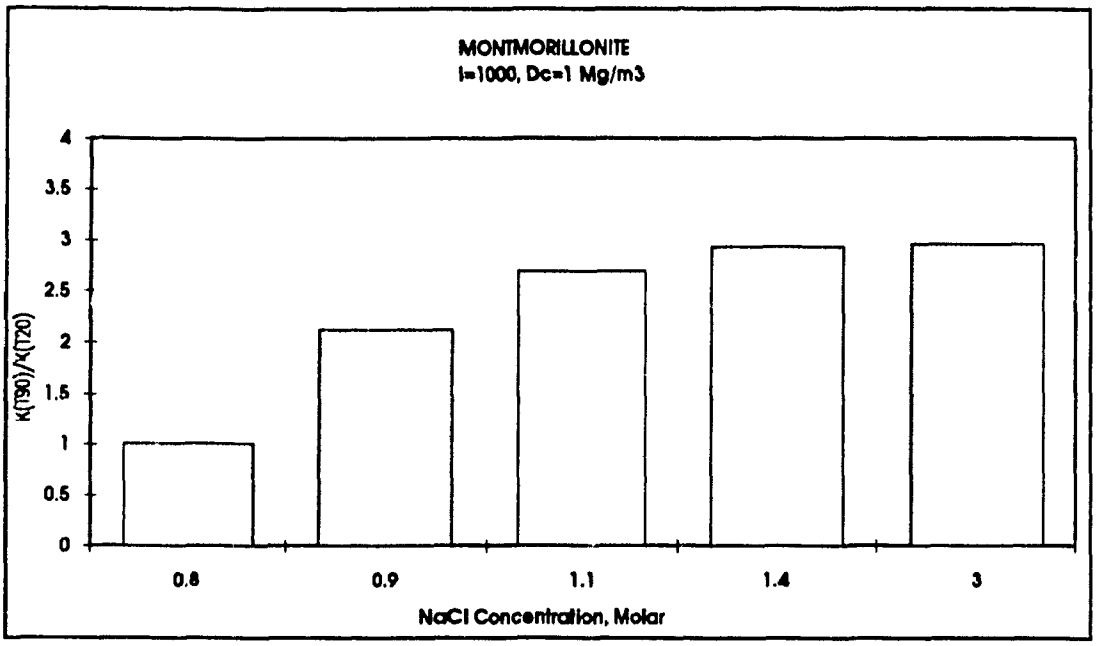

Figure C-55 Montmorillonite, K90/K20 vs NaCl concentration at i = 1000 and γ_c = 1 Mg / m^3 (Model results)

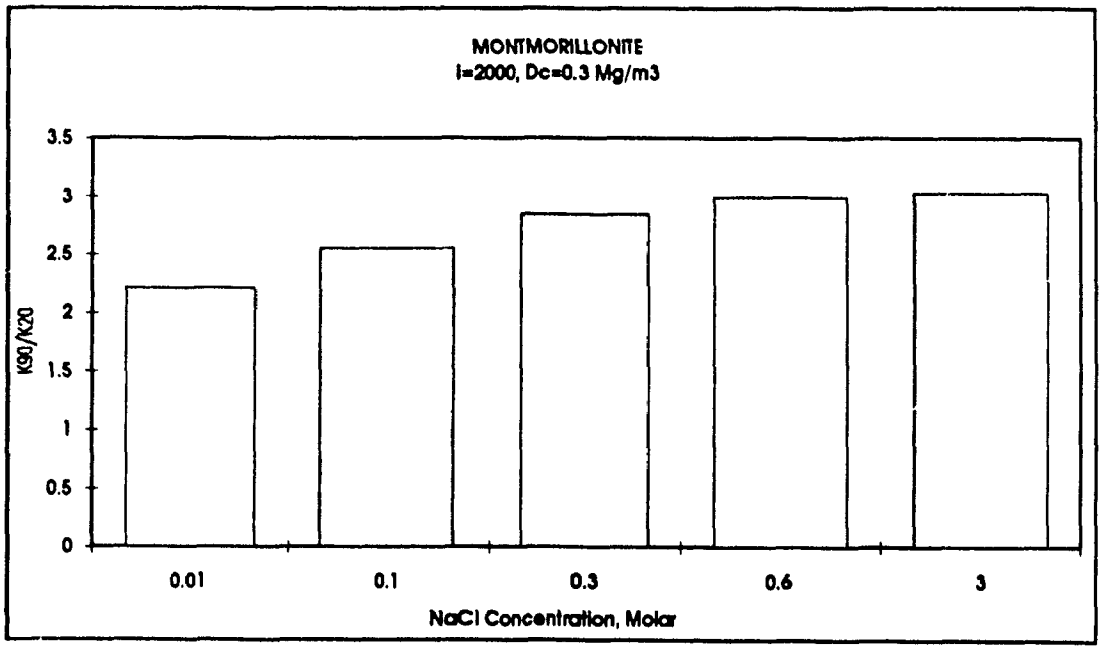

Figure C-56 Montmorillonite, K90/K20 vs NaCl concentration at i = 2000 and γ_c = 0.3 Mg / m^3 (Model results)

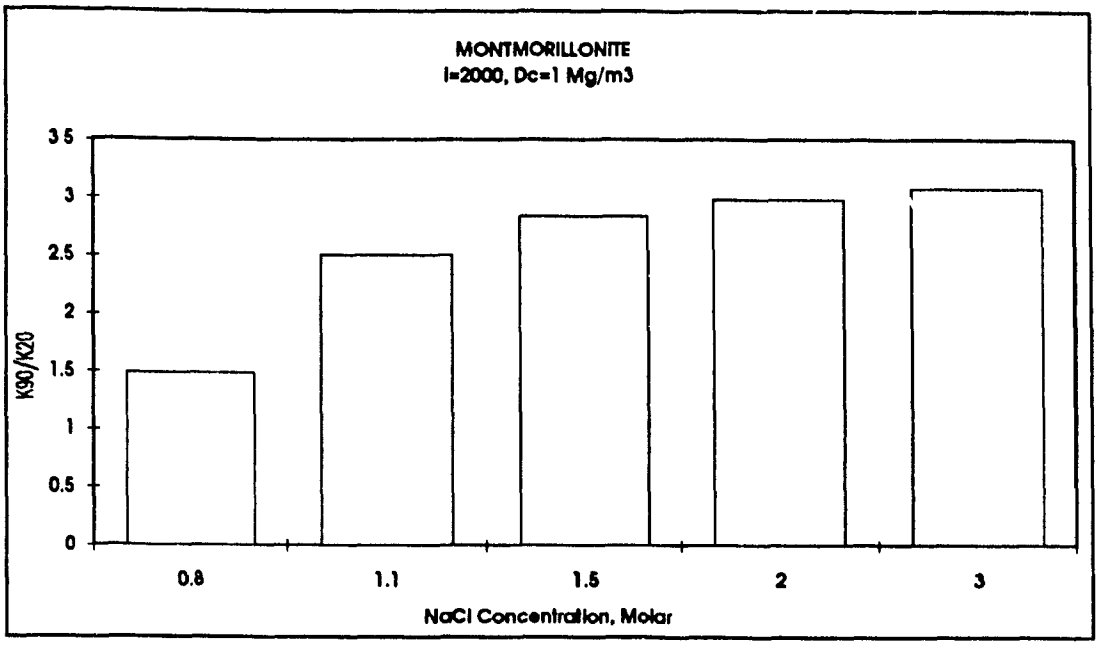

Figure C-57 Montmorillonite, K90/K20 vs NaCl concentration at i = 2000 and γ_c = 1 Mg / m^3 (Model results)

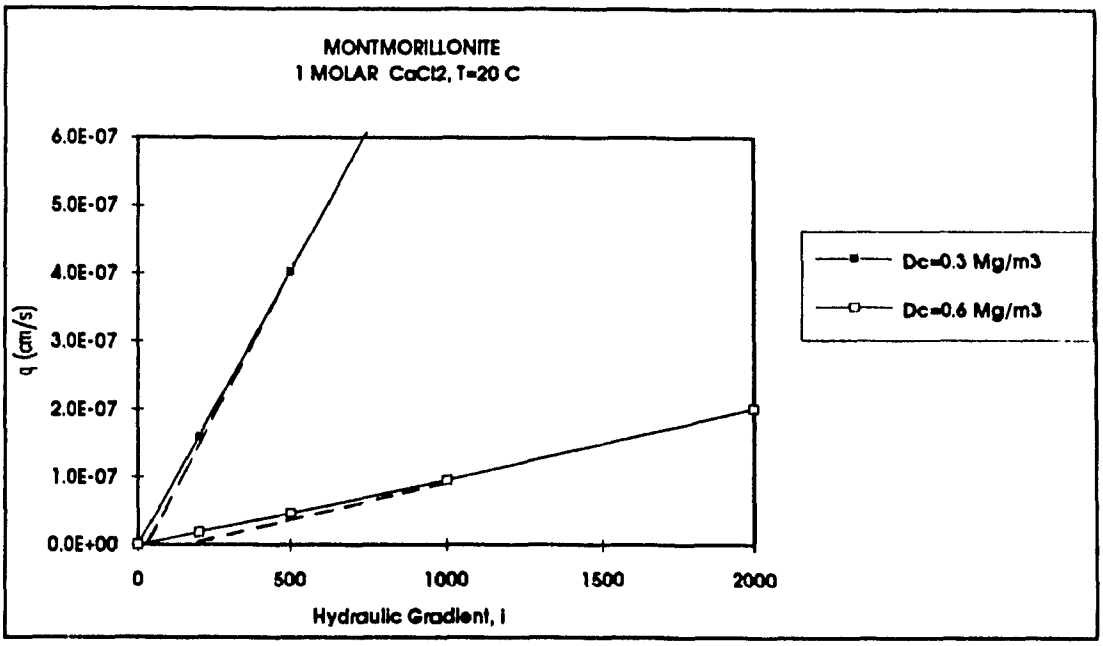

Figure C-58 Montmorillonite, q (cm/s) vs i at 1 M $CaCl_2$ and γ_c = 0.3 and 1 Mg / m^3 (Model results)

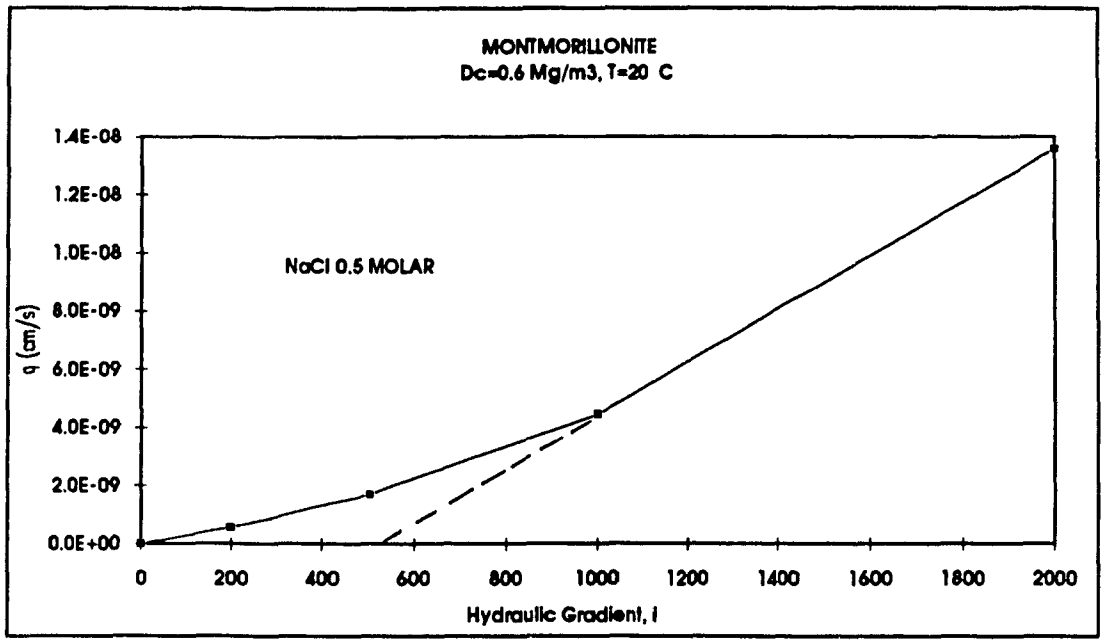

Figure C-59 Montmorillonite, q (cm/s) vs i at 0.5M NaCl and $\gamma_c = 0.6$ Mg / m^3 (Model results)

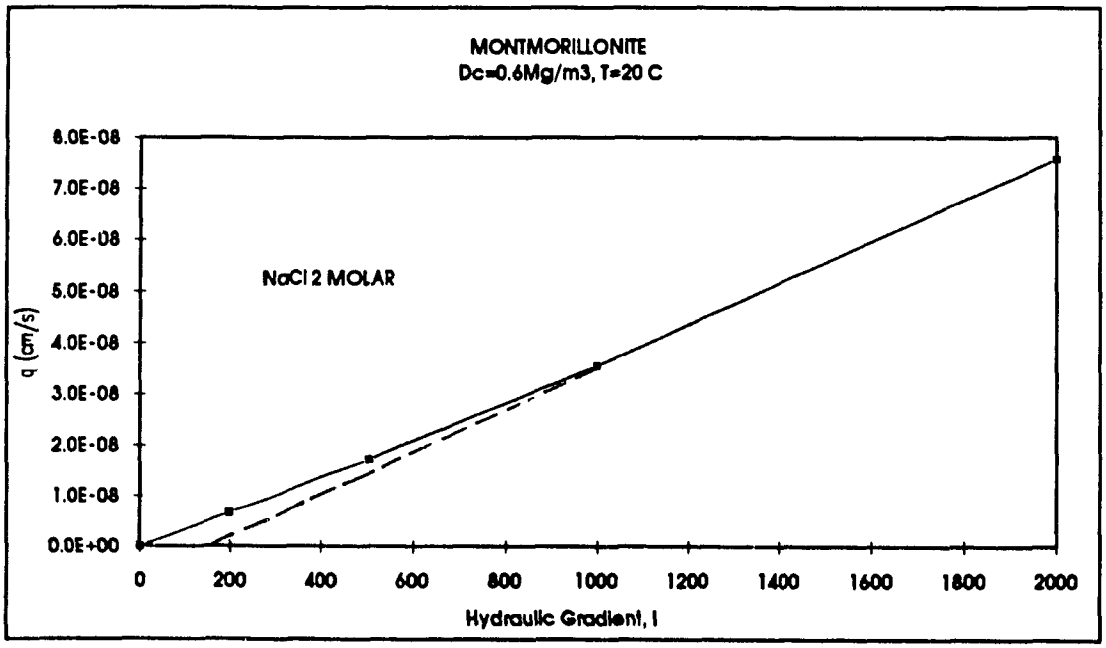

Figure C-60 Montmorillonite, q (cm/s) vs i at 2M NaCl and $\gamma_c = 0.6$ Mg / m^3 (Model results)

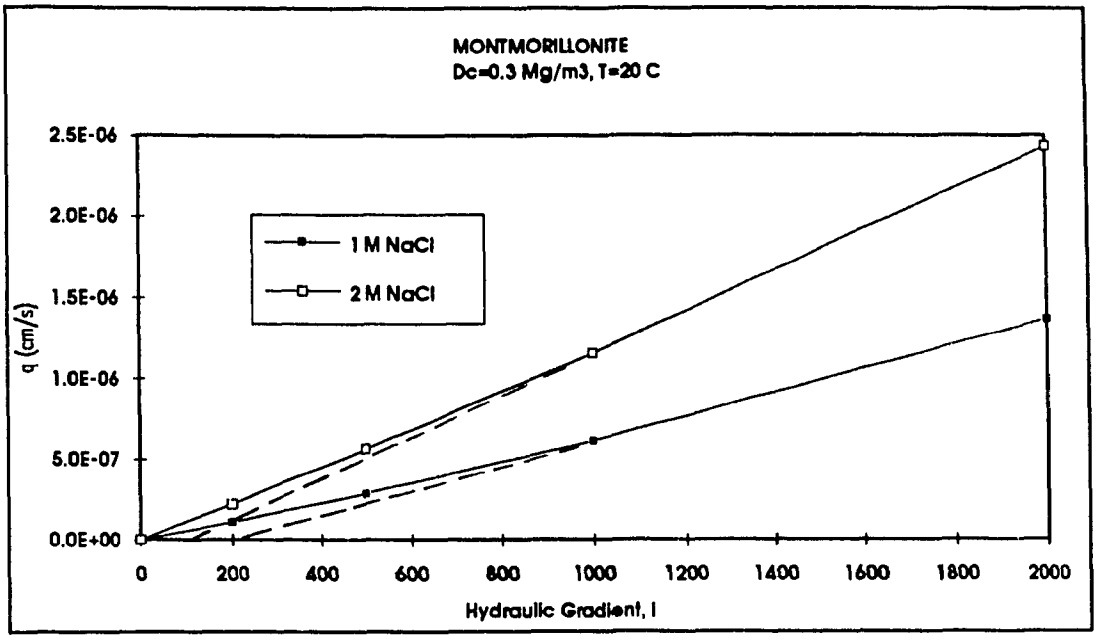

Figure C-61 Montmorillonite, q (cm/s) vs i at 1M and 2M NaCl and $\gamma_c = 0.3$ Mg / m^3 (Model results)

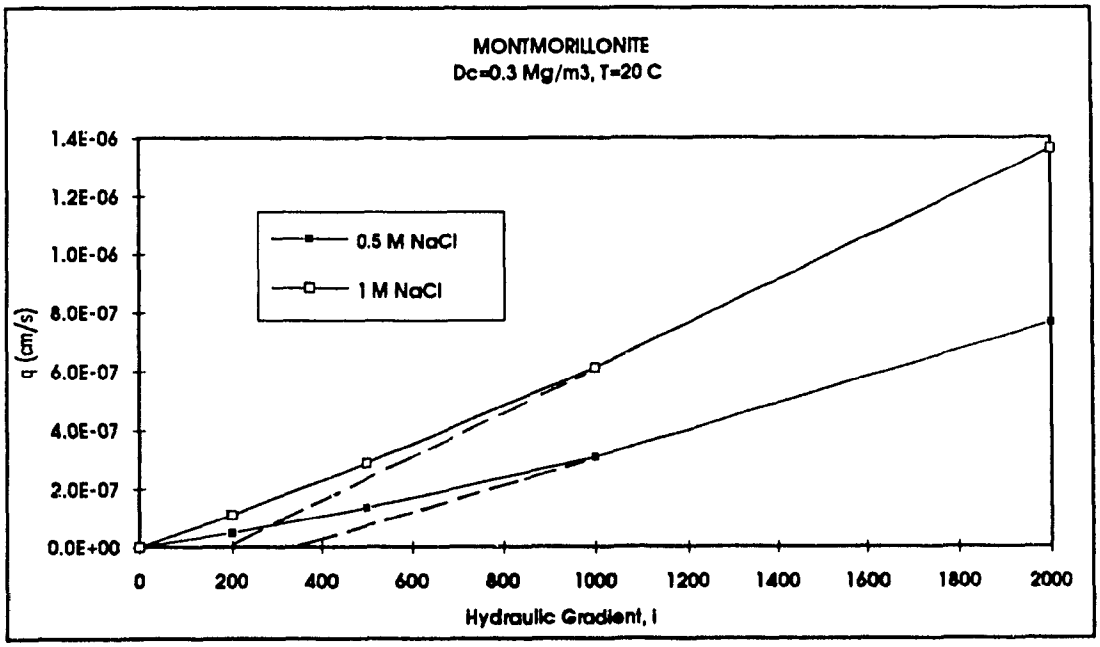

Figure C-62 Montmorillonite, q (cm/s) vs i at 0.5M and 1M NaCl and $\gamma_c = 0.3$ Mg/m^3 (Model results)

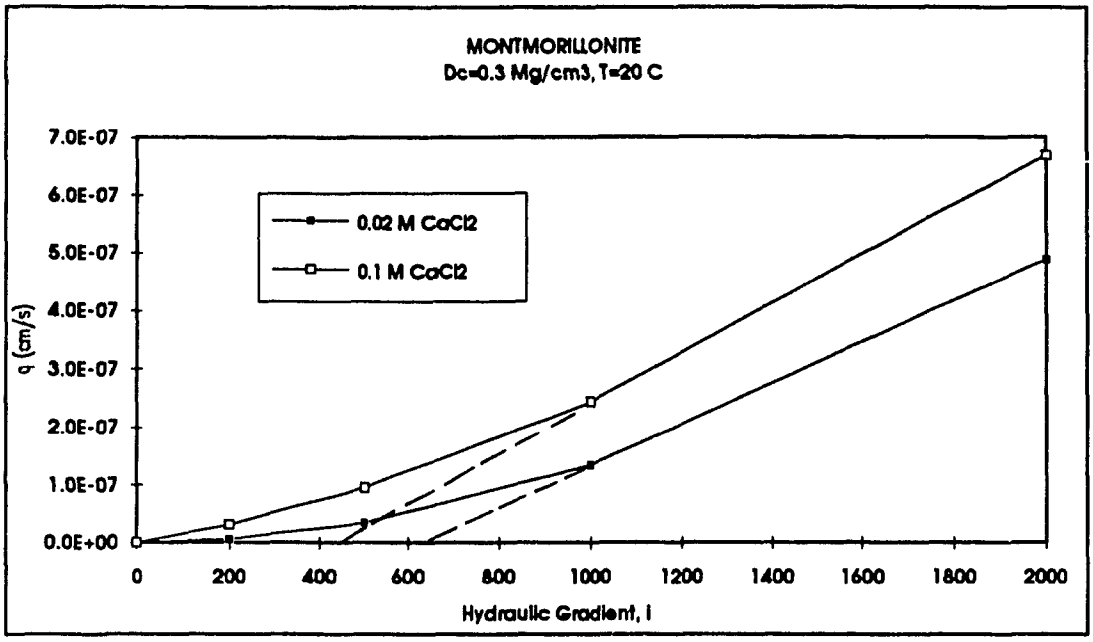

Figure C-63 Montmorillonite, q (cm/s) vs i at 0.02M and 0.1M $CaCl_2$ and $\gamma_c = 0.3$ Mg/m^3 (Model results)

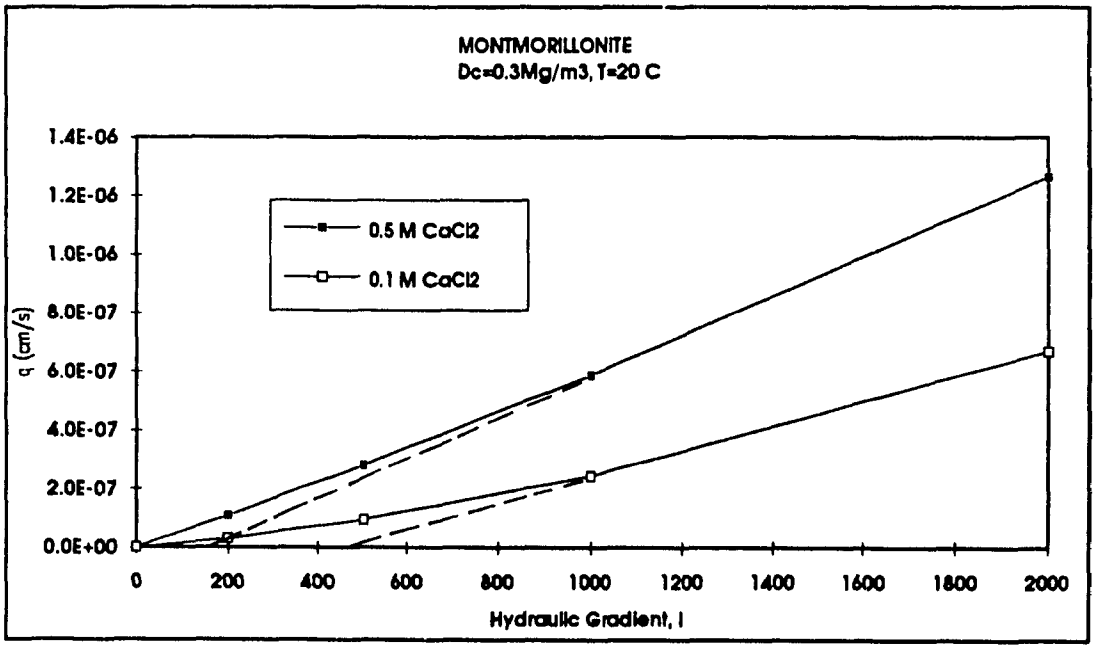

Figure C-64 Montmorillonite, q (cm/s) vs i at 0.5M and 0.1M $CaCl_2$ and $\gamma_c = 0.3$ Mg/m^3 (Model results)

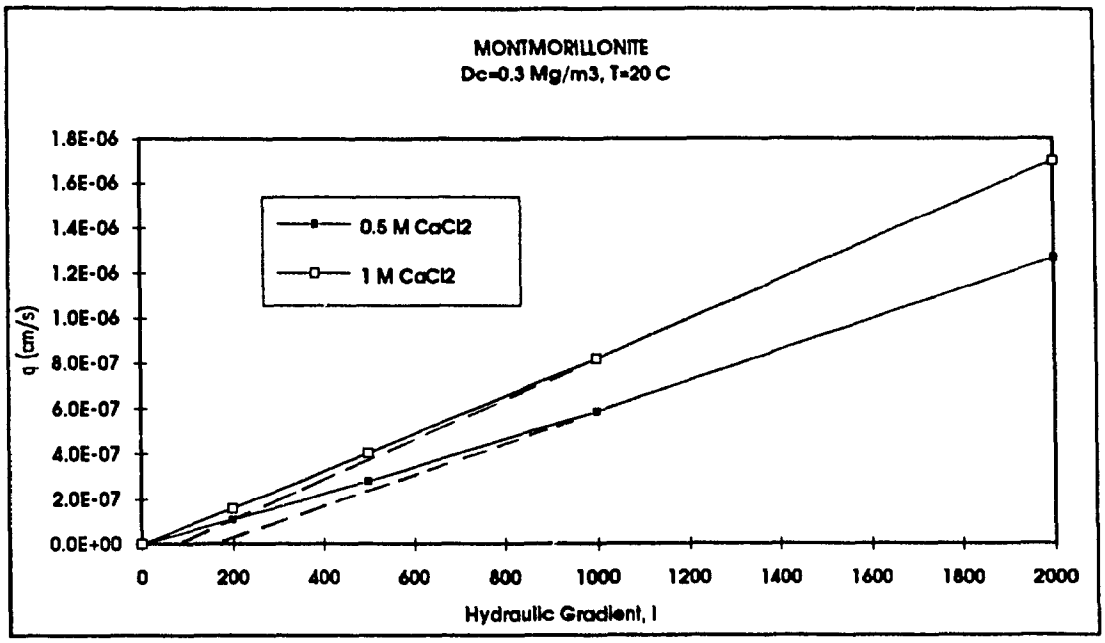

Figure C-65 Montmorillonite, q (cm/s) vs i at 0.5M and 1M $CaCl_2$ and $\gamma_c = 0.3$ Mg/m^3 (Model results)

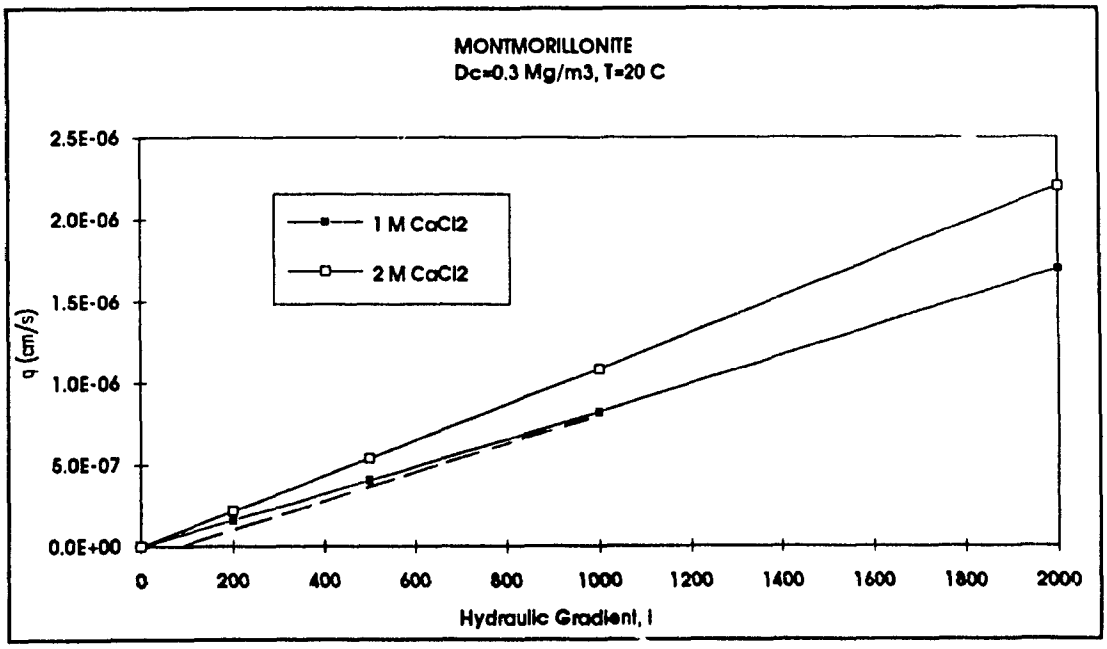

Figure C-66 Montmorillonite, q (cm/s) vs i at 1M and 2M $CaCl_2$ and $\gamma_c = 0.3$ Mg/m^3 (Model results)

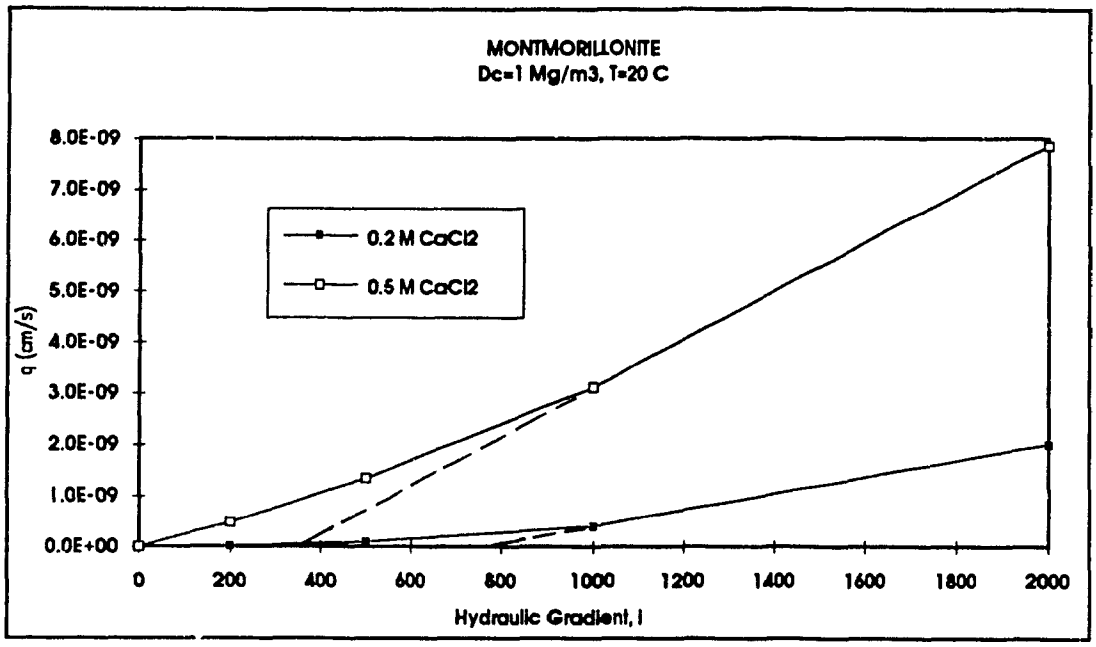

Figure C-67 Montmorillonite, q (cm/s) vs i at 0.2M and 0.5M $CaCl_2$ and γ_c = 1 Mg/m^3 (Model results)

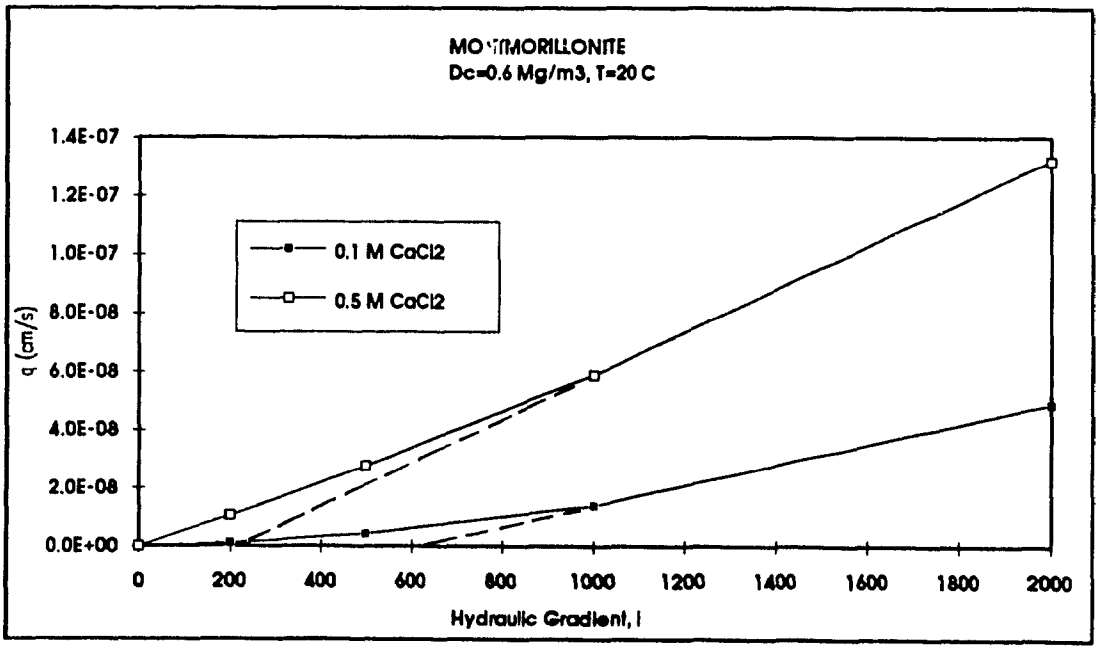

Figure C-68 Montmorillonite, q (cm/s) vs i at 0.5M and 0.1M $CaCl_2$ and γ_c = 0.6 Mg/m^3 (Model results)

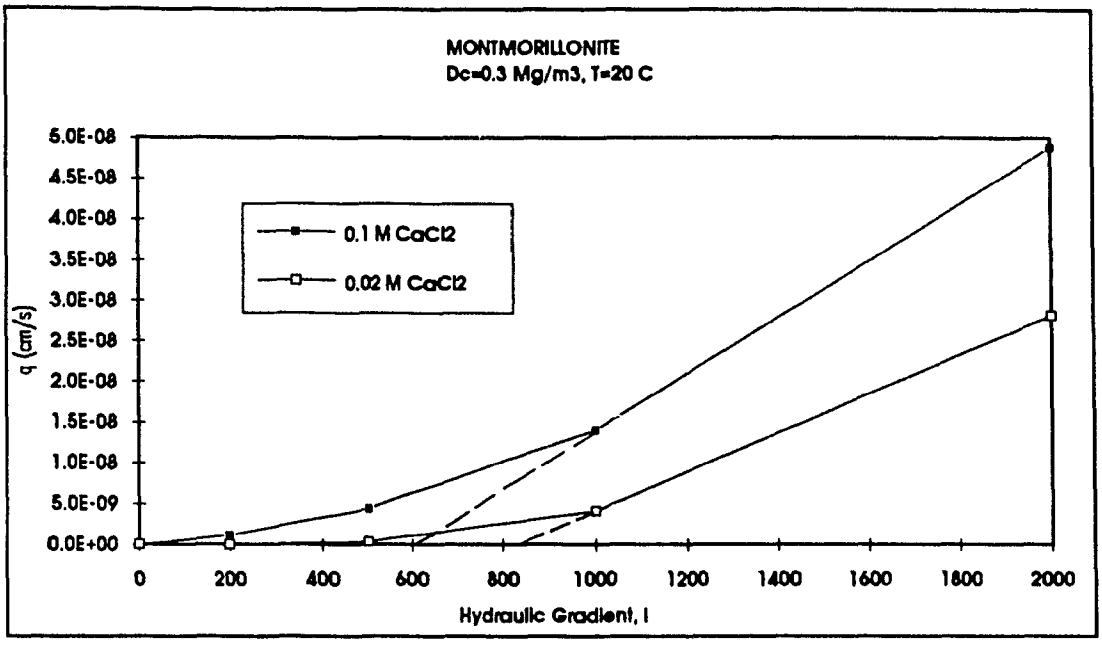

Figure C-69 Montmorillonite, q (cm/s) vs i at 0.02M and 0.1M $CaCl_2$ and $\gamma_c = 0.3$ Mg/m^3 (Model results)

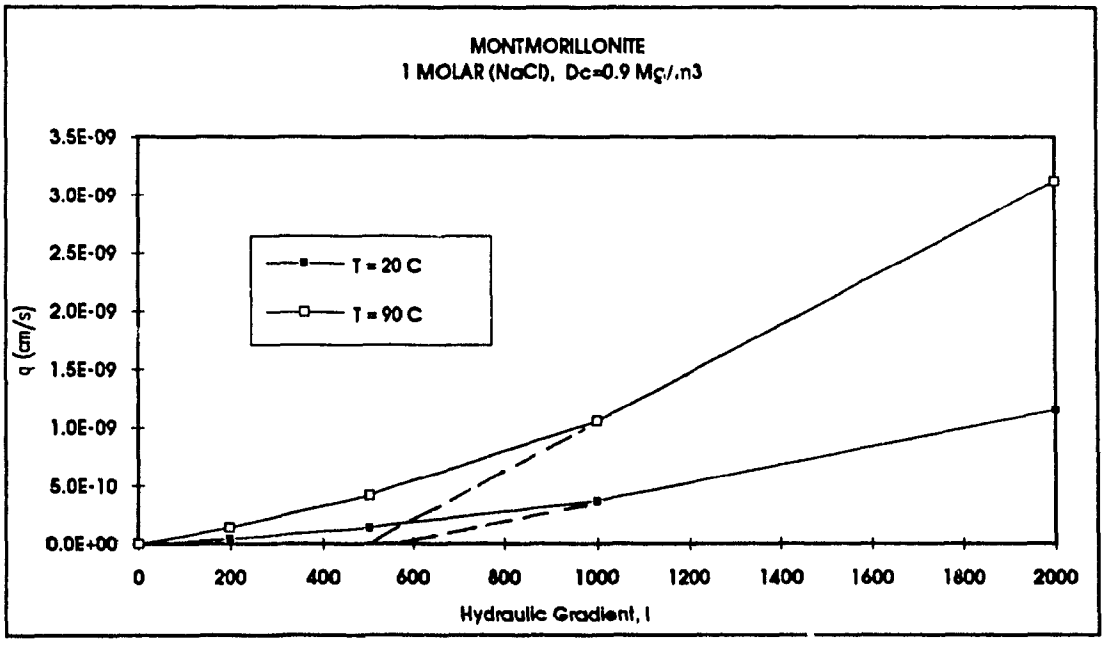

Figure C-70 Montmorillonite, q (cm/s) vs i at T=20 and 90°C, 1M NaCl and $\gamma_c = 0.9$ Mg/m^3 (Model results)

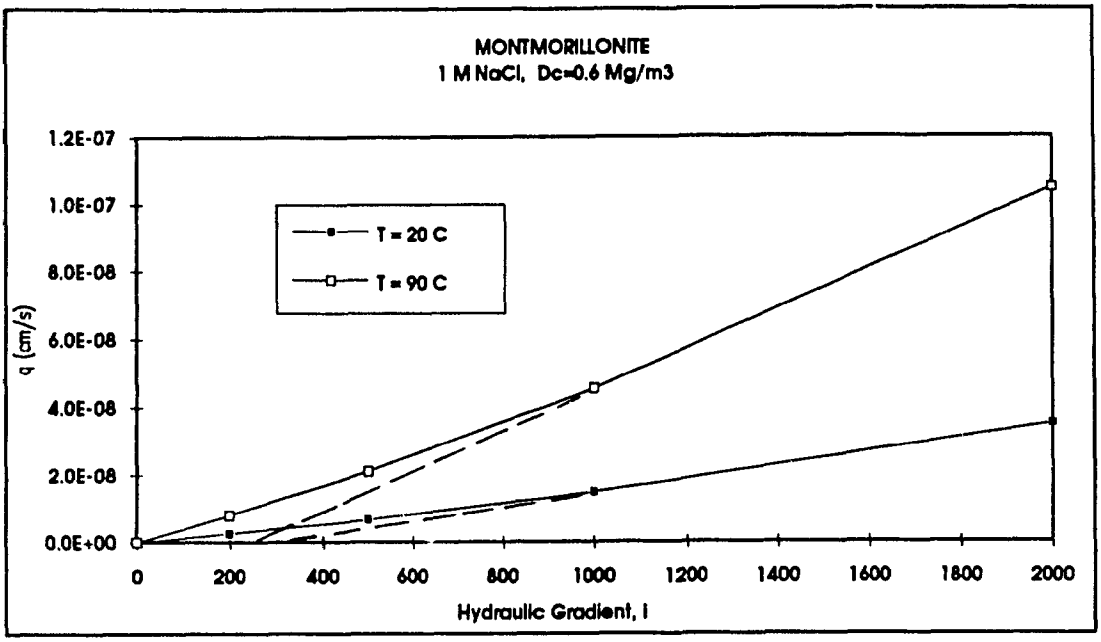

Figure C-71 Montmorillonite, q (cm/s) vs i at T=20 and 90°C, 1M NaCl and γ_c = 0.6 Mg/m^3 (Model results)

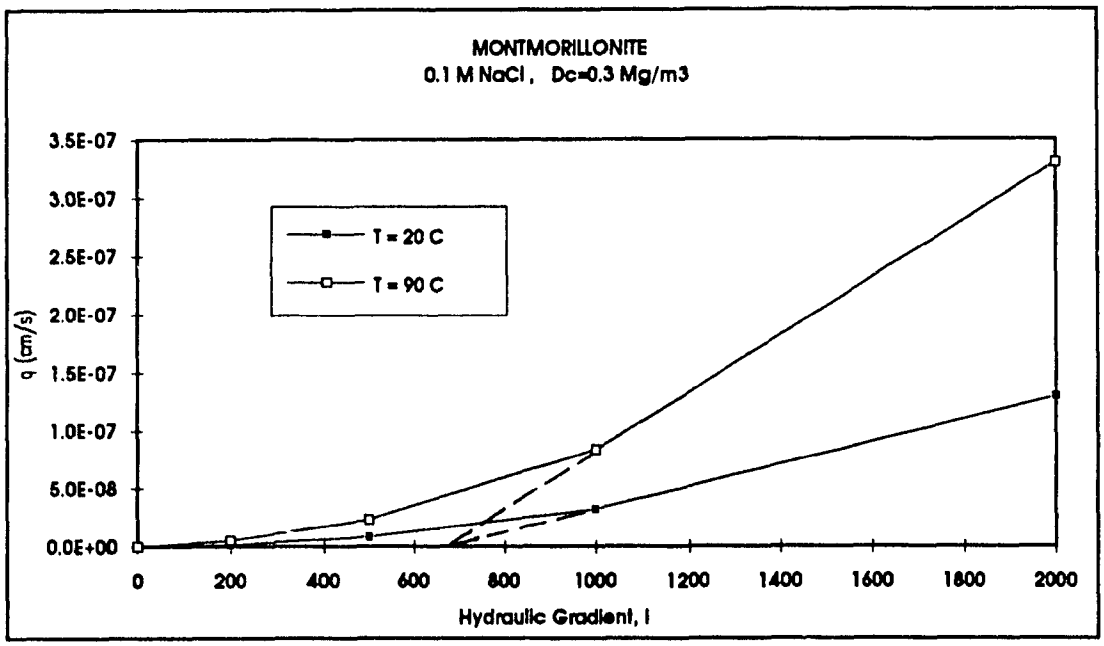

Figure C-72 Montmorillonite, q (cm/s) vs i at T=20 and 90°C, 0.1M NaCl and γ_c = 0.3 Mg/m^3 (Model results)

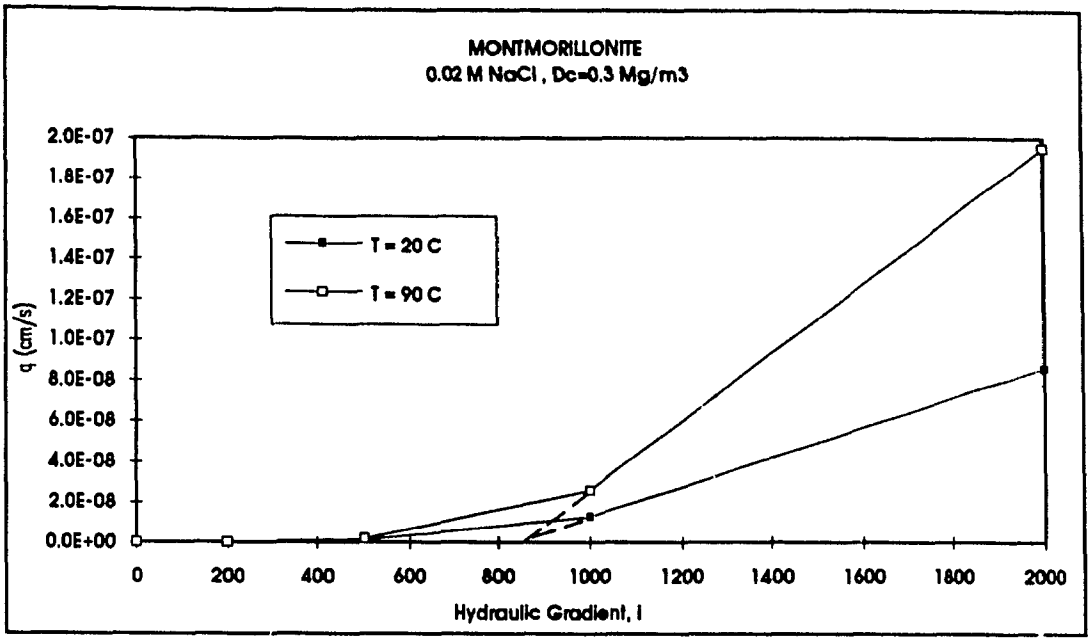

Figure C-73 Montmorillonite, q (cm/s) vs i at T = 20 and 90°C, 0.02M NaCl and γ_c = 0.3 Mg/m^3 (Model results)

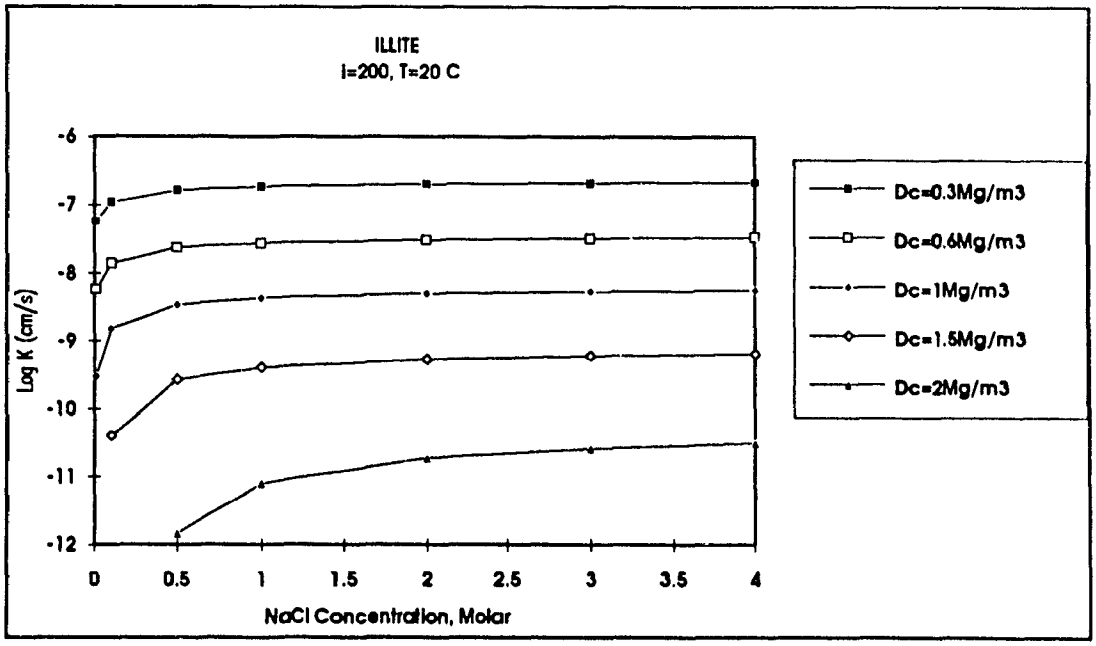

Figure C-74 Illite, Log K vs NaCl concentration at γ_c = 0.3, 0.6, 1, 1.5, 2 Mg/m^3 and i = 200 (Model results)

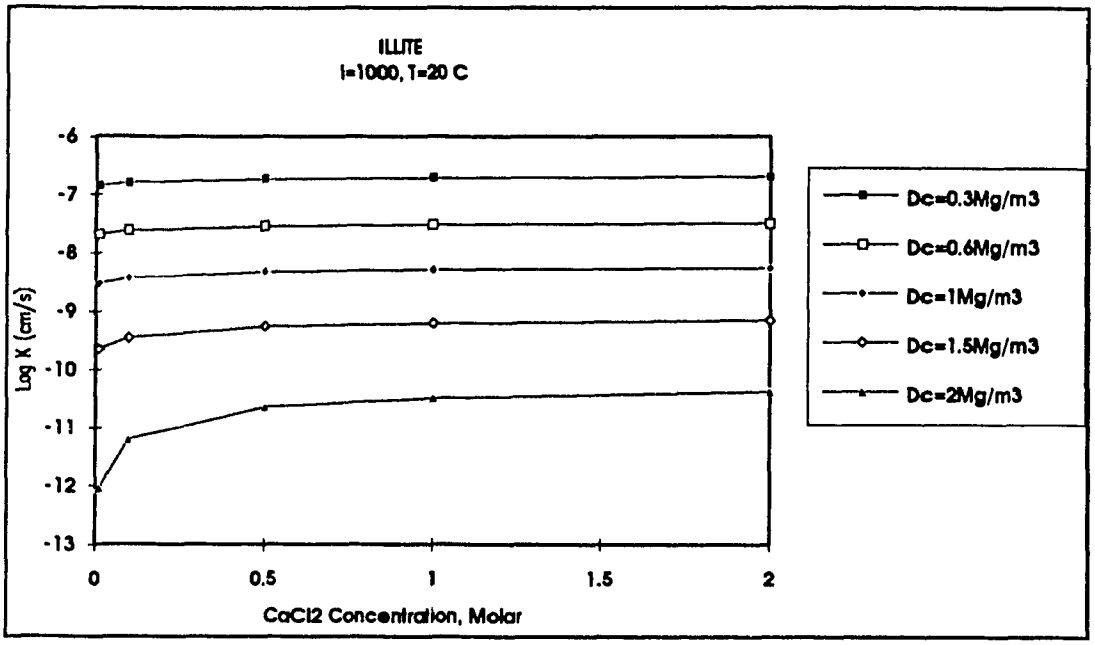

Figure C-75 Illite, Log K vs $CaCl_2$ concentration at γ_c = 0.3, 0.6, 1, 1.5, 2 Mg/m^3 and i = 1000 (Model results)

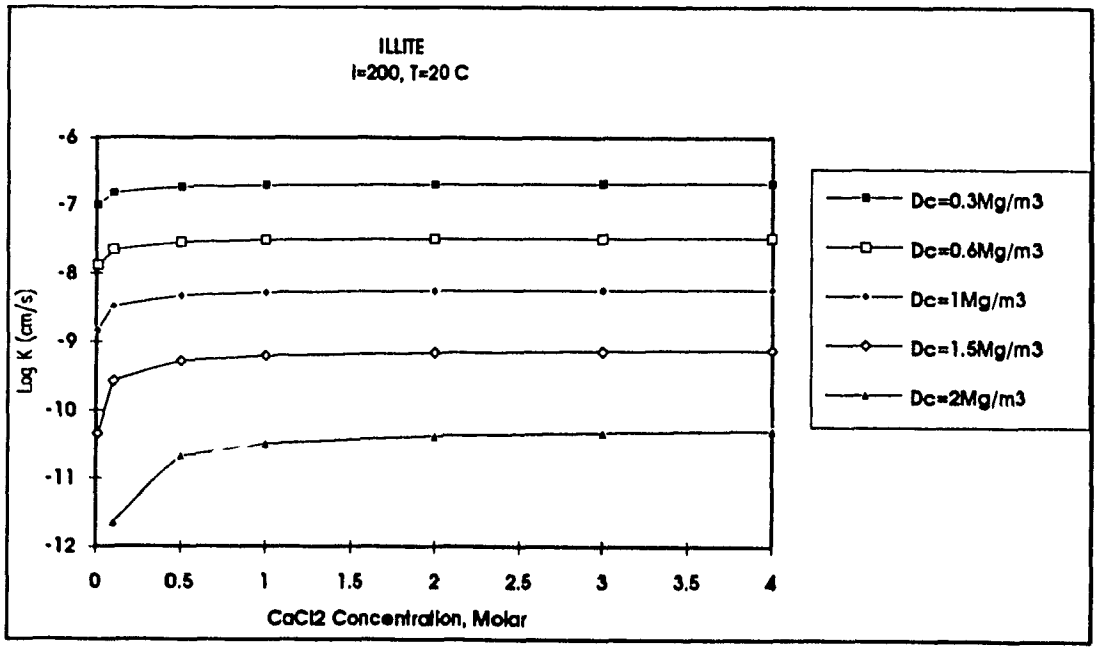

Figure C-76 Illite, Log K vs $CaCl_2$ concentration at γ_c = 0.3, 0.6, 1, 1.5, 2 Mg/m^3 and i = 200 (Model results)

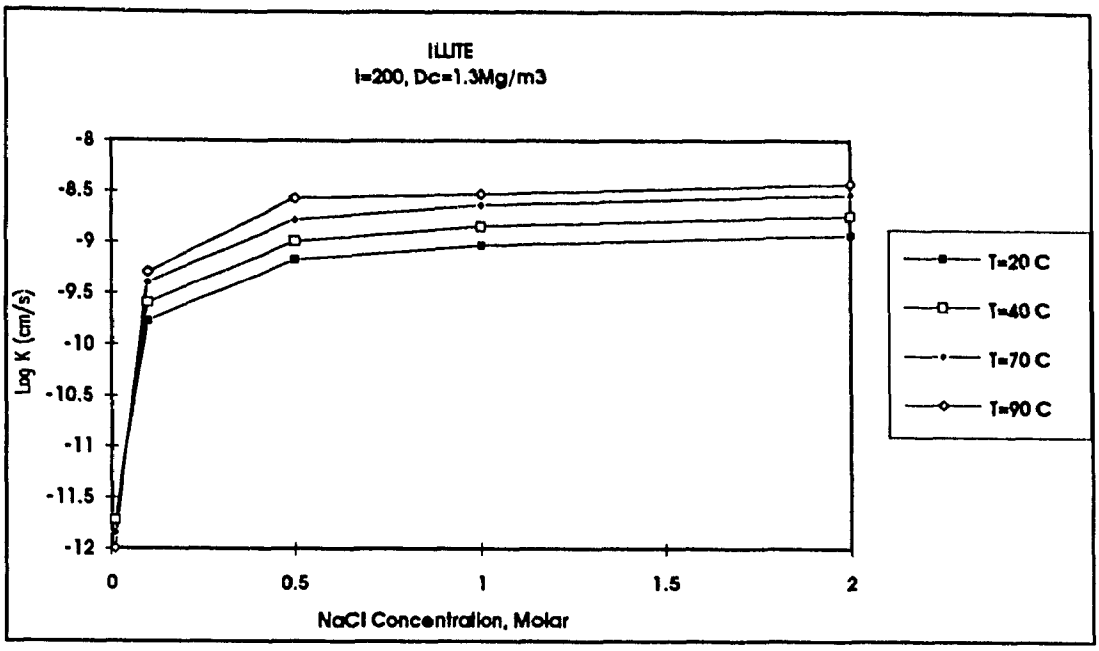

Figure C-77 Illite, Log K vs NaCl concentration at T = 20, 40, 70 and 90°C, i = 200, γ_c = 1.3 Mg / m^3 (Model results)

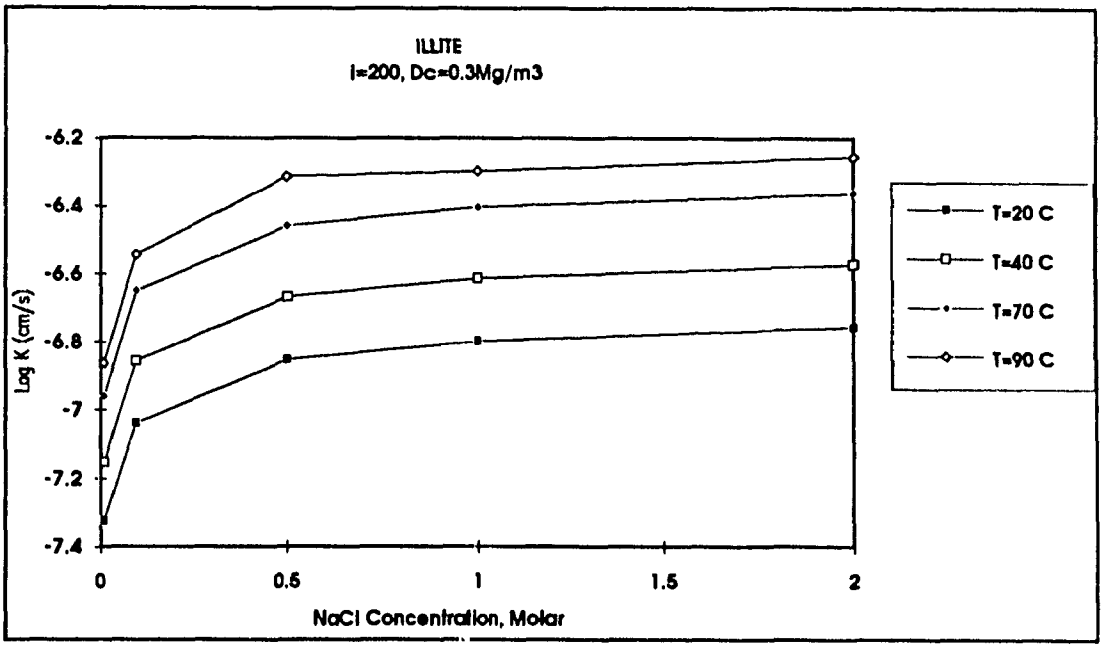

Figure C-78 Illite, Log K vs NaCl concentration at T = 20, 40, 70 and 90°C, i = 200, γ_c = 0.3 Mg / m^3 (Model results)

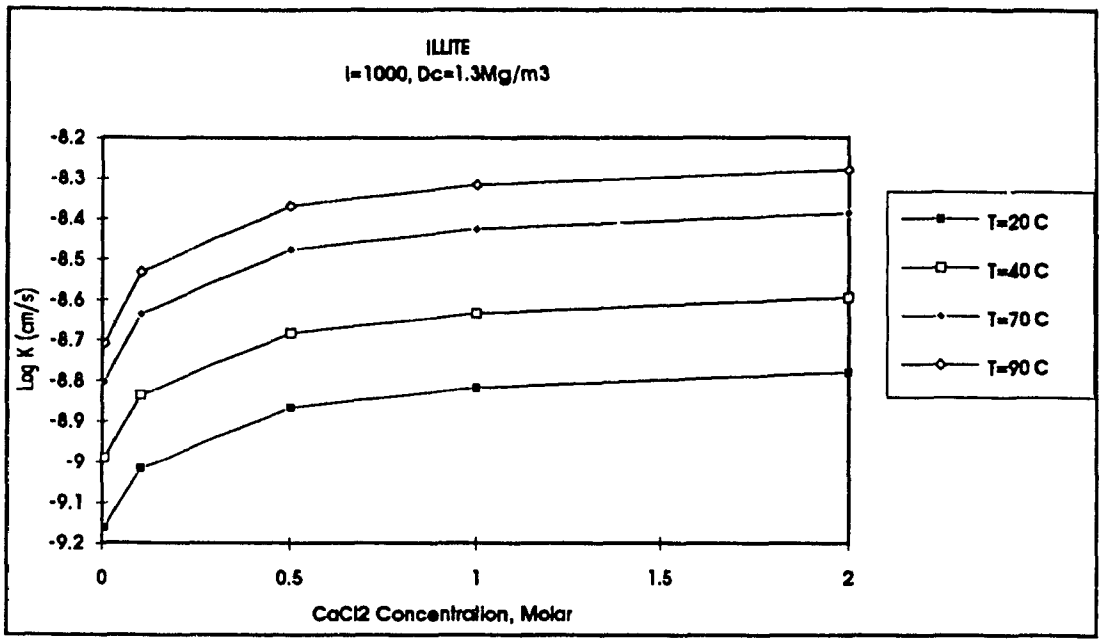

Figure C-79 Illite, Log K vs $CaCl_2$ concentration at T = 20, 40, 70 and 90°C, i = 1000, γ_c = 1.3 Mg / m^3 (Model results)

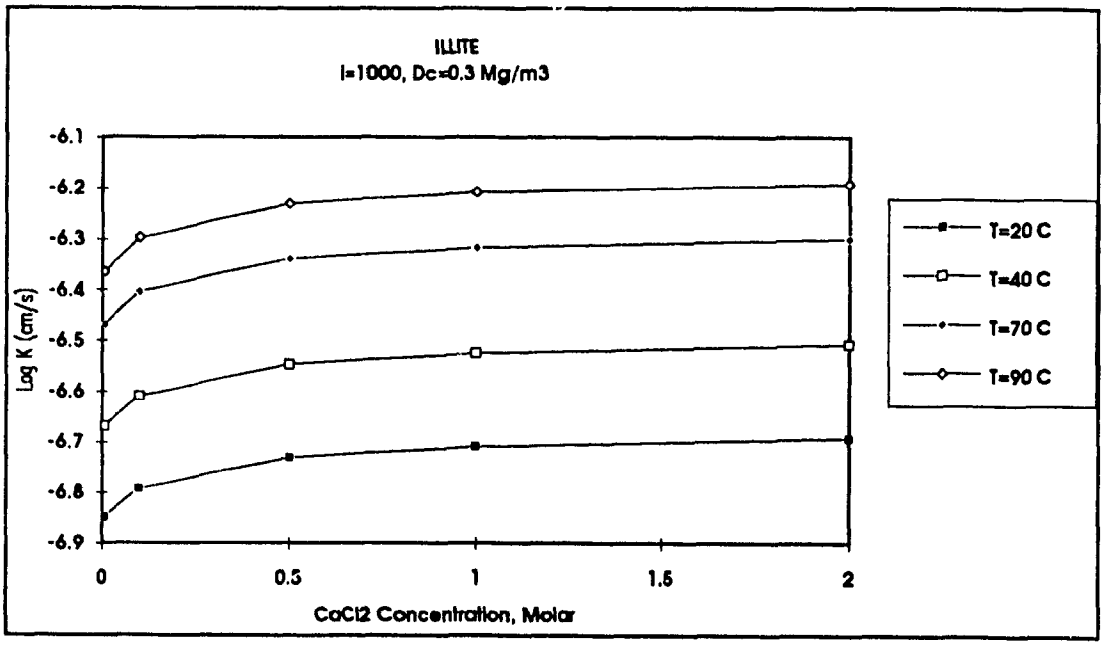

Figure C-80 Illite, Log K vs $CaCl_2$ concentration at T = 20, 40, 70 and 90°C, i = 1000, γ_c = 0.3 Mg / m^3 (Model results)

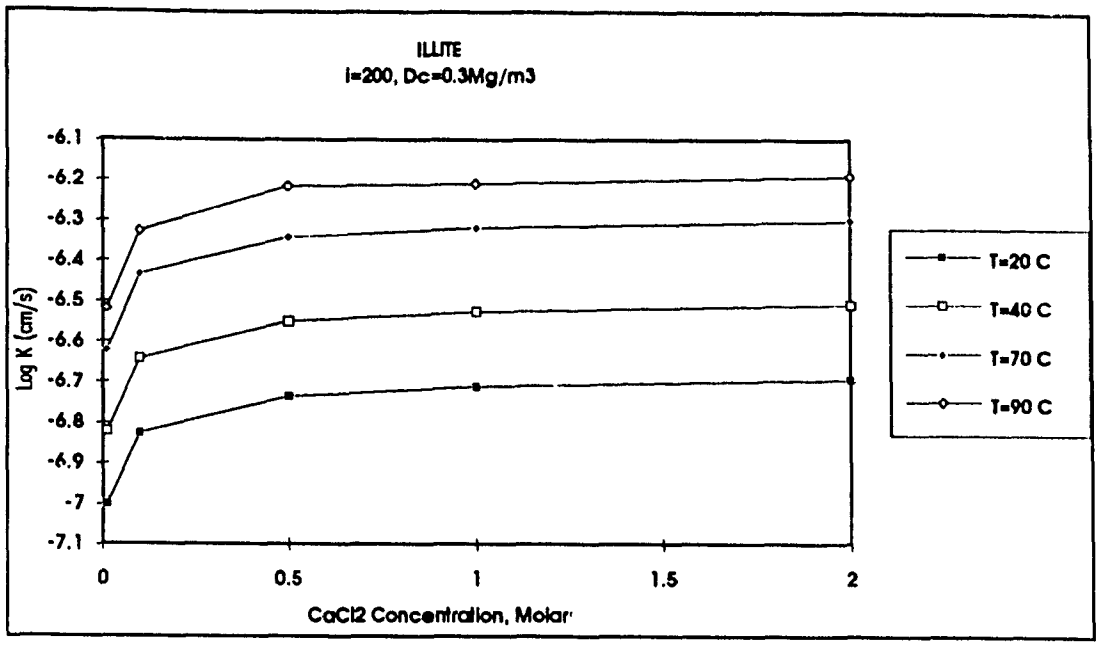

Figure C-81 Illite, Log K vs $CaCl_2$ concentration at T = 20, 40, 70 and 90°C, i = 200, $\gamma_c = 0.3$ Mg / m^3 (Model results)

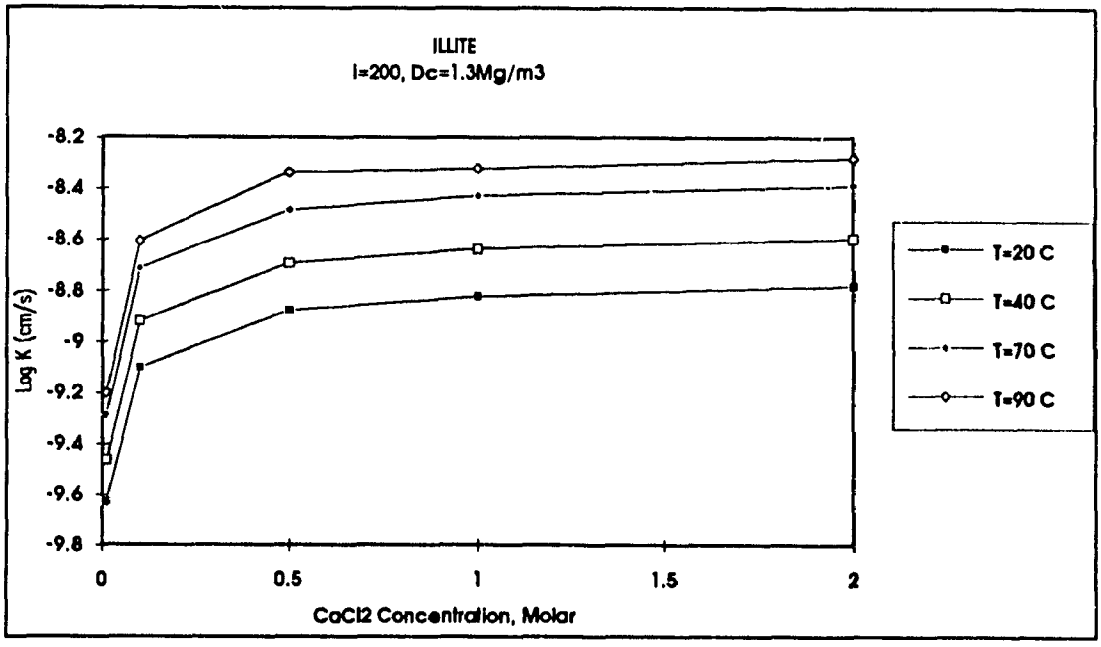

Figure C-82 Illite, Log K vs $CaCl_2$ concentration at T = 20, 40, 70 and 90°C, i = 200, $\gamma_c = 1.3$ Mg / m^3 (Model results)

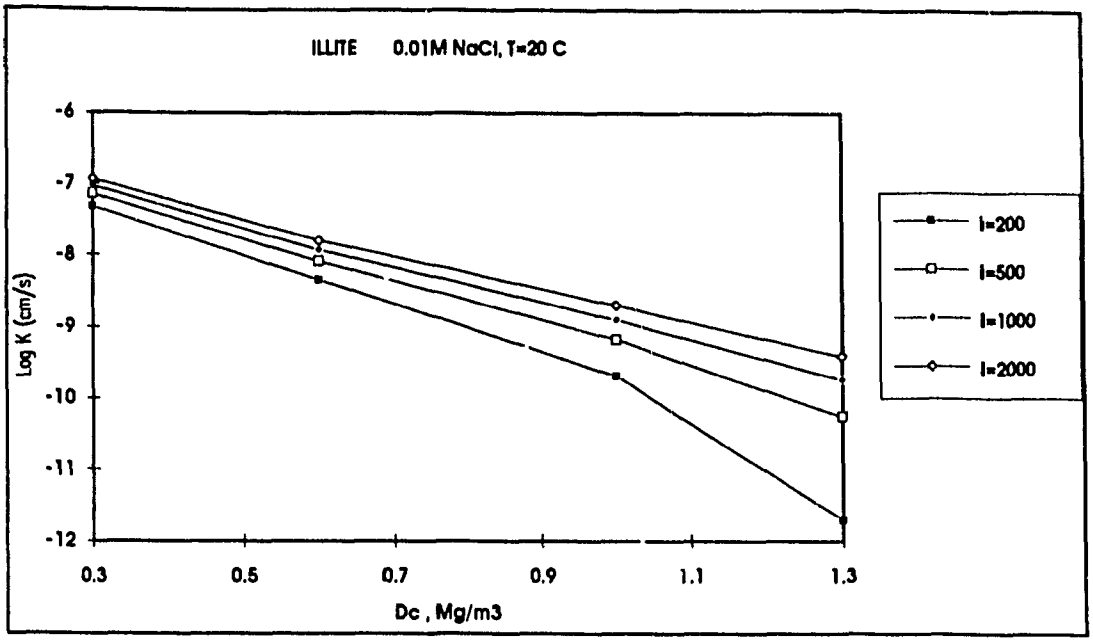

Figure C-83 Illite, Log K vs γ_c at different Hydraulic Gradient and 0.01M NaCl concentration (Model results)

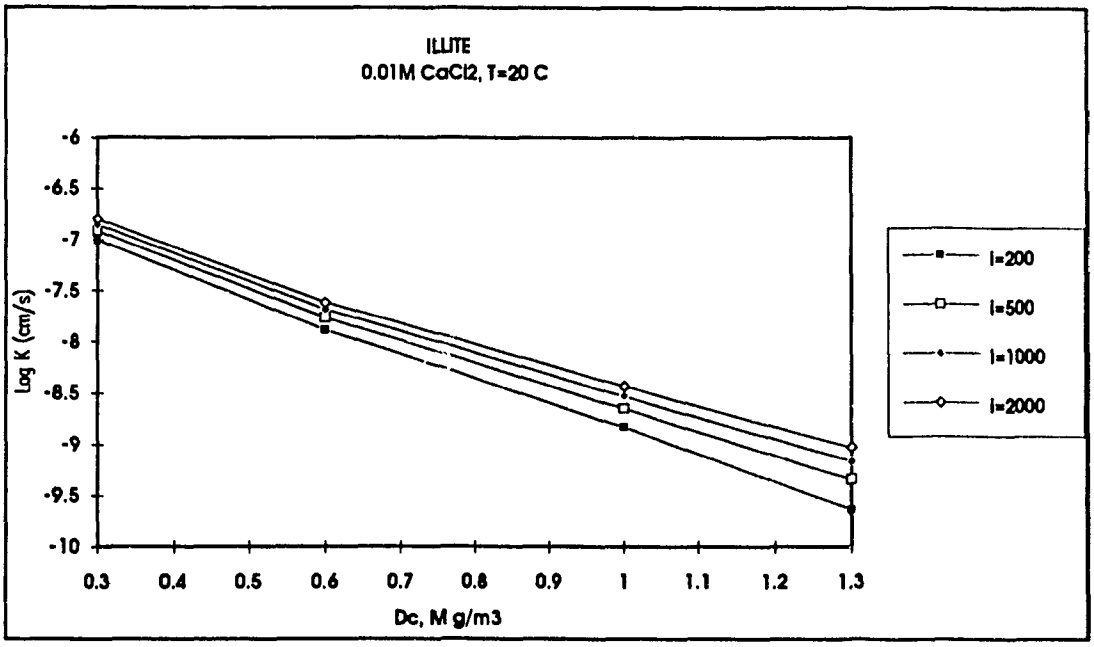

Figure C-84 Illite, Log K vs γ_c at different Hydraulic Gradient and 0.01M $CaCl_2$ concentration (Model results)

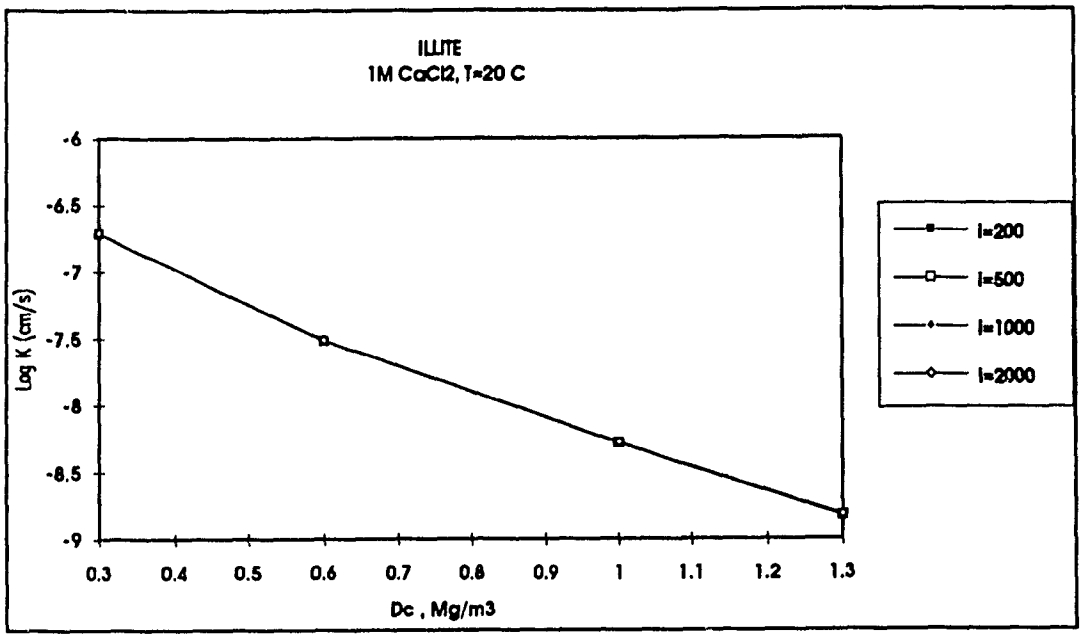

Figure C-85 Illite, Log K vs γ_c at different Hydraulic Gradient and 1M $CaCl_2$ concentration (Model results)

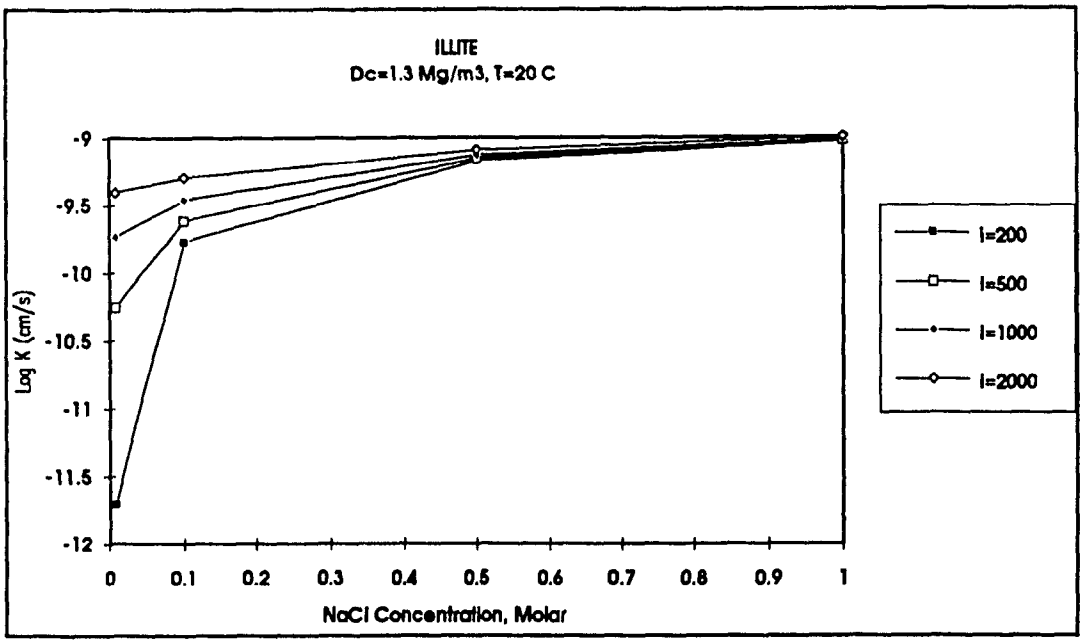

Figure C-86 Illite, Log K vs NaCl concentration at different Hydraulic Gradient and $\gamma_c = 1.3$ Mg / m^3 (Model results)

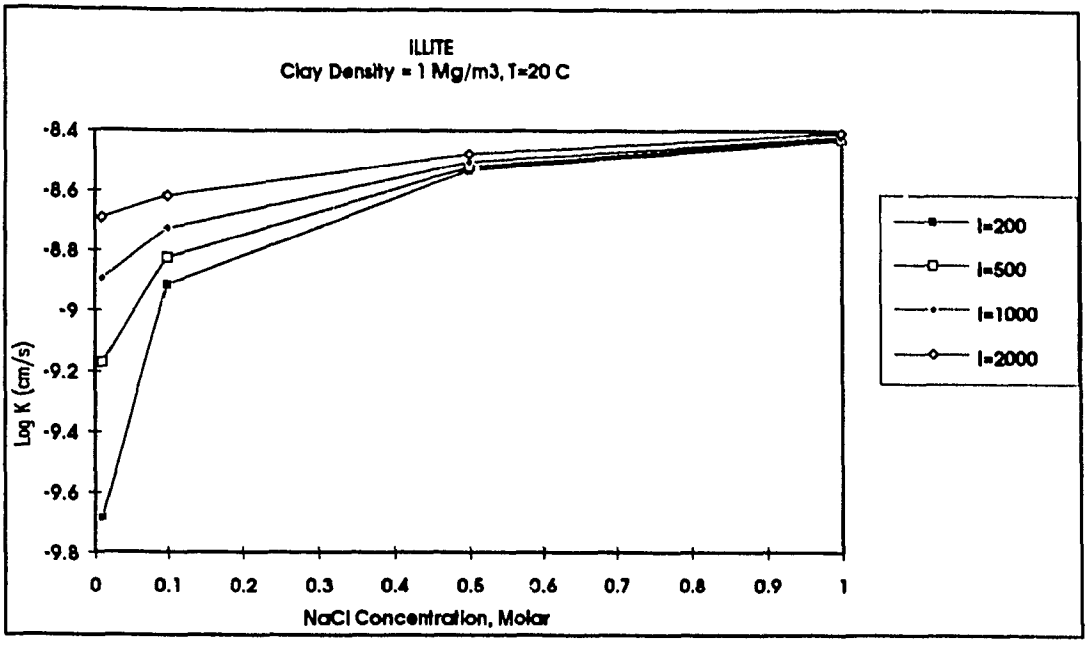

Figure C-87 Illite, Log K vs NaCl concentration at different Hydraulic Gradient and $\gamma_c = 1\ Mg / m^3$ (Model results)

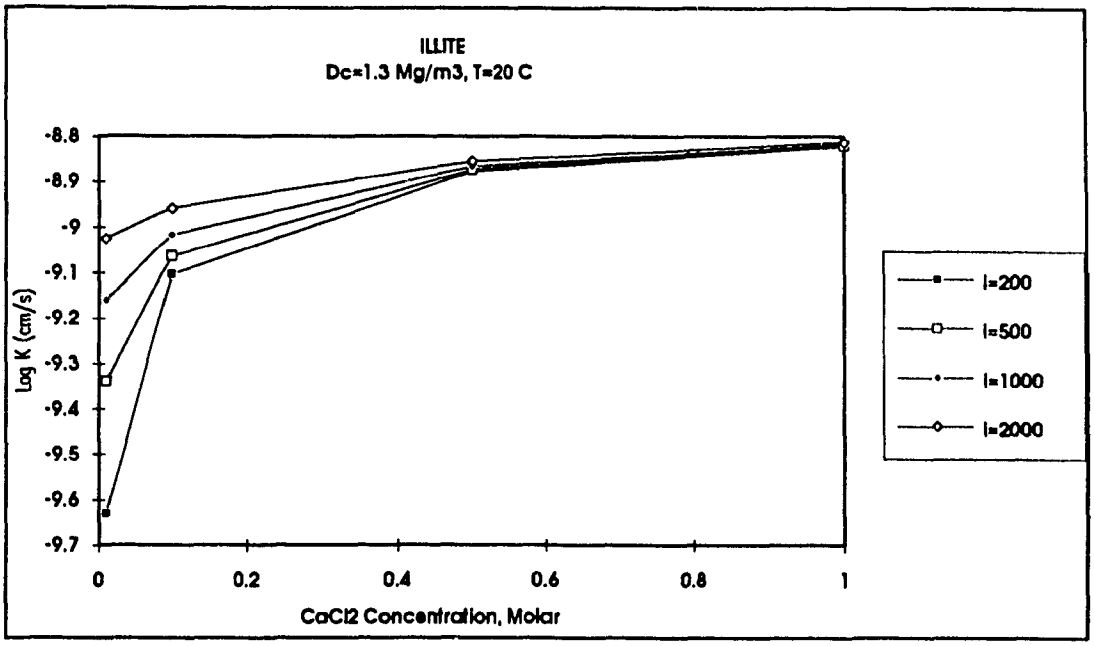

Figure C-88 Illite, Log K vs $CaCl_2$ concentration at different Hydraulic Gradient and $\gamma_c = 1.3\ Mg / m^3$ (Model results)

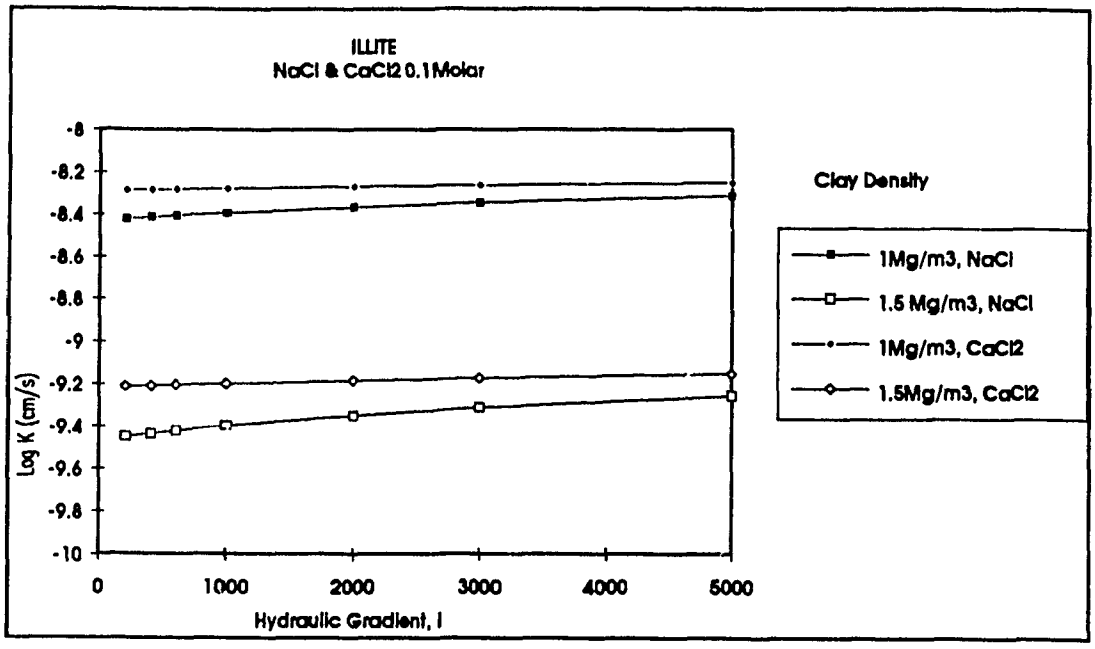

Figure C-89 Illite, Log K vs Hydraulic Gradient i for 0.1M NaCl and $CaCl_2$ and γ_c = 1 and 1.5 Mg / m^3 (Model results)

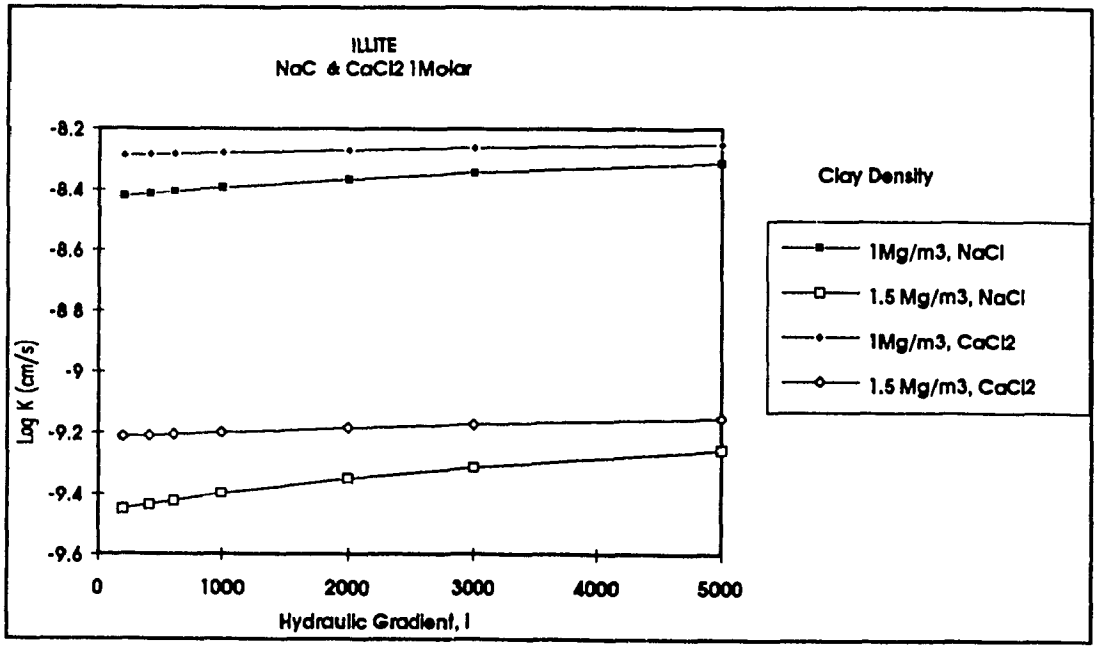

Figure C-90 Illite, Log K vs Hydraulic Gradient i for 1M NaCl and $CaCl_2$ and γ_c = 1 and 1.5 Mg / m^3 (Model results)

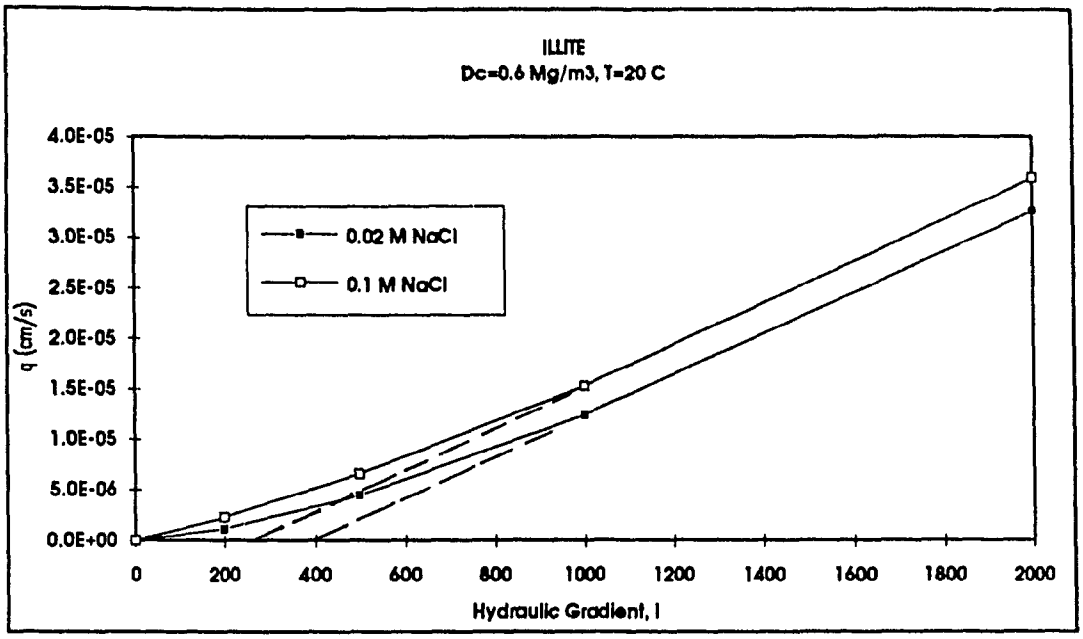

Figure C-91 Illite, q (cm/s) vs i at 0.02 M and 0.1M NaCl concentration and γ_c = 0.6 Mg / m^3 (Model results)

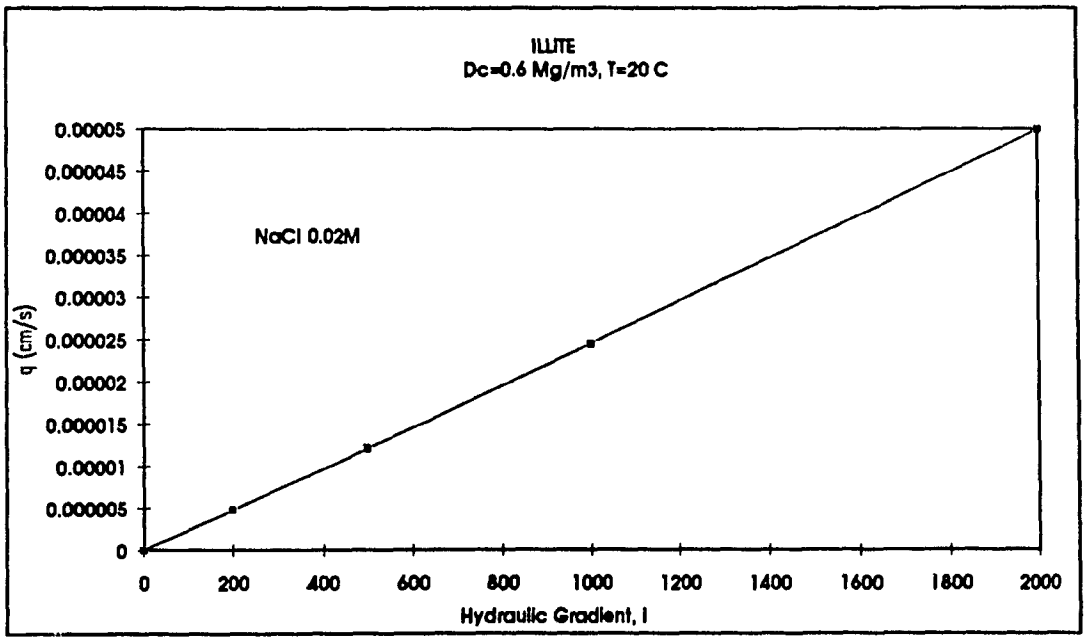

Figure C-92 Illite, q (cm/s) vs i at 0.02 M NaCl concentration and γ_c = 0.6 Mg / m^3 (Model results)

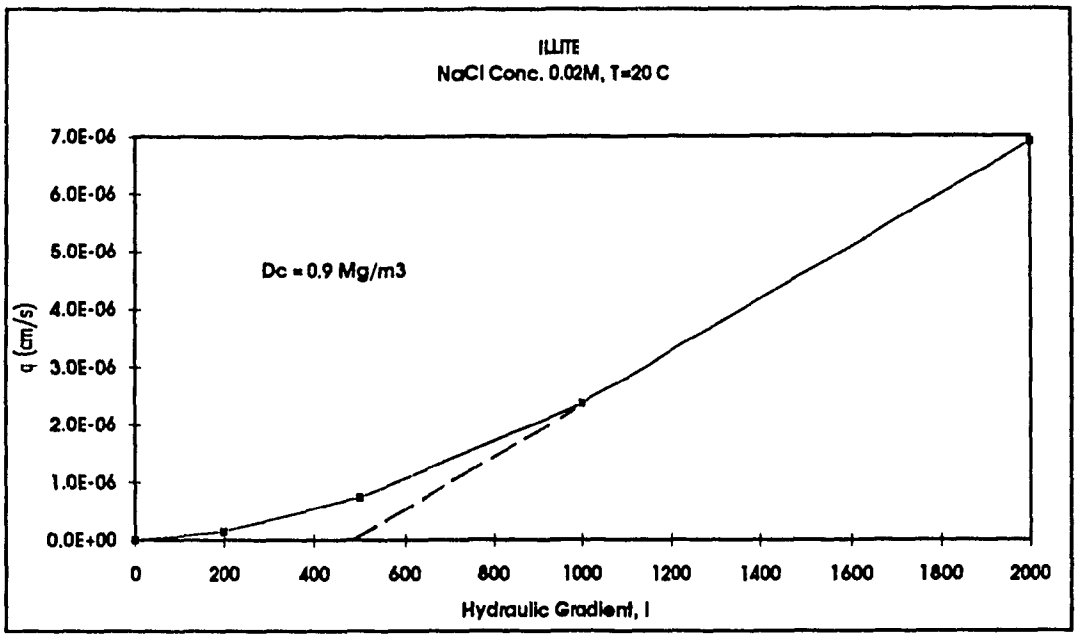

Figure C-93 Illite, q (cm/s) vs i at 0.02 M NaCl concentration and $\gamma_c = 0.9$ Mg / m^3 (Model results)

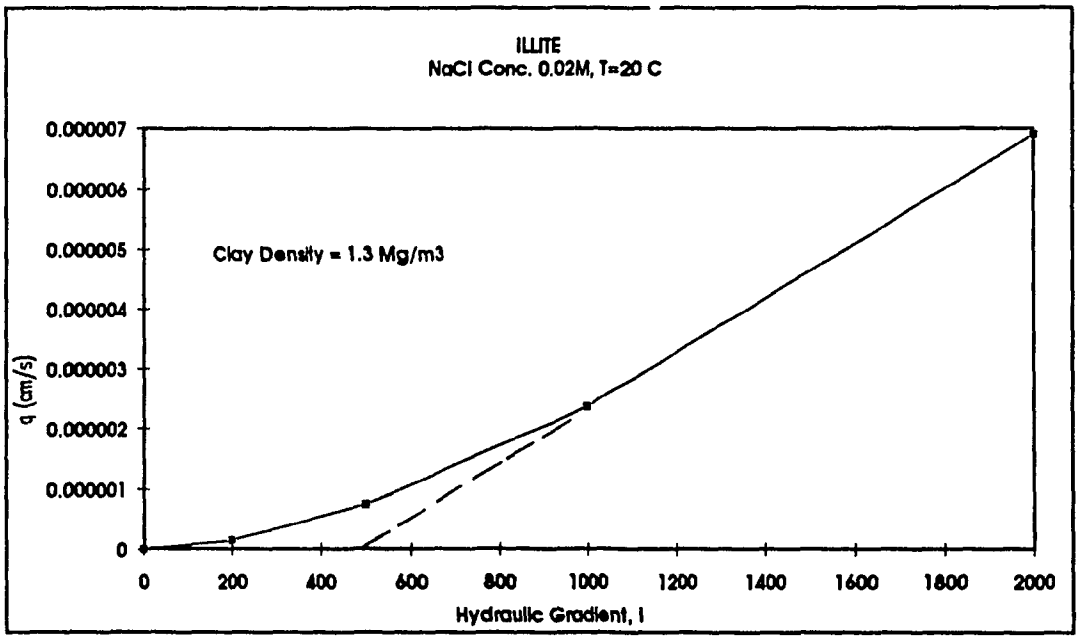

Figure C-94 Illite, q (cm/s) vs i at 0.02 M NaCl concentration and $\gamma_c = 1.3$ Mg / m^3 (Model results)

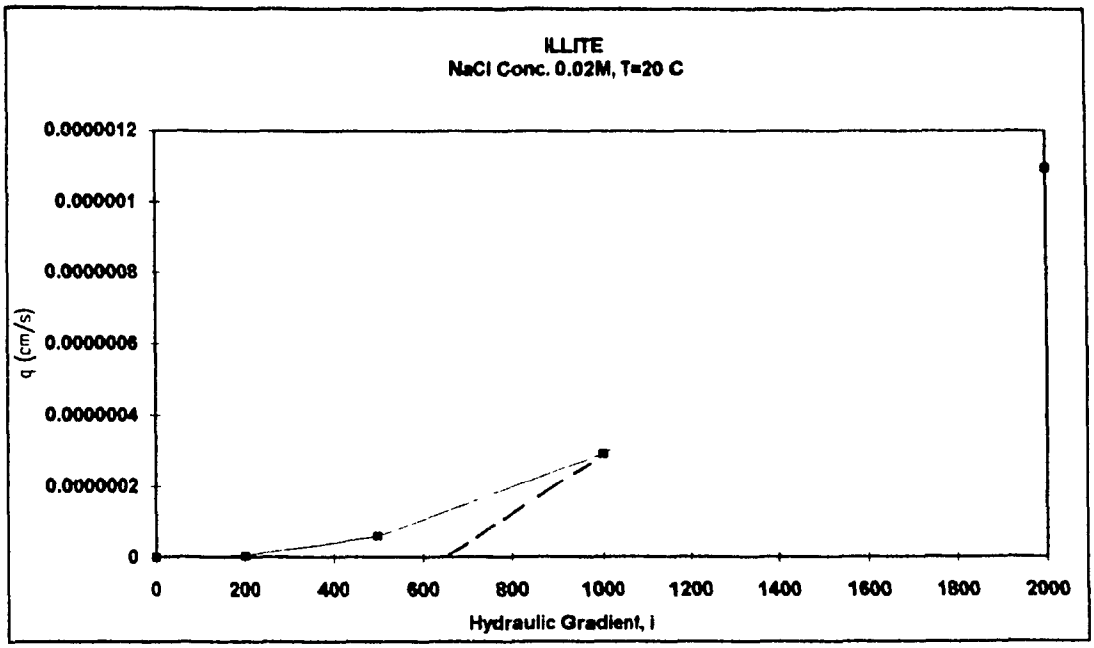

Figure C-95 Illite, q (cm/s) vs i at 0.02 M NaCl concentration and γ_c = 1.5 Mg / m^3 (Model results)

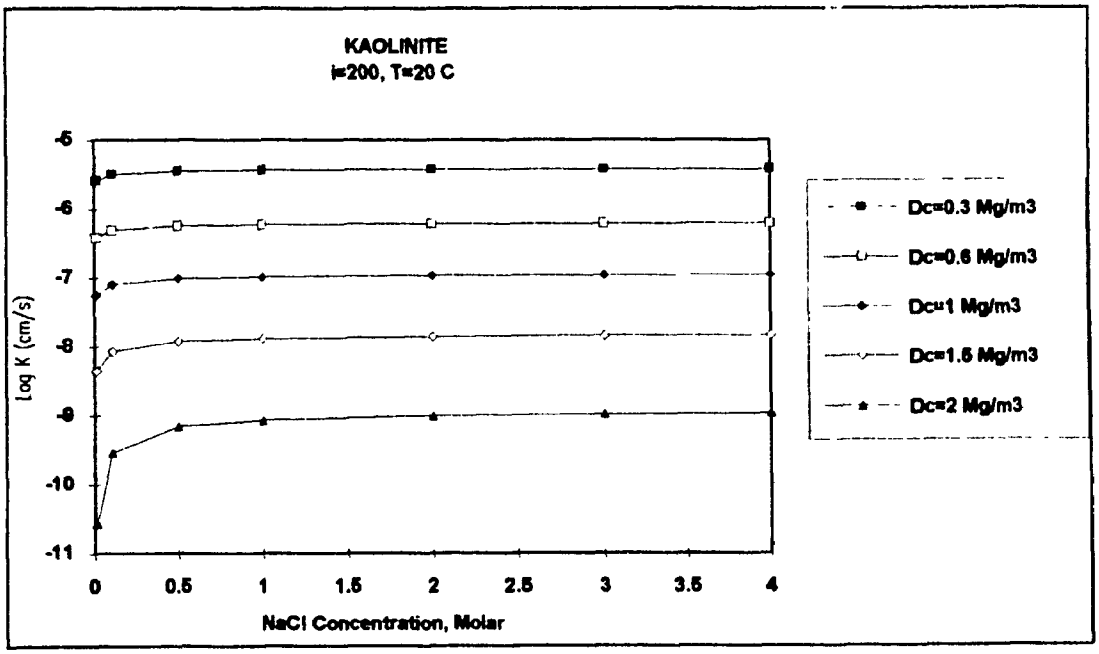

Figure C-96 Kaolinite, Log K vs NaCl concentration at γ_c = 0.3, 0.6, 1, 1.5, 2 Mg/m^3 and i = 200 (Model results)

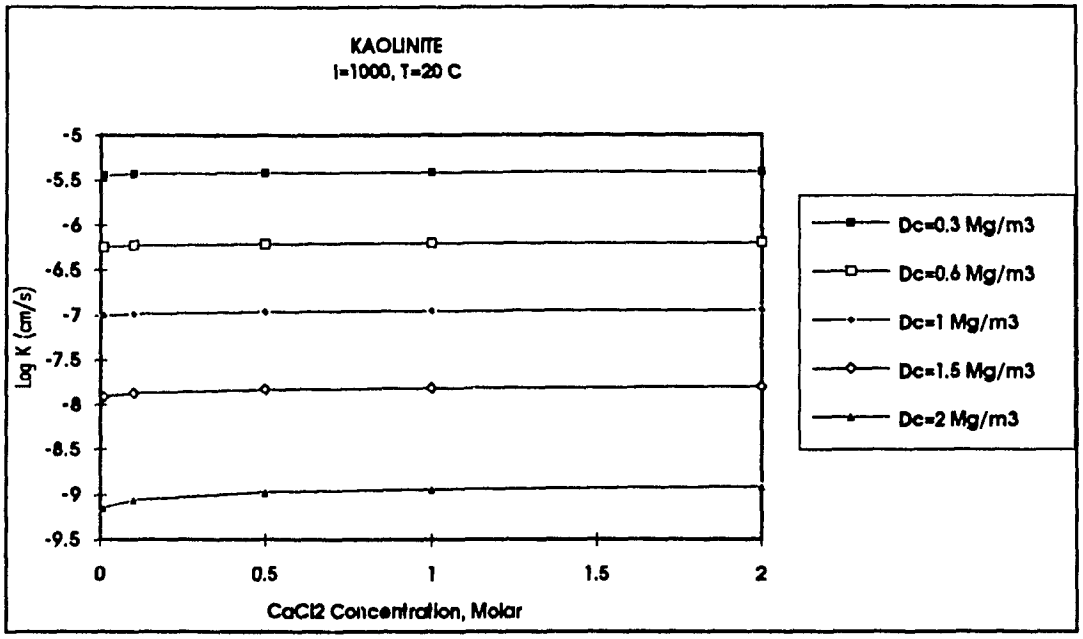

Figure C-97 Kaolinite, Log K vs $CaCl_2$ concentration at γ_c = 0.3, 0.6, 1, 1.5, 2 Mg/m^3 and i = 1000 (Model results)

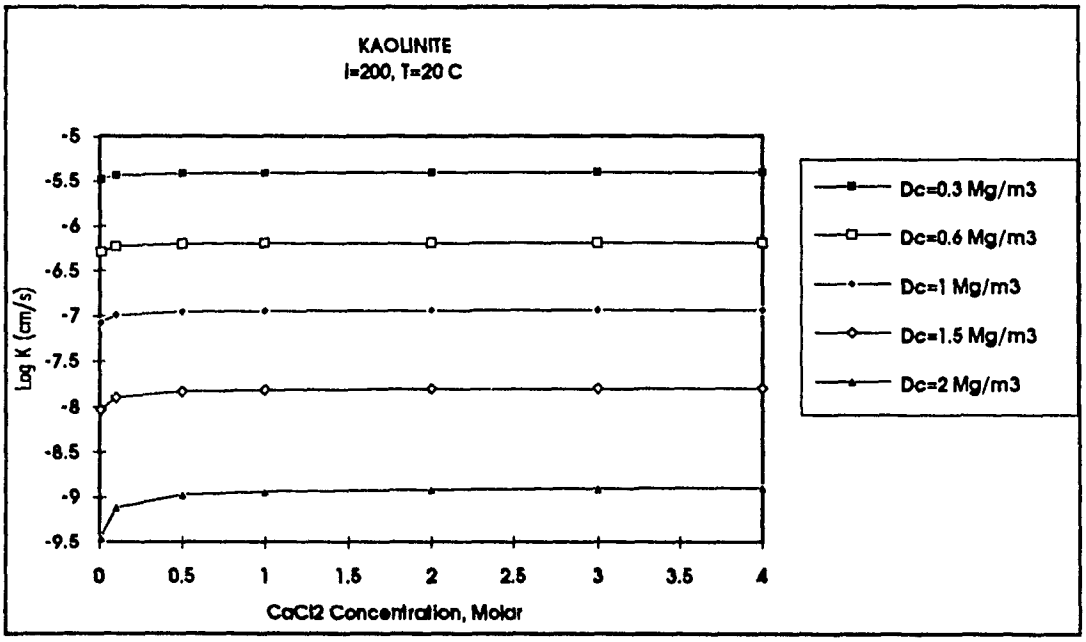

Figure C-98 Kaolinite, Log K vs $CaCl_2$ concentration at γ_c = 0.3, 0.6, 1, 1.5, 2 Mg/m^3 and i = 200 (Model results)

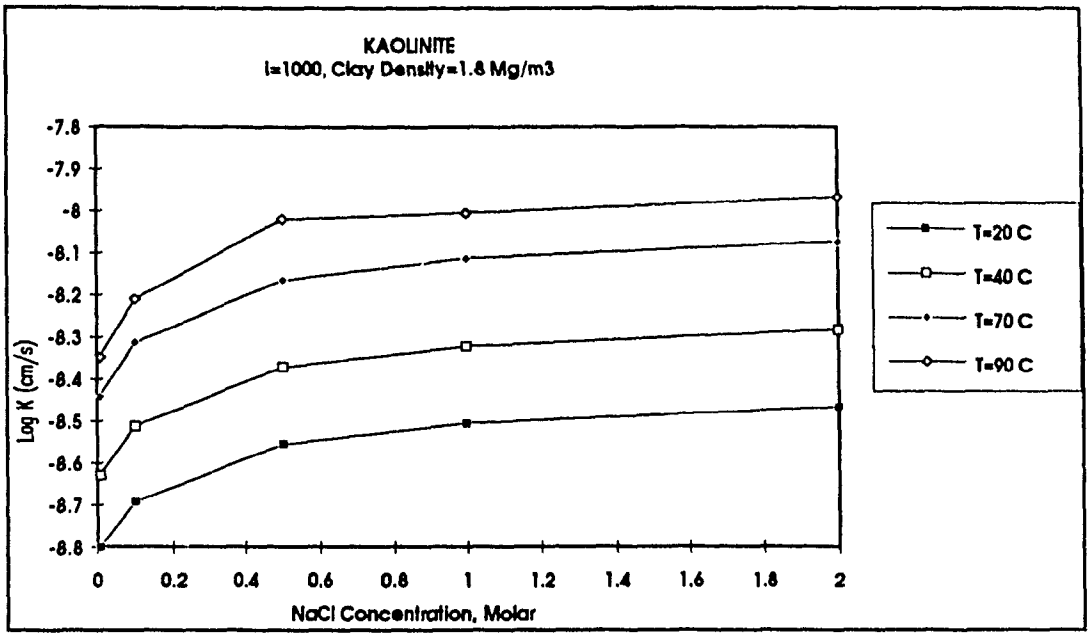

Figure C-99 Kaolinite, Log K vs NaCl concentration at T = 20, 40, 70 and 90°C, i = 1000, γ_c = 1.8 Mg / m^3 (Model results)

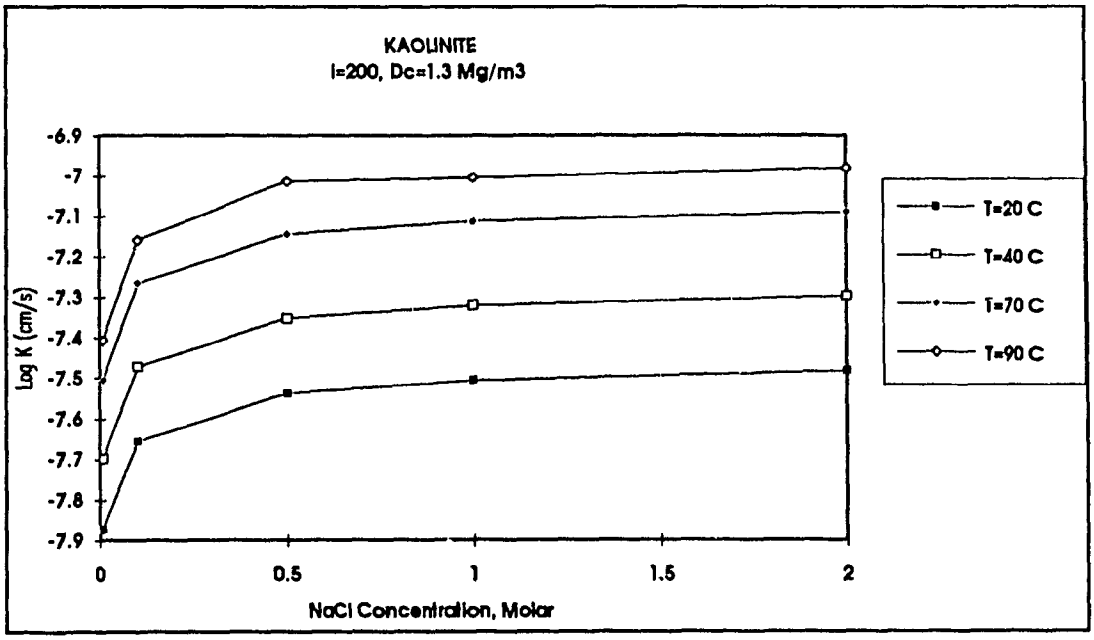

Figure C-100 Kaolinite, Log K vs NaCl concentration at T = 20, 40, 70 and 90°C, i = 200, γ_c = 1.3 Mg / m^3 (Model results)

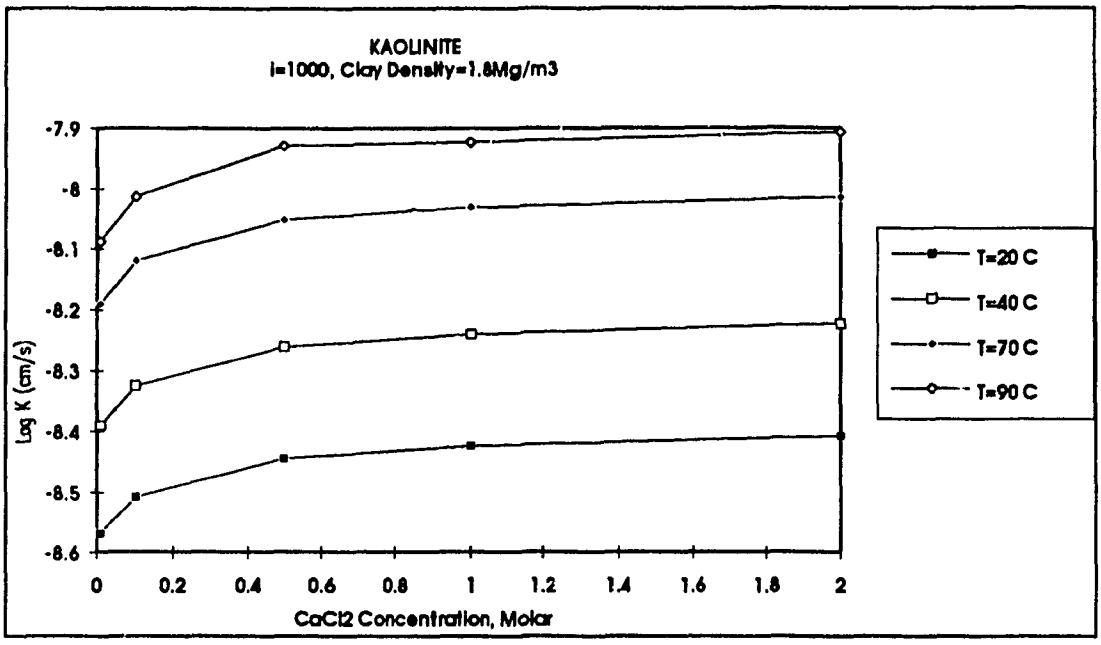

Figure C-101 Kaolinite, Log K vs $CaCl_2$ concentration at T = 20, 40, 70 and 90°C, i = 1000, γ_c = 1.8 Mg / m^3 (Model results)

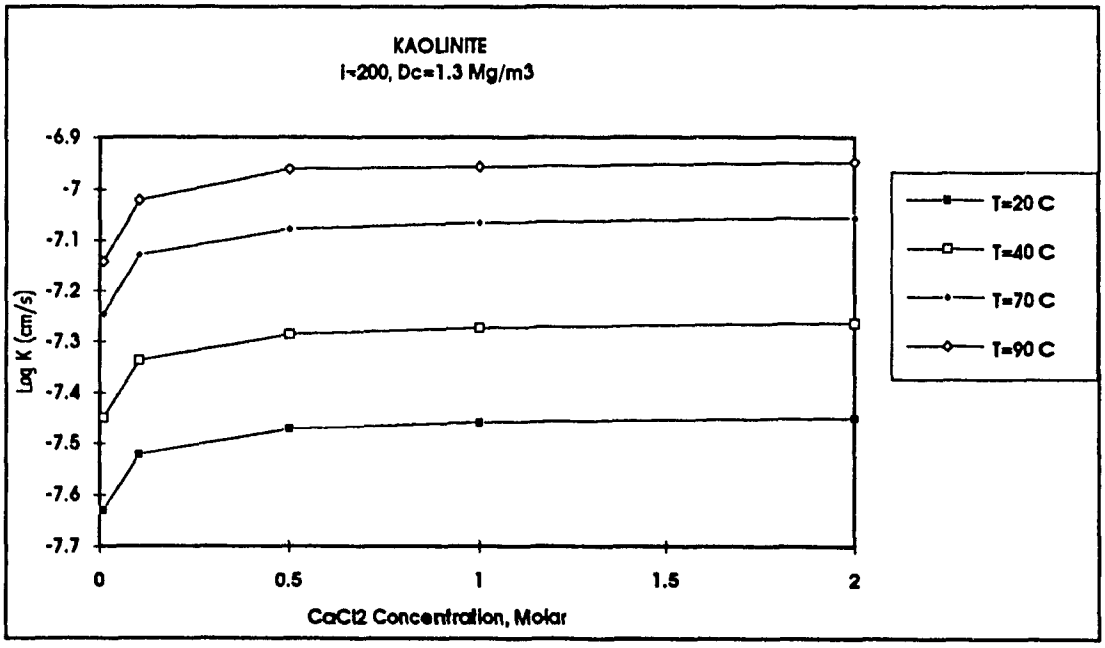

Figure C-102 Kaolinite, Log K vs $CaCl_2$ concentration at T = 20, 40, 70 and 90°C, i = 200, γ_c = 1.3 Mg / m^3 (Model results)

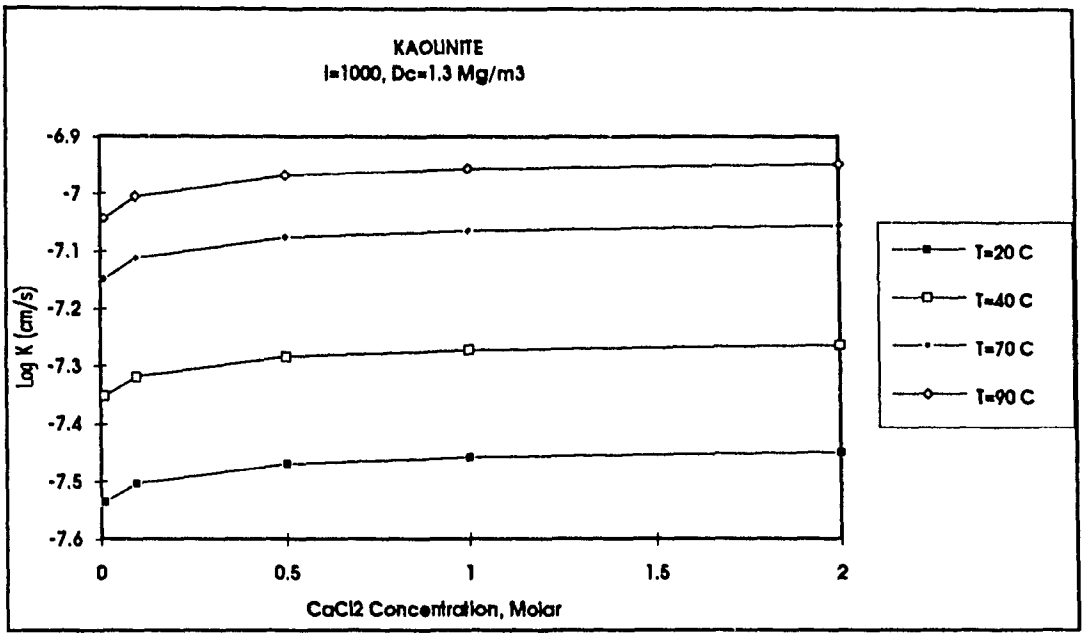

Figure C-103 Kaolinite, Log K vs $CaCl_2$ concentration at T = 20, 40, 70 and 90°C, i = 1000, γ_c = 1.3 Mg / m^3 (Model results)

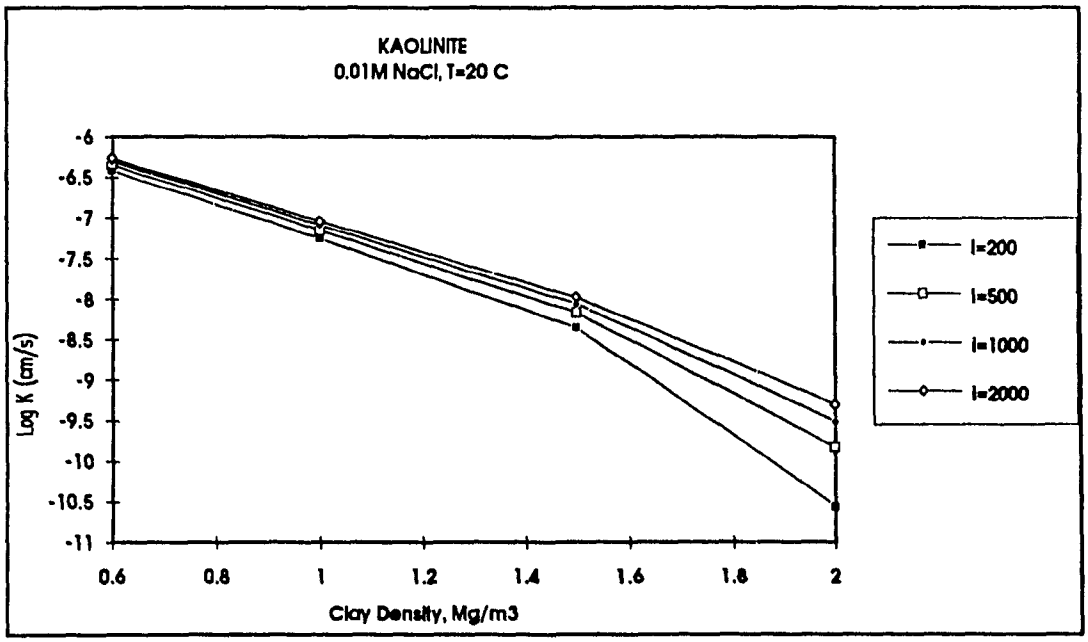

Figure C-104 Kaolinite, Log K vs γ_c at different Hydraulic Gradient and 0.01M NaCl concentration (Model results)

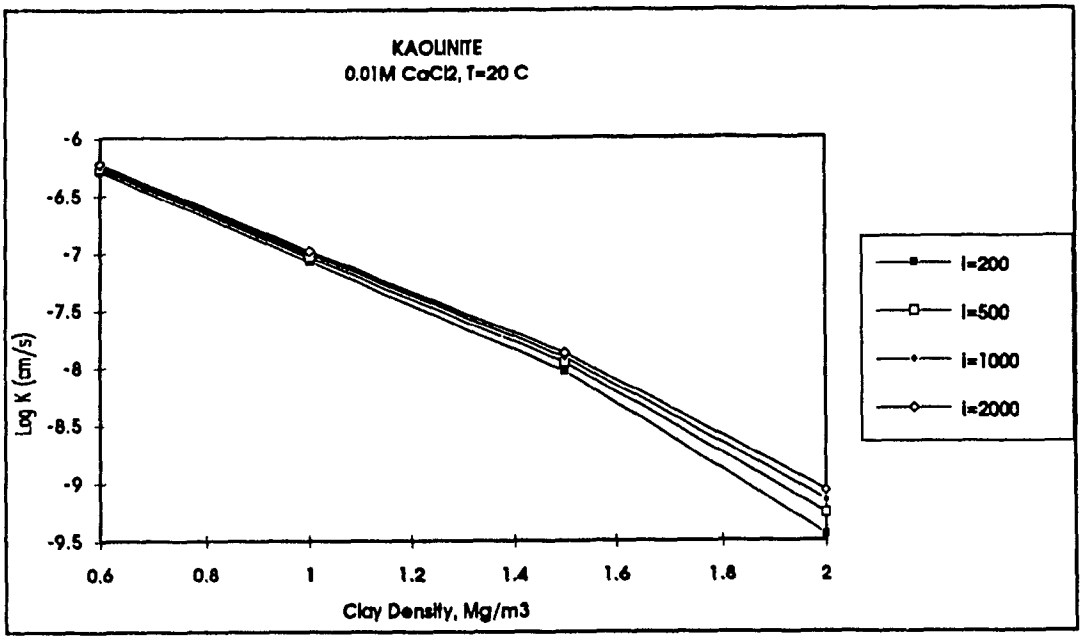

Figure C-105 Kaolinite, Log K vs γ_c at different Hydraulic Gradient and 0.01M $CaCl_2$ concentration (Model results)

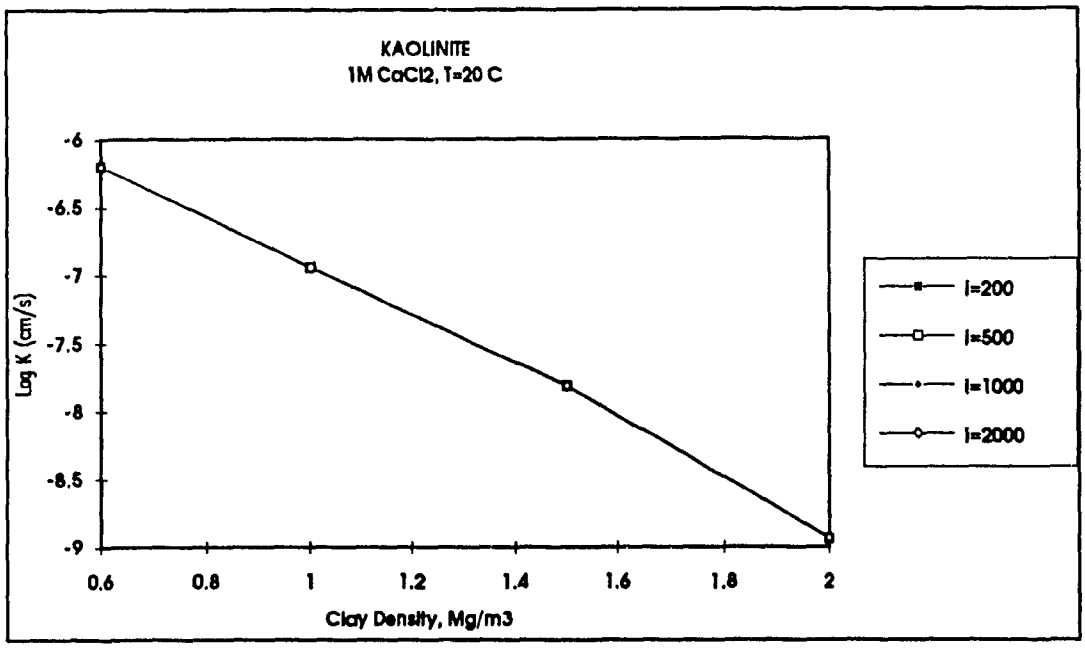

Figure C-106 Kaolinite, Log K vs γ_c at different Hydraulic Gradient and 1M $CaCl_2$ concentration (Model results)

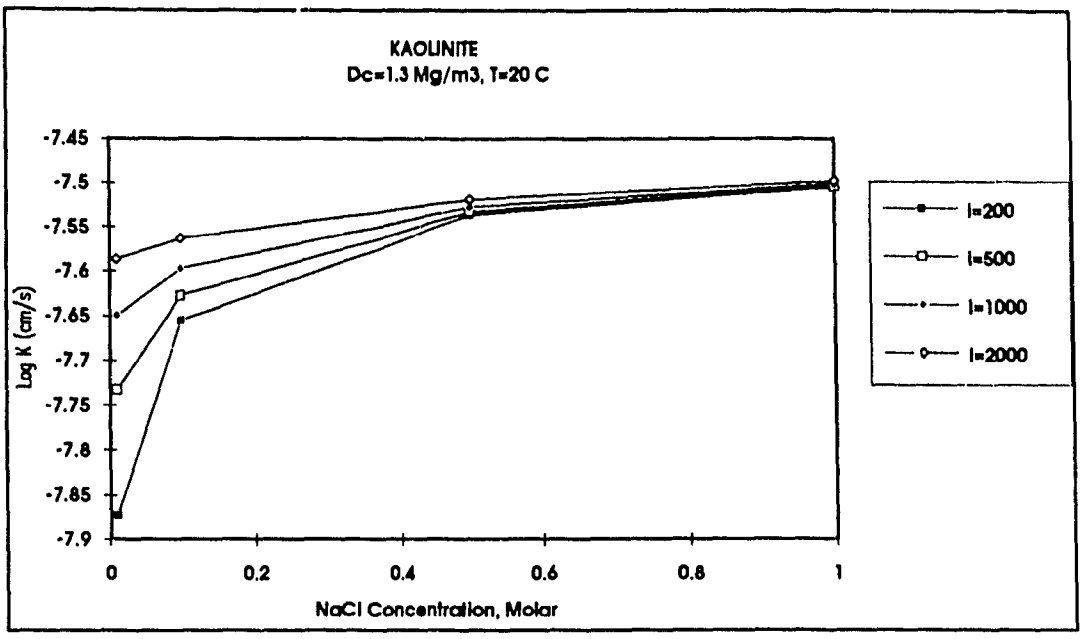

Figure C-107 Kaolinite, Log K vs NaCl concentration at different Hydraulic Gradient and γ_c = 1.3 Mg / m^3 (Model results)

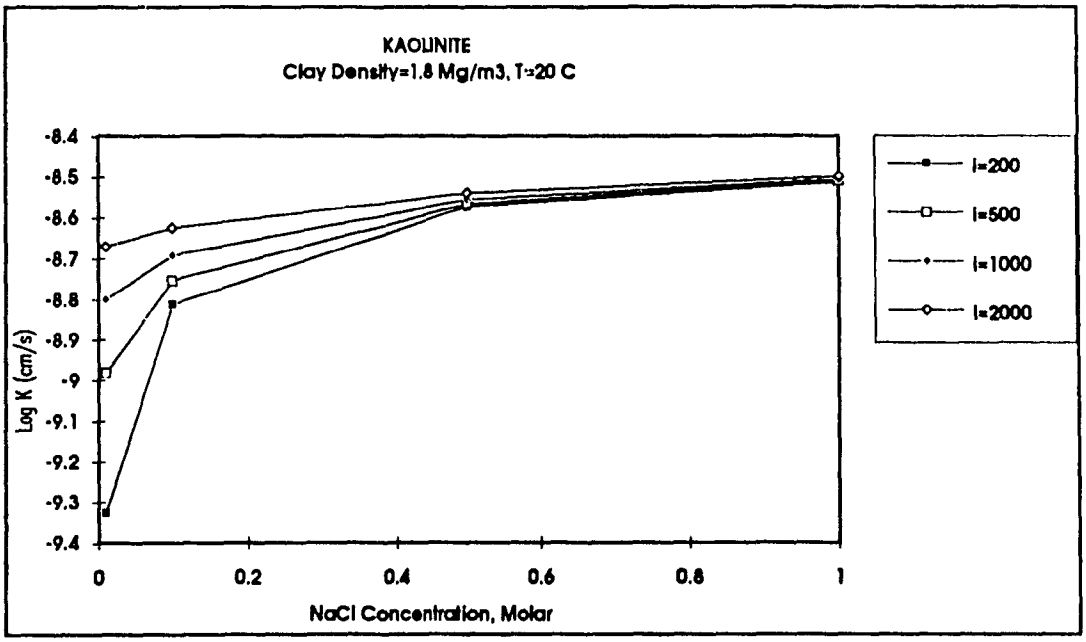

Figure C-108 Kaolinite, Log K vs NaCl concentration at different Hydraulic Gradient and γ_c = 1.8 Mg / m^3 (Model results)

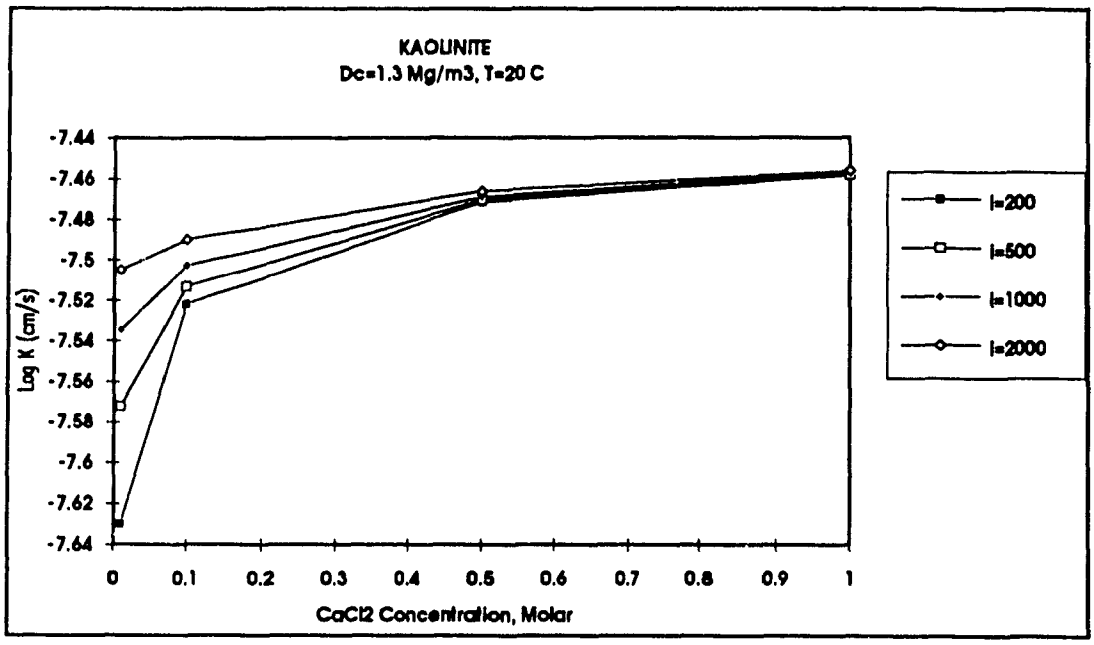

Figure C-109 Kaolinite, Log K vs $CaCl_2$ concentration at different Hydraulic Gradient and $\gamma_c = 1.3$ Mg / m^3 (Model results)

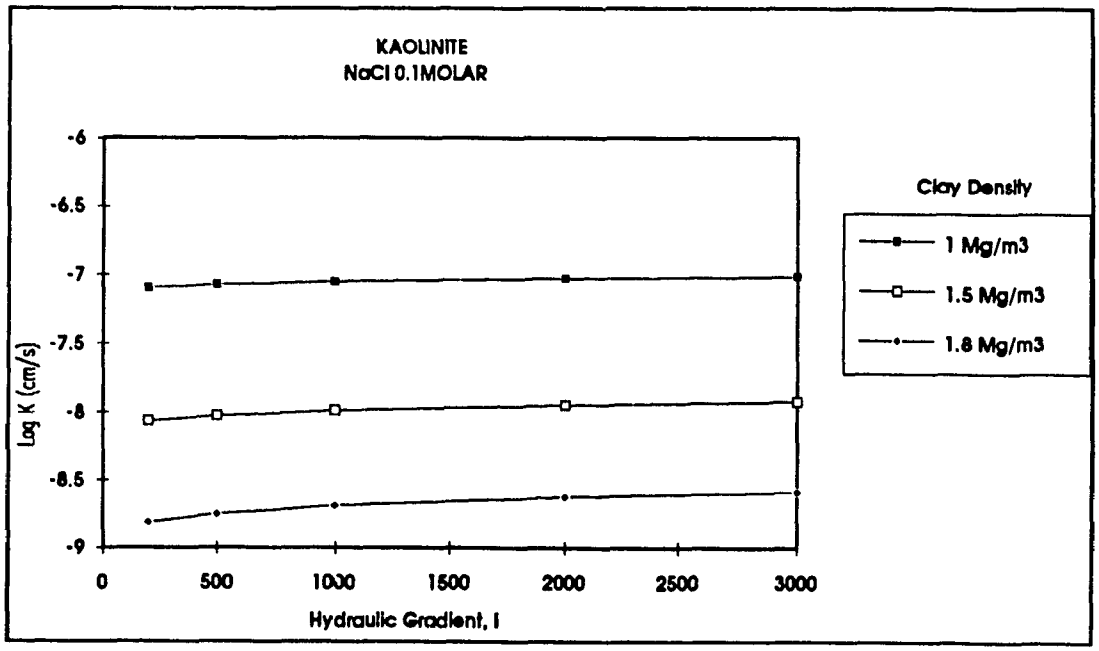

Figure C-110 Kaolinite, Log K vs Hydraulic Gradient i for 0.1M NaCl and $\gamma_c = 1$, 1.5 and 1.8 Mg / m^3 (Model results)

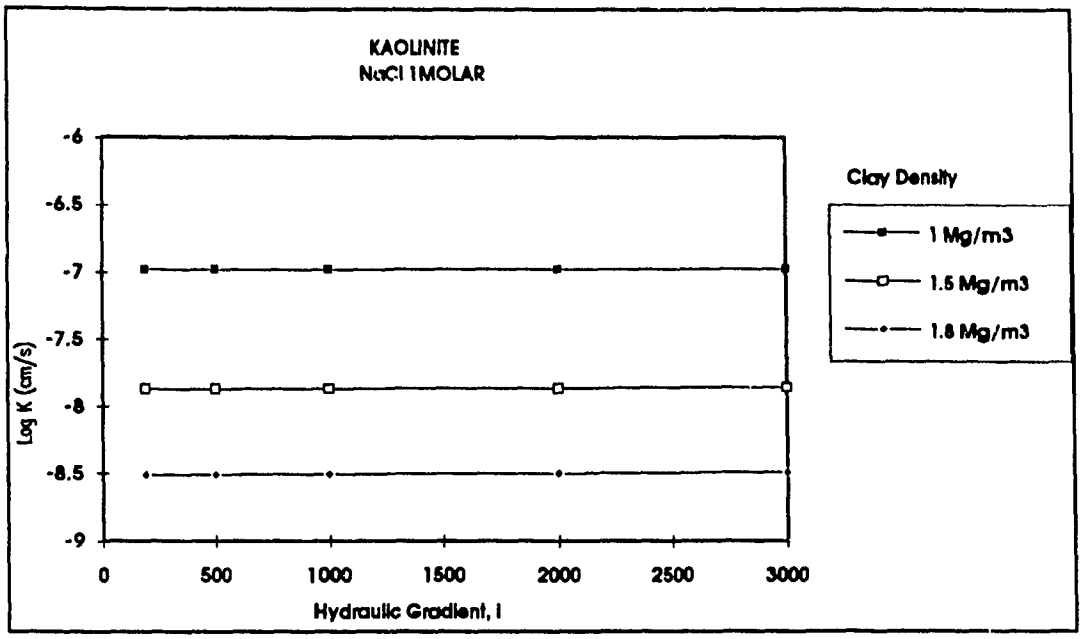

Figure C-111 Kaolinite, Log K vs Hydraulic Gradient i for 1M NaCl and γ_c = 1, 1.5 and 1.8 Mg / m^3 (Model results)

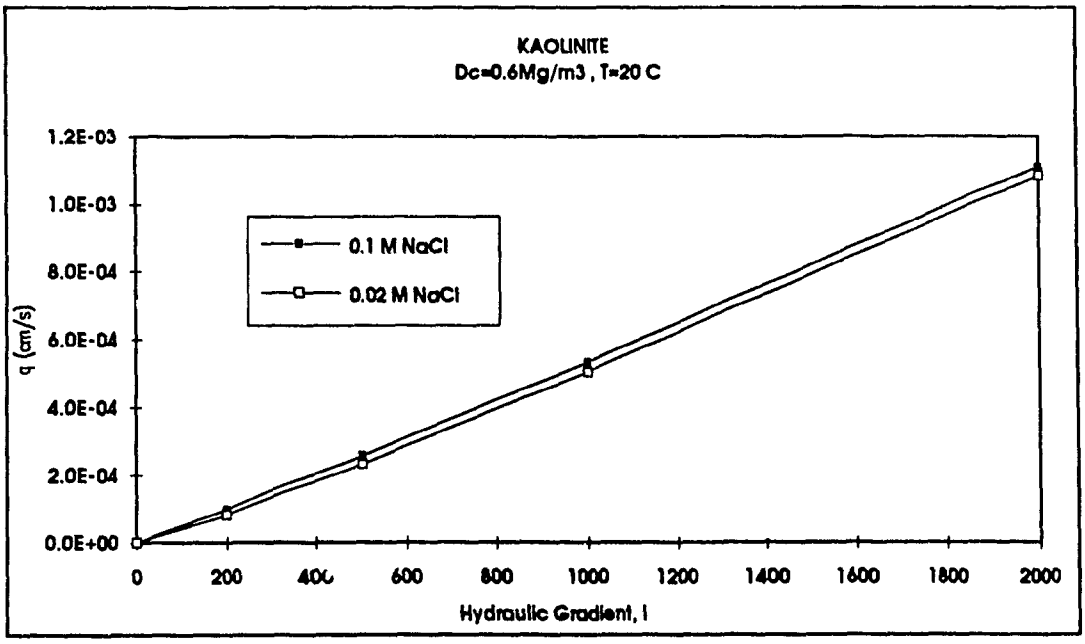

Figure C-112 Kaolinite, q (cm/s) vs i at 0.02 M and 0.1M NaCl and γ_c = 0.6 Mg / m^3 (Model results)

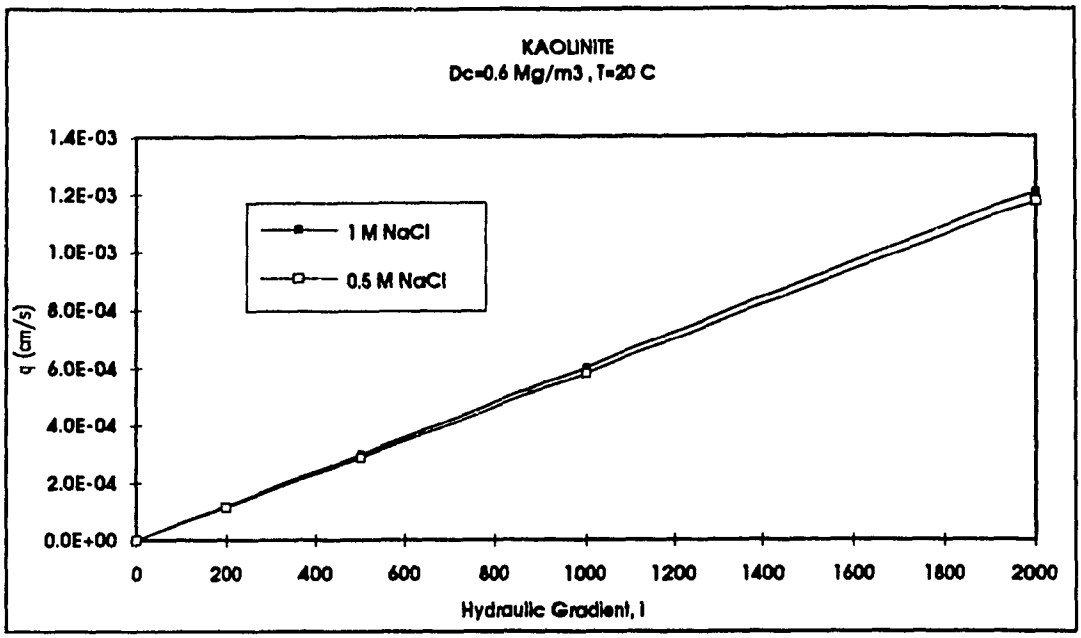

Figure C-113 Kaolinite, q (cm/s) vs i at 0.5 M and 1M NaCl and $\gamma_c = 0.6$ Mg / m^3 (Model results)

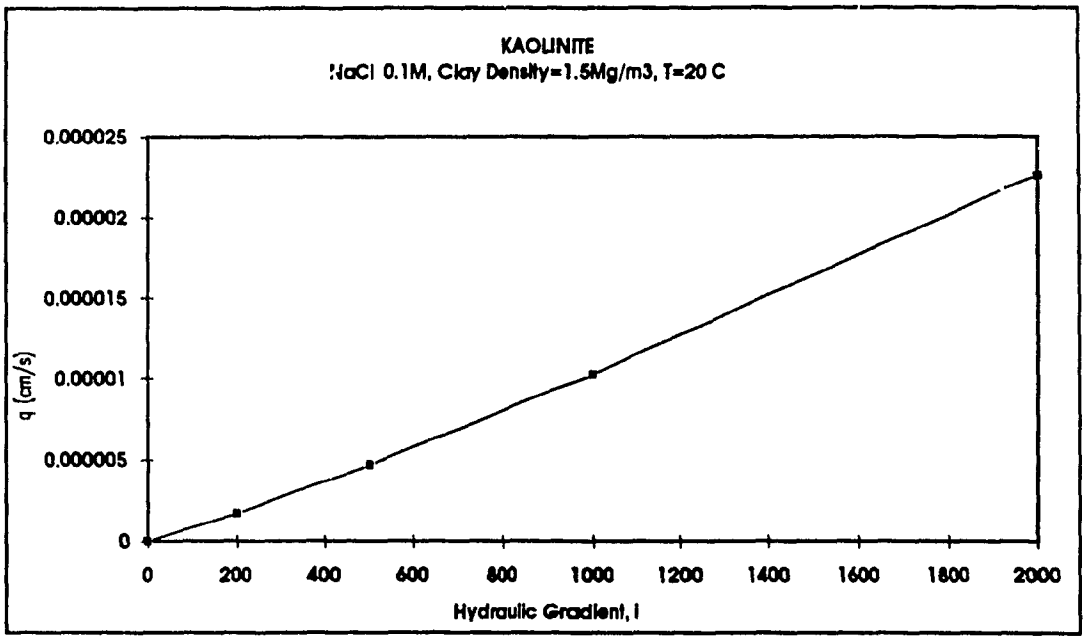

Figure C-114 Kaolinite, q (cm/s) vs i at 0.1 M NaCl concentration and $\gamma_c = 1.5$ Mg / m^3 (Model results)

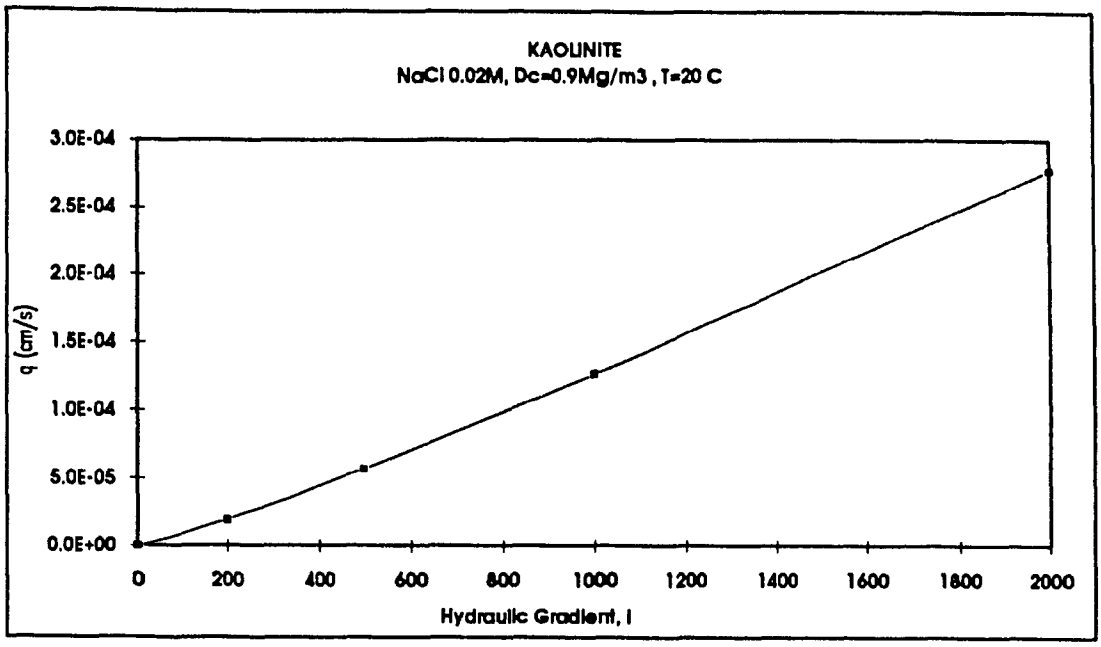

Figure C-115 Kaolinite, q (cm/s) vs i at 0.02 M NaCl concentration and γ_c = 0.9 Mg / m^3 (Model results)

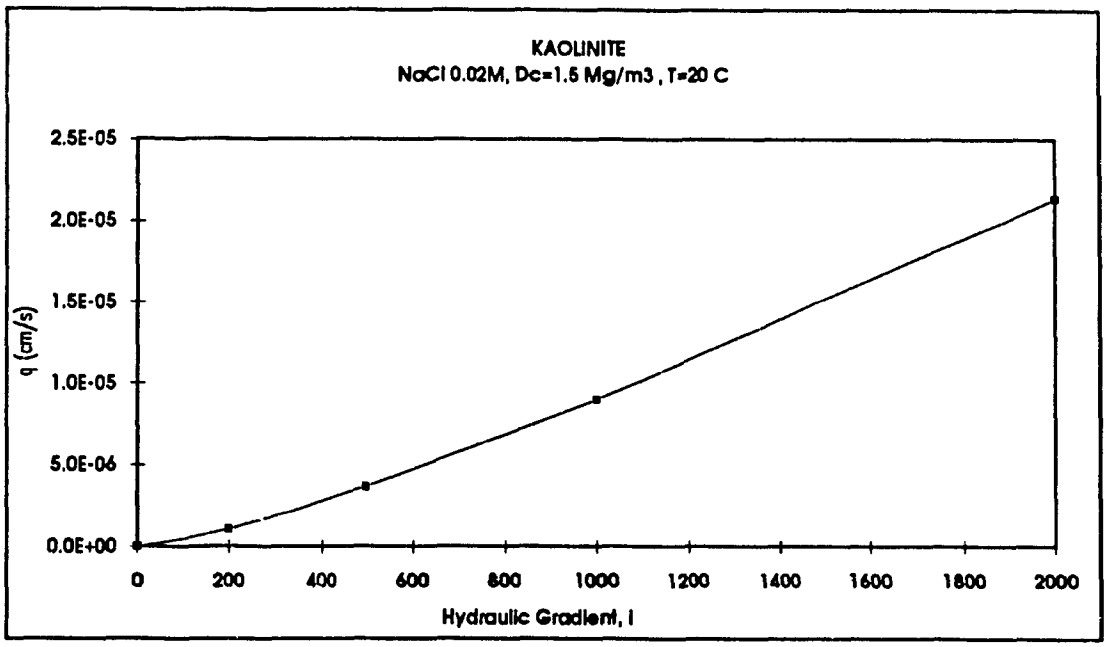

Figure C-116 Kaolinite, q (cm/s) vs i at 0.02 M NaCl concentration and γ_c = 1.5 Mg / m^3 (Model results)

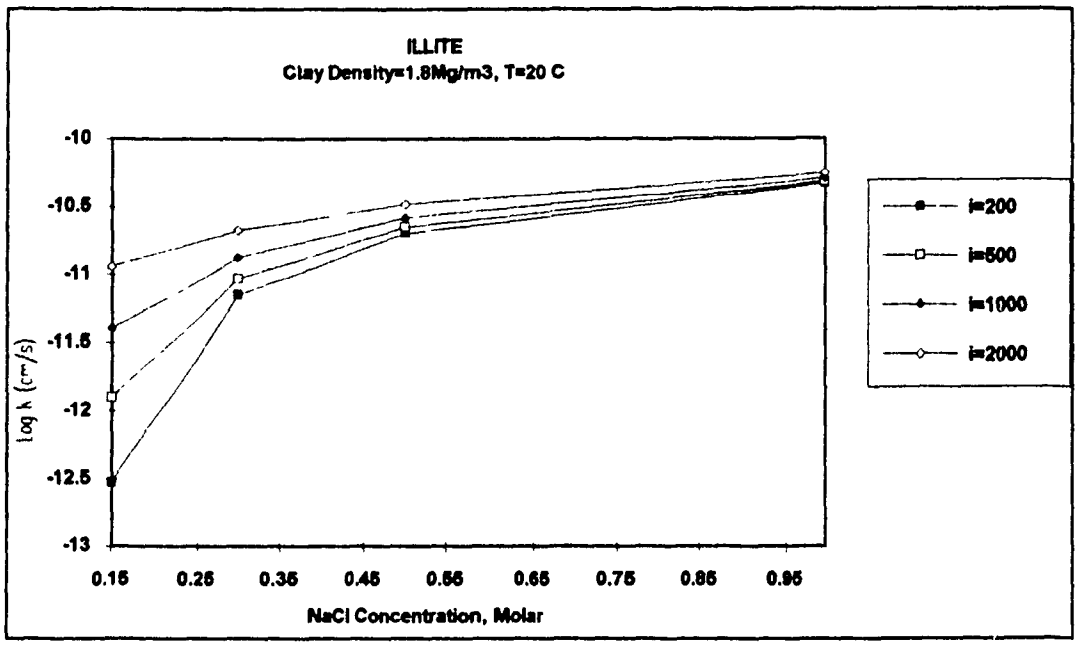

Figure C-117 Illite, Log K vs NaCl concentration at different Hydraulic Gradient and $\gamma_c = 1.8$ Mg / m^3 (Model results)

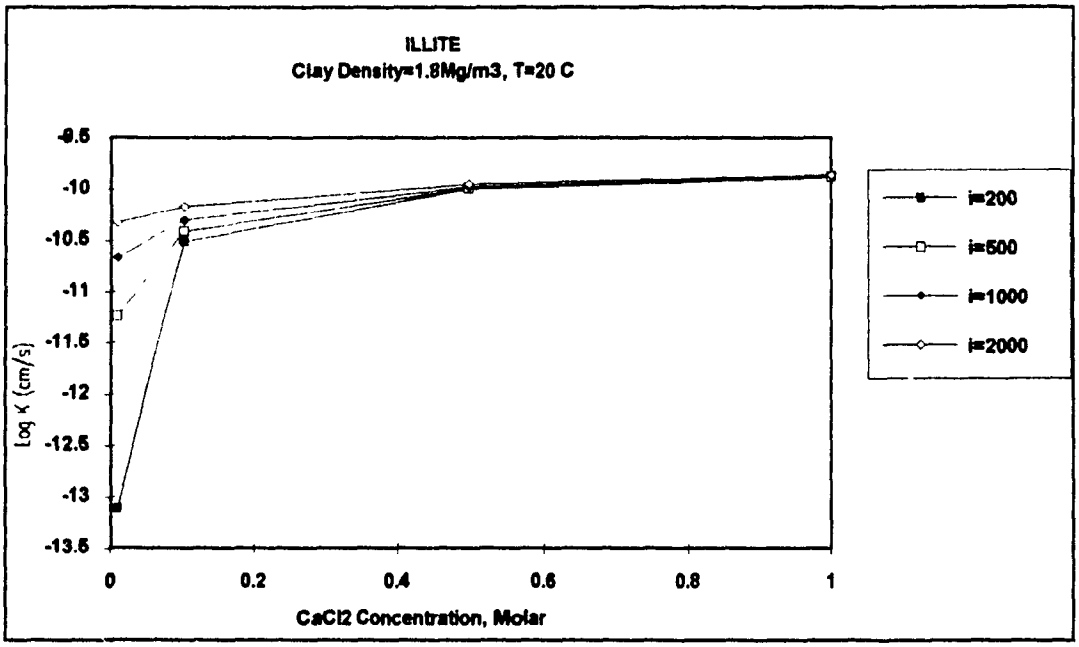

Figure C-118 Illite, Log K vs $CaCl_2$ concentration at different Hydraulic Gradient and $\gamma_c = 1.8$ Mg / m^3 (Model results)